CANADIAN THESES

THÈSES CANADIENNES

NOTICE

The quality of this microfiche is heavily dependent upon the quality of the original thesis submitted for microfilming. Every effort has been made to ensure the highest quality of reproduction possible.

If pages are missing, contact the university which granted the degree.

Some pages may have indistinct print especially if the original pages were typed with a poor typewriter ribbon or if the university sent us an inferior photocopy.

Previously copyrighted materials (journal articles, published tests, etc.) are not filmed.

Reproduction in full or in part of this film is governed by the Canadian Copyright Act, R.S.C. 1970, c. C-30.

AVIS

La qualité de cette microfiche dépend grandement de la qualité de la thèse soumise au microfilmage. Nous avons tout fait pour assurer une qualité supérieure de reproduction.

S'il manque des pages, veuillez communiquer avec l'université qui a conféré le grade.

La qualité d'impression de certaines pages peut laisser à désirer, surtout si les pages originales ont été dactylographiées à l'aide d'un ruban usé ou si l'université nous a fait parvenir une photocopie de qualité inférieure.

Les documents qui font déjà l'objet d'un droit d'auteur (articles de revue, examens publiés, etc.) ne sont pas microfilmés.

La reproduction, même partielle, de ce microfilm est soumise à la Loi canadienne sur le droit d'auteur, SRC 1970, c. C-30.

THIS DISSERTATION
HAS BEEN MICROFILMED
EXACTLY AS RECEIVED

LA THÈSE A ÉTÉ
MICROFILMÉE TELLE QUE
NOUS L'AVONS REÇUE

THE ARCHEAN ROUND LAKE BATHOLITH, ABITIBI GREENSTONE BELT: A SYNTHESIS

by

Pierre Jean Lafleur

A thesis submitted to the School of Graduate Studies in partial fulfillment of the requirements for the degree of Master of Science in Geology

University of Ottawa

ISBN 0-315-33340-5

UNIVERSITÉ D'OTTAWA
UNIVERSITY OF OTTAWA

ABSTRACT

The Round Lake Batholith, of Archean age (2.688 Ga), is intrusive into supracrustal rocks of the Abitibi Supergroup at the southern extremity of the Ontario segment of the Abitibi Greenstone Belt (circa 2.700 Ga). The batholith consists of an older phase (OP) of foliated tonalite-granodiorite and a younger phase (YP) of largely unfoliated granodiorite-tonalite that is rich in xenoliths of supracrustals and OP.

The OP is subdivided into an homogeneous foliated tonalite, grading eastward into a weakly foliated to mainly lineated, poikiloblastic (microcline) granodiorite, which passes into a granodiorite-tonalite with a cataclastic to gneissic foliation concordant to the contact. In places, the OP grades peripherally into an agmatite gneiss consisting of volcanic xenoliths, leucocratic tonalite, granitoid dykes, and a massive hornblende tonalite that occurs as distinct plutons along the western margin of the batholith.

Major element chemistry of the OP (64 to 77% SiO_2) shows trends compatible with differentiation (decrease in Al_2O_3, Fe_2O_{3TOTAL}, MgO, CaO and TiO_2; slight increase in Na_2O? and K_2O), giving support to the gradational nature of the internal subphases. The hornblende tonalite (61 to 66% SiO_2) appears to be a separate entity, possibly a hybrid subphase, since it is generally higher in Al_2O_3, Fe_2O_{3TOTAL}, MgO and CaO when compared to the OP. The YP (66 to 73% SiO_2) shows minor internal variations, also compatible with differentiation; trends are outside the field of, and subparallel to, the OP, suggesting a genetic relationship, although the YP cannot be derived from the latter. Classification diagrams (A-F-M, An-Ab-Or, Q-Ab-Or) demonstrate that the batholith belongs to the calc-alkaline suite of the trondhjemite-tonalite series.

Trace element data (Ba, Sr, Rb, Zr, Ni, Cr) for both phases is relatively scattered, showing weak compatible and in some cases antipathic correlation, such as the large ion lithophile elements (LiL) elements Ba and Sr, with differentiation. Rayleigh Fractionation is used in an attempt to outline a crystallization sequence within the OP which supports the field evidence. The lack of clear LiL elements differentiation trends is a function of mineralogical and chemical homogeneity brought upon by a crystallizing tonalitic melt subjected to chemical differentiation, as indicated by plagioclase zoning, and minimal physical separation between plagioclase crystals and residual melt.

REE data for the batholith (LREE: 20 to 50 times chondrites, Eu/Eu* of about 1.20 to 1.60, HREE: 0.5 to 3.5 times chondrites)

is compatible with partial melting (using a Batch Melting model) of a basaltic parent, at lower crustal levels, as source material for both phases.

The crystallization history of the batholith is summarized in four stages: (A) partial melting of the supracrustal greenstone pile (Abitibi Supergroup) and underlying high grade tonalitic-basic gneisses. (B) tonalitic melt mobilization along a rising diapir; to produce the OP. (C) filter pressing during magma ascent controlled the segregation of residual melt eventually becoming the granodiorite fraction of the OP. (D) subordinate tonalitic melt body(ies) produced the YP.

Emplacement of the OP produced structural patterns indicative of a diapiric mode of intrusion that is continuous from an early stage of stoping (early diapirism) with agmatite development, hybridization and dyking, through to a later stage where minor internal differentiation of the subphases and protocataclasis of the eastern margin took place (late diapirism).

Diapirism was accompanied by the development, and subsequent deflection and overturning of an early fabric in the supracrustal rocks around the batholith (D_1 event); a flattening of pillows, extensive shearing parallel to the contact (marked by a prominent schistosity), and radial shear zones. Structures parallel to the north trending margin of the YP Hope Lake Stock, at the south central margin of the batholith, overprint the diapiric fabric in the supracrustal rocks (possibly synchronous with a D_3 event).

Regional structures imposed on the batholith and country rocks include east-west trending minor fold axes, pronounced schistosity and cataclastic foliation (D_2 event); and northeast trending shear zones (up to 200 m wide) that contain quartz stockworks and gold mineralization.

The sequence of events in the Round Lake Batholith area is closely linked to the main deformation within the Abitibi belt, possibly a north-south horizontal compression (D_2 event).

Contrary to previous hypotheses, the Round Lake Batholith is a magmatic body, derived via partial melting from a mafic parent (ensialic greenstone and/or sialic basement). The magma was diapirically mobilized, slightly differentiated, and intruded into the surrounding supracrustal country rocks.

RÉSUMÉ (ABRÉGÉ)

Le batholite de Round Lake, d'âge achéenne (2.688 Ga), recoupe les unités du super-groupe de l'Abitibi à l'extrémité sud de la ceinture volcanique de l'Abitibi (âgée d'environ 2.700 Ga) en Ontario.

Les unités lithologiques constituant le batholite sont regroupées en deux phases: "older" et "younger". La phase "older" est composée de tonalite-granodiorite avec foliation accentuée à directior est-ouest, surtout le long des bordures où elle est concordante avec la strucutre des volcanites encaissantes.

La phase "older" (64 à 77% SiO_2) a des profils en éléments majeurs confirmant une différenciation peu prononcée (diminuation en Al_2O_3, Fe_2O_{3TOTAL}, MgO, CaO et TiO_2; enrichissement en Na_2O? et K_2O. Ceci supporte l'évidence d'une gradation continuelle entre les unités tonalitiques et granodioritiques. La phase "younger" (66 à 73% SiO_2) change peut en éléments majeurs; les profils chimiques affirment aussi une différenciation mineure. Les profils sonts parallèles à ceux de la phase "older", suggérant une source magmatique commune.

Les diagrammes A-F-M, An-Ab-Or et Q-Ab-Or démontre que le batholite appartient à la série calco-alcaline avec affinité trondhjemitique-tonalitique.

D'après les éléments traces et terres rares, la phase "older" est mineralogiquement et chimiquement très homogène. Cette homogenéité parvient d'une differentiation chimique seulement d'un magma tonalitique. indiquée par les plagioclase zonés, et non d'une différenciation physique entre les cristaux de plagiolcase et le magma résiduel.

Le batholite a évolué en quatre étapes: (A) fusion partielle de la croûte volcanique et de gneiss tonalitiques-basiques (avec une contribution du manteau). (B) la fusion alimente un réservoir central de magma tonalitique, resultant en un diapir ascendant (la phase "older"). (C) "filter pressing" durant l'ascension du diapir magmatique produit un magma residuel granodioritique. (D) ascension des réservoirs subsidiaires de magma tonalitique (la phase "younger") au centre et à la périphérie du réservoir central.

Les structures d'emplacement de la phase "older" indique une intrusion par diapirisme (déformation D_1). Les structures regionalles consistent de plissements avec axes de plis orientés est-ouest, schistosité prononcée et foliation cataclastique.

Ces dernières structures sont liées à une compression nord-sud (deformation D_2).

En conclusion, et contrairement aux hypothèses d'origine déjà prononcées envers le batholite de Round Lake, le batholite est entièrement magmatique, dérivé via fusion partielle d'une source mafique provenant surtout de la croûte volcanique; sans différenciation particulière, et introduit par diapirisme dans la croûte supérieure recoupant les roches volcaniques encaissantes du super-groupe de l'Abitibi.

TABLE OF CONTENTS

LIST OF TABLES

LIST OF FIGURES

MAPS

LIST OF PLATES

CHAPTER I: INTRODUCTION

Location

The Round Lake Batholith of Archean age is located near the mining community of Kirkland Lake, at the southern extremity of the Ontario segment of the Abitibi Greenstone Belt in the Superior Structural Province (Figs. 1 and 2). The batholith occupies an area of approximately 3200 km^2 between latitudes $47^{o}40'N$ to $48^{o}05'N$ and longitudes $79^{o}50'W$ to $80^{o}55'W$. It is crudely elliptical, elongated in an east-west direction. The western part of the batholith is buried beneath a mantle of younger Proterozoic sedimentary rocks of the Huronian Supergroup.

Purpose

The Round Lake Batholith has previously been interpreted as a magmatic body differentiated from a mafic parent, intruded into, and thus younger than the surrounding supracrustal country rocks (Lawton, 1954). In contrast, Ridler (1972, 1976) suggested that the batholith, or parts of it, represents diapirically remobilized pre-greenstone sialic basement.

The present study was undertaken with the ultimate goal of resolving the ambiguity between the two contrasting interpretations by defining the lithological, chemical and structural characteristics of the Round Lake Batholith and, insofar as possible, determining its origin, mechanism of emplacement, and relationship to the tectonic evolution of the region.

Previous Investigations

Geological investigations of the batholith and surrounding area have been conducted intermittently for the past 100 years. McOuat (1872), Park (1904), Knight (1907), Collins (1913), Burrows and Hopkins (1922a, b), Cooke (1922), Bell (1929), Dyer (1936), Moorhouse (1944), Lawton (1954, 1959), Grant (1963), Lovell (1964, 1967, 1972), Moore (1966), Mackean (1968), McIlwaine (1978), Johns (1980), Johns et al. (1981a, b, c), delineated the batholith's perimeter and gave some information on the internal character of the body.

Lawton (1954), in the only detailed descriptive study of the batholith, determined that it is a composite intrusion consisting of quartz diorite and hornblende granite as the two major phases. Lawton's field mapping was confined to the eastern part of the body and phase relationships on the whole were not thoroughly determined. Since Lawton's work, the batholith has been the subject of numerous special studies, from its incorporation in regional stratigraphic correlation and synthesis (Ridler, 1972, 1975, 1976; Jensen, 1978; Goodwin, 1979), in geochronological (Aldrich and Wetherill, 1960; Lowdon et al., 1963; Purdy and York, 1968; R.K. Wanless; pers. comm., 1979; Stevens et al., 1982) and metamorphic (Jolly, 1974, 1978, 1980) studies, and in gravimetric surveys (Gibb and van Boeckel, 1970; Gupta and Wadge, 1977, 1979).

Field and laboratory methods

Field work for the Round Lake Batholith project was carried out over a cumulative period of 9 weeks during the summers of 1979 and 1980. Traverses conducted within the 3200 km^2 batholith and surrounding area were restricted to roads (Highways 11, 65, 66, 112, 560, 564, and 573; secondary concession, lot, access, mine and logging roads), railroads (Ontario Northland Railway along the Swastika-Boston Creek-Englehart corridor; abandoned line near Charlton), rivers (Montreal River and its affiliated lakes; Englehart River), trails, and areas of major outcrops, particularly along internal and external contact zones.

Geological information was compiled on 1:50,000 air photos, and was subsequently transferred to topographic base maps of the same scale. Physiographic and other pertinent geographical features are summarized in Lawton (1954).

During field mapping, more than 400 hand specimens were collected, from which 73 thin sections were cut from the Round Lake Batholith older and younger phases (includes 4 amphibolitic xenoliths), and 17 from supracrustal rocks located at different external contact zones. Polished thin sections were also cut to determine magnetite-ilmenite-hematite relationships from each of the major batholith rock types (older phase tonalite, granodiorite, and hornblende tonalite; younger phase granodiorite-tonalite).

Rock nomenclature on the Round Lake Batholith map sheet (Map 1) is basically a field classification. Modal compositions

(from point counting) of selected thin sections (57) were plotted in Streckeisen's (1976) ternary diagram for plutonic rocks (Quartz-Alkali Feldspar-Plagioclase), and the corresponding nomenclature was used in conjunction with the major-element chemical scheme for tonalite/trondhjemite proposed by Barker (1979).

Fresh, 1 to 2 kg samples were used in major and trace element analyses. Most analyses were performed at the Department of Geology, University of Ottawa. Analyses from the batholith (and surrounding country rocks) were also obtained from the Geological Survey of Canada and Ontario Geological Survey. Additional country rock analyses were also compiled from the literature (Goodwin, 1979). A compilation of 84 samples (major and selected trace elements) from 16 Archean tonalite/trondhjemite type localities was also used for comparative purposes. Breakdown of analyses for the major rock types in the study area and laboratory facilities used is given as follows:

Rock Units	University of Ottawa	Geological Survey of Canada	Ontario Geological Survey
Round Lake Batholith	48	16	24
Supracrustal country rocks	4	67 (50 from Goodwin, 1979)	Nil

Analyses performed at the University of Ottawa (both major and trace elements) were carried out on a Philips 1410 automated X-ray fluorescence unit. Determinations were made on fused disks (consisting of 1.5 grams of powdered sample, 4.5 grams of $Li_2B_4O_7$ and 0.5 grams of Li_2CO_3) using a Cr tube and data reduction using alpha coefficients of De Jongh (1973). Based on duplicates and the results of runs on the standard SY-2 (Abbey, 1977), the precision[1] of amounts recorded may be taken as follows: SiO_2, Al_2O_3, $Fe_2O_{3(total)}$, K_2O: $\pm$ 2%; TiO_2: $\pm$ 3%; Na_2O, MgO, CaO: $\pm$ 4%; P_2O_5, MnO, S: $\pm$ 10%; Ba: $\pm$ 50% for the the range 10 to 40 ppm and $\pm$ 10% for values greater than 40 ppm; Sr: $\pm$ 10% (values greater than 40 ppm); Zr: $\pm$ 50% for the range 20 to 50 ppm and $\pm$ 15% for the range 50 to 500 ppm; Rb, Zn: $\pm$ 100% for values less than 20 ppm, $\pm$ 50% for the range 20 to 40 ppm, and $\pm$ 10% for values greater than 40 ppm; Cr: $\pm$ 100% for values less than 20 ppm, $\pm$ 50% for the range 20 to 50 ppm, and $\pm$ 15% for the range 50 to 500 ppm; Ni: $\pm$ 100% for values less than 40 ppm, $\pm$ 50% for the range 40 to 100 ppm, and $\pm$ 10% for values greater than 100 ppm.

Rare earth elements, Hf, Sc and Th were determined by instrumental neutron activation analyses based on the method described by Gordon et al. (1968) and Gibson and Jagam (1980). A total of 8 analyses from the Round Lake Batholith (older phase: 6; younger phase: 1; older phase hornblende tonalite: 1) were made at the University of Ottawa. Powdered samples were

irradiated (at the McMaster University Nuclear Reactor) for approximately 6 h at a flux of 10^{12} n/cm^2/s, and counted using an Aptec 2 cm^2 Ge planar detector. G-2 was the standard used (Flanagan, 1973). Based on duplicate and standard results, the precision of amounts recorded may be taken as follows: La, Ce, Sm, Eu, Yb, Th, Sc, Hf: $\pm$ 5%; Tb, Lu: $\pm$ 10%.

Harker (elements vs SiO_2) variation diagrams were computer generated using an available graph program: SPSS SCATTERGRAM (Nie et al., 1975).

Acknowledgments

I am indebted to Dr. K.D. Card, Geological Survey of Canada, for suggesting and initiating the Round Lake Batholith project. His Superior Province expertise and logistical and continued moral support simplified the task of mapping the batholith, and provided a strong incentive during the writing stages. I would also like to thank Dr. D.D. Hogarth for supervising the project, and his patience during the completion. Thanks are also extended to Drs. W.K. Fyson, R. Kretz, and Calvin Pride (all from the University of Ottawa) for discussions on Archean tectonics, migmatites, and tonalite/trondhjemite chemistry. Dr. Pride was instrumental in increasing the author's knowledge of geochemistry and trace element modelling.

Field assistants were D. Waldron (1979), J.R. Buchanan, D. Card, and P. Henshaw (all 1980); their contribution is gratefully acknowledged.

Discussion with Dr. L.S. Jensen, G.W. Johns (both from the Ontario Geological Survey, Toronto), H.L. Lovell and staff (Resident Geologist Office, Ministry of Natural Resources, Kirkland Lake, Ontario), Dr. D.R. Pyke (consultant), Dr. D. Paktunç (University of Ottawa), and H. Dillon-Leitch (Carleton University) were very helpful. Dr. Pyke also provided chemical analyses from the central part of the batholith (Ontario Geological Survey samples).

Major and trace element analyses were obtained by R. Hartree (University of Ottawa), Dr. C. Pride, and J.L. Bouvier (Geological Survey of Canada). R. Hartree, Dr. D. Paktunc and Dr. B. McQuade faciliated statistical processing of the data. Thin sections were made by A. Whitehead (Geological Survey of Canada), Robert Taylor (University of Ottawa), and Ross Taylor (Carleton University). K.C. Bencik (Geological Survey of Canada) drafted figures (1 to 28); whereas M. Steingass drafted the Round Lake Batholith-Map 1. Hand specimen photographs were taken by E. Hearn. Photomicrographs and drafting of figures benefited from advice given by E. Hearn (University of Ottawa).

Special thanks are extended to the owners of Northern Lights Campground (Dane, Ontario), Penassi Lake Lodge (on the Montreal River near Gowganda, Ontario), and particularly to Jim Reed of Reed's Cottages (Kenogami Lake, Ontario) for their hospitality. T. Wilson and K. Jones of Long Point Airways

provided float-plane support in 1980.

The chapter on Economic Geology has greatly benefited from the contributions of T. Pantalone, H. Laskowski and D. Hurd.

Field mapping during the 1980 season and laboratory research were funded through EMR and NSERC grants respectively to Dr. D.D. Hogarth.

The text was typed by B. Cox and M. MacLeod.

CHAPTER II: REGIONAL GEOLOGICAL SETTING OF THE ROUND LAKE BATHOLITH

The Archean Superior Province of northern Ontario and adjacent Quebec consists of alternating, easterly trending geological subprovinces or "megabelts" (Stockwell, 1970; Goodwin, 1972, 1978; Douglas, 1979). The subprovinces display contrasting structural trends and styles, grades of metamorphism, and lithologies.

Rocks of the Wawa-Abitibi, Wabigoon, Uchi and Gods Lake (Sachigo) Subprovinces comprise low-rank metamorphic volcanic/plutonic assemblages, whereas the Pontiac, Quetico, English River and Berens Subprovinces (Fig. 1) are characterized by high-rank metamorphic sedimentary sequences.

The Abitibi Greenstone Belt (Fig. 2) is located in the eastern part of the Wawa-Abitibi Subprovince; it is bounded on the east by the Grenville Front, the zone of contact between the Superior and Grenville Provinces, and to the west by the Kapuskasing structure, a northeast trending fault zone and high-rank metamorphic gneiss (granulite facies) that cuts sharply across the regional east-west trend of the major structural subprovinces. The Abitibi Belt, the largest and most continuous greenstone belt of the Canadian Shield (Goodwin and Ridler, 1970), extends some 700 km from the east to the west and is approximately 200 km wide. It consists of repetitive volcanic cycles ranging from ultramafic to felsic compositions, clastic sediments intercalated with the volcanic

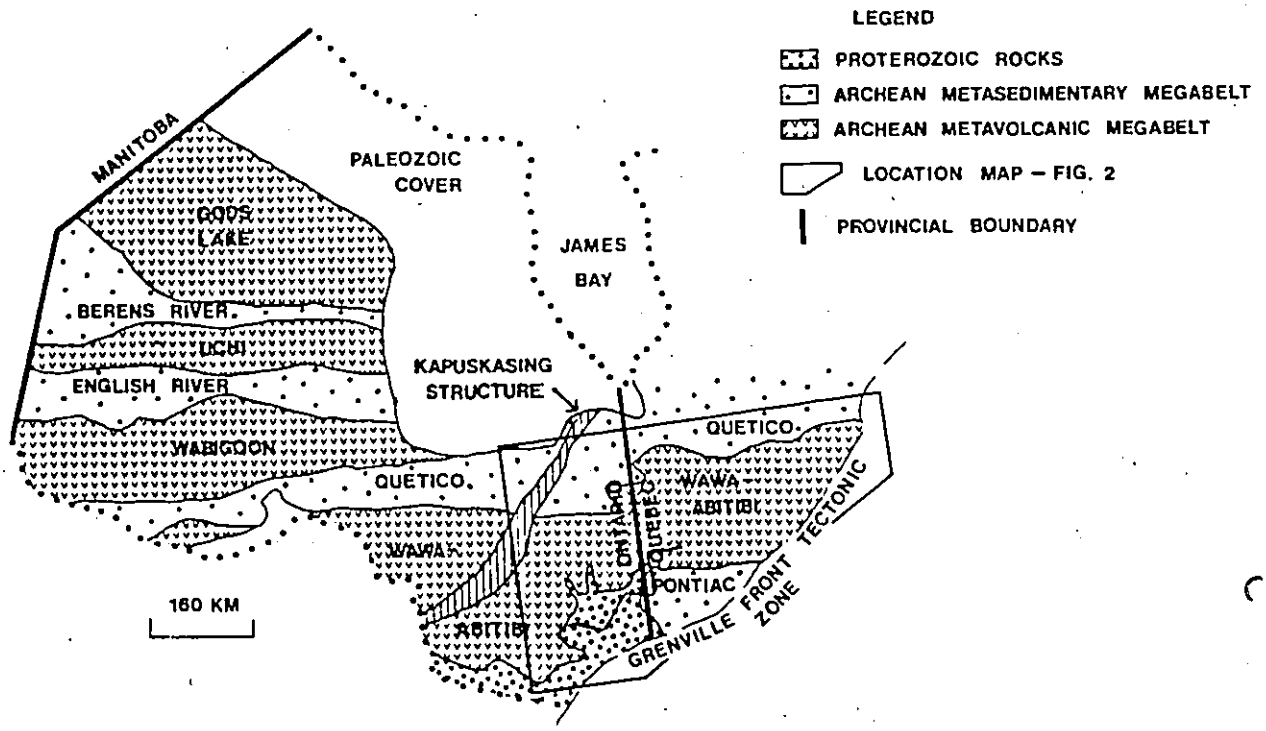

Fig. 1. Subdivision of the Superior Province of Northern Ontario and adjacent Quebec (Douglas, 1979).

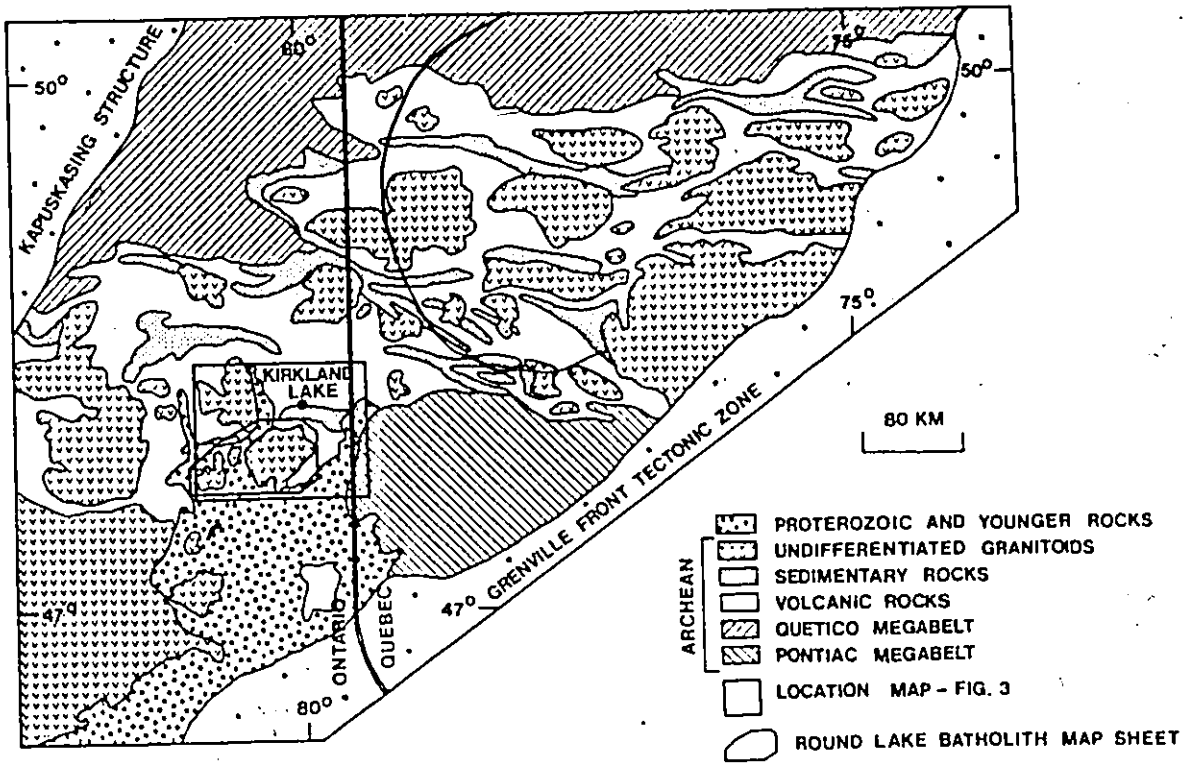

Fig. 2. Abitibi Greenstone Belt (modified from Jolly, 1978).

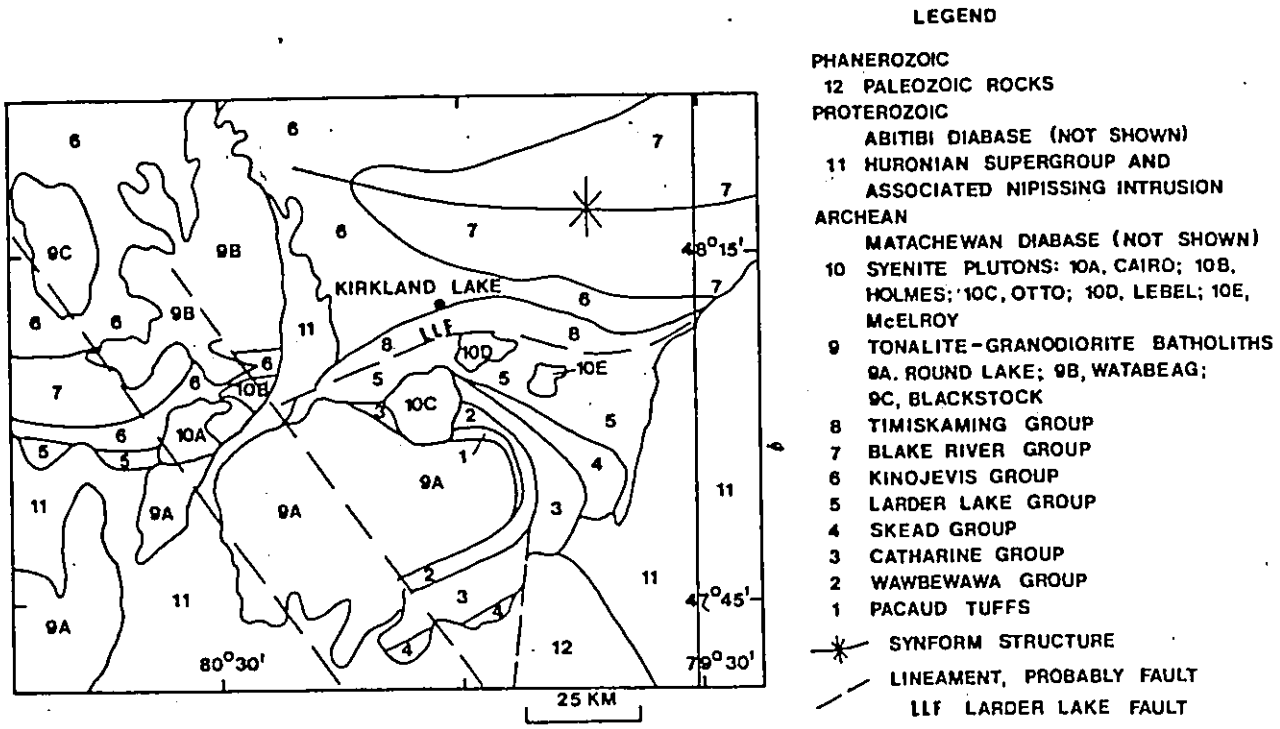

Fig. 3. Geological map of part of the Ontario segment of the Abitibi Greenstone Belt (modified from Jensen, 1980).

rocks, and in narrow, fault-bounded zones, ultramafic to mafic intrusions and granitoid complexes, all of which are represented in the study area.

The dominant structural style of the belt reflects the presence of local granitoid bodies with concordant external structures, and east-west trending isoclinal folds of regional extent (Goodwin and Ridler, 1970; Goodwin, 1979). The south trending homoclinal, easterly facing supracrustal succession, located about the eastern margin of the Round Lake Batholith, is a typical example of the former (Fig. 3). The homoclinal succession is part of the southern limb of a major east-west trending synclinorium transecting the central portion of the Ontario segment of the Abitibi Belt (Jensen, 1978).

Two major metamorphic episodes (burial and contact metamorphism) defining five metamorphic isograds (diagenesis to greenschist types with minor amphibolite facies) have been outlined in the central part of the belt, including the Round Lake Batholith area (Jolly, 1974, 1978, 1980). The metamorphic isograds show a distinct relationship between the amphibolite (and greenschist) facies metamorphism and granitoid intrusions, whereas the widest, and probably thickest part of the supracrustal pile, located north of Kirkland Lake, is of subgreenschist (prehnite/pumpellyite) facies metamorphism, and is barren of granitoid intrusions (Fig. 4). Jolly (1978) suggested that there was a gradual progression from an early

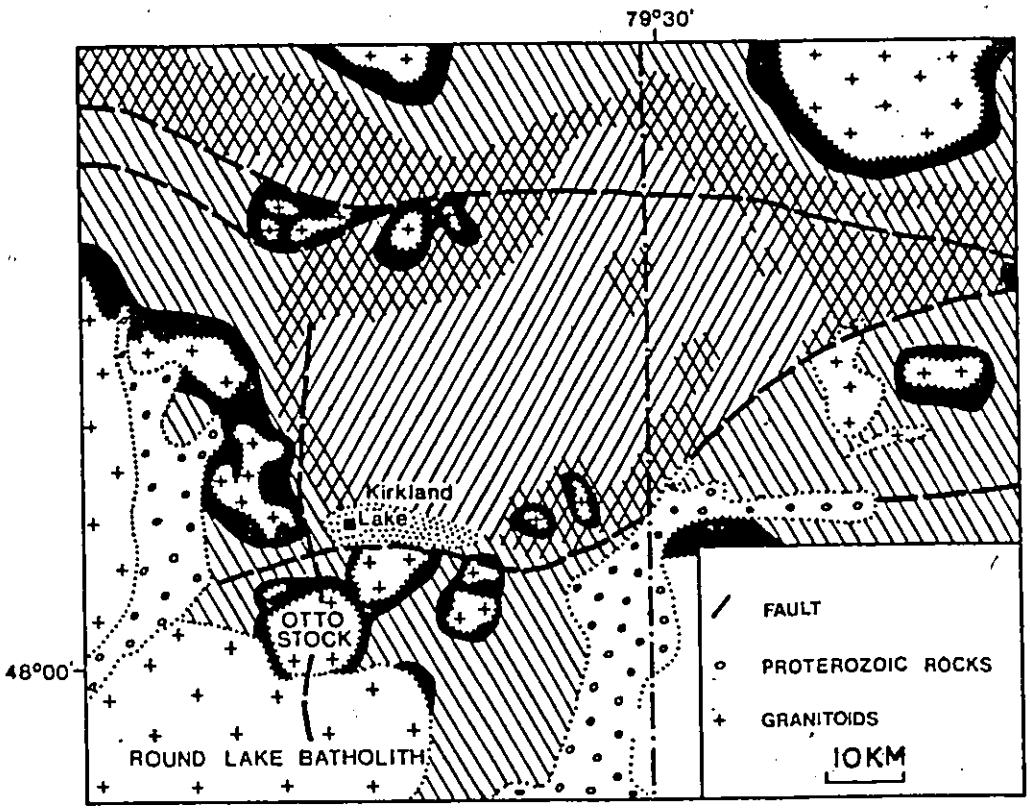

Fig. 4. Distribution of metamorphic facies in the southwestern part of the Abitibi Greenstone Belt (taken from Jolly, 1980).
Legend: ▬ Amphibolite Facies; \\\\\ Greenschist Facies; XXXXX Greenschist over Prehnite-Pumpellyite; ///// Prehnite-Pumpellyite Facies; ⋯⋯ Unmetamorphosed.

low-grade burial metamorphism in the belt, to a later high-grade contact metamorphism produced by the emplacement of granitoid complexes.

Rock units of the region can be divided into pre-batholithic, batholitic and post-batholithic sequences encompassing igneous and sedimentary rocks of Archean, Proterozoic and Phanerozoic ages.

Pre-batholithic rocks comprise a succession of supracrustal volcanic and sedimentary units termed the Abitibi Supergroup (Table 1). Jensen (1978, 1980), in a chemostratigraphic study of the Kirkland Lake area, subdivided the succession into three chemically distinct cycles of volcanic strata (Fig. 3). The first two cycles are subalkalic, each with a basal komatiitic sequence (Wawbewawa and Larder Lake Groups), a middle tholeiitic sequence (Catharine and Kinojevis Groups), and an upper calc-alkaline sequence (Skead and Blake River Groups). The third and youngest cycle, Timiskaming Group, is preserved along the Larder Lake Fault, and is characterized by shallow water sediments and alkalic volcanic rocks. The base of the first cycle overlies calc-alkalic tuffs, Pacaud Tuffs (Ridler, 1972), believed to be part of an earlier cycle (Jensen, 1978), which crops out along the northeastern margin of the Round Lake Batholith.

The supracrustal succession has been intruded by a number of granodioritic and tonalitic batholiths (Round Lake, Watabeag

Table 1. General Table of Formations for the Round Lake Batholith area, Timiskaming District, Ontario. Stratigraphy modified from Pyke et al., 1973; Jensen, 1978, 1980; Pyke, 1980

EON	ERA	GROUP, FORMATION, INTRUSIVE UNIT, DYKE SWARM, STOCK BATHOLITH	LITHOLOGY
PHANEROZOIC	PALEOZOIC	Guiges, Bucke, Thornloe, Dawson Point Formations	Chemical and clastic sedimentary rocks
		UNCONFORMITY	
	APHEBIAN or HELIKIAN	Abitibi Dyke Swarm	Diabase
		INTRUSIVE CONTACT	
PROTEROZOIC		Nipissing Diabase	Gabbro, diabase
		INTRUSIVE CONTACT	
	APHEBIAN	Huronian Supergroup Cobalt Group, Gowganda Lorrain Formations	Clastic sedimentary rocks
		UNCONFORMITY	
		Matachewan Dyke Swarm	Diabase
		INTRUSIVE CONTACT	
		Cairo, Holmes, Otto, Lebel, McElroy Stocks	Syenite
		INTRUSIVE CONTACT	
		ROUND LAKE, Watabeag, Batholiths	Tonalite, granodiorite
		INTRUSIVE CONTACT	
ARCHEAN	Abitibi Supergroup	Timiskaming Group	Trachyte lavas, clastic sedimentary rocks
		UNCONFORMITY	
		Blake River Group (not in study area)	Pyroclastic rocks, massive lavas of mafic to felsic composition
		Kinojevis Group	Pillowed and massive lavas of mafic to felsic composition, volcaniclastic sedimentary rocks
		Larder Lake Group	Pillowed to massive lavas of ultramafic to mafic composition, clastic sedimentary and felsic pyroclastic rocks
		DISCONFORMITY	
		Skead Group	Pyroclastic rocks, massive lavas of mafic to felsic composition
		Catharine Group	Pillowed and massive lavas of mafic composition, volcaniclastic sedimentary rocks
		Wawbewawa Group	Pillowed and massive lavas of ultramafic to mafic composition, minor felsic pyroclastic rocks
		Pacaud Tuffs	Volcaniclastic sedimentary rocks, pillowed and massive lavas of mafic composition

and Blackstock Batholiths) encompassing the batholithic episode, and by syenitic plutons (Cairo, Holmes, Otto, Lebel and McElroy Stocks). Field relationships indicate the batholiths are all about the same age and are older than the syenitic plutons (K.D. Card, pers. comm., 1981).

Post-batholithic rocks, in addition to the syenitic plutons, include north trending tholeiitic diabase dykes of the Matachewan Swarm which intrude the batholithic and pre-batholitic sequences. Emplacement of the Matachewan dykes was followed by deposition of Proterozoic clastic sedimentary strata, the Gowganda and Lorrain Formations of the Huronian Supergroup, which with associated Nipissing Diabase intrusions, extend into the map area from the south. The last major Precambrian igneous event was the emplacement of northeast trending alkali olivine diabase dykes of the Abitibi Swarm.

Several major north-northwest trending faults, part of the Timiskaming Fault System (Lovell and Caine, 1970) transect the central part of the study area. Normal movements on these faults resulted in the preservation of Ordovician/Silurian sedimentary rocks (Guiges, Bucke, Thornloe and Dawson Point Formations) in the southeastern part of the map area.

CHAPTER III: GEOLOGY OF THE ROUND LAKE BATHOLITH

1) Country rocks surrounding the batholith

Pre-batholithic supracrustal rocks surrounding the Round Lake Batholith consist of the Pacaud Tuffs (map-unit 1), the Wawbewawa (map-unit 2), Catharine (map-unit 3), Skead (map-unit 4), Larder Lake (map-unit 5), Kinojevis (map-unit 6), and Timiskaming (map-unit 7) Groups (map 1 in pocket).

The Pacaud Tuffs extend along the periphery of the batholith from Round Lake to Wawbewawa, a distance of approximately 25 km. The unit has a maximum surface outcrop width of 2500 m, but averages less than 500 m. It is composed of thinly bedded (on a scale of mm to a few cm), aphanitic to fine grained, mafic to intermediate tuffaceous greywacke (Lawton, 1959) interbedded with iron formation, chert, pillowed basalt, conglomerate with mafic volcanic, iron formation and felsic porphyry fragments, and finally, intruded by gabbroic sills and porphyritic dykes of felsic composition (Lawton, 1959; Grant, 1963).

The Wawbewawa Group (Jensen, 1978) has an exposed maximum width of 4000 m, and consists of ultramafic volcanic flows with olivine and pyroxene spinifex textures and polysutured flows, pillowed and massive basalts, minor tuff layers, and gabbro/peridotite sill and syenitic dykes (Moorhouse, 1944; Lawton, 1959; Grant, 1963; Jensen, 1978; Johns, 1980). Lawton (1959) believed that this mafic sequence was gradational with the

underlying Pacaud Tuffs.

Conformably overlying the Wawbewawa Group is a sequence, some 4500 m wide along the southwest, of fine grained pillowed basalts interbedded with featureless massive mafic volcanic flows, thinly bedded tuffaceous argillite, and gabbro/ peridotite sills and dykes (Moorhouse, 1944; Lawton, 1959; Grant, 1963: Jensen, 1978; McIlwaine, 1978; Johns, 1980) belonging to the Catharine Group (Jensen, 1978). The succesion is conformably overlain by the Skead Group (Jensen, 1978) consisting of at least 4500 m of mafic to felsic massive lavas and coarse-to fine-grained pyroclastic rocks, iron formation, chert and quartz-feldspar (rhyolite) porphyry bodies (Moorhouse, 1944; Lawton, 1959; Grant, 1963; Jensen, 1978; McIlwaine, 1978; Johns, 1980), the largest of which is exposed south of the Cross Lake Fault at the contact between the Catharine and Skead Groups (Johns, 1980).

Disconformably overlying the Skead and Catharine Groups is the Larder Lake Group (Jensen, 1978) which has a minimum exposed width of 6000 m south of the Larder Lake Fault, and extends in an east-west direction across the northern portion of the map area. The Larder Lake Group consists of massive, ultramafic to mafic lava flows, pillowed basalt, turbidite/ greywacke, conglomerate, iron formation, chert, felsic tuff, and gabbroic to syenitic intrusions (Abraham, 1951; Lawton, 1959; Lovell, 1964, 1967, 1972; Moore, 1966; Jensen, 1978,

1980).

The Kinojevis Group conformably overlies the Larder Lake Group (Jensen, 1978), and is exposed in the northwest portion of the map area. The outlier is predominantly composed of massive and pillowed basalts with minor intermediate to felsic lava flows and volcaniclastic sediments (Lovell, 1967).

A sliver of Timiskaming Group (see Cooke and Moorhouse, 1969, for a summary of the unit) clastic sedimentary rocks with trachyte flows crops out at the southern and eastern ends of Kenogami Lake, and is the youngest unit of Abitibi Supergroup rocks exposed in the Round Lake Batholith area (Jensen, 1978, 1980).

The Otto Stock (map-unit 10), largest of a suite of syenitic intrusions, is the most significant post-batholithic unit in the map area. It consists of a quartz syenite (map-unit 10C) core, a mafic (contaminated) porphyritic syenite (map-unit 10E) with a nepheline syenite (map-unit 10D) subphase forming a generally continuous peripheral zone, and finally, equigranular to porphyritic syenite (map-units 10A and 10F) and diorite (map-unit 10B) forming the remainder of the intrusion. The age and tectonic evolution of the stock have been, and still are, controversial because of inconsistencies between field relationships, metamorphism and geochronology.

Jolly (1978) indicated that the Otto Stock contact aureole overlapped all lithologies and structures in the area, with the

exception of the Round Lake Batholith. The aureole containing bluish-green amphiboles rimmed by faint blush actinolite which Jolly (1978) interpreted to have been developed by the later low-grade metamorphism accompanying the emplacement of the batholith. However, field evidence (based on one outcrop of the stock-batholith contact), implies that the stock is intrusive into and younger than the batholith, since xenoliths of the latter are found in an equigranular matrix of reddish syenite (Plate 1, Fig. 1) contrary to the metamorphic interpretation.

The age of the stock is interpreted to be late Archean or early Proterozoic. Matachewan diabase dykes, dated at 2.633 Ga (Rb-Sr whole rock method; Gates and Hurley, 1973) are known to crosscut other syenitic intrusions in the area (see maps by Moore, 1966; Lovell, 1967; compilation map by Pyke et al., 1973), and according to Ridler (1977), dykes of the swarm crosscut the northern part of the Otto Stock. In addition, the Huronian Supergroup Gowganda Formation, of early Aphebian age (Fairbairn et al., 1969), at Kenogami Lake, contains syenite cobbles possibly derived from the Otto Stock (Lovell, 1972). These observations are also incompatible with Rb-Sr whole-rock ages of 1.730 and 2.160 Ga (Purdy and York, 1968; Bell and Blenkinsop, 1976) on the stock, but certainly attest to a minimum age of early Proterozoic for the intrusion.

Plate 1, Fig. 1

Tonalite xenolith (T) from the Round Lake Batholith in a matrix of reddish syenite (S) from the Otto Stock. Locality, 4 km southwest of Round Lake. Pen is 15 cm long.

PLATE I

1

2) Description of the Round Lake Batholith

The Round Lake Batholith is a composite body consisting of an older cataclastically foliated, in places marginally gneissic, biotite (-hornblende) tonalite (-granodiorite) phase (map-unit 8), compositionally variable from tonalite and quartz diorite to granodiorite and monzodiorite, and a younger unfoliated to weakly foliated hornblende (-biotite) granodiorite-tonalite (map-unit 9 - Indian Chute, Hope Lake and Crooked Creek Stocks), with minor quartz monzodiorite. The younger granodiorite-tonalite contains xenoliths of the older phase and surrounding country rocks. Agmatite zones along the margin of, and within the batholith, contain amphibolite fragments permeated by leucocratic and unfoliated hornblende tonalite. The hornblende tonalite constitutes a major subunit (map-unit 8C) along the western margin of the batholith.

Modal compositions of the batholithic units are given in Table 2 and shown in Figure 5 (locations in Figure 9).

Planar fabrics in both phases are generally east-west trending, except at the eastern periphery of the older phase, where they curve parallel to the batholith outline. A similar curvature in planar structures along the western periphery is not observed. Other variations in the foliation direction result from local shearing along fault/shear structures.

Batholithic rocks vary from medium-to coarse-grained.

Table 2. Modal compositions from the Round Lake Batholith phases.

	Map-unit: 8A - Tonalite																		Agmatite gneiss				Map-unit: 8B - Granodiorite							
Minerals/Sample No.	59	69	70	125	136	140	174	195A	201A	299	305	338	367	376	391	392	394	407	14	15	311	362	21	26	31	88	156	259[3]	260[3]	381B
Plagioclase	42[1]	55	54	66	62	59	58	67	52	70	61	75	77	57	52	77	77	71	50	53	46	70	38	63	62	58	55	40	65?	60
Quartz	28	27	27	20	22	26	31	22	35	21	27	15	11	16	22	13	7.5	20	37	29	25	13	29	27	22	26	24	35	25?	17
Microline				3.5	7.5	6	tr	2.5		1.5								tr					14	1	5	3.5	6.5	15?	7	19
Mafics																												10	10	
Hornblende		7	4.5										2		12		tr				3.5							?		1.5
Biotite		5	5.5	6	5	6	3	6.5	10	5	5.5	7	6	20	9	8.5	x		6	7.5	11	10	1	2	3	3	x		x	x
Secondary Minerals																														
Chlorite	12	x	x		x	x	x	x	x	x	x	x	x	x		x	10	6	x	x	x	x	x	x	x	x	3.5			1.5
Epidote	15	5	6	3.5	1.5	2	4	1	2.5	1	2	1	2	5	1.5	1	2	1	3	6	13	3.5	6	4	3	3.5	5.5		x	x
Muscovite	3	x	2	x	1.5	x	3.5	1	x	1	4	1	x	x	x	x	2	x	3.5	4	x	3	12	3	5	5	5.5			x
Carbonate	x[2]												x										x	x	x					
Accessories																														
Opaques	tr	tr	tr	tr	tr	tr	tr	tr	tr	tr	tr	tr	1	1	2	tr	1	1	tr	tr	1	tr	tr		tr	tr	tr	x	x	tr
Apatite	tr	tr	tr		tr	tr	tr	tr	tr	tr	tr	tr	tr	tr	1.5	tr	tr	tr	tr	tr	tr	tr	tr	tr	tr	tr	tr			tr
Sphene	tr	tr	tr	tr		tr			tr		tr	tr	tr	tr				tr		tr	tr	tr	tr	tr	tr	tr				tr
Allanite		tr																							tr					tr
Zircon												?							tr		tr									
Granoblastic Material																														

Notes: [1] All numerical values given in volume percent, based on a minimum 1 000 counts per thin section.

[2] Detected but not counted.

[3] Modes visually extimated from hand specimen (± 5%).

Table 2. - continued

Map-unit: 8C - Hornblende Tonalite									Dykes			Map-units: 8D,E - Cataclastic granodiorite-tonalite								Map-unit: 9 - Granodiorite, Tonalite											Xenoliths		
165	177	204A	318	357	365	374	388	390	233C	364	363	89	151	190B	204C	228	267[3]	270[3]	271[3]	35	45	123	182	186[3]	194[3]	205	353	373	393	404	37	327	329B
43	48	62	54	47	54	56	58	55	45?	44	50	39	49	37	45	42	50	60?	50	58	59	48	52	75	70	54	63	51	52	64		39	36
17	12	11	24	17	21	18	12	16	35?	26	40	32	27	25	33	28	30	25?	20?	19	21	19	27	15	20	22	24	25	31	14		2	1
			1.5		tr		2.5			26	x	8	1	12	tr		10	10	20	10	2	8	5.5	?	7	8.5	4.5	9	6	13			
									20		10						10	10	10?					10	10								
20	28	23	8	24	19	11	15	18	x											8.5	15	18	12	x	x	10	4	11	3.5	3	70	53	56
8		1					x	x		1.5	x	x	5		x	x		x								3		x	3			
x	4.5	x	7.5	7	1.5	8	3.5	4.5	x	x		x	x		5	2		x		x	x	3.5	1.5			x	2.5	3.5	x	4	x	3	4
7	4	tr	3.5	3	2	5	7	2.5	x	x	x	6.5	8	2.5	4	7	x			3	1	x	1			x	x	x	1	x	x	2	2
3	3	x	x	x	1	x	x	1.5		1.5		4.5	2	4.5	2	3.5	x			x	x	x	x			x	x	x	x	x	30	x	x
x		7	x				1.5	x					x			x					x								x			
1.5	tr	1	1	tr	tr	1	tr	tr	x		x	tr	1	tr	tr	tr	x			1	1	1	tr		x	tr	tr	tr	1	1	x		
tr	tr	1.5	tr	1	tr	tr	tr	1	x	tr	x	tr	tr		tr	tr				tr	tr	tr	tr			1	tr	tr	tr	tr		tr	tr
			tr	tr	1.5	tr	tr	1		tr			tr		7	tr				tr	tr	2	1			1	1	tr	2.5	1		tr	1
			tr					tr																									
								tr													tr	tr	tr			tr							
												9	6	19	10	17																	

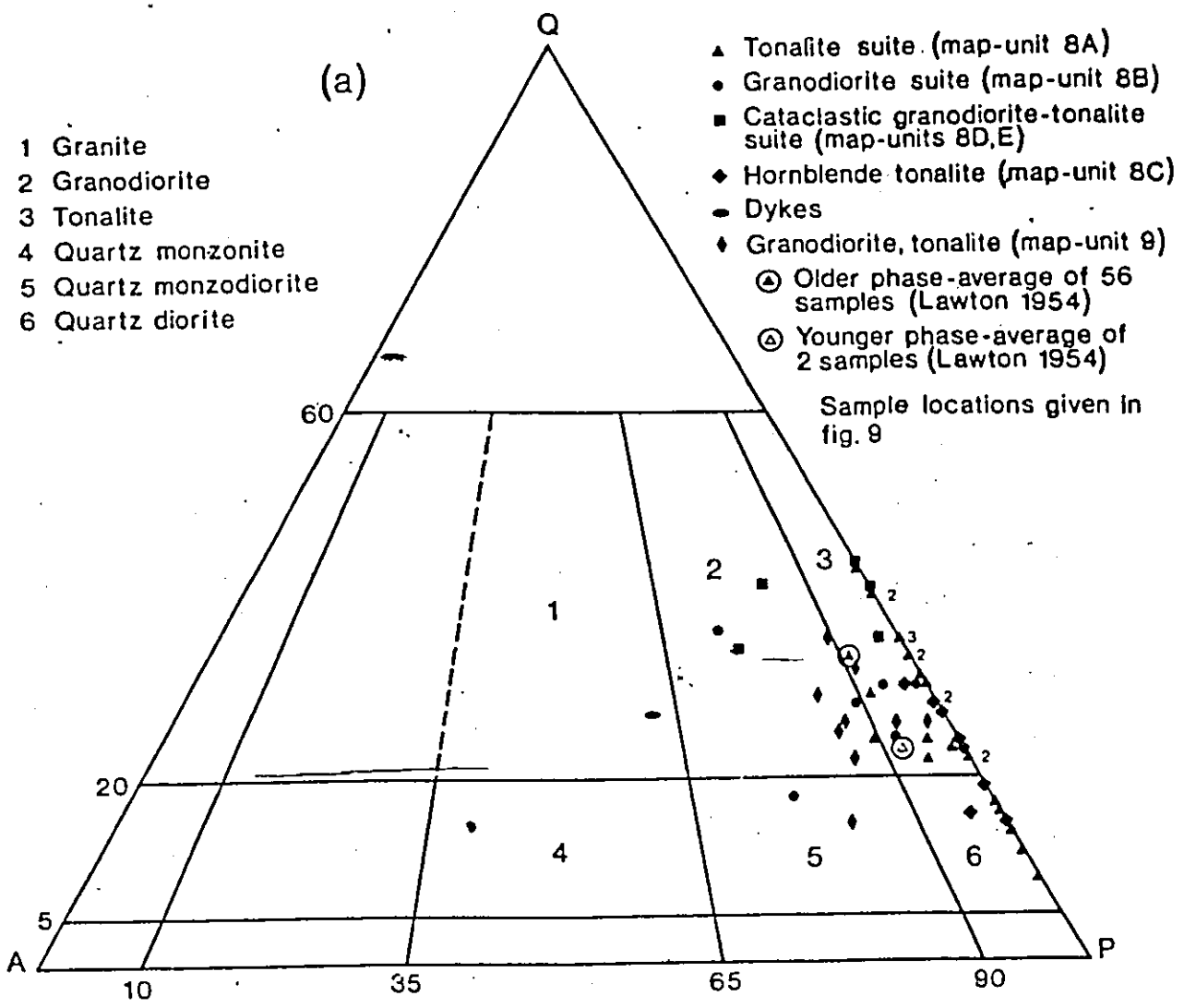

Fig. 5. Modal mineralogy of the Round Lake Batholith. (a) Q (quartz) - A (alkali feldspar) - P (plagioclase) modal diagram. (b) Q (quartz) - F (feldspar) - M (mafics) modal diagram. Plutonic rock names from Streckeisen (1976).

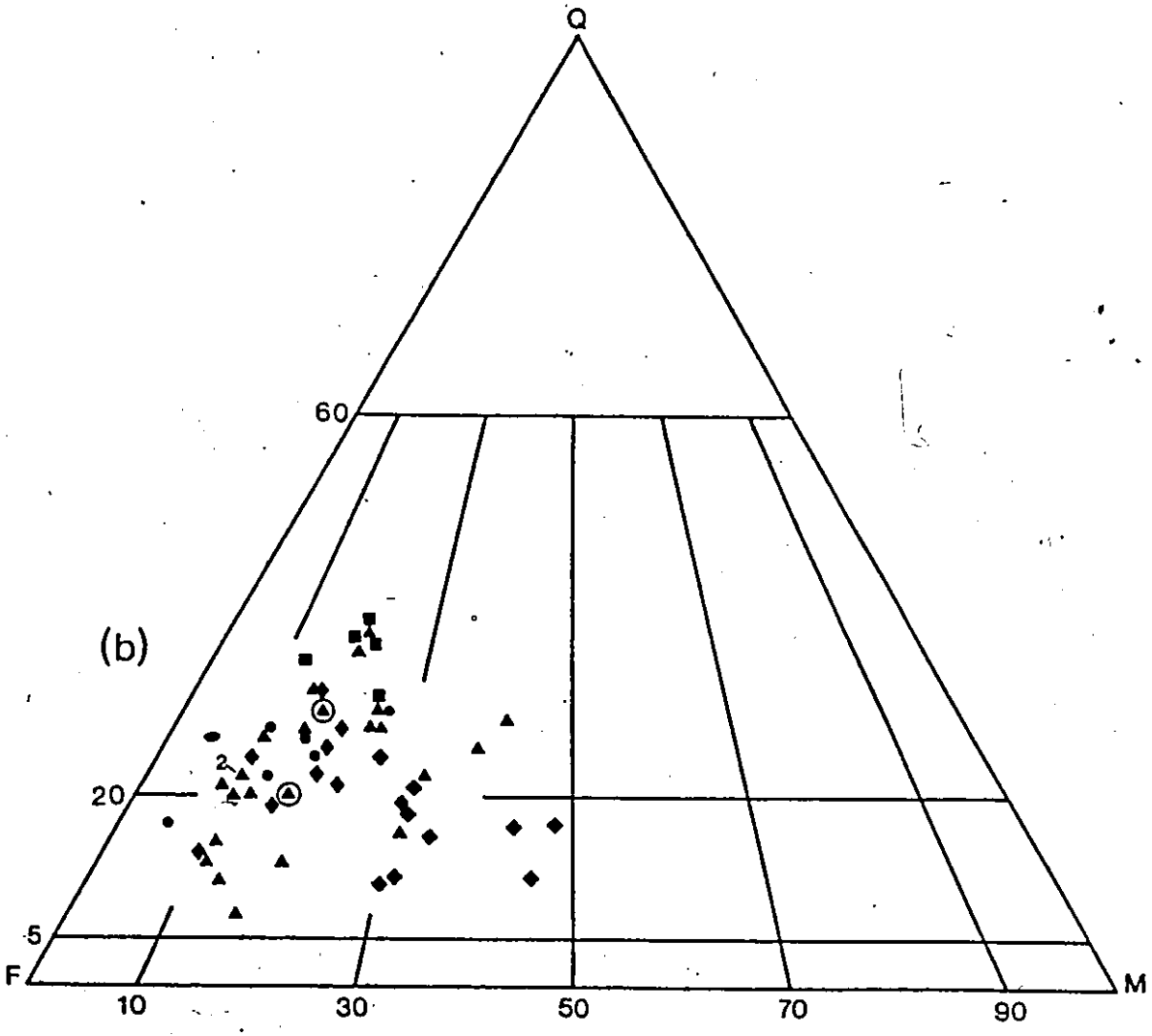
Q
60
(b)
20
5
F
10
30
50
70
90
M

The major minerals include plagioclase, quartz, microcline, biotite and hornblende. The principal opaque minerals are pyrite, ilmenite, magnetite and hematite. Ilmenite is most commonly an exsolution product of magnetite along octahedral cleavage planes. Hematite can occur as single crystals and as replacement of magnetite along crystal edges and cleavage planes. Apatite, allanite, sphene and zircon are the most common primary accessory minerals, whereas epidote, chlorite, muscovite and carbonate are the most abundant secondary alteration products.

Plagioclase is mainly albite-oligoclase, although andesine was reported in the older phase by Lawton (1954). Plagioclase crystals are tabular, average less than 3 mm in length, and are locally saussuritized to sericite and epidote in their cores. Crystals are commonly zoned with older and younger phase plagioclase cores averaging oligoclase, whereas rims are generally more albitic.

Clear quartz occurs as elongated to rounded, serrated aggregates with undulose extinction, interstitial to and overgrown on plagioclase. Microcline occurs mainly as anhedral, slightly turbid interstitial grains. It is commonly poikiloblastic (or megacrystic), with grains greater than 1 cm enclosing plagioclase and quartz. Biotite, partly and wholly altered to chlorite, occurs as disseminated and discrete

corroded flakes, and as aggregates with hornblende. Hornblende is generally found as euhedral to subhedral overgrowths on biotite/chlorite flakes, plagioclase and microcline, in some cases suggesting late crystallization. Excluding saussuritization, epidote is locally abundant, appearing as single and aggregate crystals associated with biotite, hornblende, biotite and hornblende, and allanite.

A) Older phase: tonalite (-granodiorite) (map-unit 8)

The tonalite unit (map-unit 8A), the most widespread batholithic unit (map 1 in pocket), varies compositionally from quartz diorite to tonalite.

It is weakly to moderately foliated greyish rock with a steeply dipping east-west trending cataclastic foliation defined by the orientation of mafic minerals and granulated feldspar-quartz fabric (mortar texture: Plate II, Figs. 1, 2 and 3). Where the cataclastic foliation is not well defined, and the rock is more massive, the morphology of plagioclase remains unchanged (i.e., subhedral to anhedral shapes) due to secondary overgrowths of quartz. In areas of moderate cataclasis, vein-like aggregates averaging less than 1 cm in width of recrystallized quartz ($\pm$ feldspar) are developed. These aggregates are accompanied by feldspar-quartz porphyroclasts, interstitial granoblastic material (from cataclasis), and by narrow chlorite-epidote streaks of mafic mineral remnants (Plate III, Figs. 1, 2 and 3).

Plate II, Fig. 1

Representative sample from the older phase main tonalite (map-unit 8A), showing greyish colour and weak to moderate cataclasis defined by the orientation of mafic minerals (M) and granulated feldspar-quartz fabric (FQ). Scale in cm. Sample locality, Hough Lake.

Plate II, Fig. 2

Photomicrograph from sample in Fig. 1, showing cataclastic mortar texture of feldspar and quartz indicative of weak cataclasis. Cross-nicols. Field of view is 1 cm across.

Plate II, Fig. 3

Plane-polarised light view of Fig. 2. Note cataclastic foliation defined in part by biotite aggregates (B).

PLATE II

1

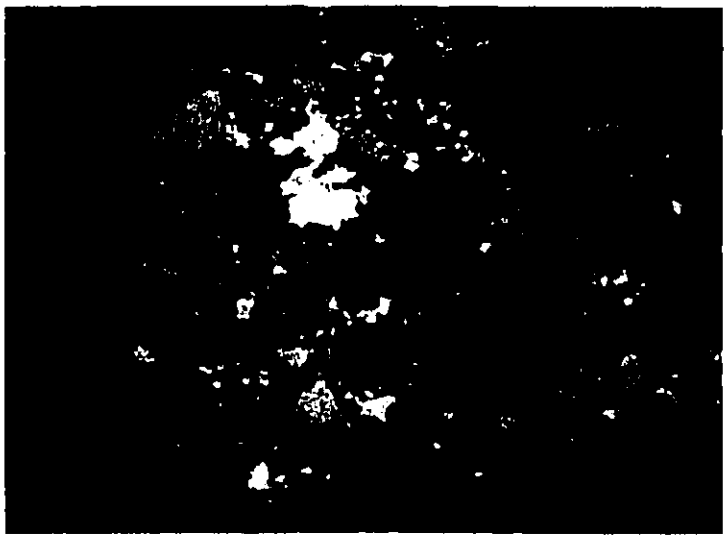

2

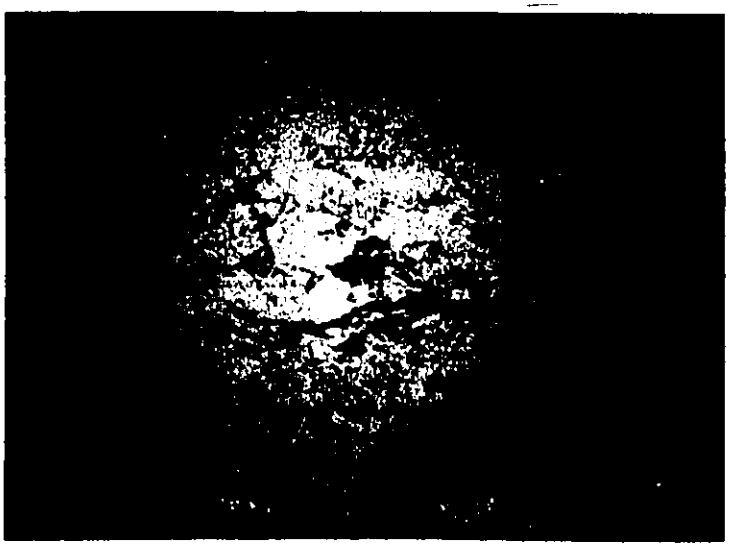

3

Plate III, Fig. 1

Sample from older phase tonalite (map-unit 8A), showing moderate cataclasis with the development of vein-like aggregates of quartz and feldspar (FQ). Scale in cm. Sample locality, 4 km due west of Chamberlain.

Plate III, Fig. 2

Photomicrograph from sample in Fig. 1, showing advanced mortar texture with the development of interstitial granoblastic feldspar and quartz (FQ). Cross-nicols. Field of view is 1 cm across.

Plate III, Fig. 3

Plane-polarised light view of Fig. 2. Note feldspar-quartz porphyroclasts (FQ) and narrow chlorite-epidote streaks (CE) possible representing "slip-shear" planes.

PLATE III

1

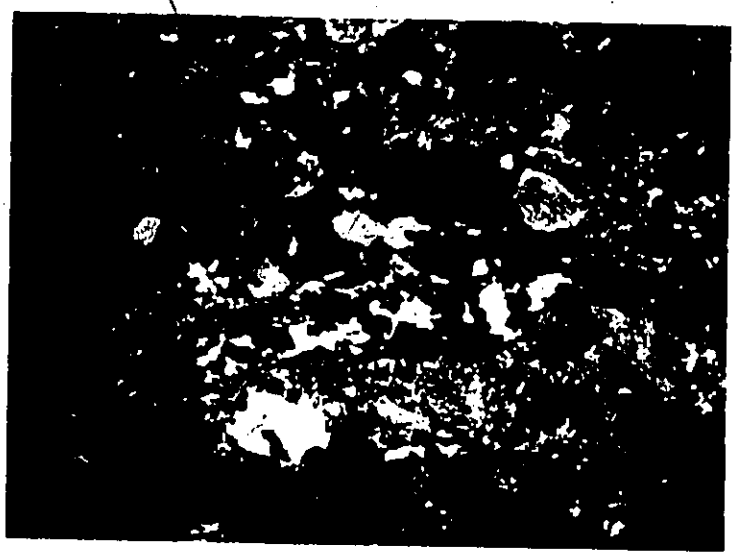

2

3

The tonalite is composed of 11 to 35% quartz, 42 to 77% plagioclase, 0 to 7.5% microcline, 0 to 12% hornblende, 0 to 20% biotite/chlorite, 1 to 15% epidote, trace to 4% muscovite, and trace to 3.5% accessories (including opaque minerals).

The older phase tonalite is crosscut by a few quartz-feldspar porphyry, felsite, biotite to pebbly lamprophyre, and diorite dykes. The diorite dykes are typically holocrystalline, mesocratic, weakly foliated, fine grained and feldspar porphyritic; contacts are sharp, and in places, irregular and contorted. Xenoliths in the main tonalitic mass are rare, and when present, consist of small (less than 25 cm long) amphibolitic varieties (Plate IV, Fig. 1).

The foliated and more massive tonalite passes gradually outward along the batholith periphery (with the exception of the eastern margin) into an inhomogeneous xenolithic gneiss (Plate V, Fig. 1) with a weakly foliated hornblende tonalite subphase (agmatite and map-unit 8C).

The gneiss is best displayed along the northern margin of the batholith from Round Lake to the area south of the Crooked Creek Stock. Here, it consists of at least two varieties of leucocratic tonalite (weakly foliated and gneissic tonalite and quartz diorite), and weakly foliated to lineated hornblende tonalite, both containing abundant,

Plate IV, Fig. 1

Amphibolite xenoliths in outcrop from the older phase tonalite (map-unit 8A), Wookey Lake area. Hammer is roughly 40 cm long.

PLATE IV

1

Plate V, Fig. 1

Xenolithic tonalitic gneiss outcrop from the northern marginal agmatite zone of the older phase tonalite (map-unit 8A). Note variable hornblende tonalite bands. Locality, due south of Round Lake, east of Highway 11. Magnet is 2.5 cm across.

Plate V, Fig. 2

Well defined elongate amphibolite xenolith in tonalitic gneiss outcrop from the northern marginal agmatite zone of the older phase tonalite (map-unit 8A). Elongation parallel to the batholith contact. Locality, roadcut along Highway 66, southwest of the Crooked Creek Stock. Hammer is roughly 40 cm long.

Plate V, Fig. 3

Sharp bordered and undeformed subangular amphibolite xenoliths (A) in tonalitic gneiss outcrop from the northern marginal agmatite zone of the older phase tonalite (map-unit 8A). Gneissosity is south facing, with the batholith contact to the right, producing an inward dipping fabric. Locality, roadcut along Highway 11, due south of Crooked Creek bridge. Field of view is roughly 15 m across.

PLATE V

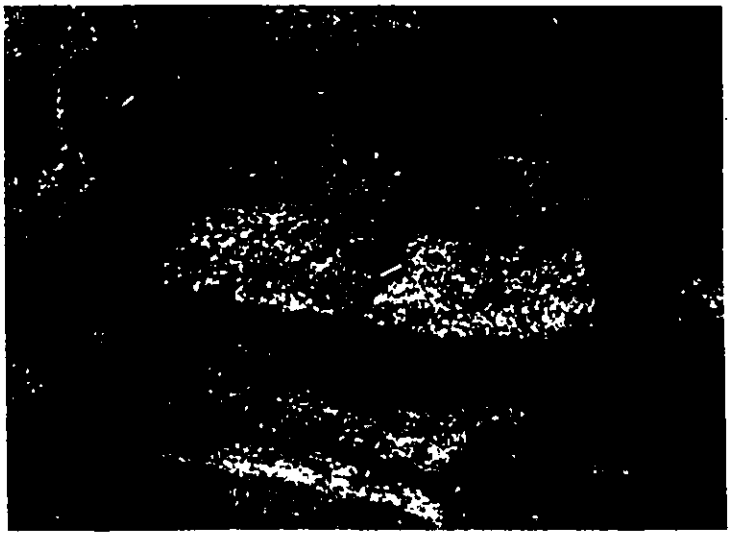
1


2


3

elongate and foliated amphibolite xenoliths (hornblende, plagioclase, epidote and quartz mineralogy) ranging from less than 1 m to approximately 2 km in length. The xenoliths are arranged with their long axis parallel to the batholith contact (Plate V, Fig. 2), and range from sharp bordered and undeformed (Plate V, Fig. 3), with recognizable primary structures (i.e. pillows), to partly assimilated types. Both varieties may be found in the same outcrop.

The gneissosity is steeply dipping and generally conformable with the batholith contact, although south of Round Lake the fabric is perpendicular to the supracrustal foliation. The gneissic rocks are also crosscut by narrow (average less than 15 cm wide) granitoid dykes consisting of leucocratic granite pegmatite, in places biotite-rich, quartz-feldspar porphyry, melanocratic tonalite, and quartz aplite. These dykes are mainly subvertical (few subhorizontal dykes were found), and are of several ages (Plate VI, Fig. 1). They are often folded about vertical axial planes with subhorizontal fold axes (Plate VI, Fig. 2).

The gneissic tonalite is composed of 13 to 37% quartz, 46 to 70% plagioclase, 6 to 11% biotite/chlorite, 0 to 3.5% hornblende, 3 to 13% epidote, trace to 4% muscovite, and trace to 1% accessories (including opaque minerals).

Plate VI, Fig. 1

Outcrop of tonalitic gneiss from the northern marginal agmatite zone of the older phase tonalite (map-unit 8A) showing several ages of leucocratic granite pegmatite dykes (numbered 1 to 3). Locality, roadcut along Highway 66, southwest of Crooked Creek Stock. Hammer is roughly 40 cm long.

Plate VI, Fig. 2

Folded granite pegmatite dyke (D) in tonalitic gneiss outcrop from the northern marginal agmatite zone of the older phase tonalite (map-unit 8A). Note vertical axial planes; fold axes is subhorizontal. Locality, roadcut along Highway 11, due south of the Crooked Creek bridge. Field of view is roughly 3 m across.

PLATE VI

1

2

The more massive hornblende tonalite (compositionally variable from quartz diorite to tonalite) occurs as distinct irregular masses along the batholith contact and within the older phase. Hornblende tonalite (Plate VII, Fig. 1) is associated with xenoliths of and along the contact is gradational into, the surrounding supracrustal rocks.

In hand specimen, the tonalite is reddish, weathering to a buff white or grey color, and contains large subhedral hornblende crystals (greater than 2 mm long), which are often poikilitic surrounding biotite/chlorite and plagioclase (Plate VIII, Figs. 1 and 2). Anhedral forms are usually found in association with biotite, chlorite, epidote, opaque minerals and sphene in subrounded mafic xenoliths. The xenolithic hornblende tonalite plutons at Everett Lake and southwest to Matachewan are mineralogically and texturally similar to their smaller homologues located elsewhere in the batholith.

Hornblende tonalite consists of 11 to 24% quartz, 43 to 62% plagioclase, 0 to 2.5% microcline, 8 to 28% hornblende, 0 to 8% biotite/chlorite, trace to 7% epidote, trace to 3% muscovite, 0 to 1.5% carbonate, trace to 2.5% accessories (including opaque minerals).

Near the eastern and western borders of the batholith,

Plate VII, Fig. 1

Older phase hornblende tonalite (map-unit 8C) outcrop crosscut by felsite dykes. Note weakly foliated nature of tonalite and buff white weathering colour. Locality, 4 km northwest of Elk Lake. Magnet is 2.5 cm across.

PLATE VII

1

Plate VIII, Fig. 1

Representative sample from the older phase hornblende tonalite (map-unit 8C) showing weak foliation, reddish colour and subhedral hornblende cyrstals. Scale in cm. Sample locality, Everett Lake.

Plate VIII, Fig. 2

Photomicrograph from sample in Fig. 1, showing subhedral hornblende (H), lineated and sericitized plagioclase (P) and interstitial quartz (Q). Note portion of remnant amphibolite xenolith (A). Cross-nicols. Field of view is 1 cm across.

PLATE VIII

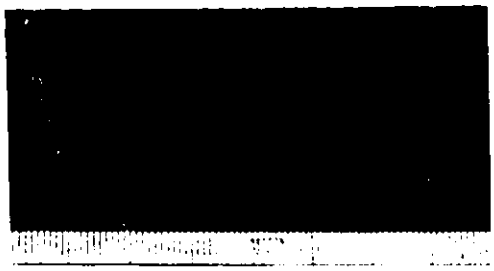

1

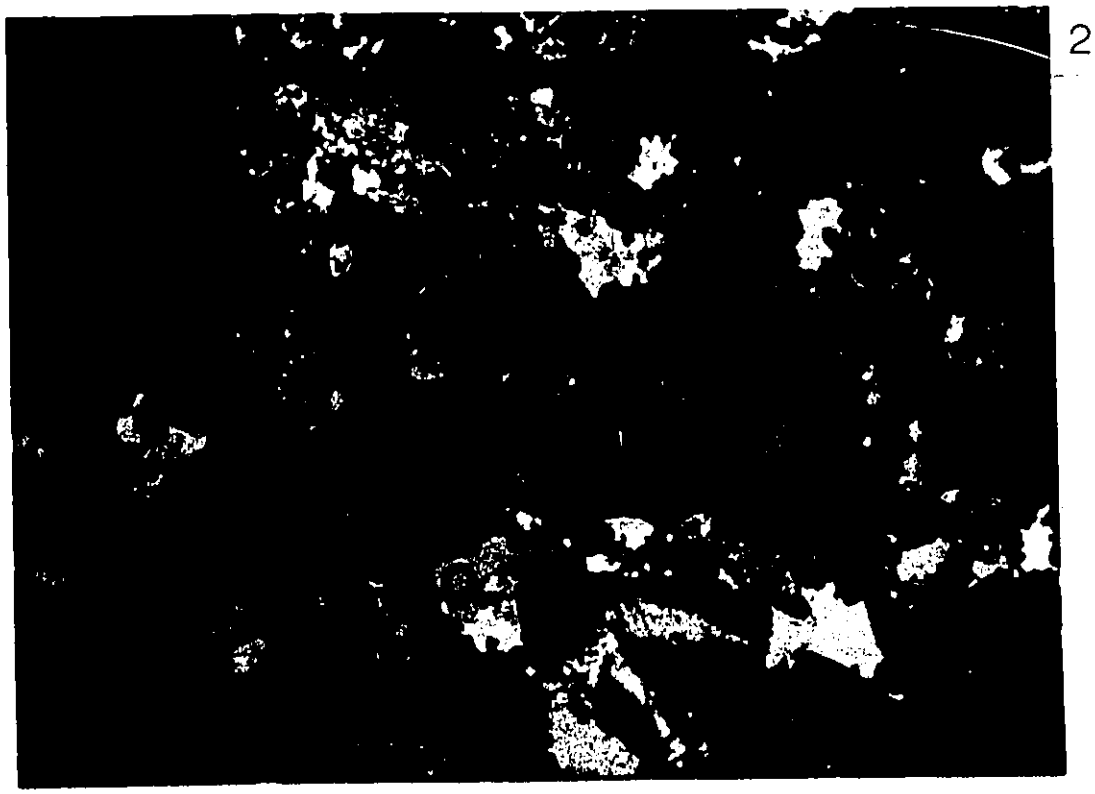

2

the predominantly greyish color of the main tonalite unit is gradually replaced by pervasive reddening due to iron oxide staining of the quartz and feldspar. In the northeast, bounded by South Mindoka, Highways 11 and 112 and the concession road to Krugerdorf, the rock is markedly less foliated and is characterized by a lack of cataclastic fabric, a linear fabric consisting of elongate feldspar and quartz rods (Plate IX, Fig. 1) plunging moderately to subvertically (60^{o}-85^{o}) southward, abundant poikiloblastic microcline, and chlorite-rich slickensided fractures. Microcline not only occurs in the northeast, but the whole eastern portion of the batholith is marked by the presence of both poikiloblastic and locally interstitial microcline (Plate IX, Fig. 2). The resulting rock ranges in composition from tonalite through granodiorite to quartz monzodiorite (map-unit 8B - poikiloblastic microcline granodiorite).

The transition between the tonalite and the granodiorite suite appears gradational from field evidence. There is gradual and pervasive color change from tonalite to granodiorite (grey to pink), both are linked by similar mineralogical and textural characteristics, and sharp intrusive contacts between the two phases were not found.

Granodioritic rocks consist of 17 to 35% quartz, 38 to 65% plagioclase, 1 to 19% microcline, trace to 10% biotite/chlorite, trace to 5.5% epidote, trace to 12% muscovite, and

Plate IX, Fig. 1

Linear fabric defined by elongate white feldspar and pale grey quartz rods in outcrop of older phase granodiorite (map-unit 8B). Locality, roughly 3 km southeast of Tarzwell. Magnet is 2.5 cm across.

Plate IX, Fig. 2

Photomicrograph showing poikiloblastic microcline from the older phase granodiorite (map-unit 8B). Note zoning pattern and sericite alteration in plagioclase (P). Cross-nicols. Field of view is 1 cm across. Sample locality, 6 km west of Wawbewawa.

PLATE IX

1

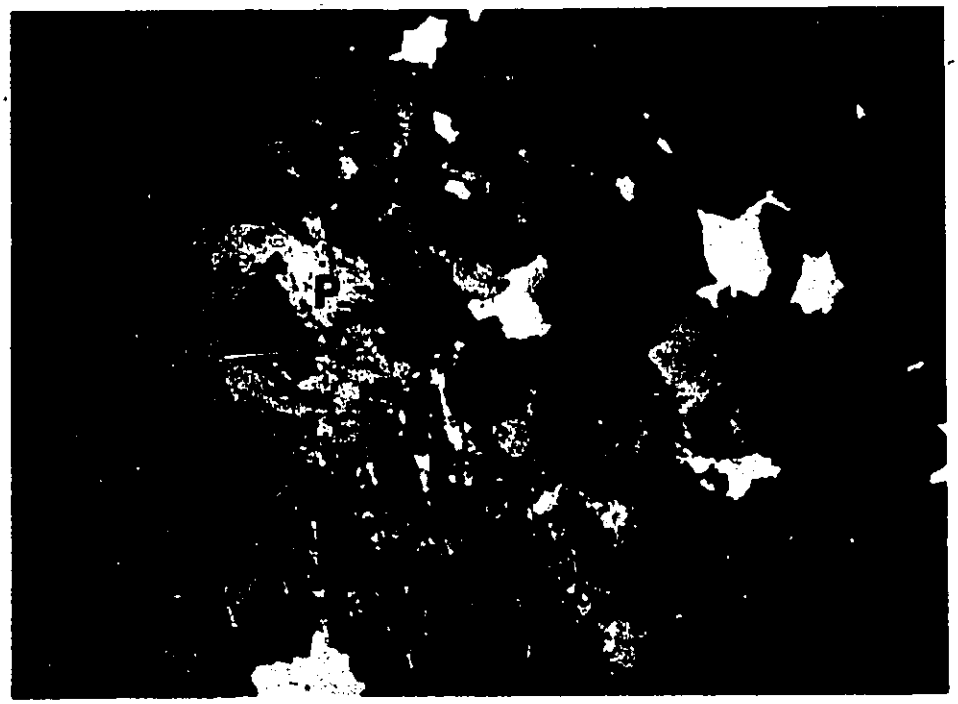

2

trace amounts of accessories and opaque minerals.

The eastern batholith periphery consists of strongly cataclastic, foliated and gneissic quartz-feldspar augen-rich tonalite-granodiorite (map-units 8D and 8E).

The gneissic and strongly cataclastic border zone varies in width from less than 1 km to approximately 3 km, extending from Round Lake to the Cross Lake Fault. The zone is characterized by extreme cataclasis of constituent minerals forming a steep to moderate inward dipping, foliated to gneissic fabric concordant to the batholith outline, and gradational with the inner main tonalite and granodiorite. The zone is also in fault contact with the peripheral agmatite gneisses of Round Lake.

The foliated, cataclastic margin is best displayed northeast of Charlton (map-unit 8D - foliated, cataclastic tonalite), where the rock is almost black and consists of reddish anhedral feldspar-rich augens or porphyroclasts (average less than 1 cm in diameter) set in a fine grained black groundmass of granoblastic material (Plate X, Fig. 1).

In thin section, the porphyroclasts are composed of partly granulated, elongated and lensoid plagioclase-quartz (-microcline) aggregates surrounded by granoblastically foliated, fine grained and somewhat recrystallized quartz (mosaics of non-undulose quartz with 120° junctions between grains) with remnant biotite. The rock is highly altered to

Plate X, Fig. 1

Foliated, cataclastic outcrop of marginal older phase tonalite (map-unit 8D), showing reddish feldspar-rich porphyroclasts (F) set in a fine-grained and foliated black groundmass of granoblastic material. Locality, roughly 3.5 km southwest of Chamberlain. Magnet is 2.5 cm across.

Plate X, Fig. 2

Photomicrograph from the older phase foliated, cataclastic tonalite (map-unit 8D), showing advanced stage of cataclasis with feldspar-quartz porphyroclasts (F) and recrystallized quartz mosaics (Q). Compare with Plate III, Fig. 2 and Plate II, Fig. 2. Cross-nicols. Field of view is 1 cm across. Locality, 250 m southeast of outcrop in Fig. 1.

Plate X, Fig. 3

Plane-polarised light view of Fig. 2. Note outline of feldspar porphyroclasts (F) defined by narrow and sinuous chlorite-epidote stringers (possible "slip-shear" planes), and the clear groundmass of quartz.

PLATE X

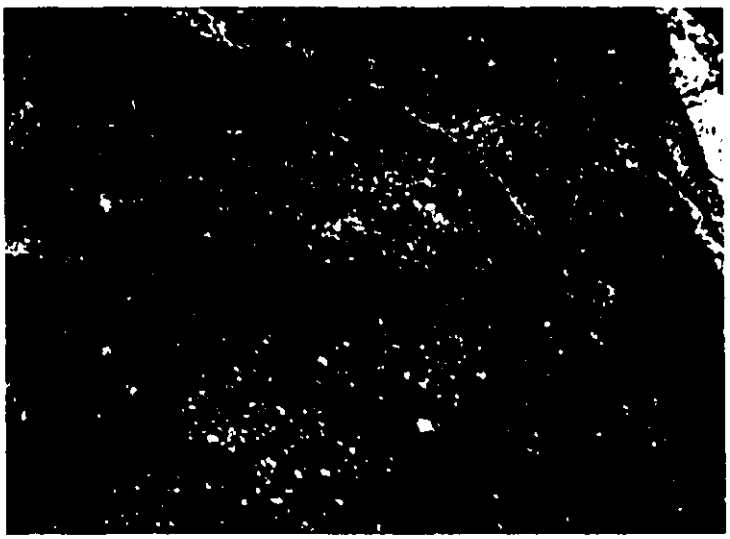
1

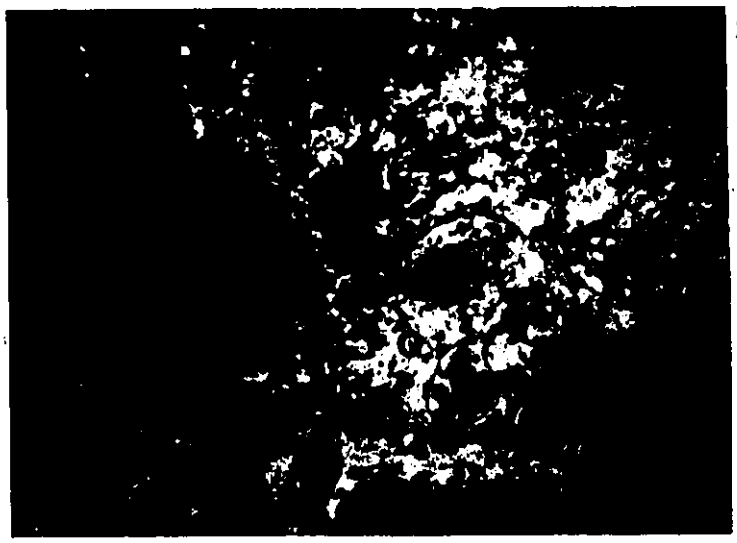
2


3

sericite (from the breakdown of plagioclase, biotite and microcline), chlorite (from biotite) and epidote (from plagioclase and biotite, but restricted to the groundmass). The mostly clear, glassy groundmass contains chlorite-epidote stringers (narrow shear planes?), less than 1 mm in width, parallel to the foliation which, with the latter, are deflected around the porphyroclasts (Plate X, Figs. 2 and 3).

Along the northeast periphery of the batholith, the cataclastic zone is characterized by progressively foliated to gneissic (last 200 m from the contact) structures as the margin is approached (map-unit 8E - gneissic, cataclastic granodiorite (Plate XI, Figs. 1, 2 and 3).

Portions of the gneissic fabric in the vicinity of Boston Creek are interpreted as deformational segregation produced by intense cataclasis. The foliated and gneissic fabrics show similarities with the cataclastically foliated variety encountered near Charlton, in that they have porphyroclasts and groundmass of the same textural characteristics, even though the rock is more leucocratic in the northeast. The strongly foliated granodiorite is again generally reddish due to iron oxide staining of the host rock in this area, but as the contact is approached greenish-grey bands (averaging less than 3 cm wide) appear interlayered with the more leucocratic layers, giving the rock a gneissic appearance (Plate XI, Fig. 3). From thin section, the darker bands

Plate XI

Series of figures from outcrops along the northeast margin of the batholith showing the progressive foliated to gneissic cataclasis structures in the older phase marginal granodiorite (map-units 8D, E).

Plate XI, Fig. 1

Note feldspar porphyroclasts (F) in foliated granoblastic groundmass. Compare with Plate X, Fig. 1. Pen is 15 cm long. Locality, 1 km east of Tarzwell.

Plate XI, Fig. 2

Note more advanced stage of cataclasis with development of gneissic fabric resulting from increased shear stresses. Pen is 15 cm long. Locality, 3.5 km southeast of Boston Creek.

Plate XI, Fig. 3

Note fully developed gneissic fabric resulting from extreme cataclasis. Leucocratic bands consist of feldspar porphyroclasts with iron oxide alteration, giving a reddish tinge, whereas the darker bands consist mostly of clear, fine-grained granoblastic quartz (± feldspar) and chlorite/biotite. Brunton compass is scale. Locality, Boston Creek.

PLATE XI

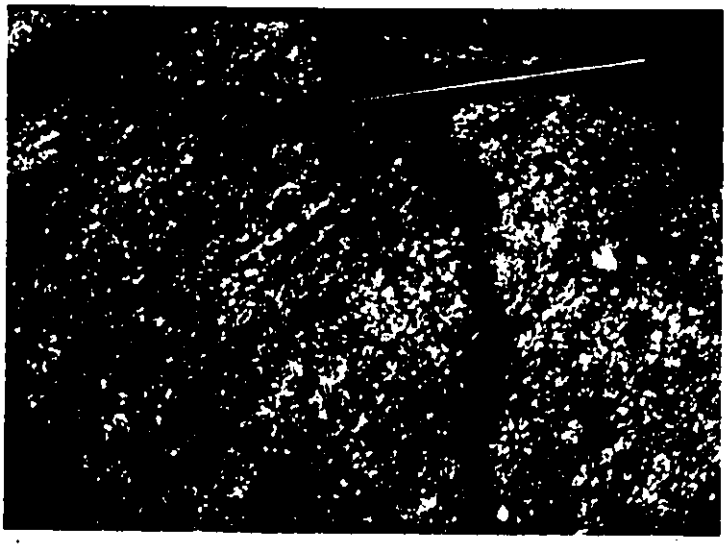

1

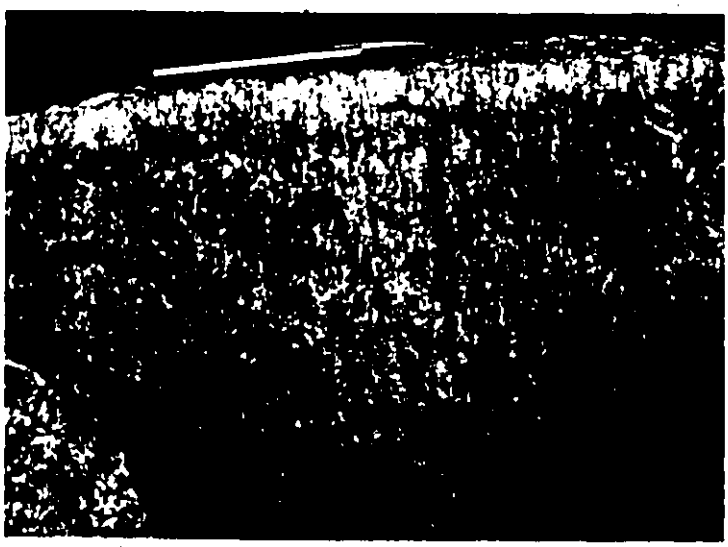

2

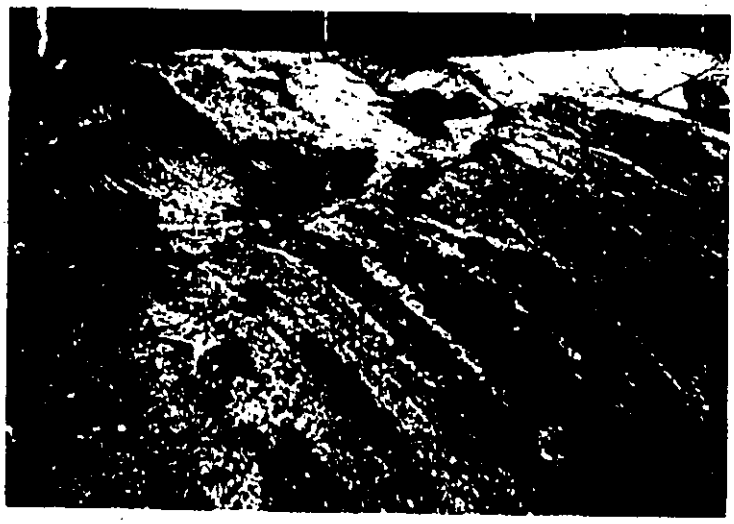

3

consist mostly of clear, fine grained granoblastic quartz (+feldspar) with abundant chlorite (/biotite) flakes and minor quartz-feldspar porphyroclasts, devoid of iron oxide apart from alteration in porphyroclasts. In contrast, the leucocratic bands are composed of feldspar with dusty iron oxide alteration and fracture filling (Plate XII, Figs. 1 and 2). In the contact zone at Boston Creek, the gneissic fabric is accentuated by cataclastically foliated, bifurcating and discontinuous leucocratic pegmatite bodies (widths in cm scale) with sharp and regular contacts subparallel and oblique to the main structural trend (Plate XIII, Fig. 1), suggesting that these were possibly early dykes subsequently deformed and sheared with the host rock.

The granodiorite-tonalite consists of 6 to 19% granoblastic material (quartz, plagioclase, ± microcline), 20 to 32% quartz, 37 to 60% plagioclase, trace to 20% microcline, trace to 5.5% biotite/chlorite, trace to 8% epidote, trace to 5% muscovite, trace to 1% accessories and opaque minerals.

Several conclusions regarding the peripheral clastic zone can be drawn from the field evidence. The peripheral cataclastic zone is devoid of country rock xenoliths when compared with the homologous peripheral agmatite gneiss west of Round Lake. Secondly, the gneissose cataclastic fabric appears along the northeast contact only. Both features, and the apparent gradation between the various structural

Plate XII, Fig. 1

Photomicrograph of leucocratic band in older phase gneissic granodiorite from the previous Plate XI, Fig. 3. Note alignment of feldspar porphyroclasts (F) and recrystallized quartz groundmass (Q). Cross-nicols. Field of view is 1 cm across.

Plate XII, Fig. 2

Plane-polarised light view of Fig. 1 photomicrograph. Note heavily altered feldspar porphyroclasts (F) and chlorite stringers (C), again possibly indicating "slip-shear" surfaces.

PLATE XII

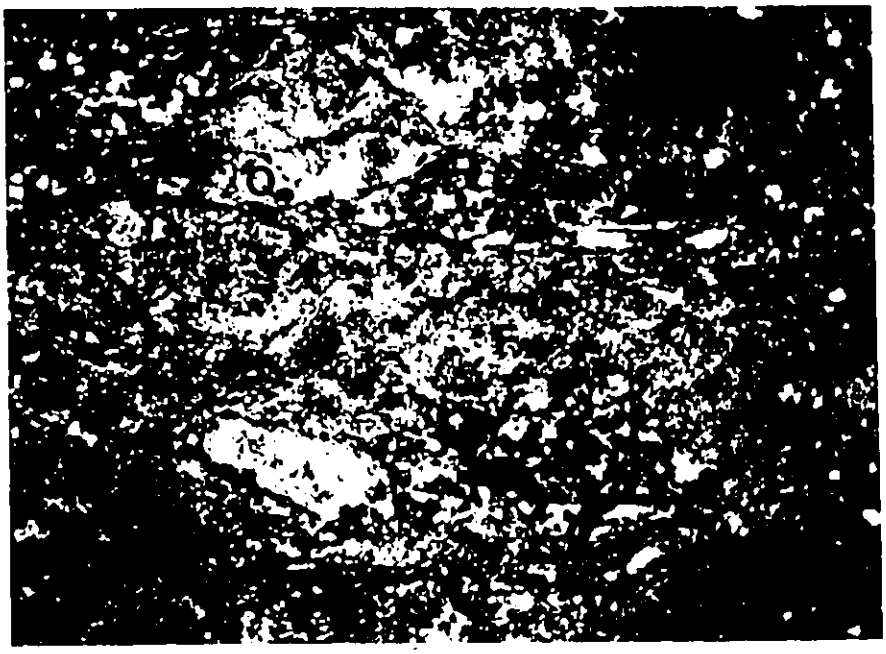

1

2

Plate XIII, Fig. 1

Cataclastically foliated, bifurcating and discontinuous leucocratic granite pegmatite dykelets in marginal older phase gneissic granodiorite (map-unit 8E) outcrop. Note slight oblique trend of dykelets to gneissossity. Locality, Boston Creek. Magnet is 2.5 cm across.

PLATE XIII

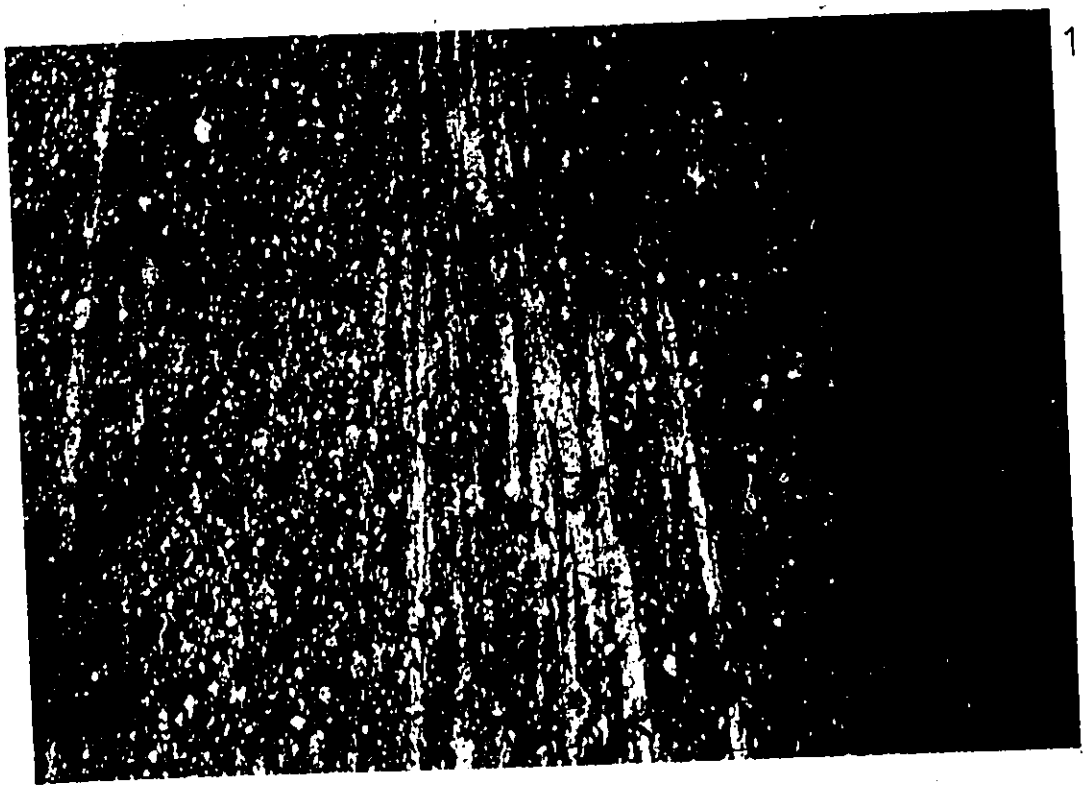

elements encountered in the batholith east of the Cross Lake Fault, were probably produced during emplacement. Shearing stresses originating from late-stage movement in a viscous fluid-crystal mush, prior to complete solidification, could induce peripheral cataclasis of the type observed here. The model may explain the unfoliated and lineated northeast granodiorite portion of the batholith, since the granodiorite would represent a crystallized remnant of a continually rising (near vertical as defined by the subvertical lineation) less viscous magma, during which most of its adjoining and partly crystallized periphery was cataclastically deformed. The extensive deformation would have obliterated any evidence of country rock xenoliths present in the peripheral zone, such that xenoliths were emplaced at lower levels, assimilated and sheared beyond recognition at the present erosional level. As for the lack of a gneissosse fabric in the Charlton area, fabric variability (from cataclasis expressed by schistose foliation and gneissosity) may reflect differences in the intensity of shear associated with magma movement, viscosity and density contrasts between magma and host rock, emplacement level and confining stresses.

B) <u>Younger phase: granodiorite-tonalite (map-unit 9)</u>

The younger granodiorite-tonalite, with quartz monzodiorite

affinities, is a homogeneous red to mottled white rock with a weak east-west trending foliation, accentuated by oriented xenoliths which average 5% of the rock. It completely lacks the cataclastic fabric of the older phase (Plate XIV, Fig. 1). The younger phase occupies the central part of the batholith, (the Indian Chute Stock), and flanking cupolas, including the Crooked Creek and Hope Lake Stocks (map 1, and Fig. 9). These bodies display both concordant and discordant intrusive relationships toward the older tonalite.

The Crooked Creek (Moore, 1966; Lovell, 1972) and Hope Lake Stocks, also intrude the supracrustal country rocks; and near the Hope Lake Stock, predominantly southwest trending structures in the volcanic succession have been reoriented northerly.

The stocks consist of cumulate tabular plagioclase and subhedral quartz crystals set in matrix of quartz, poikiloblastic microcline, and euhedral hornblende (Plate XIV, Fig. 2). Sphene, the commonest accessory mineral, occurs as large euhedral wedge-shaped grains averaging almost 1 mm in length.

The granodiorite-tonalite is composed of 14 to 31% quartz, 48 to 75% plagioclase (may include microcline), 2 to 13% microcline, 3 to 18% hornblende, 0 to 4% biotite/chlorite, trace to 4% epidote, trace muscovite, trace to 3.5% accessories, including opaque minerals.

The younger phase is characterized by rounded to elongate xenoliths less than 1 cm to greater than 1 m in diameter

Plate XIV, Fig. 1

Outcrop surface of younger phase granodiorite-tonalite (map-unit 9). Note variable types and sizes of xenoliths in a reddish homogeneous and unfoliated host. Locality, roughly 8 km northeast of Indian Chute Falls, Council Creek. Pen is 15 cm long.

Plate XIV, Fig. 2

Photomicrograph of representative younger phase granodiorite-tonalite (map-unit 9), showing plagioclase (P), subhedral quartz (Q), poikiloblastic microcline (M), and euhedral hornblende (H). Cross-nicols. Field of view is 1 cm across. Locality, 2.75 km northeast of the northern tip of Kushog Lake.

PLATE XIV

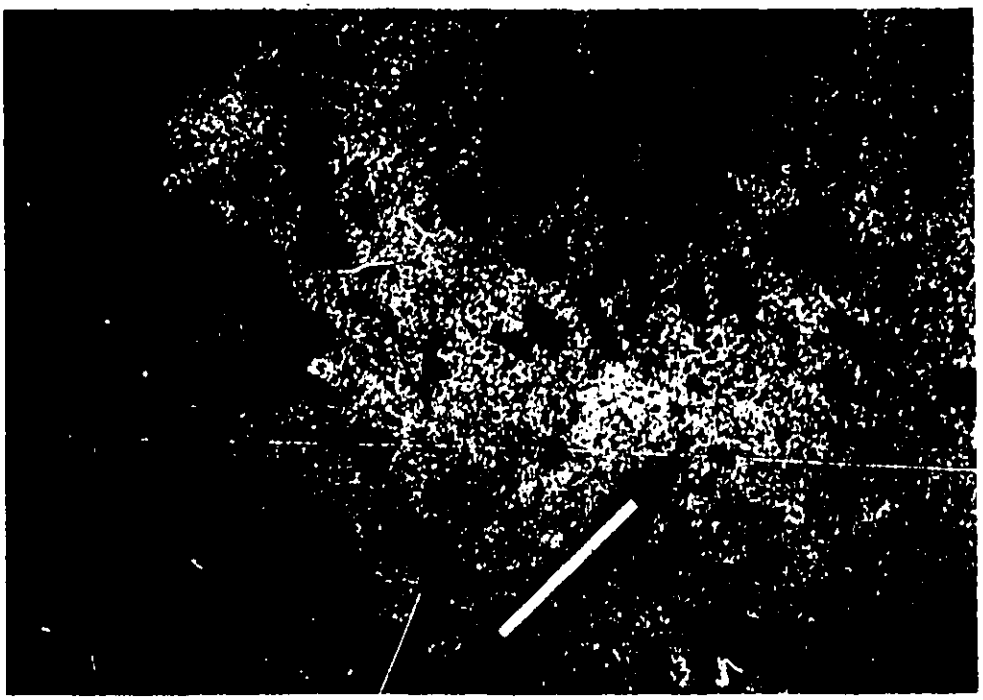

1

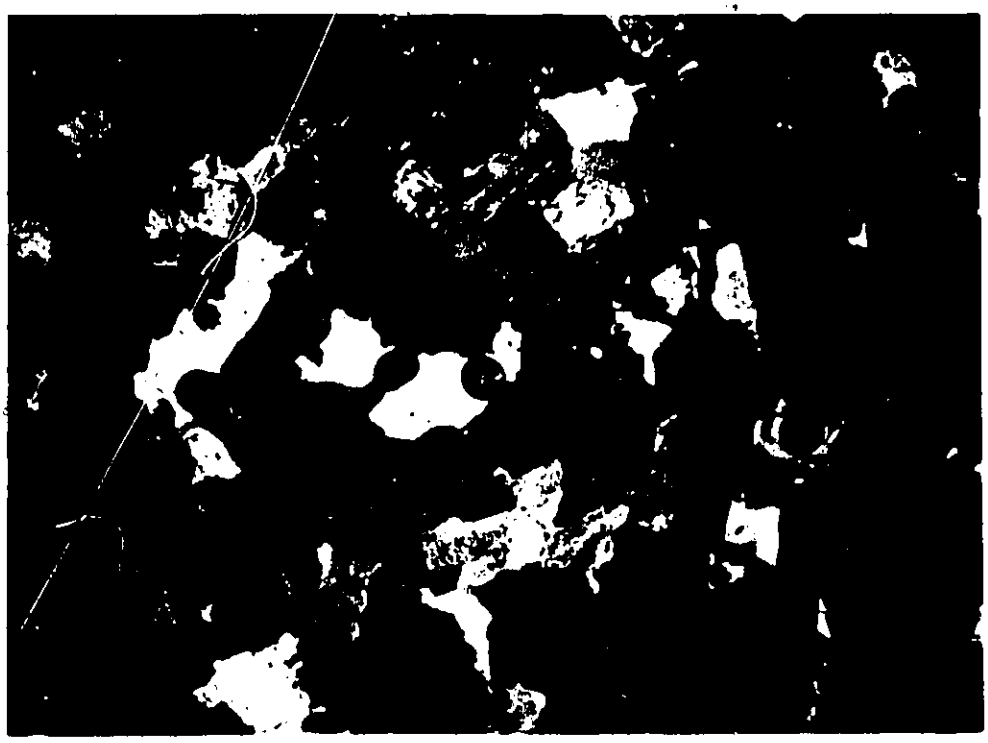

2

Plate XV

Series of figures from the younger phase granodiorite-tonalite (map-unit 9) showing the variety of xenoliths: amphibolite (Fig. 1), foliated mafic volcanic (Fig. 2), hornfels (Fig. 3), autoliths of intermediate composition? (Fig. 4), and foliated tonalite (Fig. 5) most likely from the older phase of the batholith. Fig. 6 represents an extremely granitized fragment recognizable by the dispersed and remnant mafic mineral aggregates.

Scales: Figs 1 and 6 - quarter, 2 cm in diameter
Figs 2 and 4 - magnet, 2.5 cm across
Figs 3 and 5 - camera lens cap, 5 cm in diameter.

Locality: Figs 1 to 5 - dam/power station at Indian Chute Falls on Council Creek
Fig. 6 - 8 km northeast of Indian Chute Falls.

PLATE XV

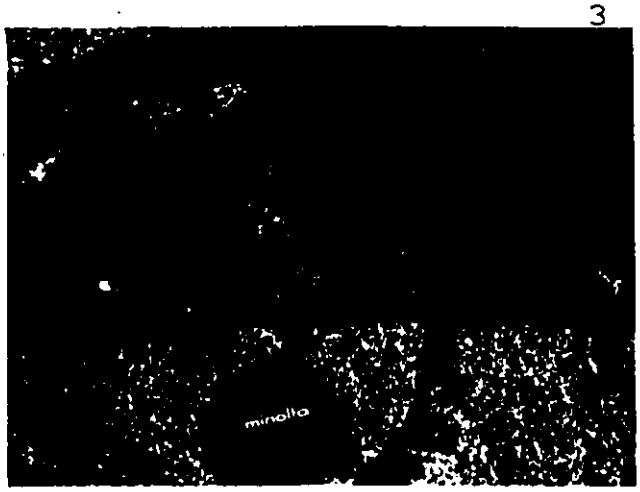

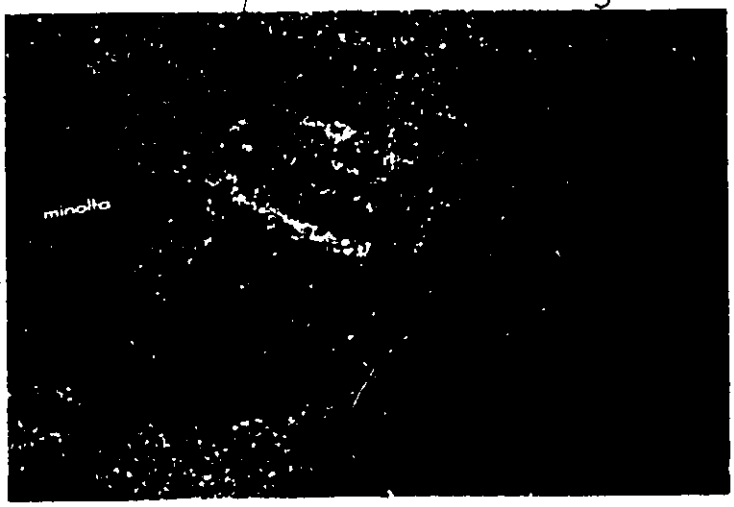

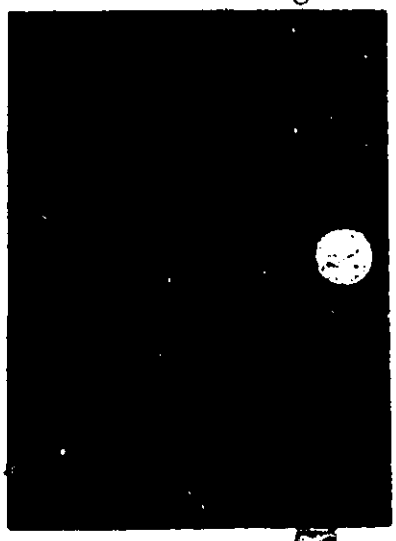

consisting of:

1) recrystallized ultramafic and mafic (volcanic?) fragments (Plate XV, Figs. 1 and 2)
2) granitized hornfelsic fragments (sediment or felsic volcanic in origin) (Plate XV, Fig. 3)
3) autoliths of intermediate composition, possibly representing an earlier phase of the granodiorite-tonalite, and containing the above xenolith types (Plate XV, Fig. 4)
4) foliated tonalite fragments, probably from the older phase (Plate XV, Fig. 5).

Xenoliths show varying degrees of assimilation in a single outcrop, with extremely granitized fragments recognizable only by the dispersed and remnant mafic mineral aggregates (Plate XV, Fig. 6). However, the bulk of mafic and intermediate xenoliths have a mineralogical composition similar to the surrounding granodiorite-tonalite (hornblende, quartz, plagioclase, chlorite (-biotite), epidote, sphene, apatite and opaque minerals; no microcline), although they differ in proportion (hornblende in excess of 50%, quartz approximately 40%) and in texture (finer grained and anhedral shapes).

3) Physical properties of batholith

The total magnetic field (Geological Survey of Canada and Ontario Department of Mines Aeromagnetic Maps, 1970a, b; Geological Survey of Canada Aeromagnetic Maps, 1965, 1981)

over most of the Round Lake Batholith is relatively consistent, ranging from under 2000 to over 2300 gammas (Fig. 6), due to an almost total lack of magnetic minerals (magnetite). Minor variations (i.e. linear patterns) occur at the northwest trending Montreal River and Cross Lake Faults, and over the northeast trending diabase dykes of the Abitibi Swarm. Major changes also occur along the eastern periphery (east of the Montreal River Fault), where the batholith contact roughly corresponds to the 2100-2200 gammas contour. The adjacent Wawbewawa and lower Catharine Groups volcanic rocks (ultramafic to mafic in composition) attain higher magnetic fields, exceeding 2500 gammas between Charlton and Boston Creek. The contact zone magnetic response is not as distinct west of the Montreal River Fault, partly due to the prominence of diabase dykes of the Matachewan Swarm which extensively crosscut the batholith, but mainly resulting from the thick cover of Huronian Supergroup rocks. Nevertheless, the contact can be traced as a magnetic discontinuity beneath the cover rocks, extending from the Matachewan area, westerly to Elmer Lake, then southwesterly along Duncan Lake, and southeasterly, eventually joining with the batholith-country rock contact at Penassi Lake and into the Elk Lake area.

In addition, the batholith corresponds to a distinct negative Bouguer gravity anomaly (Dominion Observations Branch Gravity Map, 1966), with values ranging from less than -70 to -40

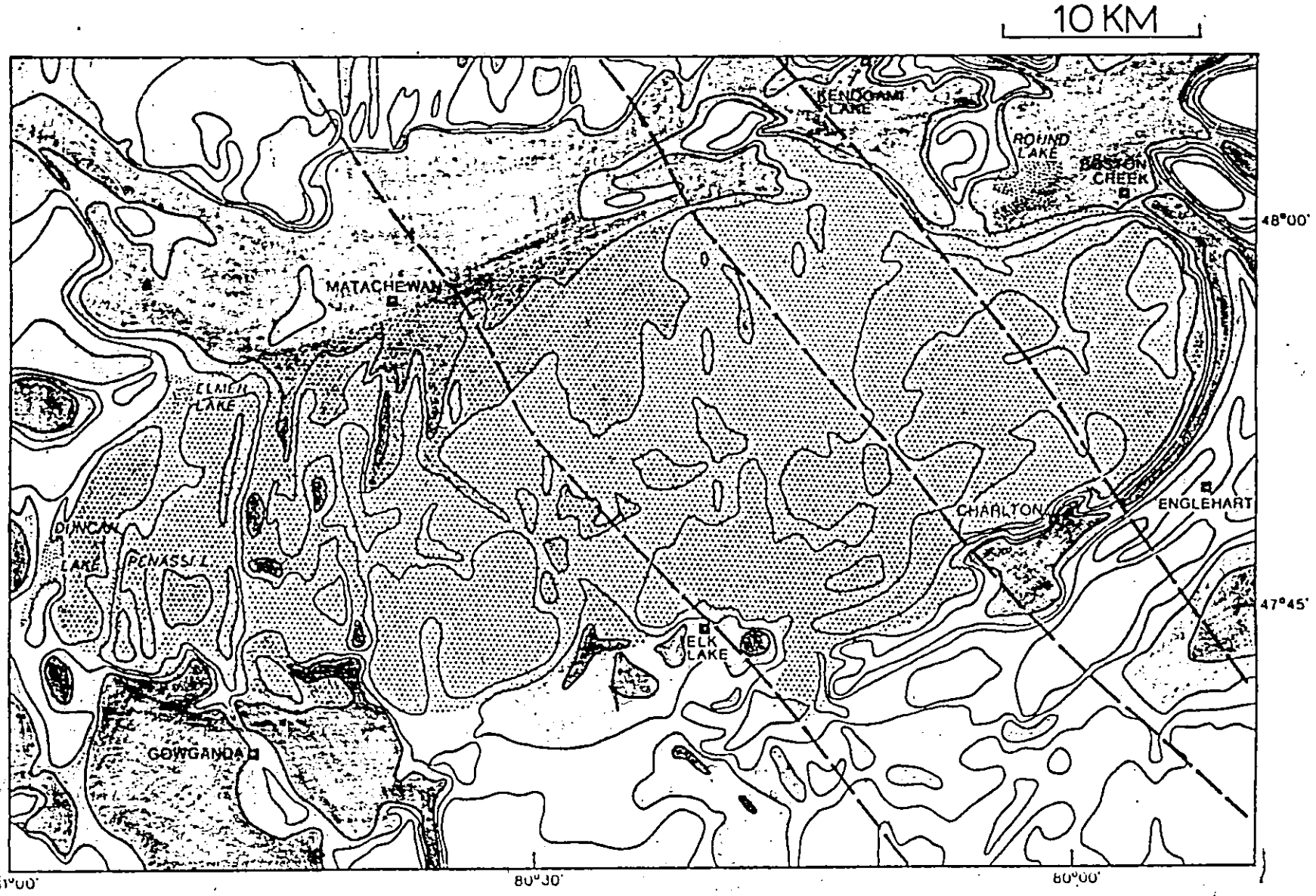

Fig. 6. Aeromagnetic map of the Round Lake Batholith area (simplified from Geological Survey of Canada and Ontario Department of Mines Aeromagnetic maps, 1970a, b; and Geological Survey of Canada Aeromagnetic Maps, 1965, 1981).
Legend: magnetic fields, ☐ <2000 gammas; ☐ 2000-2100; ☐ 2100-2200; ☐ 2200-2300; ☐ 2300-2500; ■ >2500.
Stippled pattern corresponds to the Round Lake Batholith (includes extrapolated portions under the Proterozoic cover rocks). Heavy dashed lines correspond to faults of the Timiskaming System.

milligals east of the Montreal River Fault. West of the fault, the gravity field over the batholith decreases to -60 to -30 milligals (Fig. 7), and blends in with the regional northwest trending contours. Significantly, the -50 milligals contour extends west of the Montreal River Fault for more than 30 km, indicating the probable presence of light granitoid material in this area, and the possible subsurface extension of the batholith The sharp magnetic contrast along the eastern periphery also corresponds to a sharp gravity increase to -20 milligals across the contact zone, a distance of less than 5 km. Both major northwest trending faults alter the negative anomaly from east to west by -70 to -65 milligals across the Cross Lake Fault, and by -55 to -50 milligals at the Montreal River Fault. These "anomaly breaks" suggest that both faults contributed to the present configuration of the batholithic phases.

Any model used to explain the negative anomaly must take into account the large density contrast between the tonalitic composition of the batholith, which is probably less than the crustal average (approximately 2.75 g/cm^3 for this part of the Superior Province. This approach has already been utilized to estimate the thickness of the Round Lake Batholith as between 4 and 10 km (Gibb and van Boeckel, 1970).

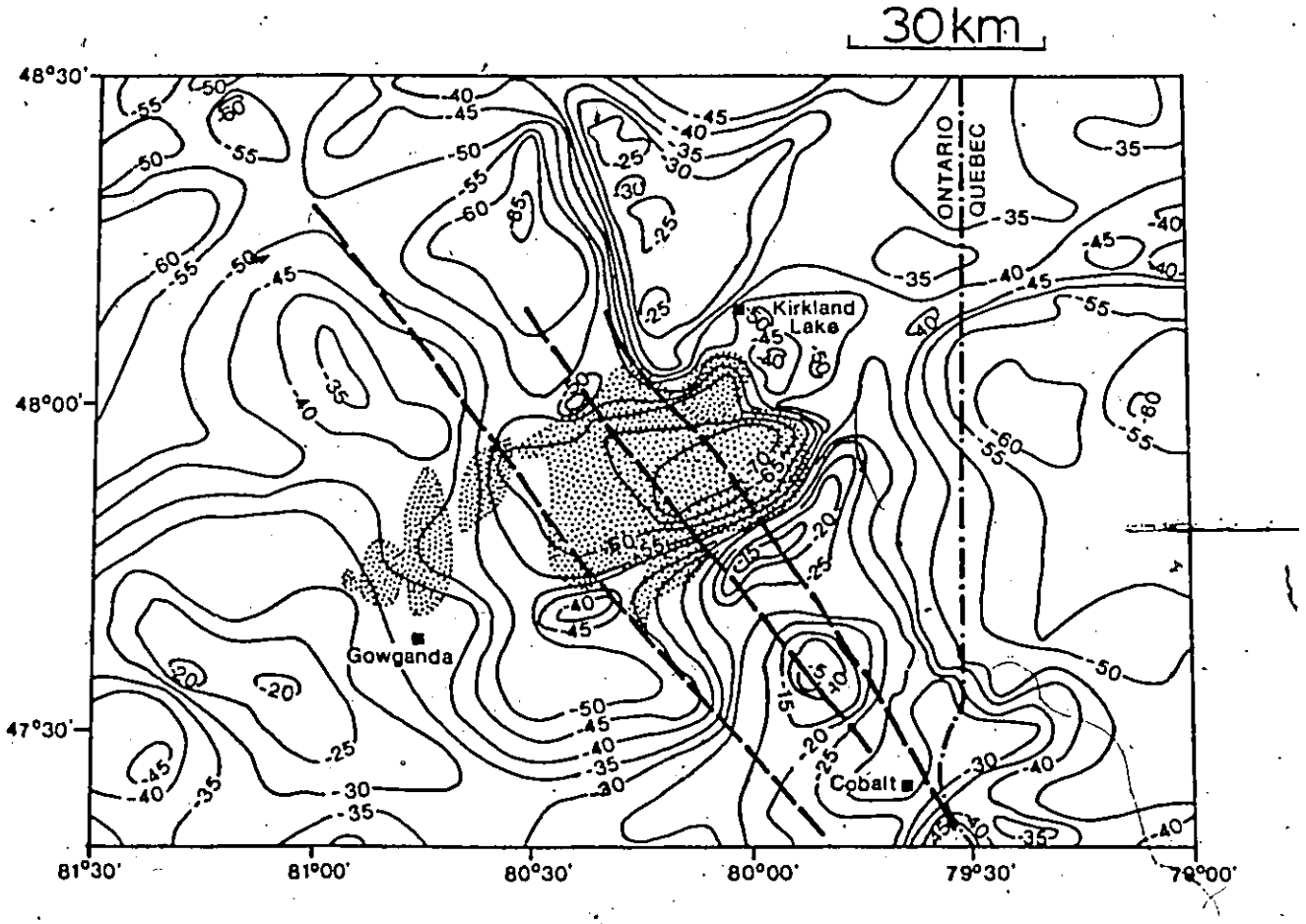

Fig. 7. Bouguer gravity anomaly map of the Round Lake Batholith area (taken from Dominion Observations Branch, 1966: Gravity map No. 58).
Legend: contour intervals at 5 milligals; stippled pattern corresponds to the Round Lake Batholith (and Otto Stock); heavy dashed lines correspond to faults of the Timiskaming System.

CHAPTER IV: GEOCHEMISTRY OF THE ROUND LAKE BATHOLITH

The geochemistry of igneous rock suites is useful not only for classification purposes, but also for determining magma sources and cogenetic relationships. These approaches will be utilized for the Round Lake Batholith to:

1) classify the major phases and subphases,
2) support the field evidence of large scale homogeneity within the batholith, and of a spatial relationship between the older phase tonalite, poikiloblastic granodiorite and peripheral tonalite-granodiorite (fractionation link),
3) determine the source of the batholith.

Major and trace elements are useful in determining sources and postulating fractionation models for igneous rocks. Element concentrations have been inherited from the parent magma, and partitioned between successive liquid and crystalline fractions. Mineral phases precipitating from a liquid will accomodate specific major elements in their structures, and depending on the compatibility of trace elements (based on partition coefficients - K_D), these will preferentially enter (or be rejected from) the mineral framework. Continued separation of mineral phases will deplete or enrich the residual liquid in major and trace elements. Compatible trace elements ($K_D > 1$) will be restricted to the mineral phases. For example, during fractionation of an acid magma involving mainly

plagioclase, the major oxides, Al_2O_2, CaO, tend to decrease and SiO_2, Na_2O, K_2O increase along a liquid line of descent, and there is a complementary increase in the trace elements Rb, Ba, REE's and decrease in Sr, with the particular pattern giving a valuable hint as to the fractionation sequence itself (K_d^{Sr} for plagioclase $>$ 1; for others $<$ 1).

Major and trace element concentrations allow qualitative estimates of source regions for parent magmas which can be compared to chemically and petrographically defined source material (for example, either amphibolite or eclogite). The source region is of importance, particularly when it is necessary to determine whether an igneous complex was entirely or partly derived from a primary source such as the mantle or represents reworked sialic material.

The succeeding sections in this chapter will contain a brief review of Archean tonalite/trondhjemite chemistry an petrogenesis; and a summary of major and trace element concentrations from the batholith that will include chemical classification, identification of trends, and a comparison with analyses from worldwide occurrences of Archean tonalite/trondhjemite[1] suites. The latter part of the chapter will be concerned with fractionation and petrogenesis of the batholith.

1) <u>Review of Archean tonalite/trondhjemite chemistry and petrogenesis</u>

Worldwide, Archean tonalite/trondhjemite suites (partial

---

[1]Streckeisn (1976) defines trondhjemite as a light coloured tonalite containing less than 10% mafics, and oligoclase or andesine as the plagioclase.

listing in Appendix IV) have the following chemical characteristics (from Glikson, 1979; Barker, 1979; and Appendix IV):

1) SiO_2 ranges between 68 and 75 weight %; Al_2O_3 is between 13% and 16%, generally 15% Al_2O_3 at 70% SiO_2 and less than 14% at 75% SiO_2; CaO is generally between 1.5 and 3.0%, although values may exceed 4% or be lower than 1%; Na_2O is generally 4.0 to 5.5%, some as low as 3.5% or as high as 6.5%; K_2O is generally less than 2.5%, but may range to higher than 5%; Fe_2O_{3TOTAL} (FeO+Fe_2O_3) + MgO is generally less than 3.5%, and again there are many exceptions since some exceed 6.5% (Fe_2O_{3TOTAL}: MgO greater than 2); and finally, TiO_2 is less than 0.5%.
2) Tonalites follow a calc-alkaline trend in the triangular A-F-M variation diagram.
3) All are quartz normative. Normative corundum is uncommon, since magma derived from the anatexis of igneous parents are diopside normative. It has been shown in some cases that at greater than 65% SiO_2 calc-alkaline rocks change from diopside to corundum normative. In normative triangular variation diagrams (Q-Ab-Or, An-Ab-Or), tonalitic rocks generally plot close to the Q-Ab and An-Ab tie lines (with minor Or enrichment).

4) Sr and Ba are usually less than 1000 ppm, whereas Rb is less than 200 ppm (quite commonly less than 30 ppm); all three large ion lithophile (LiL) elements (Sr, Ba, Rb) display weak correlations to major element abundances, and generally show a wide range of dispersion. Ba/Sr is generally greater than 1, whereas Rb/Sr is less than 0.15.

5) Most initial Sr^{87}/Sr^{86} range between 0.700 and 0.705 for the 2.5 to 3.0 Ga tonalite age group.

6) All have steep chondrite normalized REE patterns with LREE 30 to 200 times chondrites and HREE 1 to 5 times chondrites; La/Yb range from 20 to 70; slight positive, or no Eu anomaly (Eu/Eu* averages 1).

These chemical characteristics have led many workers (Arth and Hanson, 1972, 1975; Barker and Arth, 1976; Arth et al., 1978; Glikson, 1979; Gower et al., 1982) to set constraints in developing models of origin for tonalite/trondhjemite magmas. These are reported here, along with the most referred-to model or origin:

1) In any fractionation or partial melting model involving major and trace elements plagioclase cannot be a residual (or precipitating) phase, whereas garnet and, in all probability, amphibole are obligatory phases of the residue. Garnet and amphibole would produce the HREE depletion needed in tonalitic magmas ($K_D^{Yb,Lu}$ much greater than 1).

2) Low initial Sr^{87}/Sr^{86} and K and Rb contents, in addition to the predicted behaviour of REE (LREE enrichment, Eu/Eu* greater than or equal to 1; HREE depletion) in tonalites suggest that the magma originated from the mantle or undifferentiated crustal rocks with a short residence time, containing low levels of K, Rb, Zr, U, Th, total REE, and low initial Sr^{87}/Sr^{86}.

3) Field evidence, melting and fractionation models, and $K_{D's}$ suggest that tonalitic magmas can be derived by partial melting of rocks of basaltic or gabbroic compositions such as eclogite, amphibolite and basic granulite. Formation of tonalite by fractionation of a basaltic magma, under hydrous conditions would necessitate more than 70% fractional crystallization (producing a pyroxene and garnet cumulate). In most cases, field evidence demonstrates that there is insufficient parental basaltic magma to produce tonalite by crystal fractionation. Secondly, tonalite-gabbro bimodal assemblages show no intermediate rock composition between gabbro and tonalite as would be predicted by differentiation.

4) Initial working models for the genesis of tonalites stem from evidence gathered in Archean granite-greenstone belt complexes of Minnesota and northwestern Ontario.

The commonest petrogenetic model states that tonalite/trondhjemite melts were formed by 20% partial melting (although 5 to 35% is acceptable) of eclogite (or amphibolite), leaving a residue consisting predominantly of garnet and clinopyroxene. further modifications to this scheme resulted in modally specific and alternative parental rocks to be chosen, which vary from basic granulite (from two pyroxene-garnet-bearing to amphibolite-two pyroxene-garnet-bearing and garnet-free amphibolite). Figure 8 represents a summary of proposed partial melting and fractionation models in the genesis of tonalite/trondhjemite melts in general as derived from a basic parent (basic granulites not included, but may be equivalent in composition to a gabbro). On theoretical grounds, eclogite has been excluded as a source rock for Archean tonalites, since Archean geothermal gradients did not intersect the stability of eclogite (Figure 25, p. 62; Glikson, 1979). Other non-igneous source rocks such as short-lived Archean greywackes are also excluded as source rocks, since these would produce potassic-rich melts (Winkler, 1975), and not sodic-rich melts required for tonalites.

Whatever the mantle or lower crustal source, the parent must not only be basic in nature, but must satisfy experimental

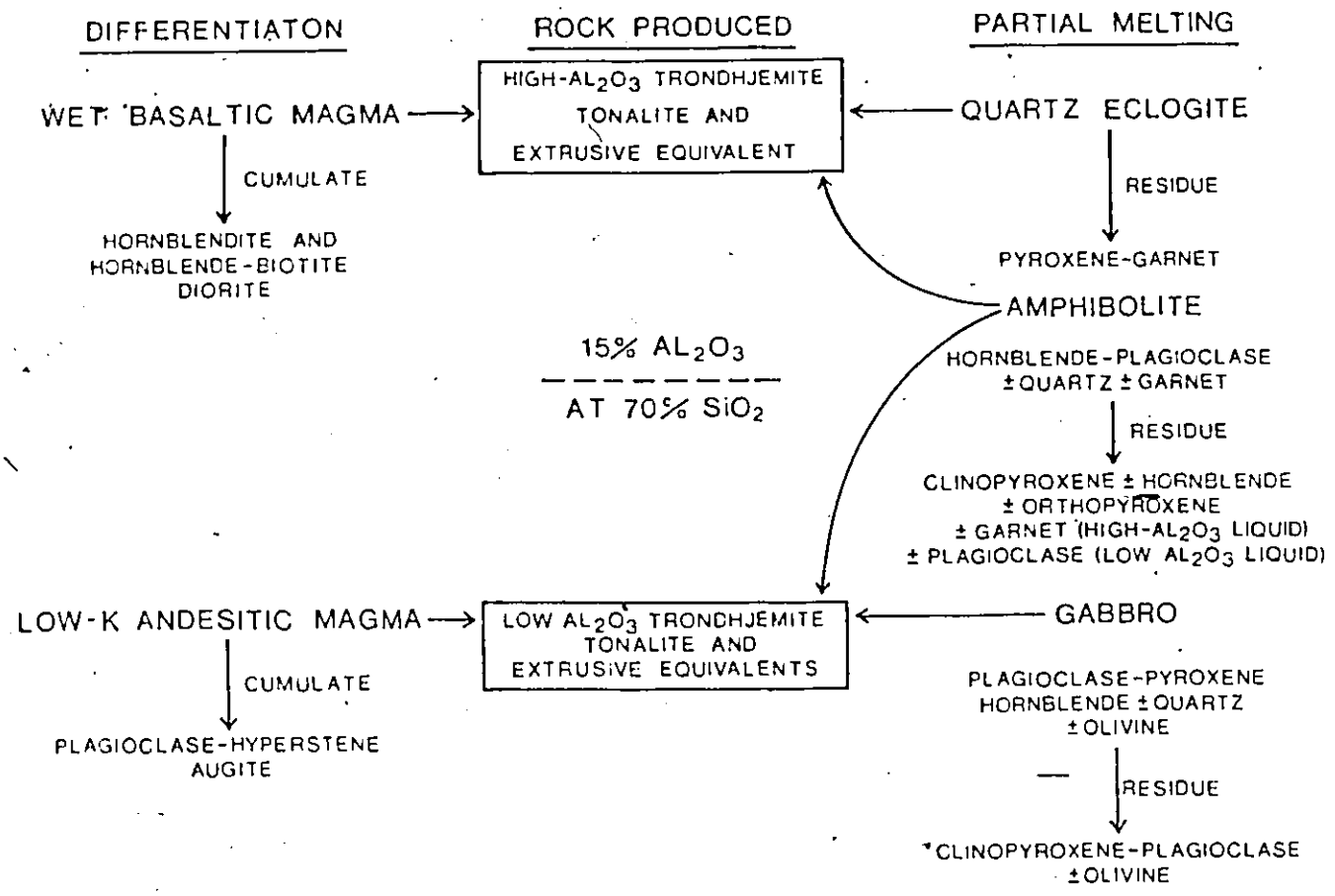

Fig. 8. Models of tonalite-trondhjemite genesis (Barker and Arth, 1976

studies in the series granite-tonalite-gabbro with H_2O (Wyllie, 1979).

Based on Archean geothermal gradients of either 30 to 35°C/km (Baer, 1977) or 40 to 50°C/km (Glikson, 1979), melting of basic crust to produce anhydrous tonalite liquid requires a minimum temperature of 1200°C (Figure 25, p. 62; Glikson, 1979). Similarly, Wyllie et al. (1976) and Wyllie (1979) showed that even if tonalites represent primary anhydrous melts (2% dissolved H_2O) formed by anatexis of lower continental crust (andesitic or tonalitic gneisses), the liquidus temperature would be still in excess of 1000°C (Figure 17-14B, p. 513; Wyllie, 1979). Both temperatures are beyond the upper limit of normal crustal metamorphism (less than 900°C for granulite facies metamorphism (Figure 17-14A, p. 513; Wyllie, 1979), although conditions in the Archean may have allowed for extreme temperatures in the lower crust. Addition of heat from the mantle to the lower crust (Wyllie, 1979) would be a plausible mechanism regulating the temperature.

The generation of Archean tonalites by melting of a basic parent, possibly ultramafic-mafic greenstones at lower crustal levels, temperatures greater than 1000°C and depths greater than 35 km, as suggested by Glikson (1979), is consistent with major and trace element modelling.

2) Chemical Analyses from the Round Lake Batholith

Major and trace element analyses from the Round Lake

Batholith and surrounding Abitibi Supergroup are listed in Appendices II and III, respectively, whereas REE and Th, Hf, and Sc from the major batholithic phases are listed in Table 4 (sample locations given in Figure 9; Ontario Geological Survey and Geological Survey of Canada samples are not included). Chemistry from the compilation of worldwide Archean tonalite/trondhjemite occurrences and the suite from Finland are listed in Appendix IV.

Sample distribution and laboratory facilities where analyses were performed are tabulated in Appendix I.

Analyses from the Ontario Geological Survey and Geological Survey of Canada were used to complement analyses of the batholith and surrounding supracrustal units, from areas that were not fully investigated or sampled. Ontario Geological Survey analyses supplement the tonalite (map-unit 8A), hornblende tonalite (map-unit 8C), granodiorite-tonalite (map-unit 9), and dyke category. Ontario Geological Survey samples are located in the central part of the batholith bounded by the twin northwest trending faults of the Timiskaming System. Geological Survey of Canada analyses are scattered throughout the batholith, wherever gaps in the sampling occurred. Abitibi Supergroup analyses from the Pacaud Tuffs were taken from the Boston Creek area along the northeast margin of the batholith, those of the Catharine-Wawbewawa from the northeastern and southwestern portions of the map area, and the Skead were taken

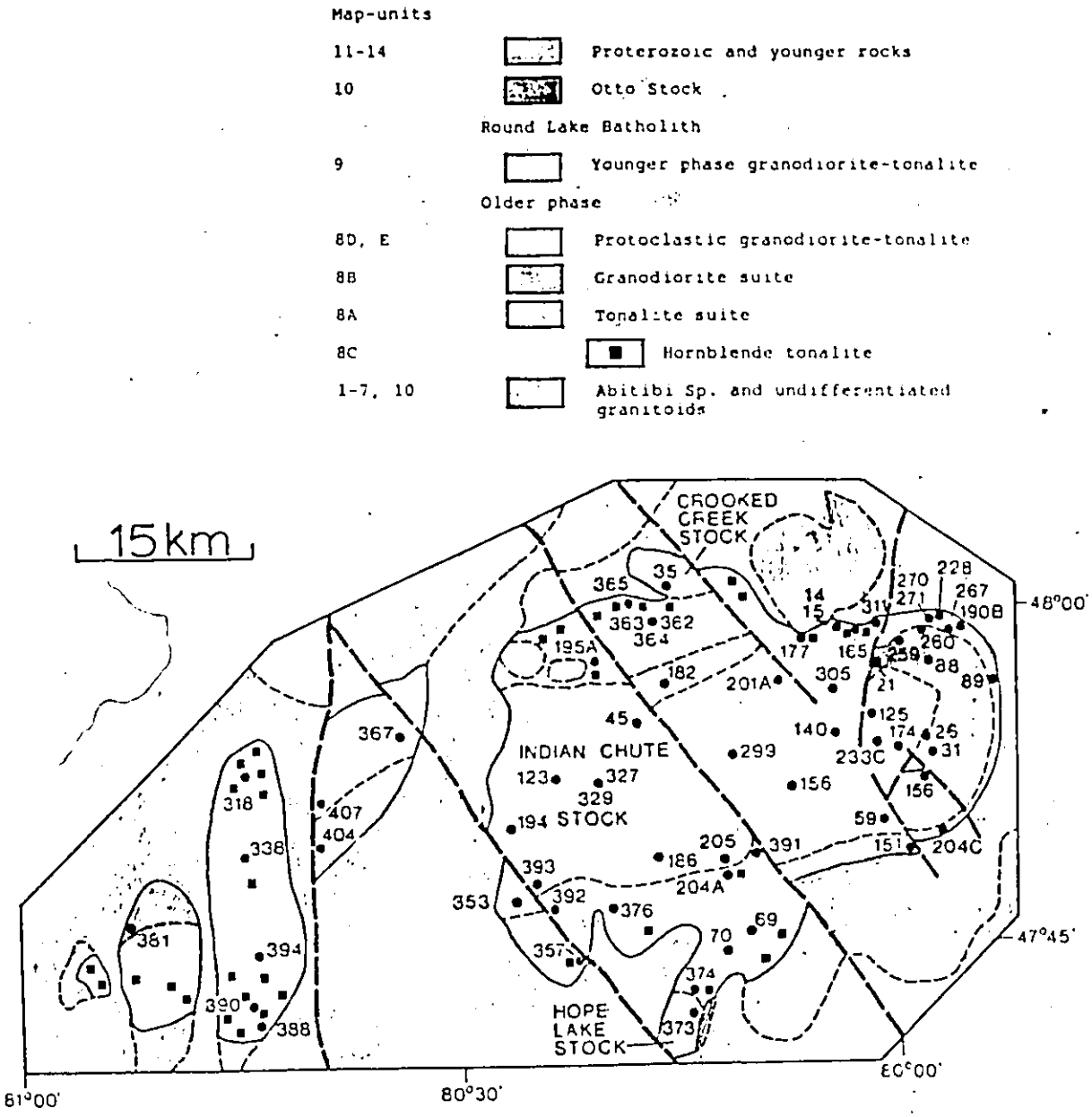

Fig. 9. Generalized geologic map of the Round Lake Batholith area showing locations of samples used in this study. OGS samples from the batholith and samples from the Abitibi Sp. are not included. Dashed, heavy set lines correspond to faults. Legend above.

from outside the map area to the east.

In Harker and triangular variation diagrams, analyses were plotted with symbols depicting rock types and laboratory facilities. The laboratory symbol subdivision shows the variability of analyses within a single map-unit, and enables a separation of trends largely controlled by either inter-laboratory bias (see Abbey, 1979) or magmatic differentiation. If each group of analyses from a single map-unit plots in a different portions of the diagram, so as to form a linear trend, this could be conceived as an erroneous variability brought about by inter-laboratory bias. Alternatively, if groups intermix with each other and form a linear trend, this trend may be interpreted as differentiation.

A) Results: major and trace element concentrations

A summary of major and trace element concentrations from the Round Lake Batholith and Abitibi Supergroup, in terms of mean chemical compositions and ranges, is given in Table 3. Included in Table 3 is a mean chemical composition for the volcanic pile of the Kirkland Lake-Timmins-Noranda area (from Goodwin, 1979), which is to be used in conjunction with the partial melting model of origin for the batholith.

The following patterns and interpretations are noted in the analytical data:

1) Field evidence demonstrates spatial and genetic relationships between the older phase tonalite

Table 3. Averaged (mean) chemical analyses from the Round Lake Batholith and Abitibi Supergroup. Oxide mean and range in weight %; trace element mean and range in ppm. σ -standard deviation; n-samples. For the complete listing of analyses see Appendices II and III.

Round Lake Batholith

	Map-unit 8A – Tonalite					Map-unit 8B – Granodiorite					Map-unit 8D, E – Granodiorite-tonalite					Map-unit 8C – Hornblende tonalite					Map-unit 9 – Granodiorite-tonalite				
Oxides	Mean	σ	Range		n	Mean	σ	Range		n	Mean	σ	Range		n	Mean	σ	Range		n	Mean	σ	Range		n
SiO_2	68.51	2.81	63.50	- 70.29	29	72.66	1.95	70.75	- 76.79	8	71.85	1.31	69.67	- 73.36	8	61.81	2.67	57.04	- 65.31	10	67.25	1.98	62.89	- 72.33	26
Al_2O_3	16.26	0.72	13.60	- 16.55	do	15.30	1.17	12.79	- 16.55	do	15.16	0.68	13.70	- 15.96	do	16.91	1.37	15.09	- 19.97	do	15.90	0.56	15.10	- 17.10	do
$Fe_2O_3TOT^3$	2.68	1.31	1.04	- 5.76	do	1.21	0.31	1.00	- 1.93	do	1.38	0.38	0.86	- 2.45	do	5.25	0.96	3.38	- 6.38	do	2.85	0.64	1.28	- 4.28	do
MgO	1.21	0.71	0.36	- 2.92	do	0.51	0.18	0.26	- 0.76	do	0.59	0.25	0.32	- 0.96	do	3.13	0.63	2.21	- 3.53	do	1.97	0.60	0.90	- 3.32	do
CaO	3.21	0.98	0.66	- 5.01	do	2.09	0.54	1.01	- 2.69	do	2.09	0.62	1.37	- 3.44	do	5.00	0.98	3.98	- 7.19	do	2.77	0.63	0.97	- 3.65	do
Na_2O	5.13	0.62	3.95	- 6.06	do	5.32	0.37	4.63	- 5.93	do	4.81	0.58	4.00	- 5.68	do	4.74	0.62	4.07	- 6.16	do	5.89	0.54	5.38	- 7.97	do
K_2O	1.33	0.39	0.80	- 3.73	do	1.76	0.36	1.29	- 2.22	do	2.18	0.66	1.21	- 2.98	do	1.54	0.38	1.05	- 2.37	do	1.59	0.33	0.69	- 2.08	do
TiO_2	0.30	0.16	0.11	- 0.58	do	0.13	0.03	0.08	- 0.19	do	0.15	0.07	0.09	- 0.29	do	0.35	0.08	0.46	- 0.68	do	0.34	0.07	0.19	- 0.56	do
P_2O_5	0.09	0.03	0.02	- 0.19	do	0.03	0.02	0.00	- 0.05	do	0.03	0.04	0.00	- 0.08	do	0.18	0.07	0.07	- 0.31	do	0.13	0.03	0.06	- 0.21	do
MnO	0.04	0.02	0.01	- 0.08	do	0.02	0.01	0.01	- 0.03	do	0.03	0.01	0.01	- 0.05	do	0.08	0.02	0.05	- 0.11	do	0.05	0.01	0.02	- 0.07	do
S	0.01	0.01	0.00	- 0.03	do	0.01	0.01	0.00	- 0.02	do	0.01	0.01	0.00	- 0.03	do	0.01	0.01	0.00	- 0.03	do	0.01	0.01	0.00	- 0.03	do
Trace elements																									
Ba	665	286.88	200	- 1541	23	512	176.59	265	- 718	do	508	235.61	291	- 1178	do	347	289.17	180	- 996	9	563	180.06	163	- 850	25
Cr	13	10.69	0	- 42	24	13	17.52	0	- 44	6	10	10.78	0	- 32	7	56	24.41	25	- 96	10	38	32.80	5	- 140	21
Zr	127	24.02	95	- 169	17	99	17.02	69	- 119	do	89	17.95	67	- 121	do	165	28.63	116	- 202	9	125	32.48	88	- 200	12
Sr	564	168.63	237	- 842	do	396	210.76	271	- 786	do	352	123.25	207	- 538	do	593	233.95	305	- 1038	do	657	198.03	239	- 1024	do
Rb	23	12.60	11	- 66	do	32	12.01	18	- 69	do	30	17.41	25	- 80	do	33	17.51	8	- 55	do	28	11.63	17	- 68	6
Zn	23	20.90	0	- 91	do	13	16.39	0	- 63	do	12	7.96	0	- 21	do	50	20.20	31	- 93	do	33	19.08	0	- 52	do
Ni	14	7.37	3	- 36	23	13	9.52	3	- 30	do	9	3.63	4	- 13	do	42	18.63	13	- 69	10	32	9.49	19	- 50	19
K/Rb			286.27	- 876.86				358.09	- 594.95				309.23	- 505.82				257.35	- 1161.67				336.95	- 629.80	
Rb/Sr			0.02	- 0.19				0.02	- 0.12				0.07	- 0.27				0.01	- 0.16				0.02	- 0.10	
Ca/Sr			13.79	- 119.62				16.11	- 32.66				23.23	- 73.83				27.60	- 102.71				19.26	- 64.76	
K/Sr			10.16	- 54.22				13.62	- 33.91				30.16	- 107.88				10.00	- 61.64				11.49	- 31.62	
K/Ba			11.43	- 39.85				15.21	- 70.82				18.46	- 51.22				13.09	- 30.73				17.01	- 33.16	
Ba/Rb			9.32	- 76.38				5.00	- 39.11				6.76	- 27.40				6.37	- 79.30				9.39	- 28.38	
Ba/Sr			0.38	- 2.15				0.39	- 1.33				0.81	- 2.19				0.36	- 1.98				0.42	- 1.36	

Map-unit 1 – Pascal Tuffs					Map-units 2,3 Catharine-Mawbeewawa Gps					Map-unit 4 – Stead Gp					Abitibi Supergroup[1]			Kirkland Lake-Timmins-Noranda[2]	
Mean	σ	Range		n	Mean	σ	Range		n	Mean	σ	Range			Mean	σ	n	Mean	n
50.87	6.25	42.04 -	65.50	19	48.38	4.75	42.20 -	74.90	62	56.96	4.90	46.40 -	61.90	10	50.37	5.88	71	53.20	1046
13.98	1.53	11.30 -	16.40	do	13.42	1.36	10.00 -	16.00	do	14.31	1.42	11.60 -	16.50	do	13.72	1.46	do	14.90	do
11.19	3.36	6.90 -	17.30	do	13.33	2.77	6.20 -	19.10	do	9.88	0.97	6.90 -	7.80	do	12.02	3.88	do	9.39	do
6.54	2.16	1.92 -	9.02	do	5.71	1.79	0.66 -	9.26	do	5.04	1.17	3.50 -	7.30	do	5.70	1.83	do	5.30	do
9.31	3.00	6.70 -	15.00	do	9.69	2.90	2.12 -	14.25	do	5.97	1.50	4.20 -	8.30	do	9.20	2.59	do	7.10	do
2.31	1.03	0.30 -	3.90	do	2.69	0.83	1.10 -	5.00	do	3.02	1.67	0.10 -	5.00	do	2.63	1.03	do	3.20	do
0.66	0.90	0.08 -	3.96	do	0.35	0.30	0.00 -	1.16	do	1.88	1.63	0.50 -	5.20	do	0.63	0.93	do	0.30	do
0.87	0.38	0.37 -	1.63	do	1.18	0.38	0.30 -	2.36	do	0.50	0.10	0.38 -	0.64	do	1.00	0.63	do	1.01	do
				0	0.10	0.02	0.00 -	0.18	28					0	0.07	0.04	43	0.16	410
0.20	0.06	0.06 -	0.33	19	0.23	0.06	0.11 -	0.43	62	0.25	0.55	0.09 -	1.24		0.24	0.14	71	0.19	1066
				0	0.23	0.20	0.00 -	0.69	10						0.19	0.22	21		
110	81.03	20	- 301	17	91	76.34	30	- 390	39	523	845.55	130	- 2909	10	162	337.81	66	236	1012
211	131.93	7	- 421	do	198	149.36	8	- 510	28	196	67.18	110	- 330	8	202	127.23	53	188	934
75	27.22	42	- 120	13	106	79.98	32	- 340	34	93	20.55	72	- 120	6	96	63.76	53	100	1008
154	53.14	62	- 270	19	163	140.70	65	- 960	39	326	172.38	160	- 730	10	184	139.70	68	172	993
31	45.38	8	- 104	3											31	45.38	8		
56	26.72	28	- 86	do											56	26.72	do	73	1002
126	62.90	11	- 230	18	182	69.55	67	- 320	do	202	44.67	150	- 290	do	170	70.08	67	154	987

[1]Mean (and standard deviation) chemical composition of the Abitibi Supergroup used in this study.

[2]Mean (and standard deviation) chemical composition in the Kirkland Lake-Timmins-Noranda area (Table 6 in Goodwin, 1979).

[3]Total iron, in Table 3 and appendices II, III, IV, is given as Fe_2O_3.

(map-unit 8A), granodiorite (map-unit 8B), and marginal cataclastic granodiorite-tonalite (map-units 8D, E). Chemically, there are somewhat minor variations in the chemistry of older phase units. Means for SiO_2, Al_2O_3, Fe_2O_{3TOTAL}, CaO, Na_2O(?) and TiO_2 tend to decrease from tonalite to the cataclastic granodiorite-tonalite, whereas K_2O tends to increase. The trace elements Ba, Sr and Rb (the LiL elements) manifest considerable dispersion about their means in all three units. Ba ranges from 200 to 1541 ppm, with a mean of 445 ppm, in the tonalite; 245 to 718 ppm in the granodiorite (mean of 512 ppm); and 291 to 1178 ppm in the cataclastic granodiorite-tonalite (mean of 508 ppm). Sr ranges from 237 to 842 ppm, 271 to 786 ppm, and 207 to 538 ppm for the same three units (means of 564, 594 and decreasing to 352 ppm respectively). Rb ranges from 11 to 66 ppm, 18 to 49 ppm, and 23 to 80 ppm with increasing means of 23, 32 and 50 ppm. Cr, Zn and Ni values are too low to be of significance, whereas Zr appears to decrease. Trace element, and major to trace element ratios (Rb/Sr, Ba/Rb, Ba/Sr, K/Rb, K/Sr, K/Ba, Ca/Sr) offer a wide range of values with no consistent variation between the units.

Interpretation: perhaps the most striking

feature of these analyses is the nominal amount of variation across the older phase of the batholith considering its large dimensions. The compositional homogeneity in the mineralogy and chemistry depicts a single source - single magma origin for the older phase, with the internal variations caused by minor differentiation.

2) The younger phase granodiorite-tonalite (map-unit 9) oxide data resemble that of the older phase tonalite (map-unit 8A). Trace element means are generally higher for Ba, Cr, Sr, Zn and Ni, and equivalent for Zr and Rb. Trace, and oxide to trace element ratios offer a narrower range of values than the older phase tonalite, and there is a significant overlap.

Interpretation: major elements from the younger phase granodiorite-tonalite and the older phase tonalite demonstrates that both units have a common origin, probably the same parent, although their age difference and trace element discrepancies promote two distinct evolutionary lines.

3) Hornblende tonalite of the older phase (map-unit 8C) has lower mean values for SiO_2, and higher Al_2O_3, Fe_2O_{3TOTAL}, MgO and CaO when compared to the other units in general. Trace element values show the same type of dispersion about their means as depicted by

the other batholithic units, or the means approaching those of the younger phase granodiorite-tonalite.

Interpretation: features such as these mafic indicators, in addition to the mafic xenolith content of the tonalite and the latter's proximity to the Abitibi Supergroup, suggests a possible link to the supracrustal rocks surrounding the batholith, whether via derivation or contamination. In addition, the possibility of a link between the hornblende tonalite and the younger phase is plausible, since both have a similar spatial distribution (margin of the batholith), lack a strong foliation, and are xenolith-rich. Alternatively, the hornblende tonalite may also be a late pulse, emplaced along contact zones between older phase tonalite and either Abitibi Supergroup rocks or younger phase granodiorite-tonalite (Fig. 9).

4) Means from the Abitibi Supergroup show considerable variability in SiO_2, Fe_2O_{3TOTAL}, CaO, K_2O, Ba, Sr and Ni between the mixed Pacaud Tuffs and komatiitic-tholeiitic Catharine-Wawbewawa Groups, and the calc-alkaline Skead Group. Skead Group rocks are generally higher in SiO_2, Na_2O, K_2O, Ba, Sr and Ni, and lower in Fe_2O_{3TOTAL} and CaO. The overall mean of the Supergroup approximates the regional composite ~~from~~ the Abitibi Belt.

Table 4. Rare earth elements, Th, Hf and Sc in ppm from the Round Lake Batholith. Chondritic meteoritic values from Haskin et al. (1968) were used to normalize rare earth values of Eu/Eu*, and in Figs. 11, 13 and 24. For sample locations see Fig. 9.

Map-Unit	8A				8B	8E	8C	9
Sample No.	14	70	136	299	88	228	390	35
La	22	11	10	6	8	15	46	16
Ce	42	22	50	12	16	25	109	35
Sm	2	25	1	1	1	1.5	9	2.5
Eu	0.8	0.8	0.9	0.3	0.5	0.6	2	1
Tb	0.2	0.3	0.2	0.1	0.1	0.2	0.8	0.2
Yb	0.3	0.7	0.3	0.1	0.2	0.5	1	0.5
Lu	0.07	0.12	0.04	0.03	0.03	0.07	0.21	0.07
Th	3	1.5	4	1	1	2	5.5	2.5
Hf	4	3	5	2	3	3	3	3
Sc	2.5	6.5	3	1.5	2	3	13	6
ΣREE	67.4	37.4	62.4	19.5	25.8	42.9	168	55.3
Eu/EU*[1]	1.4	1.2	2.4	1.4	1.5	1.4	0.9	1.0
La/Yb	86	15	29	60	36	32	38	35

[1] Eu/Eu* = observed Eu value ÷ value obtained by interpolation between Sm and Tb (or Sm and Gd as in some REE data of Appendix IV).

Interpretation: in granite-greenstone belt development, the formation of plutonic tonalite/trondhjemite suites is believed to be accompanied by acid volcanism (see Glikson, 1979). Dacitic to rhyolitic lenses would be emplaced above early greenstone cycles intruded by the batholith and below upper greenstone cycles which postdate the intrusions. This cyclic scenario is certainly consistent with the volcanic stratigraphy for the Kirkland Lake segment of the Abitibi Belt. The Skead Group, representing a calc-alkaline sequence of basaltic to rhyolitic lavas and pyroclastics, and rhyolitic porphyries would be an equivalent to these acid volcanic lenses emplaced above the precursor cycle (Pacaud Tuffs) and below the second cycle (Larder Lake Group). According to the scenario, the Skead Group would be classified as an extrusive differentiate of the Round Lake Batholith, the batholith being the closest major tonalitic intrusion to the Skead. A model encompassing this scenario would not only have to contend with the lower SiO_2 and higher Fe_2O_3, MgO, CaO, Cr and Ni values of the Skead, when compared to any unit of the Round Lake Batholith (which is incompatible with differentiation) and also the intrusive relationship of the batholith with the

post-Skead Larder Lake Group. Details of the origin of the volcanic pile, particularly the Skead Group, are beyond the scope of the thesis. The Abitibi Supergroup analyses are presented here for comparative and batholith modelling purposes only.

REE are 19 to 67 ppm for tonalite (map-unit 8A), about 26 ppm for granodiorite (map-unit 8B) and 43 ppm for cataclastic granodiorite (map-unit 8E). All feature a small positive Eu anomaly (Eu/Eu* between 1.2 and 2.4), and all are LREE enriched (La/Yb) ranges between 15 and 86 for the tonalite, and is 36 and 32 for the granodiorite and cataclastic granodiorite, respectively). Th ranges from 1 to 4 ppm, Hf from 2 to 5 ppm and Sc from 1.5 to 6.5 ppm; all relatively low values.

The younger phase granodiorite-tonalite REE and Th, Hf, Sc values overlap with those of the older phase units with the exception of a lower Eu/Eu* at 1.0. Hornblende tonalite is higher in all REE (total REE of 168 ppm), and Th and Sc values than either the older or younger phases. The Eu anomaly is slightly negative (Eu/Eu* at 0.9), whereas the Hf content of 3 ppm is compatible with the others. The anomalously high REE values may be related to the above normal sphene and apatite contents in sample 390 (1% each; Table 2) and trace allanite and zircon, since accessory minerals such as these are important in controlling concentrations of REE (see Table 5).

The REE data and Th, Hf, Sc values from the older and

younger phases, with the possible exception of the hornblende tonalite, are consistent with an origin from the same parent, and reaffirm the contention that the older phase is chemically homogeneous.

B) Variation diagrams: classification, comparison and trends

Chemical analyses from the Round Lake Batholith (Table 3 and Appendix II) are compatible with other Archean tonalite/trondhjemite suites. One significant deviation is the relativley low Rb content of the batholith, at less than 80 ppm overall, compared to Archean suites which range up to 200 ppm. This characteristic probably reflects the Rb depleted nature of the parent. Compatibility also encompasses the quartz normative character of all batholithic units. In contrast, corundum normative rocks are mostly restricted to the older phase, with the exception of the hornblende tonalite which is predominantly diopside normative, as is the younger phase granodiorite-tonalite. Conversion from diopside to corundum normative occurs at approximately 65% SiO_2, which is consistent with the division employed by Barker (1979).

Harker diagrams (Fig. 10) for both Round Lake Batholith phases, including hornblende tonalite, show major element trends with negative and poor positive correlations in terms of SiO_2. Al_2O_3, Fe_2O_{3TOTAL}, MgO and CaO exhibit negative correlations with SiO_2, whereas Na_2O and K_2O exhibit a poor positive correlation. Trends for

Fig. 10. SCATTERGRAM - generated Harker diagrams for the Round Lake Batholith and Abitibi Supergroup Pacaud Tuffs, and Wawbewawa-Catharine-Skead Groups. (a) Map-units 1-4 (1: Pacaud Tuffs, 2: Wawbewawa group, 3: Catharine Group, 4: Skead Group) and 8 (Round Lake Batholith older phase), including dykes and xenoliths. (b) Map-units 1-4, 8, and 9 (Round Lake Batholith younger phase), including dykes and xenoliths.

Symbol nomenclature[1]:

Round Lake Batholith

Dotted line field	▲ △ ▲	Tonalite (map-unit 8A)
	● ○	Granodiorite (map-unit 8B)
	■ □	Cataclastic granodiorite-tonalite (map-units 8D,E)
	◆ ◇	Hornblende tonalite (map-unit 8C)
	● ⊙	Dykes
	◆ ◇ ◈	Granodiorite-tonalite (map-unit 9)
	⊞	Xenoliths (amphibolite; OP-in 8A, YP-in 9)

Abitibi Supergroup

	◪ ◪	Pacaud Tuffs (map-unit 1)
Solid line field	⊟	Catharine-Wawbewawa Groups (map-units 2, 3)
	◫	Skead Group (map-unit 4)

[1]Filled symbol: sample analysed at the University of Ottawa

Open symbol: sample analysed at the Geological Survey of Canada

Dotted open symbol: sample analysed at the Ontario Geological Survey

(10 a)

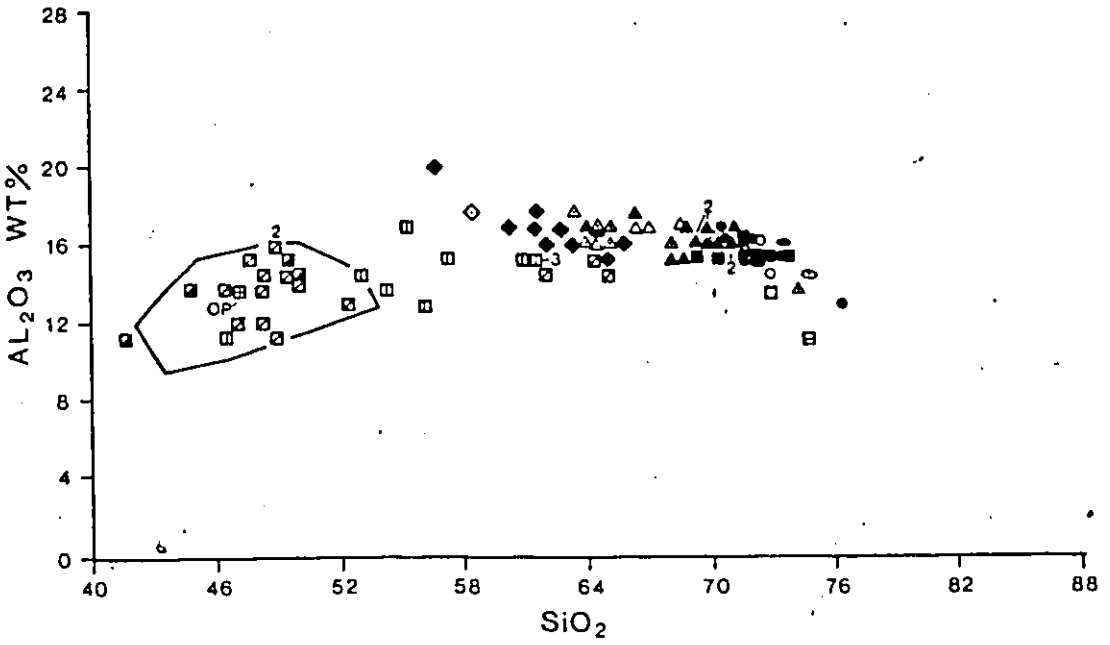
28
24
20
16
12
8
4
0
AL_2O_3 WT%
OP
40
46
52
58
64
70
76
82
88
SiO_2

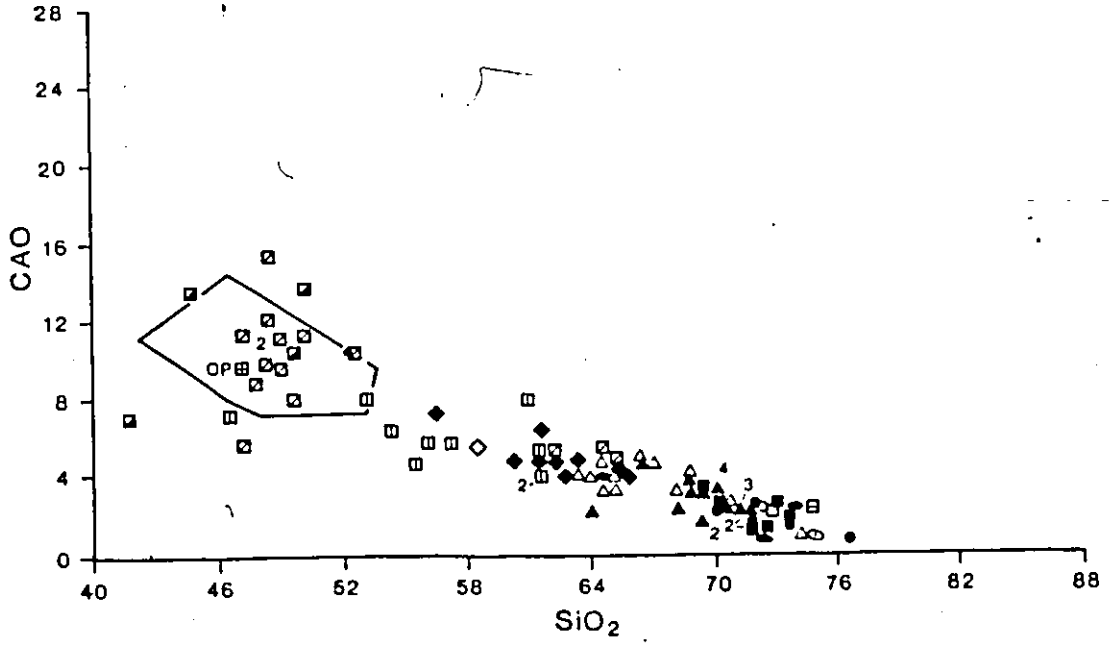
28
24
20
16
12
8
4
0
CAO
OP
40
46
52
58
64
70
76
82
88
SiO_2

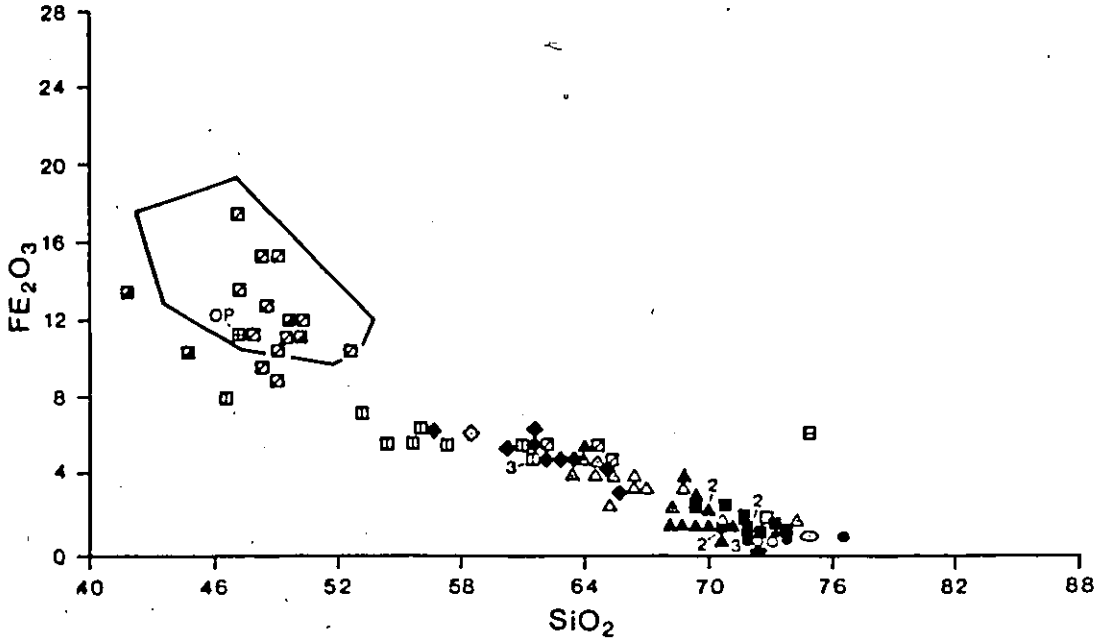
28
24
20
16
12
8
4
0
FE_2O_3
OP
40
46
52
58
64
70
76
82
88
SiO_2

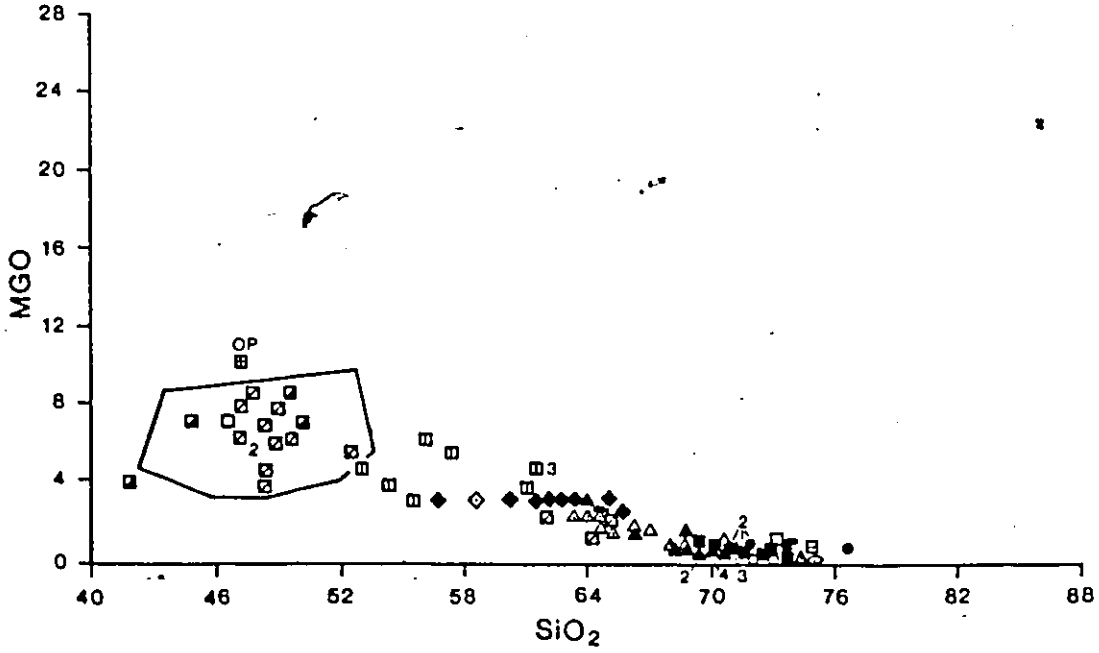
28
24
20
16
12
8
4
0
MGO
OP
40
46
52
58
64
70
76
82
88
SiO_2

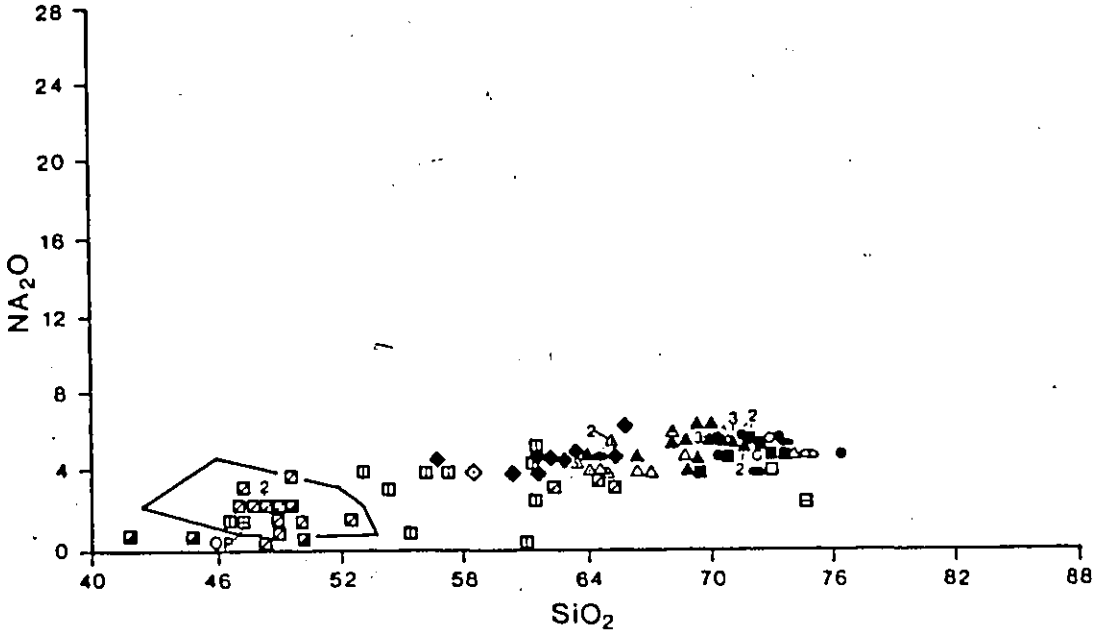
28
24
20
16
12
8
4
0
NA_2O
40
46
52
58
64
70
76
82
88
SiO_2
OP

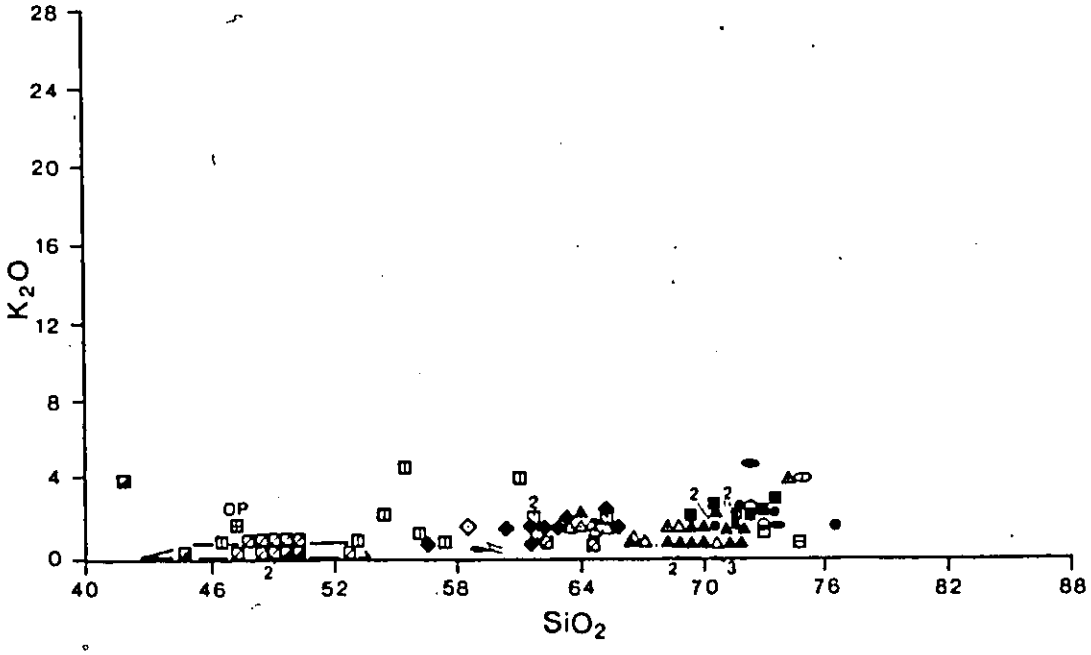
28
24
20
16
12
8
4
0
K_2O
40
46
52
58
64
70
76
82
88
SiO_2
OP

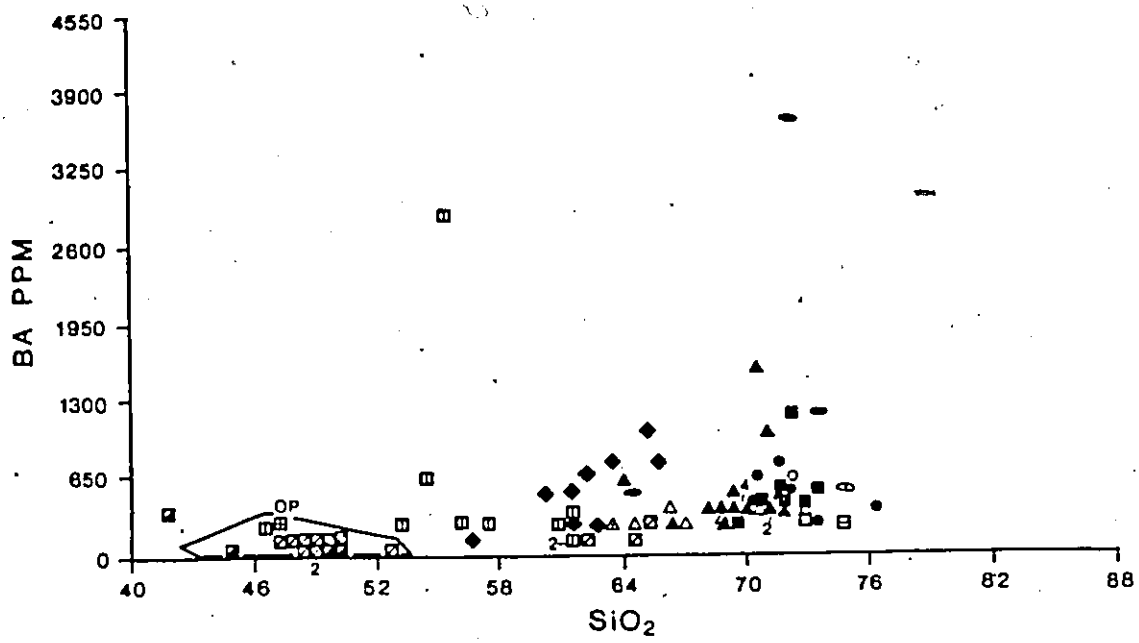
4550
3900
3250
2600
1950
1300
650
0
BA PPM
OP
2
2
2
40
46
52
58
64
70
76
82
88
SiO2

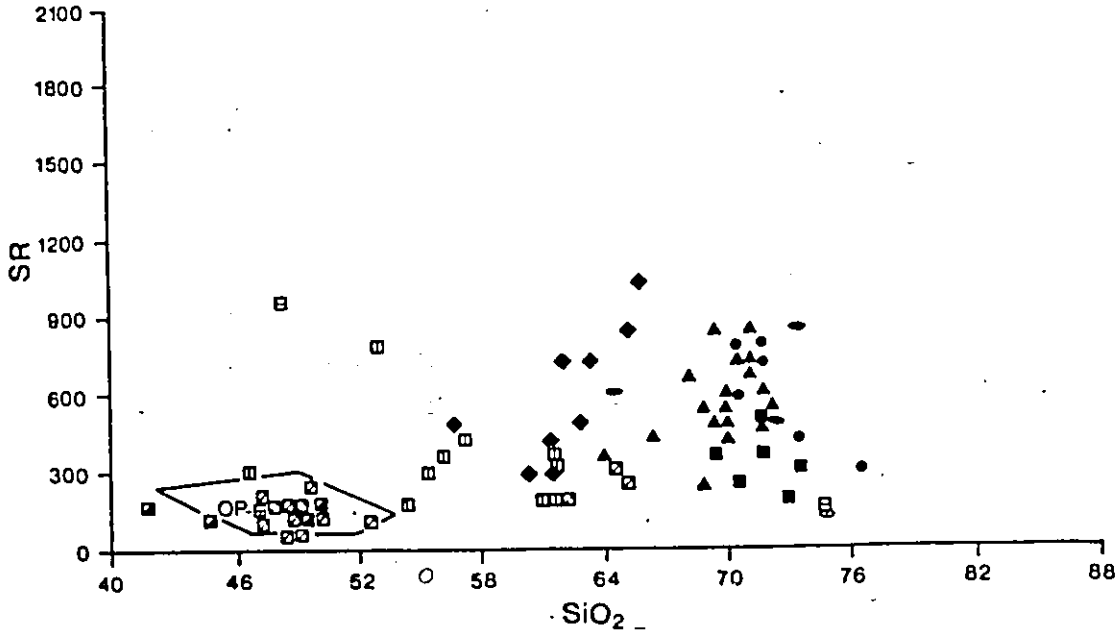
2100
1800
1500
1200
900
600
300
0
SR
OP
40
46
52
58
64
70
76
82
88
SiO2

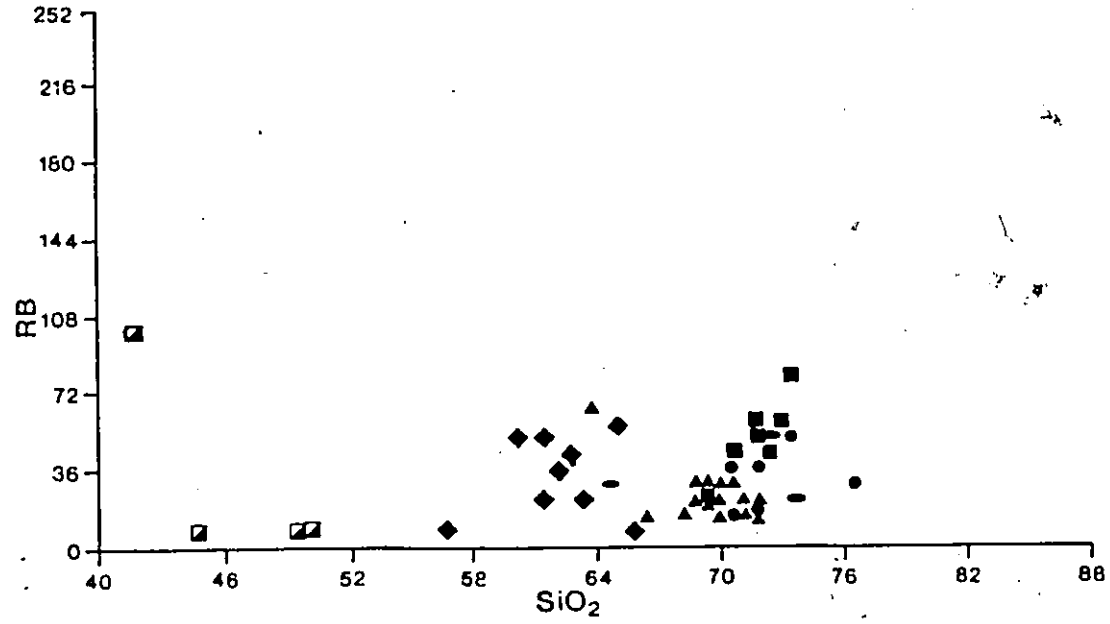
252
216
180
144
108
72
36
0
RB
40
46
52
58
64
70
76
82
88
SiO2

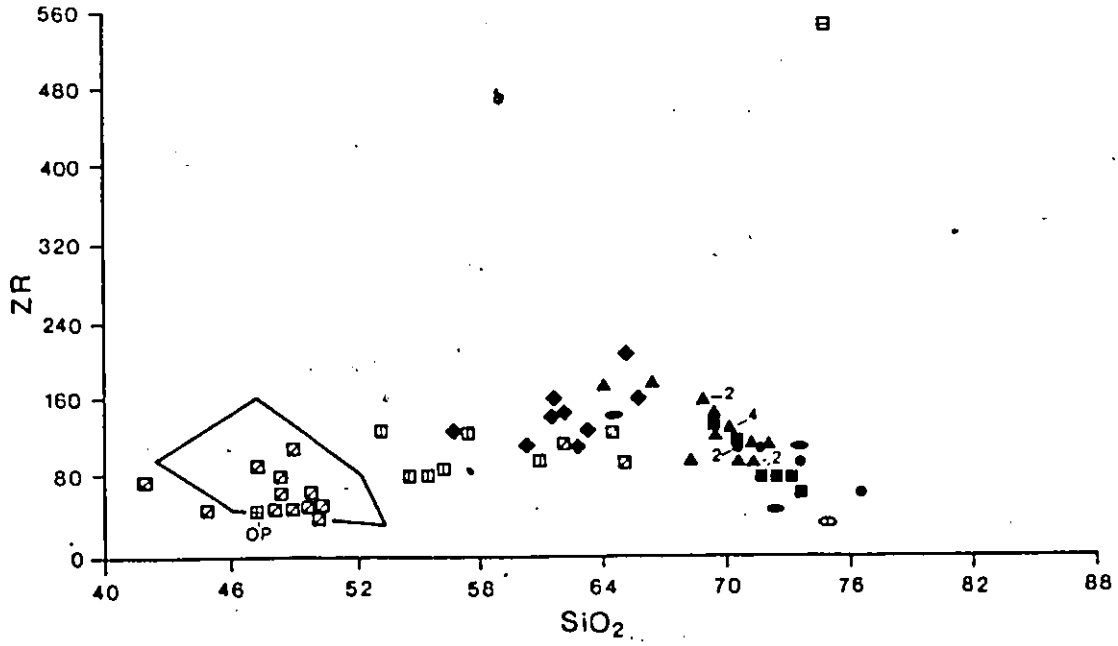
560
480
400
320
240
160
80
0
ZR
OP
40
46
52
58
64
70
76
82
88
SiO2

(10 b)

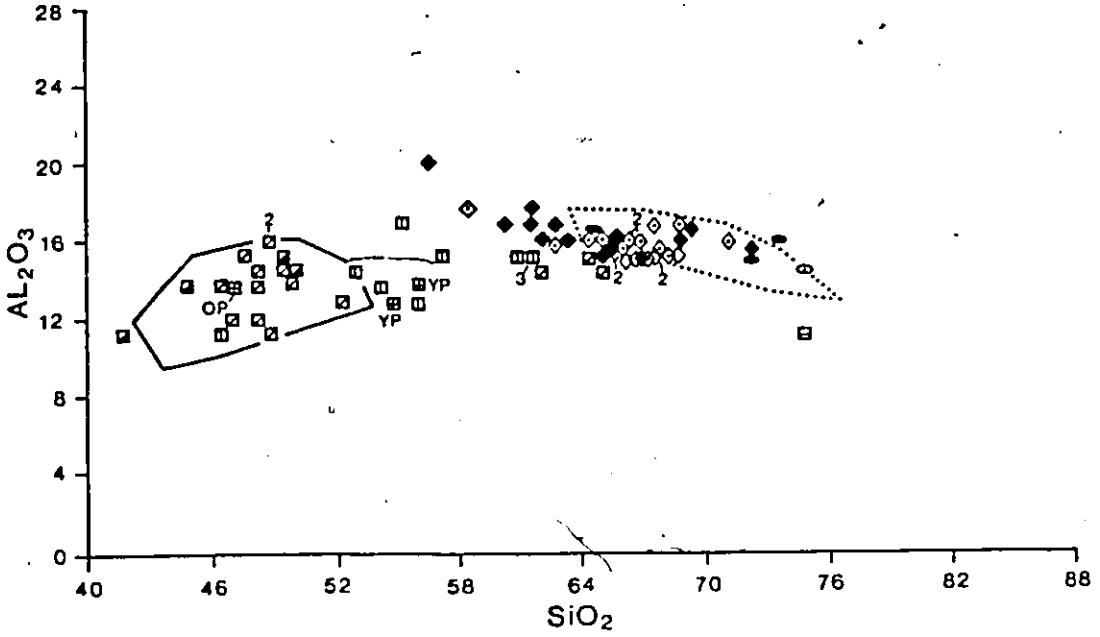
28
24
20
16
12
8
4
0
AL_2O_3
40
46
52
58
64
70
76
82
88
SiO_2
OP
YP
YP
?
2
2
2
3

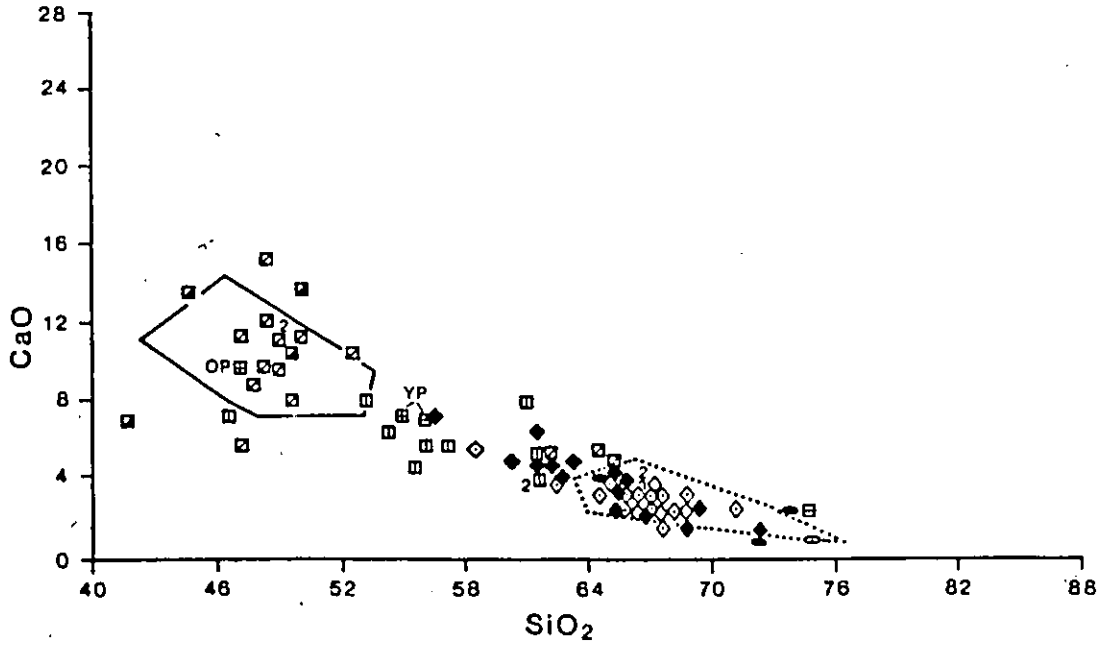
28
24
20
16
12
8
4
0
CaO
40
46
52
58
64
70
76
82
88
SiO_2
OP
YP
?
2

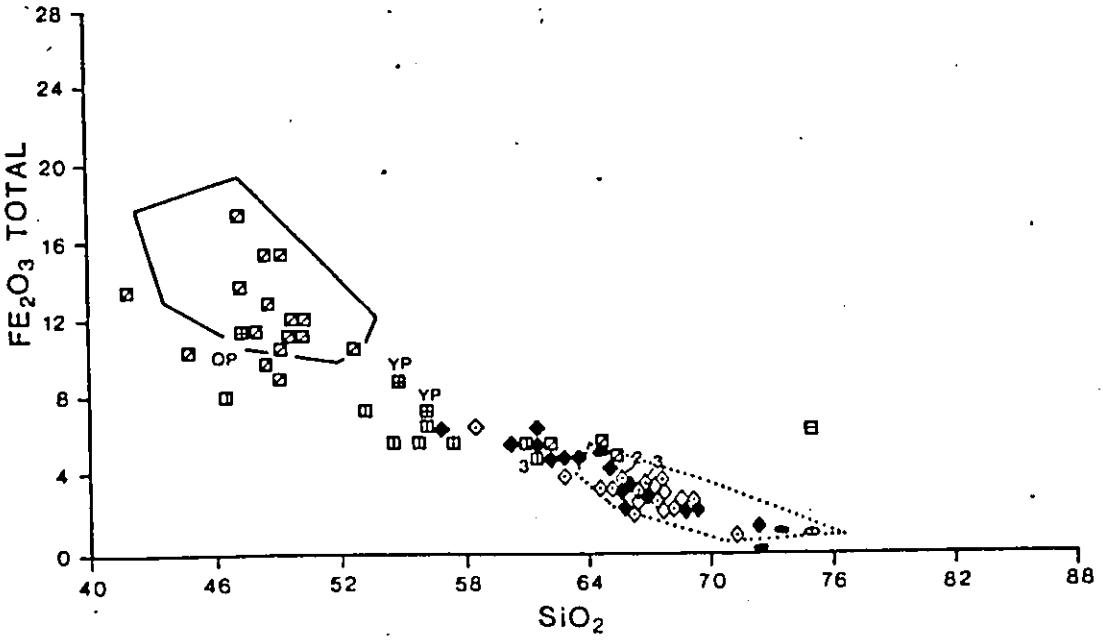
28
24
20
16
12
8
4
0
FE_2O_3 TOTAL
OP
YP
YP
3
2
3
40
46
52
58
64
70
76
82
88
SiO_2

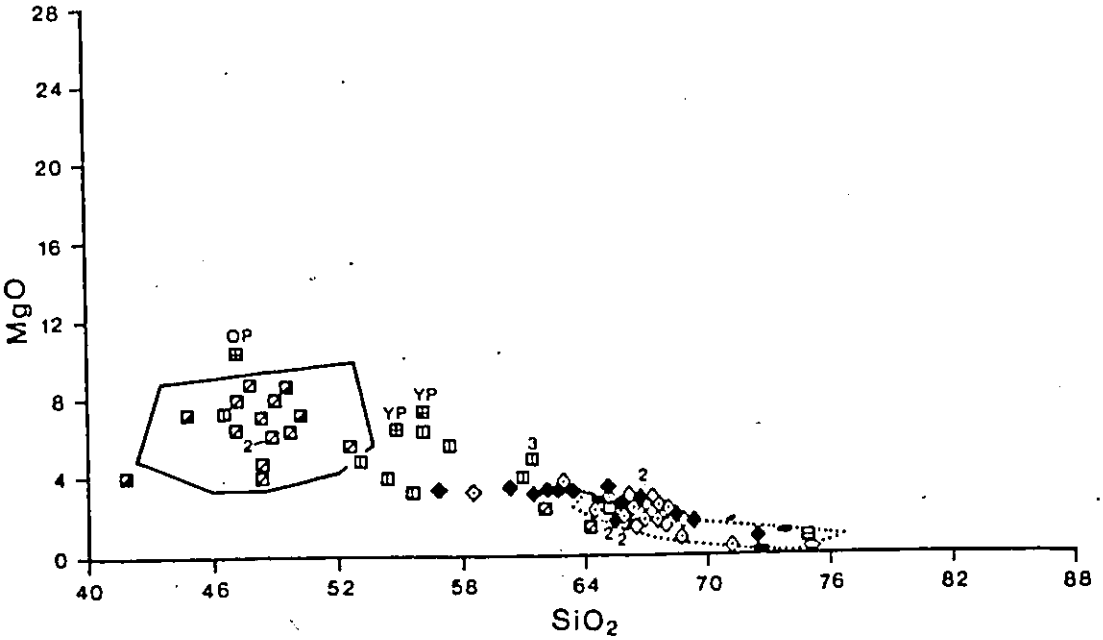
28
24
20
16
12
8
4
0
MgO
OP
YP
YP
2
3
2
2
2
40
46
52
58
64
70
76
82
88
SiO_2

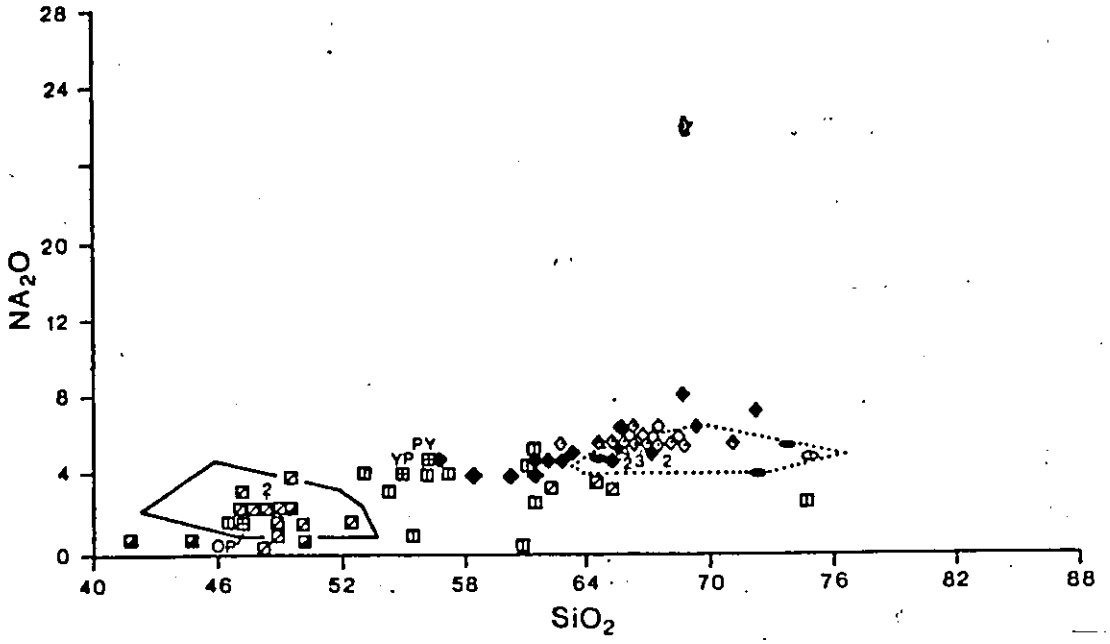
28
24
20
12
8
4
0
NA_2O
40
46
52
58
64
70
76
82
88
SiO_2
PY
YP
OP
?
2
3

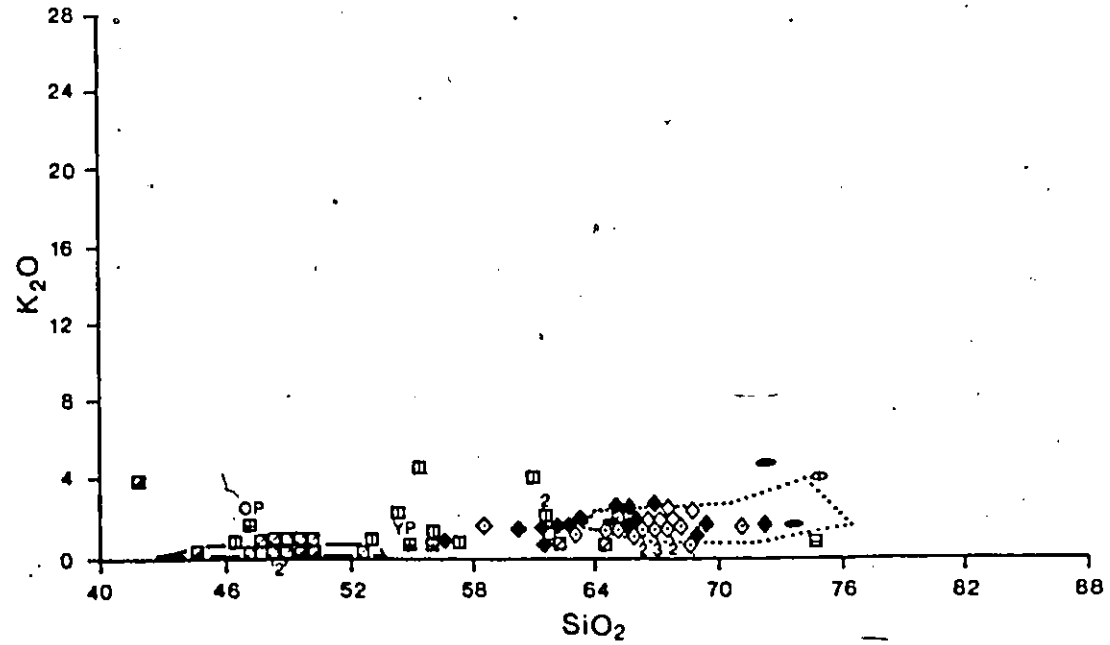
28
24
20
16
12
8
4
0
K_2O
40
46
52
58
64
70
76
82
88
SiO_2
OP
YP
2
3

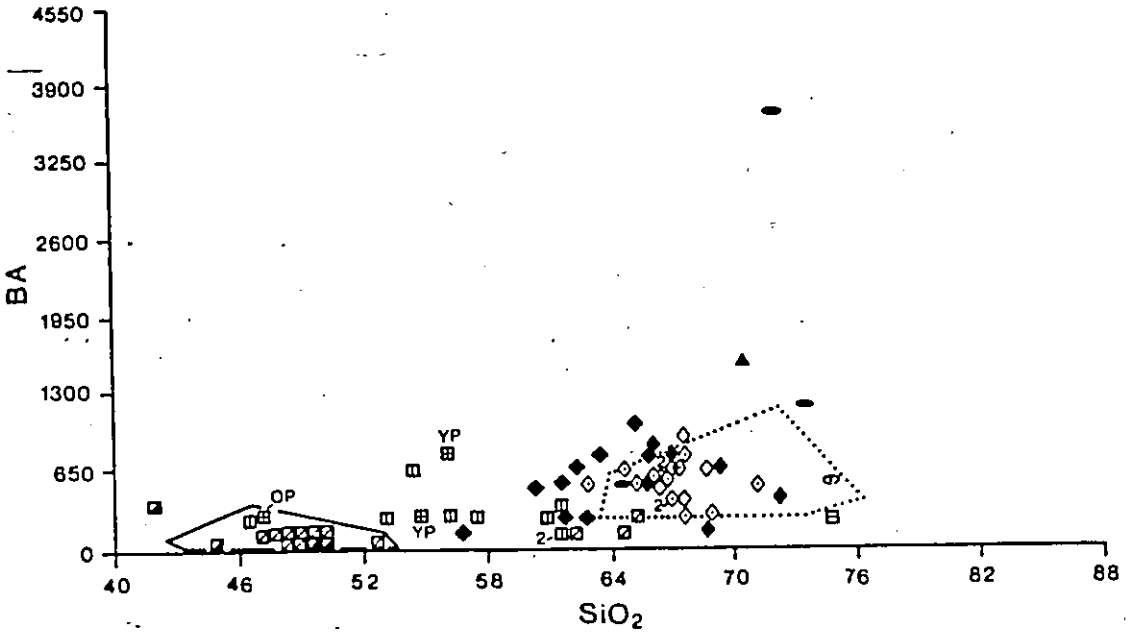
4550
3900
3250
2600
1950
1300
650
0
BA
YP
OP
YP
2
2
40
46
52
58
64
70
76
82
88
SiO2

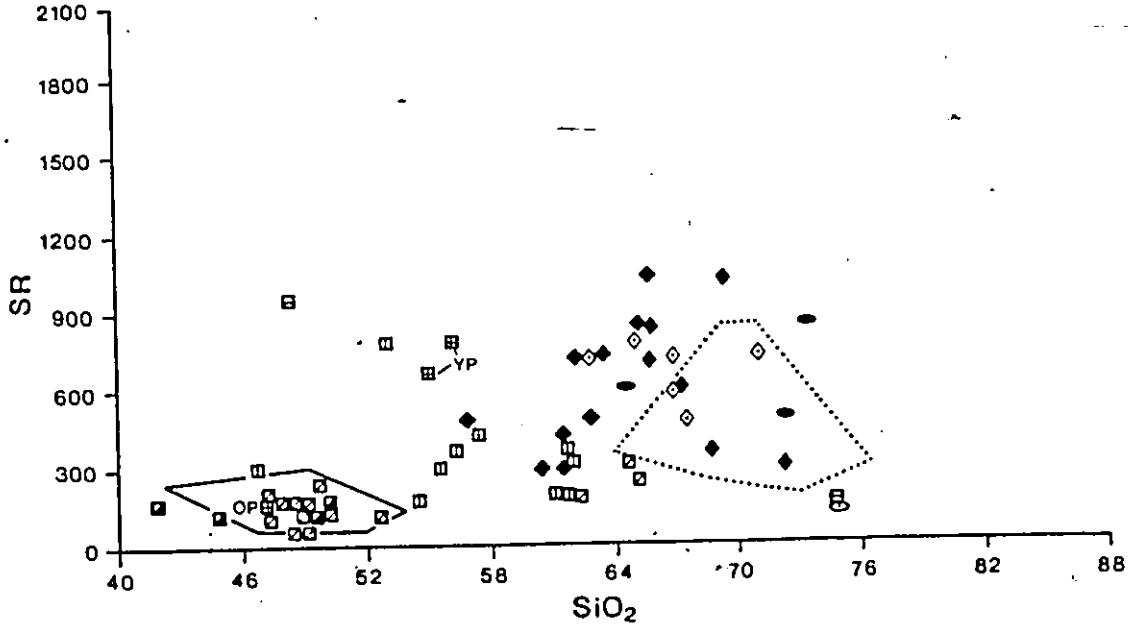
2100
1800
1500
1200
900
600
300
0
SR
YP
OP
40
46
52
58
64
70
76
82
88
SiO2

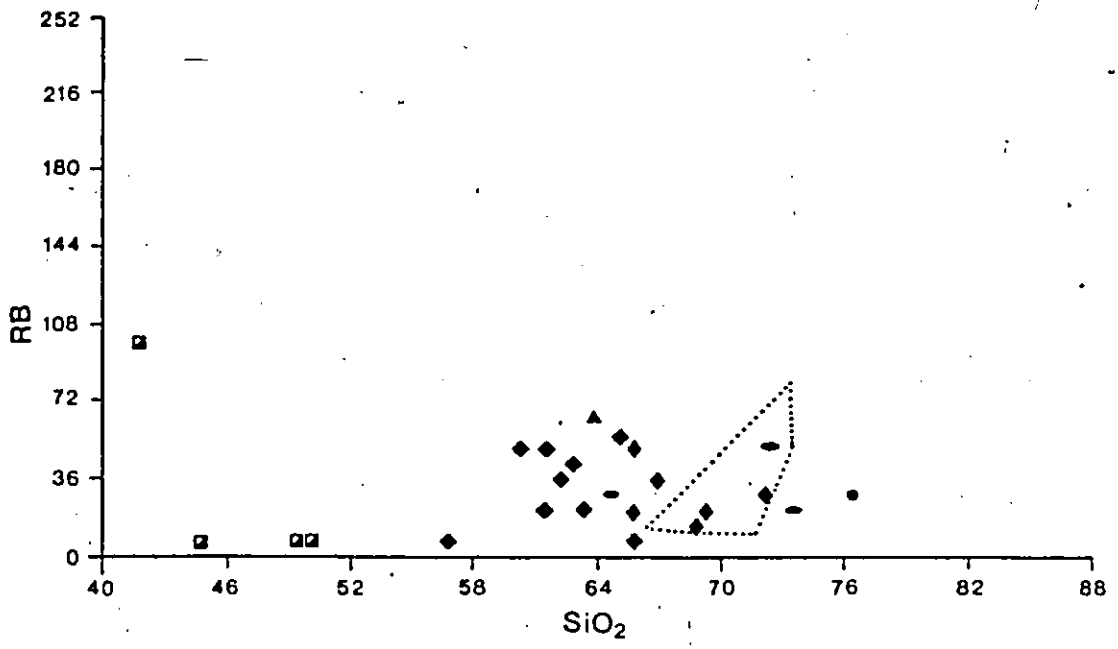
252
216
180
144
108
72
36
0
RB
40
46
52
58
64
70
76
82
88
SiO2

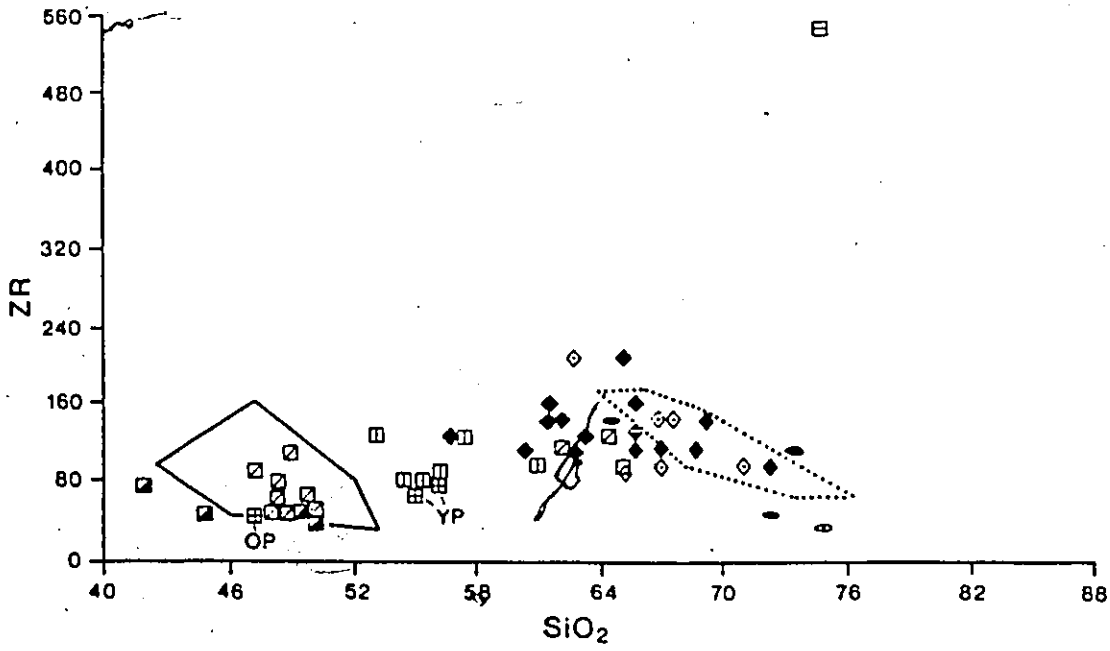
560
480
400
320
240
160
80
0
ZR
OP
YP
40
46
52
58
64
70
76
82
88
SiO2

the younger phase are generally less marked, with a clustering of results between 64 and 70% SiO_2. Trace element trends from both phases (excluding the hornblende tonalite) are vague owing to few results and the scattered distribution of data points. Nevertheless, Ba and Rb from the older phase tonalite, granodiorite and cataclastic marginal unit show a somewhat weak positive correlation, and Zr shows a significant negative correlation. Within the older phase hornblende tonalite, Ba and Sr exhibit a strong positive correlation, whereas Zr shows a poor positive correlation.

Both pegmatite and aplite dykes plot closely, or slightly within, the older phase field for all elements (data points at roughly 72, 73.5 and 75% SiO_2). The quartz-feldspar porphyry dyke (at 64.5% SiO_2) plots in proximity to the younger phase clusters of analyses and within the hornblende tonalite field.

Analyses from the Abitibi Supergroup Pacaud Tuffs, and Catharine-Wawbewawa and Skead Groups are included in the Harker diagrams (Fig. 10). With few exceptions, the Pacaud and Catharine-Wawbewawa units plot in the same field, whereas Skead Group rocks plot outside the field (mostly because of higher SiO_2) and define a trend extending from the other two units. Overall, Al_2O_3 shows the only distinct positive correlation with SiO_2; Na_2O and K_2O are weakly positive; and Fe_2O_{3TOTAL}, MgO and CaO show a strong negative correlation.

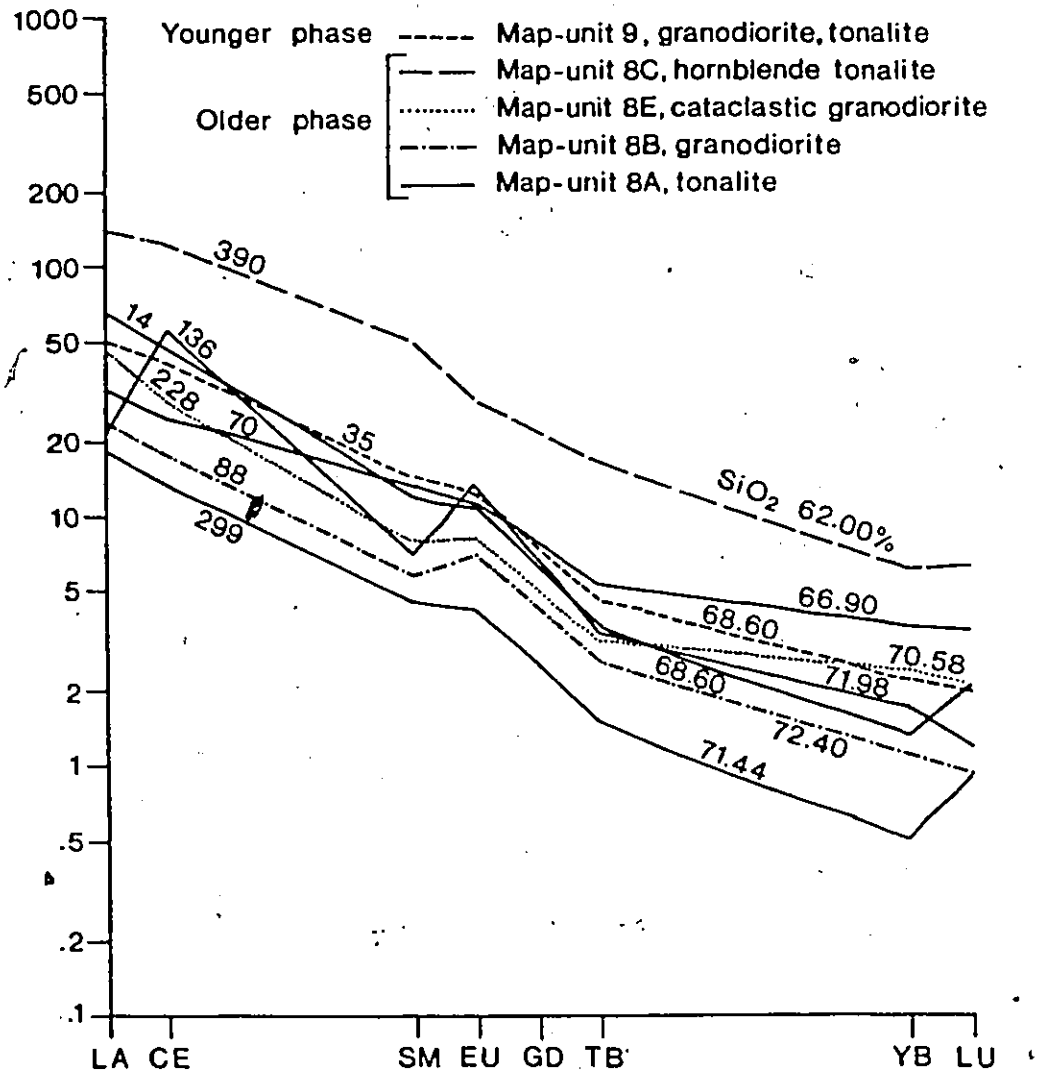

Fig. 11. Chondrite-normalized REE patterns from the Round Lake Batholith. Sample numbers are given at the LRE element side of curves.

Ba and Rb concentrations are low and generally too scattered to exhibit any trends, whereas Sr and Zr show a weak positive correlation.

The older phase amphibolite xenolith, found in agmatite gneiss near the Crooked Creek Stock, plots within the Pacaud Tuffs and Catharine-Wawbewawa fields, suggesting an origin from similar rocks. The two younger phase amphibolite xenoliths plot in proximity to the Skead Group field, although the xenoliths are slightly lower in Al_2O_3 and Zr, and higher in Fe_2O_{3TOTAL}, MgO, CaO, Na_2O and Sr than the Skead average.

Chondrite-normalized REE curves (Fig. 11) graphically demonstrate the chemical homogeneity of the Round Lake Batholith: LREE enriched and depleted HREE concentrations with positive to slightly negative Eu anomalies. The lowest SiO_2 value of 66.90% from the older phases tonalite corresponds to the highest REE concentration, with the higher SiO_2 samples containing lower REE values. Both features suggest a little to a more differentiated sequence. But the minimal SiO_2 range in older phase samples (66.90 to 72.40%; excluding hornblende tonalite) and the insignificant modifications to the shape of the REE curves (such as continuous enrichment or depletion of the LREE, HREE and Eu) preclude any insight into the fractionation history of the older phase.

In summary, Harker diagram trends and chondrite-normalized plots reinforce several conclusions previously documented:

1) Even with the separation of laboratory facilities in the analyses, trends shown here appear to be real, i.e., caused by magmatic processes. Certain analytical clusters in major element analyses of the older phase tonalite reflect the similar composition of rocks from the sampling area, and the spatial gradation between the tonalite and the granodiorite and cataclastic granodiorite-tonalite.

2) It should be stressed that very smooth variation in major element composition cannot be solely taken as evidence for simple differentiation. Smooth variation result in part from normalization of the oxide sums to 100%. However, from the Harker diagrams, the least differentiated older phase analyses belong to the tonalite, whereas the most differentiated belong to the cataclastic granodiorite-tonalite, the overall range of differentiation being quite narrow with significant overlap as suggested by the field evidence.

3) Overlap between the older phase (excluding hornblende tonalite) and younger phase granodiorite-tonalite substantiates the genetic link between the two phases, since trends tend to be subparallel. Hornblende tonalite overlaps within, and extends, the trend of the younger phase in major elements only, and not in the trace elements, suggesting that both units are

not part of the same differentiation sequence.

4) There is definitely no genetic correlation between the Abitibi Supergroup rocks and the Round Lake Batholith phases in terms of the upper supracrustal package being partly derived from the batholith as differentiation products. Units follow antipathic major and trace element trends, even though some of the Pacaud Tuffs and Skead Group rocks plot near, though generally outside, the fields of the older and younger phases of the batholith.

Comparison of major and trace elements between the Round Lake Batholith phases (excluding dykes) and other Archean tonalite/trondhjemite suites (Appendix IV) is graphically presented in Harker's diagrams of Figure 12, chondrite-normalized REE plots of Figure 13, and REE vs SiO_2 plots of Figure 14. Also included in these figures are 18 analyses from the Proterozoic gabbro-trondhjemite suite of southwest Finland (also in Appendix IV; Arth et al., 1978).

Harker diagrams clearly show that Round Lake Batholith analyses overlap and exceed the narrower fields of Archean

Fig. 12. SCATTERGAM-generated Harker diagrams comparing the Round Lake Batholith (field: ◌) excluding dykes and xenoliths, worldwide Archean tonalite/trondhjemite suites (field: ▽ , symbol: x), and the gabbro-trondhjemite suite of southwest Finland (symbol: *). Both the Archean and Finland suites are listed in Appendix IV.

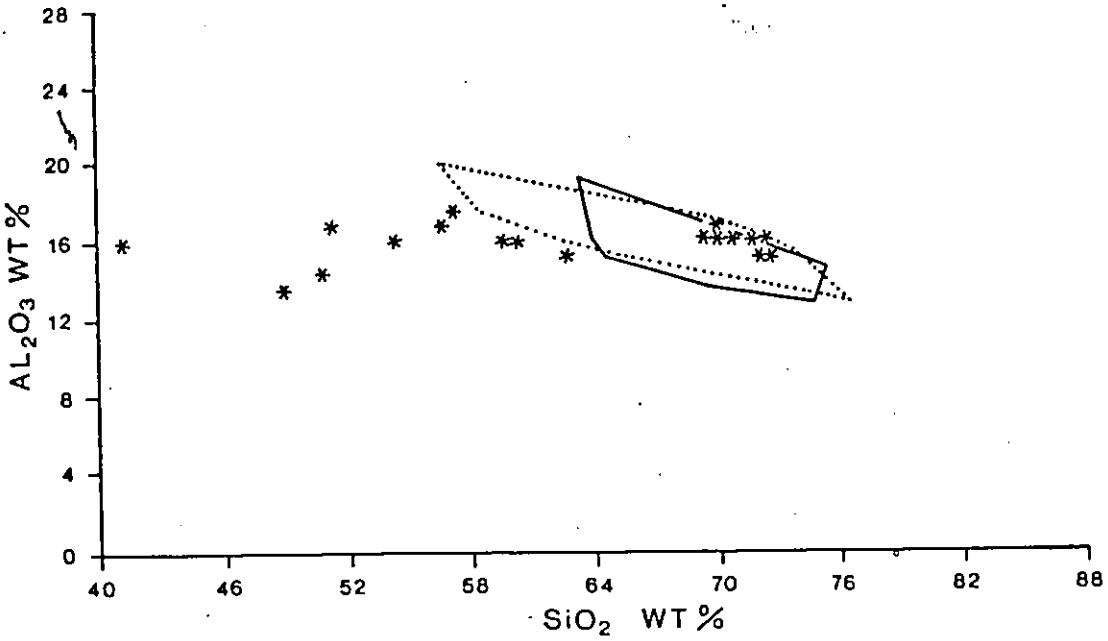
28
24
20
16
12
8
4
0
AL_2O_3 WT %
40
46
52
58
64
70
76
82
88
SiO_2 WT %

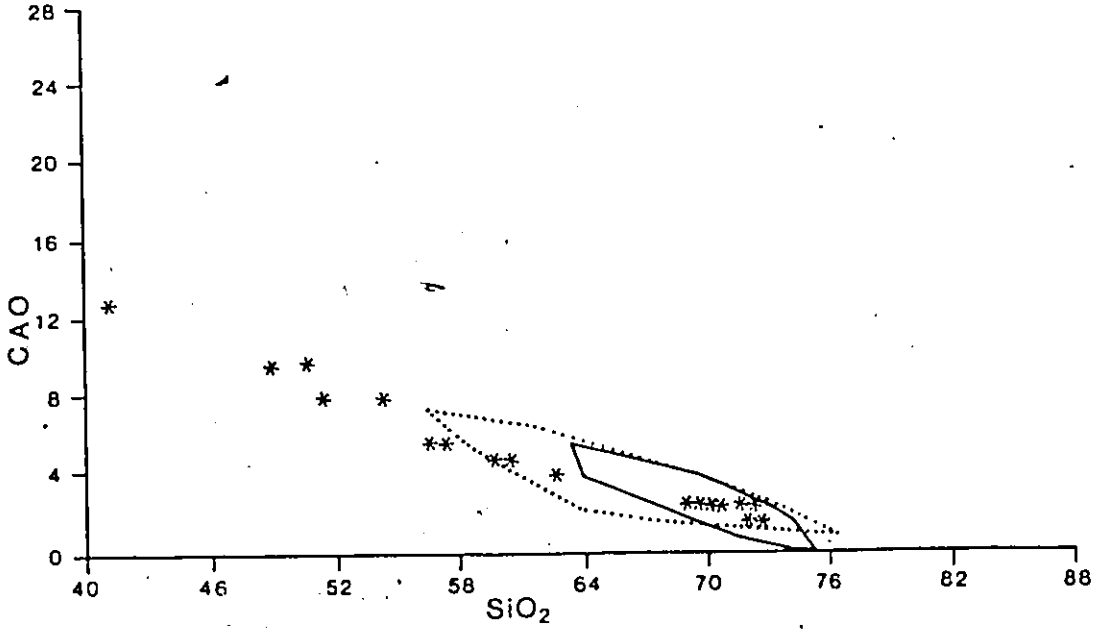
28
24
20
16
12
8
4
0
CAO
40
46
52
58
64
70
76
82
88
SiO_2

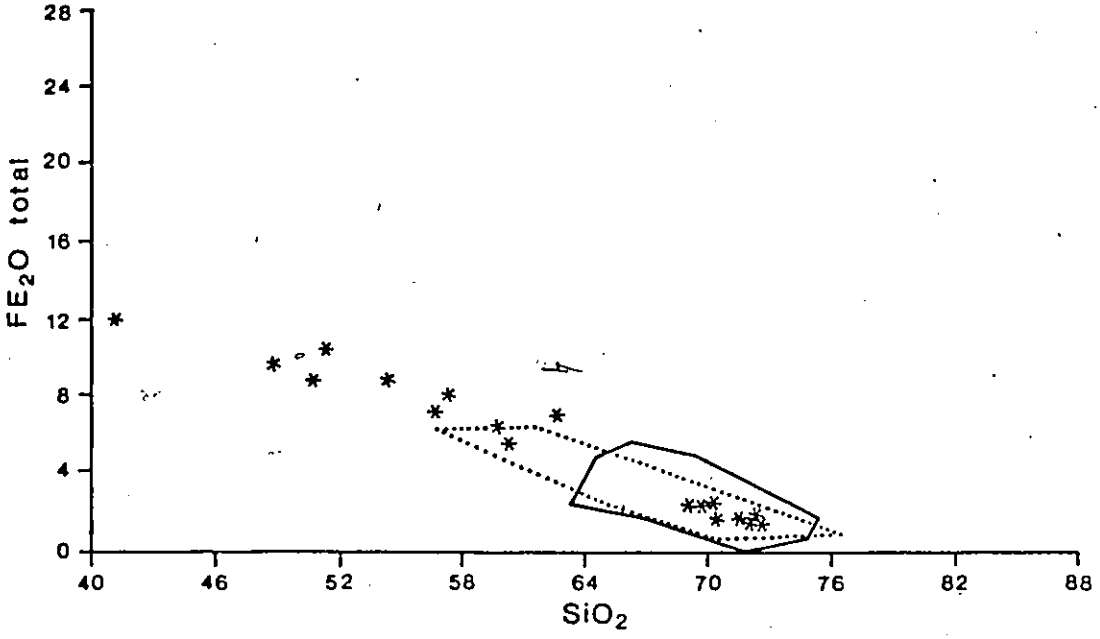
28
24
20
16
12
8
4
0
FE2O total
40
46
52
58
64
70
76
82
88
SiO2

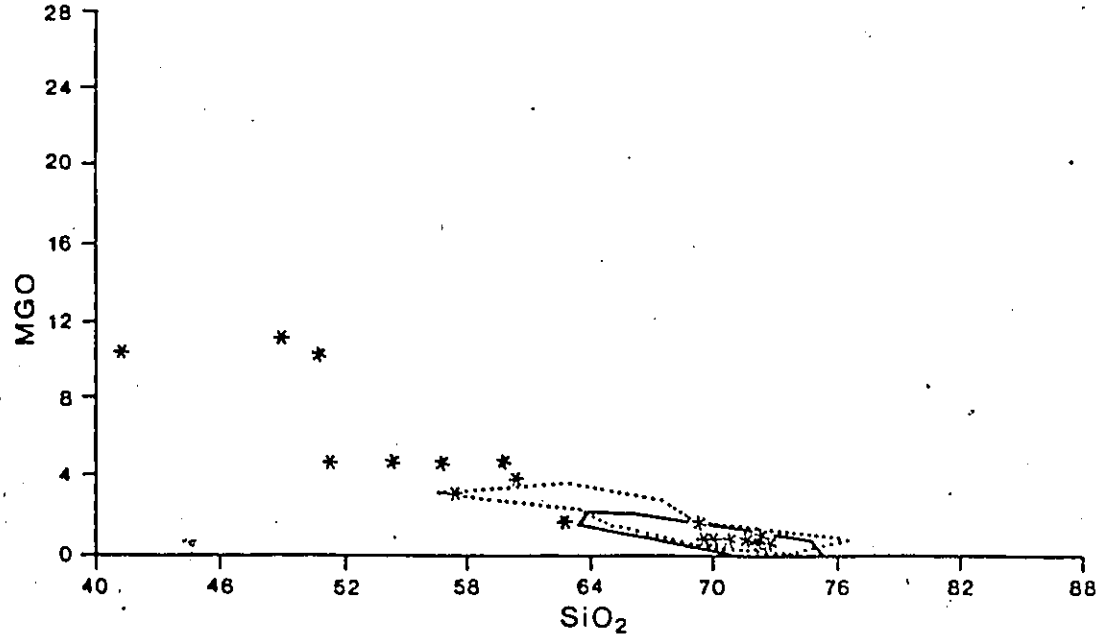
28
24
20
16
12
8
4
0
MGO
40
46
52
58
64
70
76
82
88
SiO2

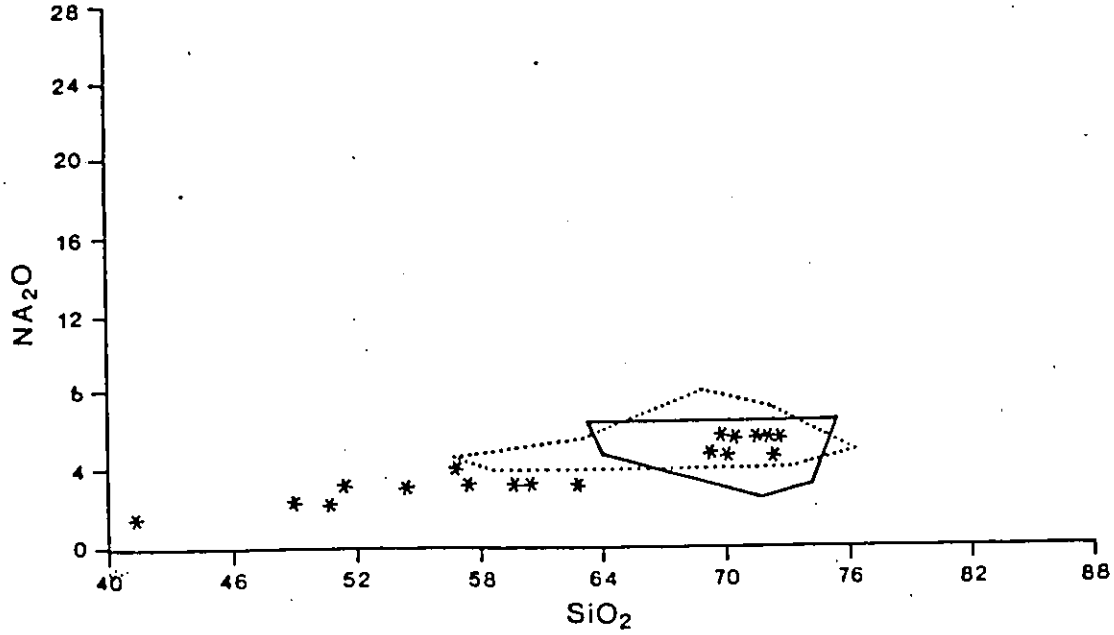
28
24
20
16
12
8
4
0
NA_2O
40
46
52
58
64
70
76
82
88
SiO_2

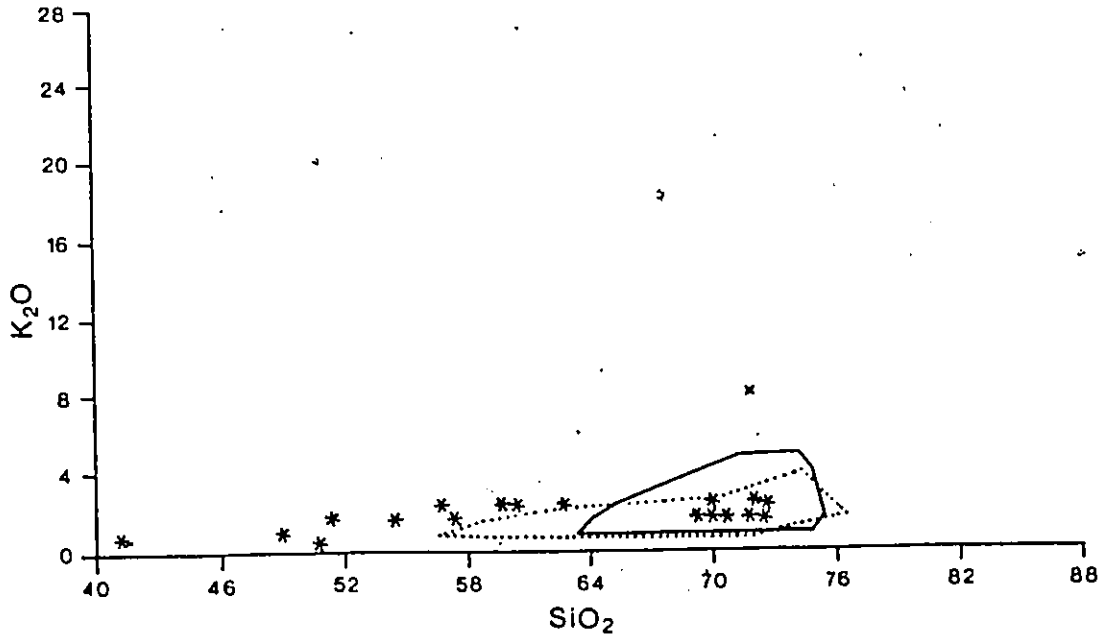
28
24
20
16
12
8
4
0
K_2O
40
46
52
58
64
70
76
82
88
SiO_2

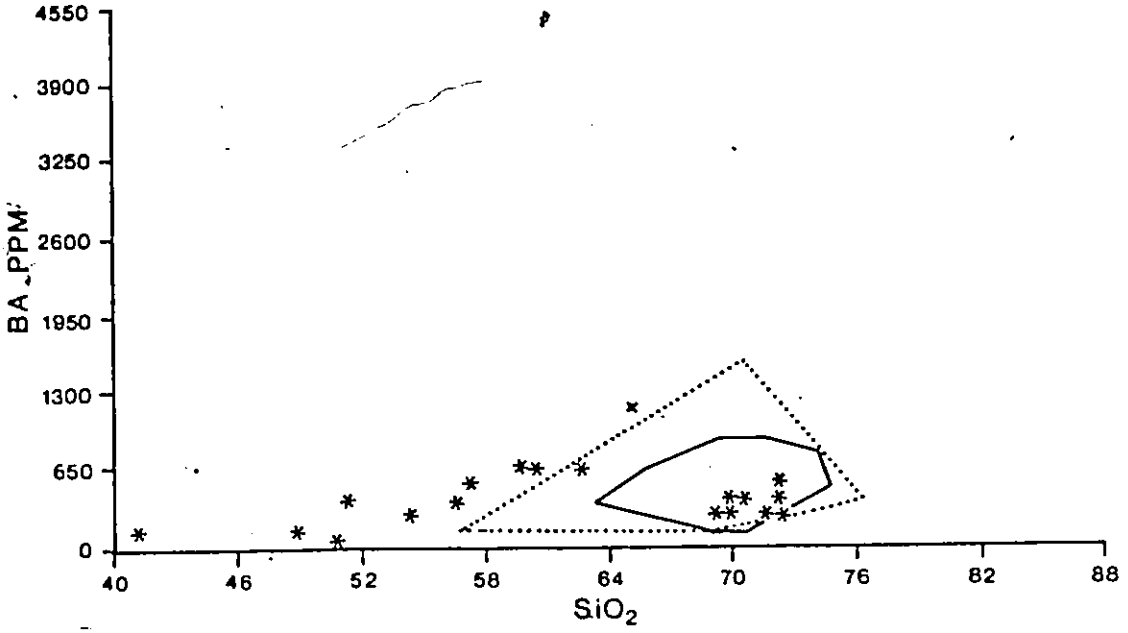
4550
3900
3250
2600
1950
1300
650
0
BA_PPM
40
46
52
58
64
70
76
82
88
SiO2

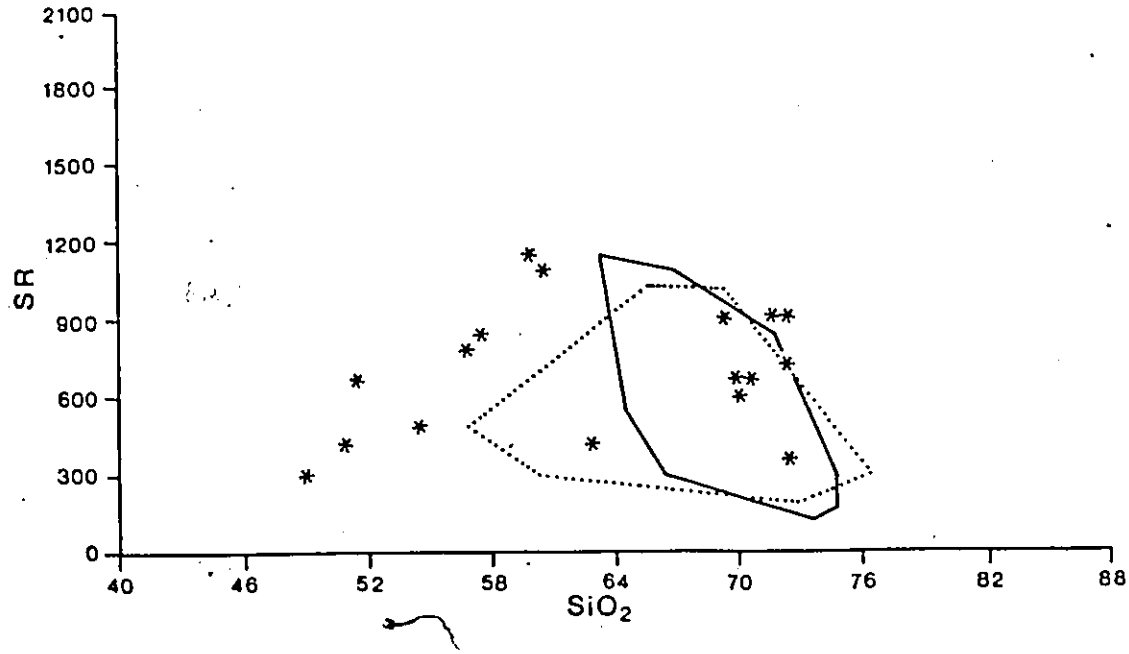
2100
1800
1500
1200
900
600
300
0
SR
40
46
52
58
64
70
76
82
88
SiO2

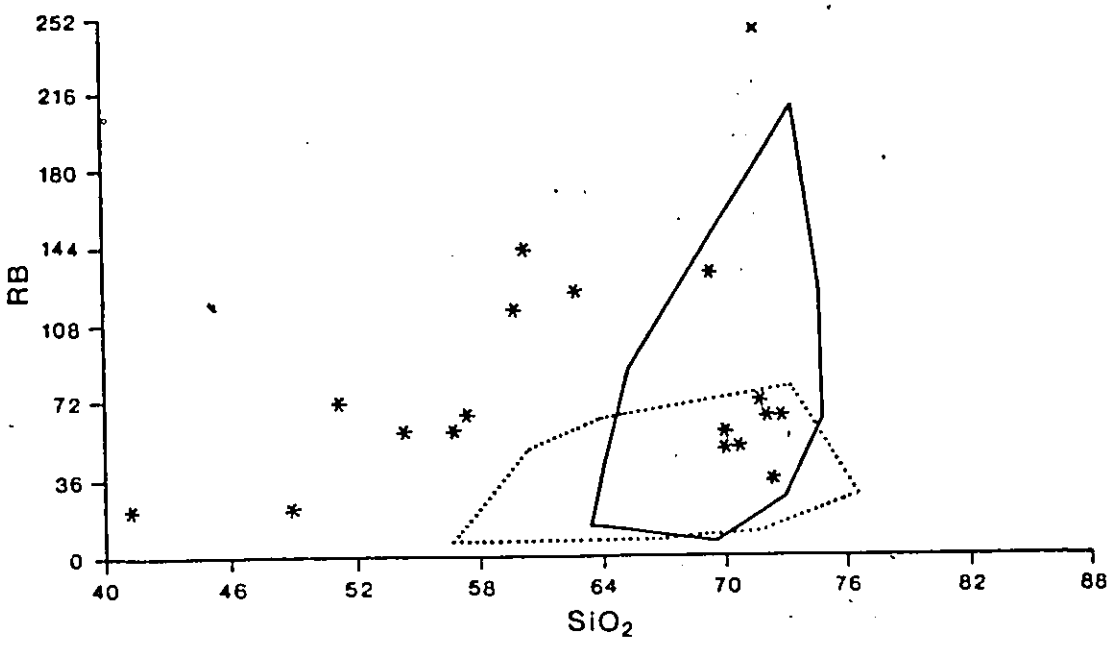
252
216
180
144
108
72
36
0
RB
40
46
52
58
64
70
76
82
88
SiO2

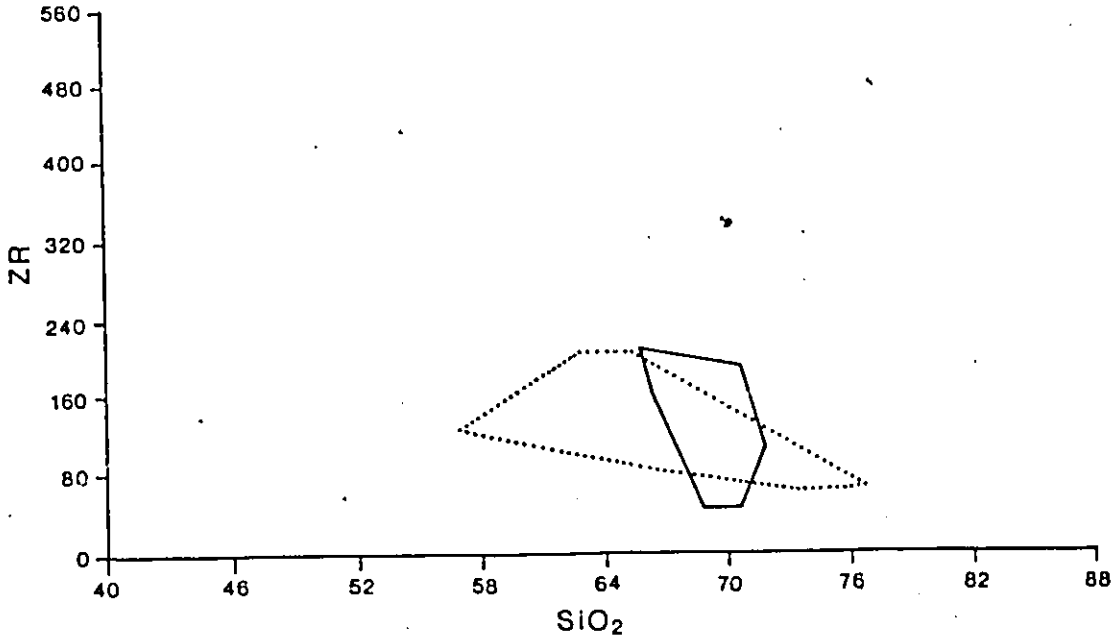
560
480
400
320
240
160
80
0
ZR
40
46
52
58
64
70
76
82
88
SiO2

suites with respect to major elements and Ba, Sr and Zr. Overlap with the most differentiated tonalite-trondhjemite samples of the Finland suite is also evident, although batholithic trends for Al_2O_3, Na_2O, K_2O, Sr and Rb are generally outside the evolutionary line for a typical gabbro to trondhjemite differentiation sequence.

Chondrite-normalized REE data from the Round Lake Batholith (Fig. 13) plot in the lower half of the field defined by Archean suites. Four curves from the least to most differentiated samples of the Finland suite (sequentially UK-10, UK-8, UK-15 and UK-12) are also plotted. The Finland pattern shows a general decrease in total REE concentrations and an increase in the Eu anomaly with increasing SiO_2 (from 60.43 to 72.39%). The only significant correlation of the Finland suite with the batholithic patterns is the position of curves relative to SiO_2 content: UK-10 at 60.43% SiO_2 is similar to the older phase hornblende tonalite curve at 62.00% SiO_2, whereas the field encompassing the younger phase and other older phase units (ranging from 66.90 to 72.40% SiO_2) is consistent with samples UK-8, UK-15 and UK-12.

REE plots (total REE, La/Yb and Eu/Eu* vs SiO_2; Fig. 14) for the Round Lake Batholith exhibit a generally tight cluster of data points in all three diagrams at about 70% SiO_2, which overlaps with other Archean suites. The REE plots also

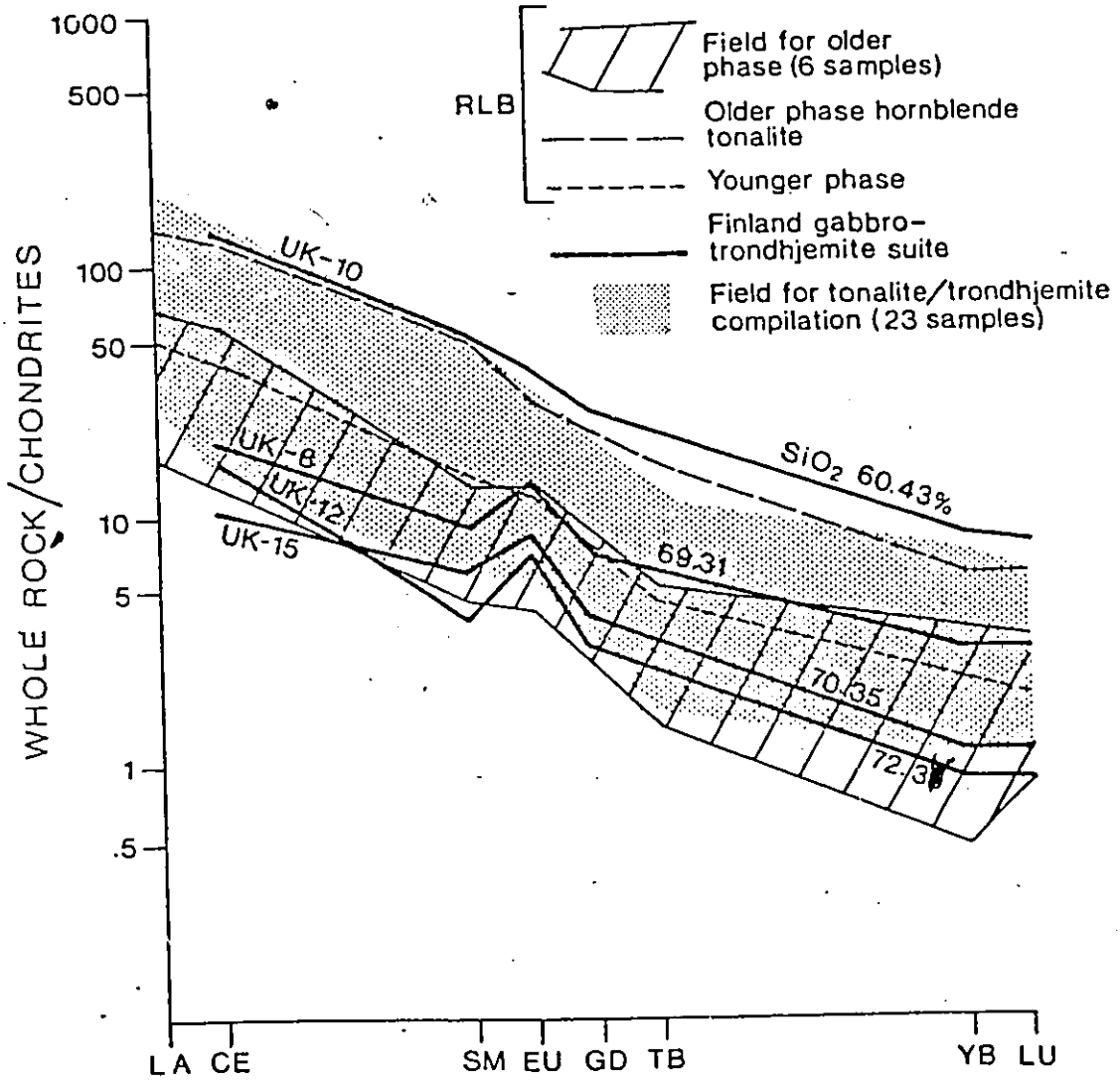

Fig. 13. Comparison of chondrite-normalized REE patterns from the Round Lake Batholith (RLB) with other Precambrian tonalite/trondhjemite suites.

Fig. 14. REE plots (REE, La/Yb and Eu/Eu* vs SiO_2) for the Round Lake Batholith, Elzevir Batholith of eastern Ontario (Table 3: Pride and Moore, 1983), Archean tonalite/trondhjemite suites, and gabbro-trondhjemite suite of southwest Finland. Symbols are: Tonalite (map-unit 8A), ▲ ; Granodiorite (map-unit 8B), ● ; Cataclastic granodiorite (map-unit 8E), ■ ; Hornblende tonalite (map-unit 8C), ◆ ; Granodiorite-tonalite (map-unit 9), ◆ ; Archean suite, ▱ (field; with 70% of samples falling below the dividing line at roughly 80 ppm REE); Finland suite, ↗ (arrow); Elzevir Batholith, +.

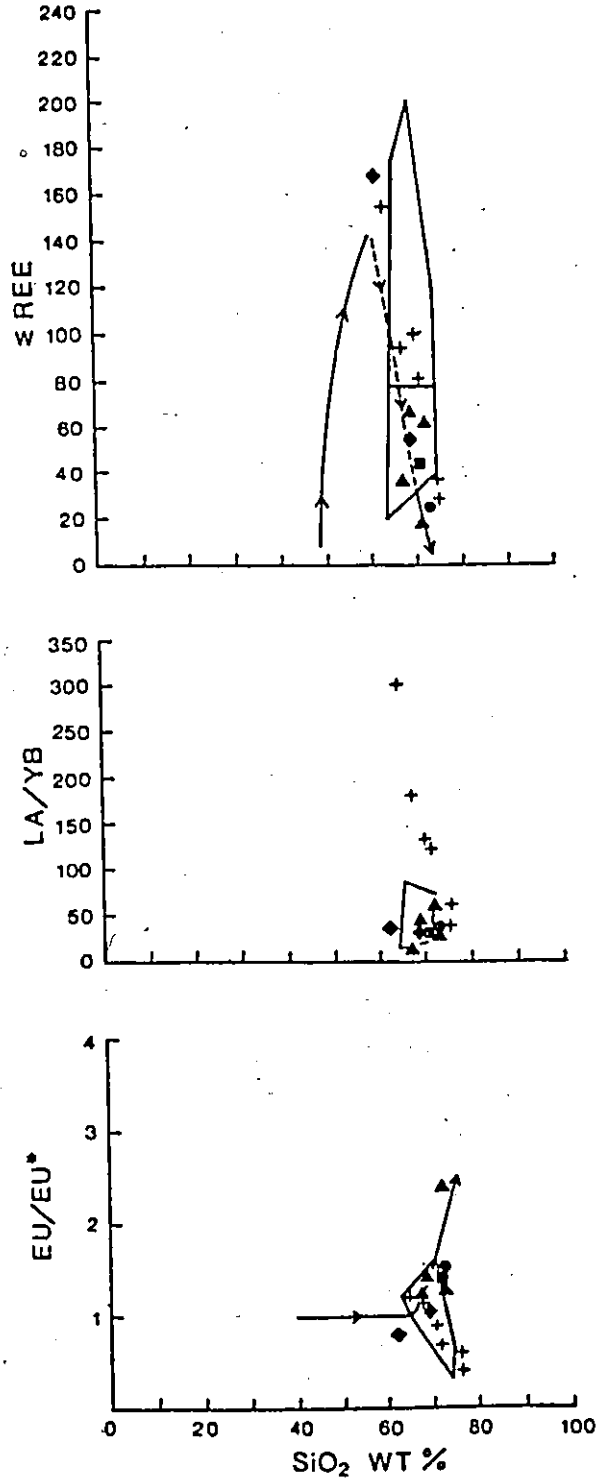
Σ REE
240
220
200
180
160
140
120
100
80
60
40
20
0
LA/YB
350
300
250
200
150
100
50
0
EU/EU*
4
3
2
1
0
20
40
60
80
100
SiO2 WT %

contain two distinct differentiation sequences, the Grenvillian Elzevir Batholith of trondhjemite composition (Pride and Moore, 1983) and the familiar Finland suite. The Elzevir Batholith features a marked decrease in REE, La/Yb and Eu/Eu* with increasing SiO_2, even over a narrow range of SiO_2 values (roughly 64 to 75% SiO_2). The Finland suite initially increases, then decreases in REE, and (in contrast to the Elzevir Batholith) increases in Eu/Eu*, over a wide range of SiO_2 values (40 to 75% SiO_2). The Round Lake Batholith older phase REE data does not obviously follow either of the two contrasting differentiation trends.

Triangular classification diagrams (A-F-M, An-Ab-Or and Q-Ab-Or) for the Round Lake Batholith indicate that phases display calc-alkaline affinities of the tonalite-trondhjemite series (Fig. 15), which is consistent with other Archean suites and the Finland trondhjemitic rocks (Fig. 16).

On an A-F-M diagram (Fig. 15a), the Round Lake samples plot along a narrow field extending towards the alkali corner, whereas most Abitibi Supergroup Pacaud Tuffs and Catharine-Wawbewawa samples show an $FeO+Fe_2O_3$ enrichment indicative of tholeiitic affinities. Four samples of the Pacaud, and all of the Skead (with the exception of one sample), plot in the calc-alkaline field; and as in the Harker diagrams, both units show trends that are incompatible with the batholithic phases.

Fig. 15. Triangular compositional diagrams for the Round Lake Batholith: (a) A-F-M (wt %) plot of Irvine and Baragar (1971); (b) An-Ab-Or (cation normative) plot of Barker (1979); (c) Q-Ab-Or (cation normative) plot of Barker and Arth (1976). (a) Map-units 1-4 (1: Pacaud Tuffs, 2: Wawbewawa Group, 3: Catharine Group, 4: Skead Group), 8 (Round Lake Batholith older phase), including dykes and xenoliths. (b-c) Map-units 8 and 9, including dykes and xenoliths. Symbol nomenclature same as in Figure 10.

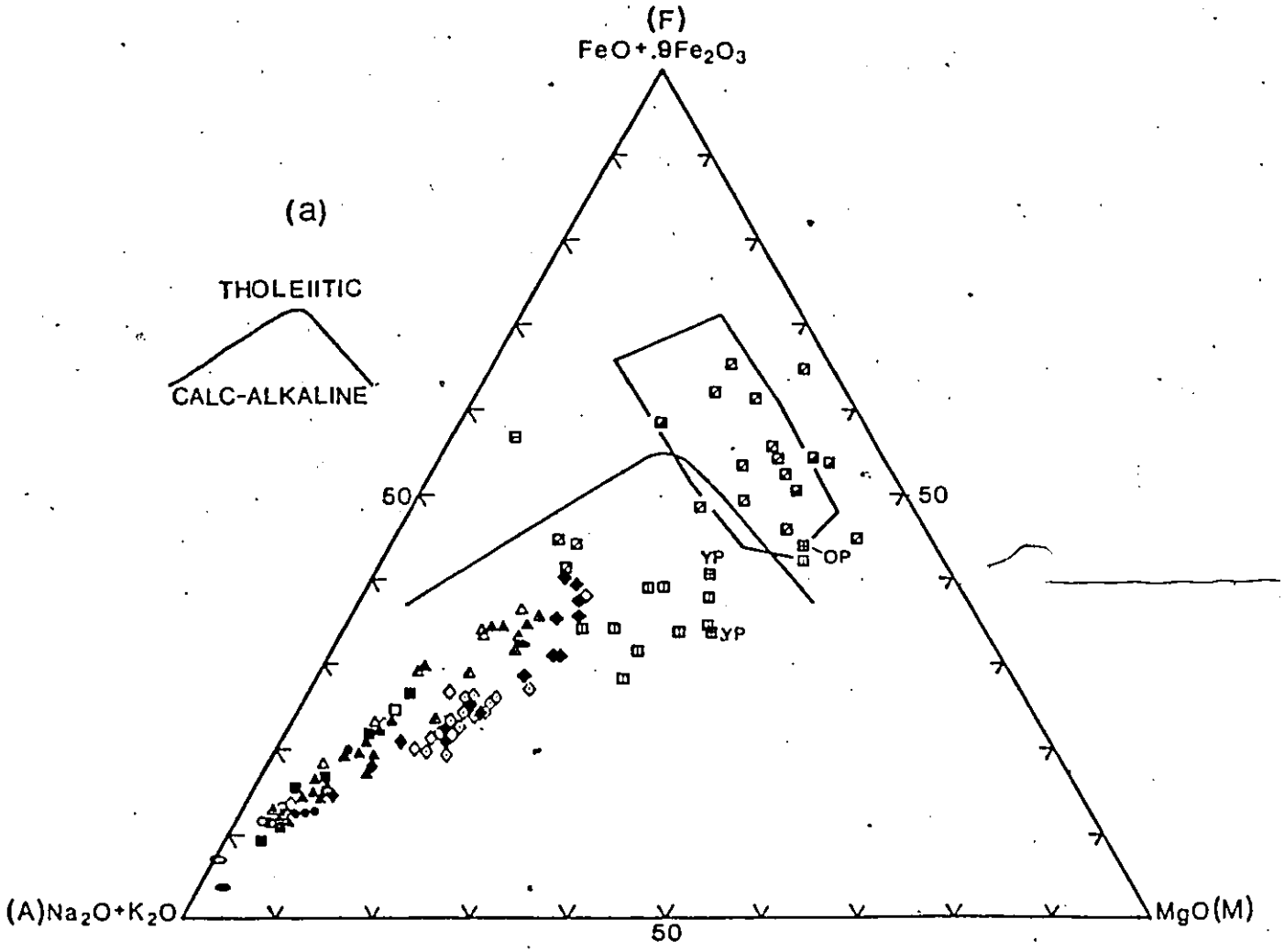
(F)
FeO+.9Fe2O3
(a)
THOLEIITIC
CALC-ALKALINE
50
50
YP
OP
YP
(A)Na2O+K2O
50
MgO(M)

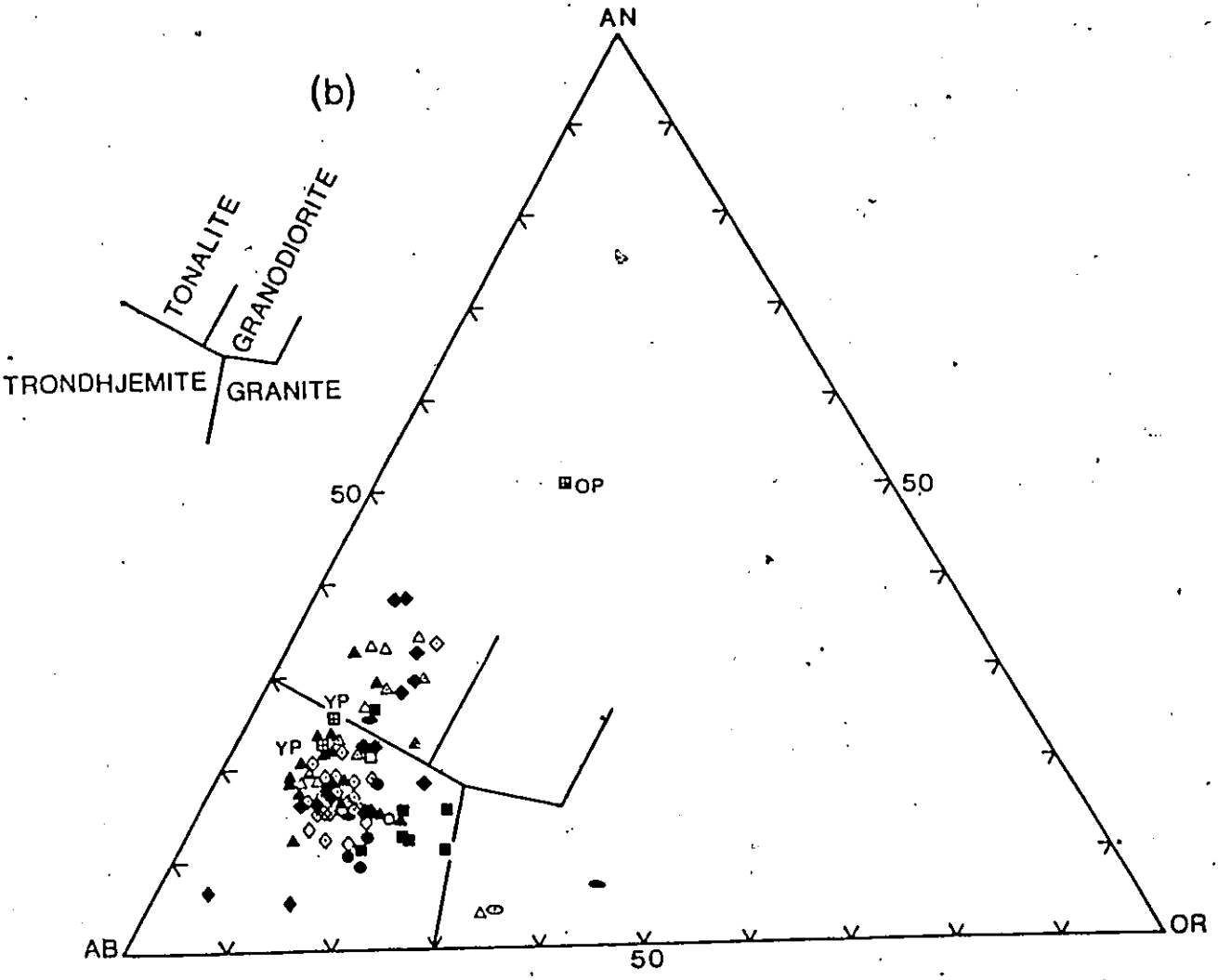
(b)
AN
TONALITE
GRANODIORITE
TRONDHJEMITE
GRANITE
50
OP
50
YP
YP
AB
50
OR

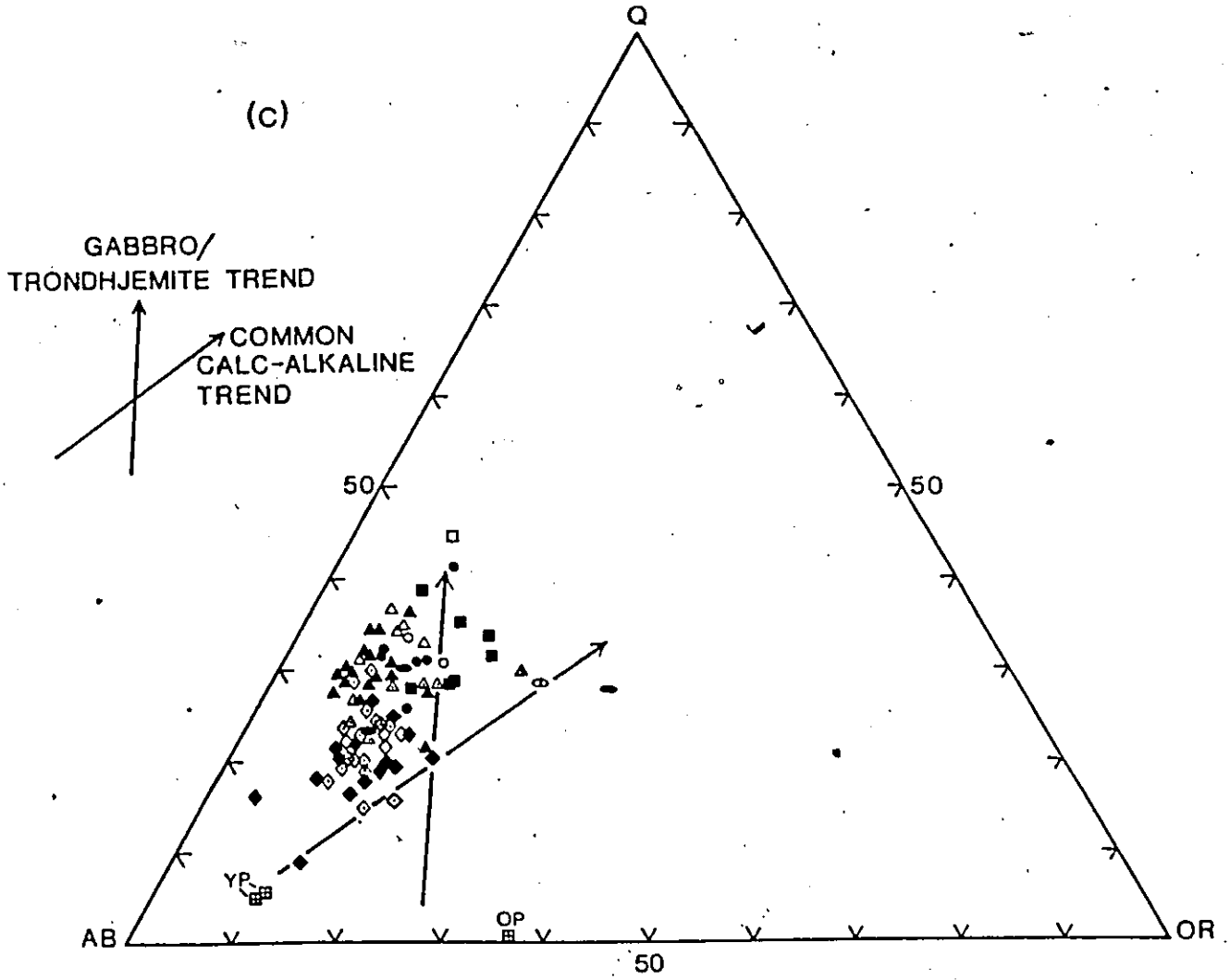
(c)
Q
GABBRO/
TRONDHJEMITE TREND
COMMON
CALC-ALKALINE
TREND
50
50
YP
OP
AB
OR
50

Fig. 16. Triangular classification diagrams comparing the Round Lake Batholith, excluding dykes and xenoliths, worldwide Archean tonalite/trondhjemite suites, and the gabbro-trondhjemite suite of southwest Finland. (a) A-F-M. (b) An-Ab-Or. (c) Q-Ab-Or. Classification same as in Figure 15. Symbol nomenclature same as in Figure 10.

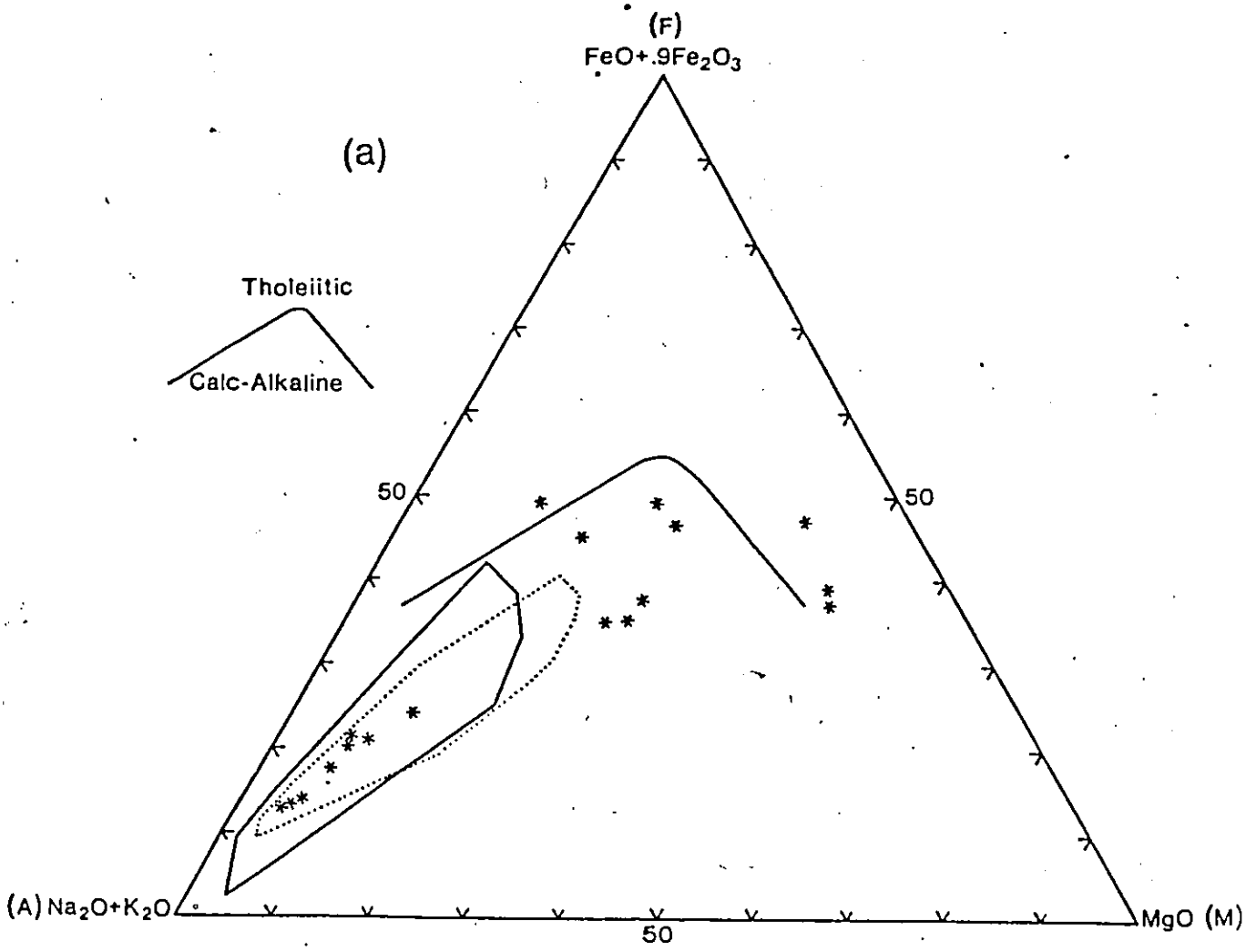
(F)
FeO+.9Fe2O3
(a)
Tholeiitic
Calc-Alkaline
50
50
(A) Na2O+K2O
50
MgO (M)

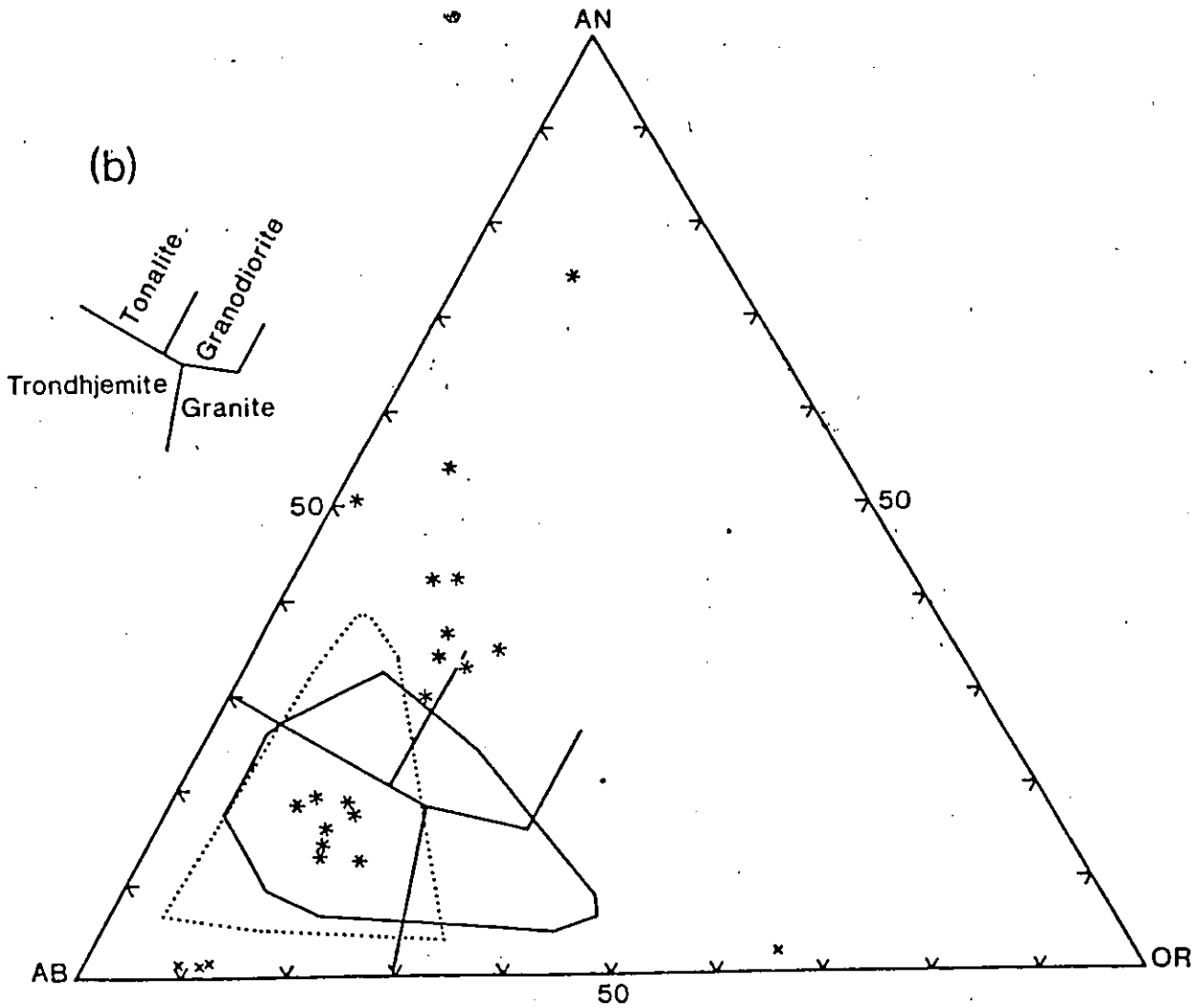
(b)
Tonalite
Granodiorite
Trondhjemite
Granite
AN
AB
OR
50
50
50

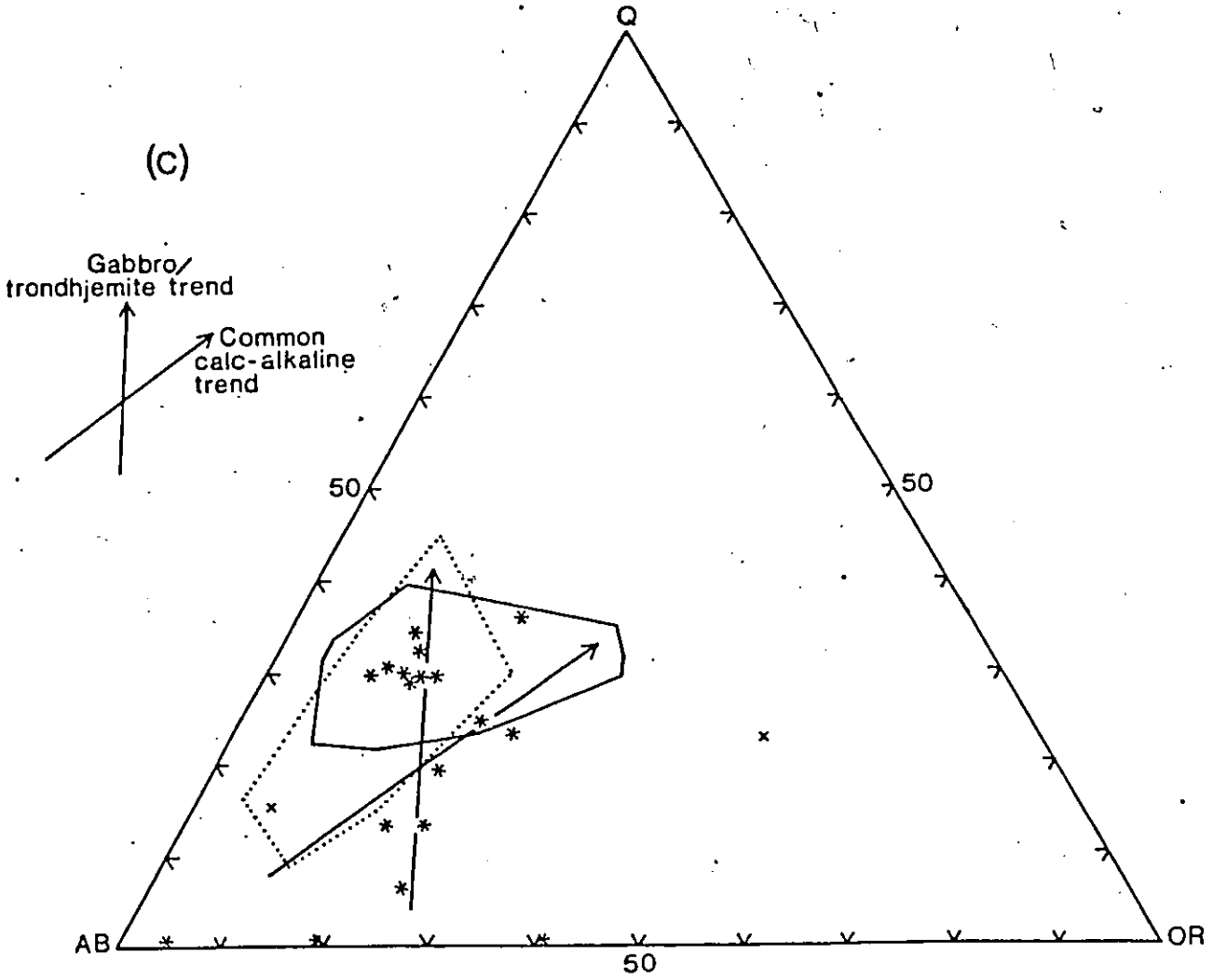
(c)
Gabbro/
trondhjemite trend
Common
calc-alkaline
trend
Q
50
50
AB
50
OR

On a normative An-Ab-Or diagram (Fig. 15b), the Round Lake samples occupy the tonalite and trondhjemite fields of Barker (1979) with two dykes and one older phase tonalite plotting in the granite field. According to this diagram, both younger phase xenoliths are chemically indistinct from other "tonalite-trondhjemite" rocks of the batholith, contrary to the older phase xenolith.

On a normative Q-Ab-Or diagram (Fig. 15c), the cluster of data points illustrates the homogeneity not only of the older phase but of the whole batholith. Here, all three xenoliths plot outside of the main envelope of the batholith analyses. Based on the Harker and triangular diagrams, the younger phase amphibolite xenoliths are not of a precursor intrusive phase, but are likely akin to the surrounding supracrustal rocks, as suggested previously.

In comparison, the minor Or enrichment shown by Archean tonalite/trondhjemite suites is not evident in the Round Lake Batholith cluster (excluding dykes) (Fig. 16a,b,c). The lack of Or enrichment depicts a plagioclase involvement in the crystallization history of batholith. Petrographic evidence from the batholith attests to a very pronounced plagioclase involvement, since the plagioclase content varies from 38 to 77% overall (see Table 2).

3) Fractionation within the batholith: an enigma

It is difficult to envisage large plutonic bodies of the

dimensions of the Round Lake Batholith without differentiation. Most well known large plutonic masses, such as the Phanerozoic Sierra Nevada Batholith (Bateman et al., 1963), consist of many mineralogically, texturally and chemically zoned plutons ranging from gabbroic to granitic compositions. The Archean Round Lake Batholith, as with many other early Precambrian tonalite/trondhjemite complexes of similar tectonic setting does not exhibit the same degree of heterogeneity, typical of differentiation, of many of the Phanerozoic batholiths. The absence of diverse phases (gabbro and granite) in Archean plutonic bodies, as shown by the abundance of tonalitic rocks throughout the ancient shield areas, must reflect their common source and subsequent crystallization history.

Hyndman (1984) postulated partial melting as the characteristic mechanism producing voluminous amounts of chemically homogeneous parent, followed by rapid solidification of the magma near its source. This is a feasible process for Archean tonalites. Partial melting of vast amounts of amphibolite at depth, shown by Barker and Arth (1976) as the most likely source rock and possibly representing the base of the greenstone pile, would produce a tonalitic melt. The melt would subsequently crystallize, allowing chemical, and not physical, differentiation. Zoning in plagioclase, the main component mineral of tonalites, infers either a depletion or enrichment of certain elements from the residual melt. However,

this (chemical) differentiation would be negligible assuming that the residual melt would not physically separate from early formed plagioclase crystals. Ultimately, the residual melt would remain practically in-situ, and probably crystallize as K-feldspar and quartz.

The scenario may well apply to the Round Lake Batholith older phase. However, prior to advocating such a model, it is essential to examine and evaluate all possible processes which could lead to mineralogical and chemical homogeneity as depicted by the Round Lake Batholith older phase.

In all, there are three possible processes that may create the same pattern of homogeneity. These are:

1) homogeneity through alteration, a consequence of either regional metamorphism or autometamorphism.
2) homogeneity through the previously outlined partial melting of a chemically homogeneous parent, via either a single pulse (or multiple magmatic pulses), with rapid crystallization and no differentiation.
3) homogeneity through a combination of partial melting with a single pulse of tonalitic melt (as in 2), subject to differentiation that would have been inhibited by a lack of physical separation between crystals and residual melt.

Alteration is judged the least likely process contributing to chemical homogeneization. Differentiation within the older

phase of the batholith as shown by the apparent eastward gradation of subphases from tonalite to granodiorite, coupled with a minor variability in major elements, nullifies any significant modifications brought upon by alteration.

Arth et al. (1978), in their study of the tonalite-trondhjemite rocks of the Finland suite, suggested that the trace elements Sr and Rb were transported into, and Ba out of, the magmatic system during low temperature alteration brought upon by (the exchange of) fluids rich in water originating from surrounding metamorphosed country rocks. Both biotite and hornblende from the Round Lake Batholith appear to give metamorphic ages (Chapter VI: Geochronology of the Round Lake Batholith). The petrographic evidence in the older phase supports the metamorphic interpretation: micas (biotite and muscovite) are late growth minerals. Saussuritization of plagioclase is the sole mode of formation of muscovite, whereas biotite occurs as disseminated corroded flakes and, most importantly, as aggregates with the late forming euhedral to subhedral hornblende. Hydrous minerals such as micas would not be part of most tonalites primary mineral assemblages. Tonalites, in general, are "dry" rocks; based on experimental work, water content probably does not exceed 2% (Wyllie, 1979). Peraluminous systems are mica bearing, although the Round Lake Batholith as a whole does not fit this category.

Another approach in establishing the role of metamorphism

in the modification of chemistry would be to correlate between modal micas and the compatible trace elements Ba and Rb (K_D^{Ba} and K_D^{Rb} are greater than 1 for micas; Table 5). A strong positive correlation would imply an influence from metamorphism/alteration. Results of the correlation are shown in Fig. 17. No apparent correlation exists between modal micas and Ba and Rb, even owing to imprecise modal counts from the cataclastic marginal subphases, and to the precision of Rb which exceeds $\pm$ 50% of values under 40 ppm. Micas are strictly minor constituents in the older phase, and probably did not control Ba concentrations as much as feldspar which constitutes at least half to three-quarters of the minerals (K_D^{Ba} for plagioclase and K-feldspar are 1.21 and 12.9 respectively; Table 5). Rb is generally low throughout the batholith, even with the influx of late micas. Therefore, Rb can not be reliably used in petrogenetic modelling shemes.

The second process is also excluded on the single premise that differentiation was active in the older phase of the Round Lake Batholith. Ubiquitous zoning of plagioclase throughout the older phase attests to a chemical differentiation.

The third process invokes partial melting resulting in a single tonalitic melt pulse being subjected to chemical differentiation only, with the residual melt remaining at or near the site of plagioclase nucleation probably throughout most of the crystallization history. Examples of the link

Table 5. Crystal-liquid partition coefficients used in this study. Some values were added for comparison.

Mineral	Element															
	Ba		Sr		Rb		La		Sm		Eu		Tb		Yb	
	A	B	A	B	A	B	A	B	A	B	A	B	A	B	A	B
Quartz	0.001[1]	-	0.001[1]	-	0.001[1]	-	-	-	-	-	-	-	-	-	-	-
Plagioclase	1.21[1]	0.23[2]	4.12[1]	1.83[1]	0.091[1]	0.071[2]	-	0.1[4]	-	0.11[5]	-	0.73[5]	-	0.01[4]	-	0.031[5]
K feldspar	12.9[1]	-	3.55	-	1.04[1]	-	-	-	-	-	-	-	-	-	-	-
Biotite	3.21[1]	1.1[3]	0.08[1]	0.08[3]	2.31[1]	3.1[3]	-	0.03[3]	-	0.03[3]	-	0.03[3]	-	0.03	-	0.04[3]
Muscovite	2.66[1]	-	0.104[1]	-	1.54[1]	-	-	-	-	-	-	-	-	-	-	-
Hornblende	0.046[2]	0.42[2]	0.022[2]	0.46[2]	0.014[2]	0.29[2]	-	0.2[4]	-	3.99[5]	-	3.44[5]	-	1[4]	-	4.29[5]
Orthopyroxene	0.0029[2]	0.001[3]	0.083[2]	0.0017[2]	0.0027[2]	0.022[2]	-	0.002[4]	-	0.01[5]	-	0.013[5]	-	0.04[4]	-	0.049[5]
Clinopyroxene	-	0.001[3]	-	0.07[3]	-	0.031[3]	-	0.07[4]	-	0.95[5]	-	0.68[5]	-	0.3[4]	-	1.39[5]
Garnet	-	0.023[2]	-	0.012[2]	-	0.042[1]	-	0.005[4]	-	2.66[5]	-	1.50[5]	-	3[4]	-	39.9[5]
Apatite	-	-	-	-	-	-	-	8.6[4]	-	20.7[5]	-	10.5[5]	-	15.4[4]	-	9.8[5]
Zircon	-	-	-	-	-	-	-	3	-	3.14[5]	-	3.14[5]	-	3	-	270[5]
Sphene	-	-	-	-	-	-	-	80	-	102[5]	-	101[5]	-	100	-	37.4[5]
Allanite	-	-	-	-	-	-	-	5000	-	300	-	300	-	300	-	100

A. K_D values for intermediate to felsic compositions; B. K_D values for basic to intermediate compositions

Sources: 1. Mittlefehldt and Miller (1983); 2. Arth and Hanson (1975); 3. Cox et al. (1979); 4. Allègre et al. (1977); 5. Hanson (1980); others are approximations based on previous sources and Miller and Mittlefehldt (1982).

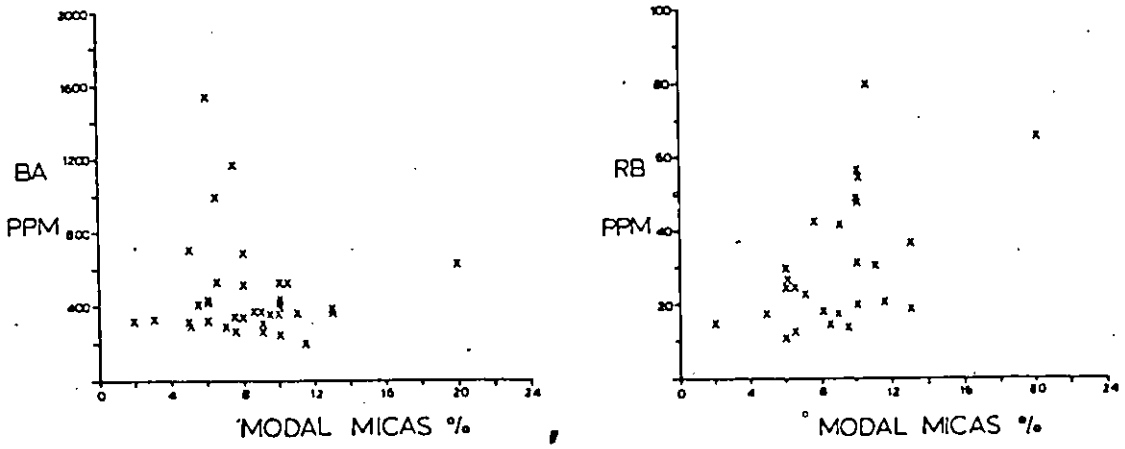

Fig. 17. Ba and Rb vs modal micas from the older phase (excluding hornblende tonalite) of the Round Lake Batholith.

between chemical homogeneity and the degree of separation of early formed crystals from residual melts during crystallization in granitoid rocks have been described by McCarthy and Hasty (1976), Tindle and Pearce (1981), and Lee and Christiansen (1983).

The effect of having intercumulus melt (residual melt), during crystallization, imparts a melt character to the solids (crystallized portions), and tends to suppress the degree of enrichment or depletion of elements in late solids and melts. Hence, chemical homogeneity occurs with a clustering of elements in variation diagrams instead of normal liquid lines of ascent and descent.

The large ion lithophile elements Ba, Sr and Rb would be the best parameters in modelling the crystal melt evolution during crystallization of the older phase of the Round Lake Batholith, since they occur in major silicate minerals of tonalites. LiL elements would readily fluctuate as changes in the crystallization sequence of minerals took place, even though major elements would show consistent trends. Rb will be excluded from the fractionation modelling of the older phase because of its low concentration.

Ba and Sr data from the older phase are presented in a logarithmic plot (Fig. 18). Samples have been subdivided according to a chemical classification instead of the field/ modal mineralogy classification, since alteration has probably

modified the modal mineralogy to some extent. CaO was used as the classification index, since the element exhibits one of the best trends in major element differentiation. Secondly, CaO is also selected on the basis that it is the element (with SiO_2) which exemplifies best the modal-chemical relationship of the older phase in general. CaO-bearing minerals include plagioclase, hornblende, epidote and sphene. General relations between amounts of CaO and modal mineralogy are shown in Fig. 19. Older phase samples of Figure 18 were subdivided into three discrete data groups based on CaO and the proportion of K-feldspar: K-feldspar-poor portion of the older phase (least differentiated) at CaO content greater than 2.75%, with the next division set at 2.25%, which is the arbitrary boundary between the K-feldspar-rich portion (greater than 10% K-feldspar) at CaO less than 2.25% (most differentiated) and intermediate values (less than 10% K-feldspar) at CaO between 2.25 and 2.75%.

Fig. 18 also includes vectors showing theoretical effects on melt composition from crystallizing mineral phases, assuming Rayleigh Fractionation[1] and using partition coefficients listed in Table 5. Rayleigh Fractionation is used here since

---

[1] Rayleigh Fractionation equation:

$C_l/C_o = F^{(Di-1)}$ assuming Henry's Law for Ba and Sr distribution

where C_o = concentration of element i in the original melt.

C_l = concentration of element i in the residual melt.

F = weight fraction of melt remaining.

D_i = bulk partition coefficient for the element i.

$D_i = \sum_{i=1}^{n} X_i K_i$, where K_i = partition coefficient of the element in the given mineral phase, X_i = weight fraction of the mineral phase in the solid assemblage.

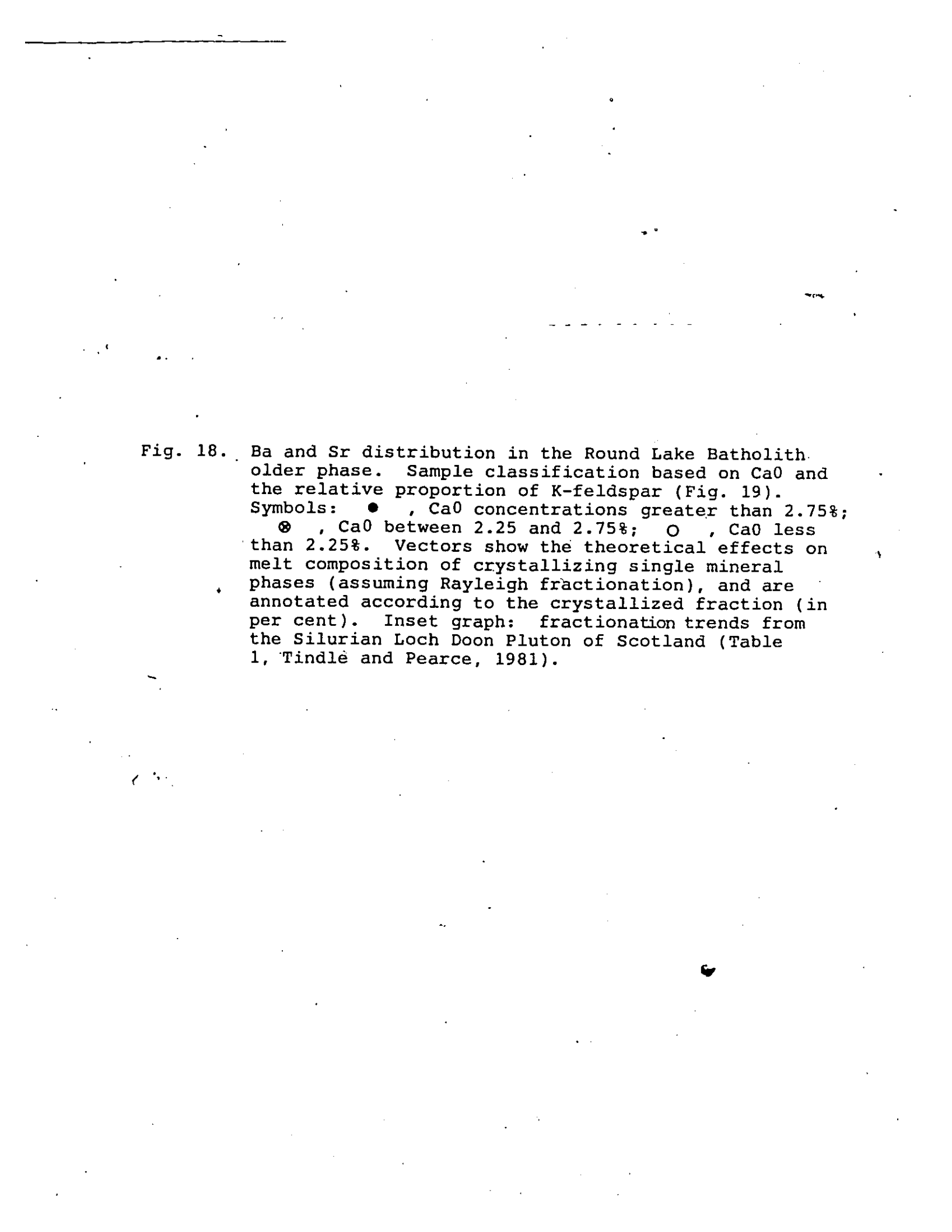

Fig. 18. Ba and Sr distribution in the Round Lake Batholith older phase. Sample classification based on CaO and the relative proportion of K-feldspar (Fig. 19). Symbols: ● , CaO concentrations greater than 2.75%; ⊗ , CaO between 2.25 and 2.75%; ○ , CaO less than 2.25%. Vectors show the theoretical effects on melt composition of crystallizing single mineral phases (assuming Rayleigh fractionation), and are annotated according to the crystallized fraction (in per cent). Inset graph: fractionation trends from the Silurian Loch Doon Pluton of Scotland (Table 1, Tindle and Pearce, 1981).

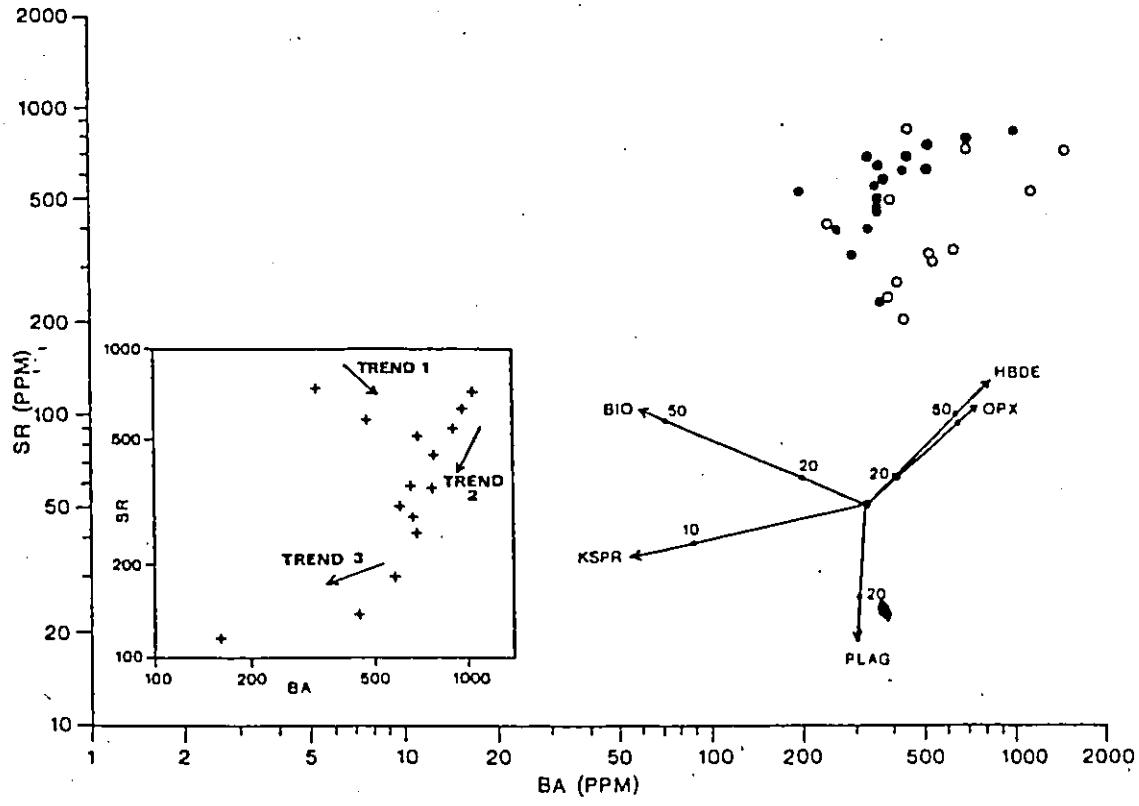
SR (PPM)
BA (PPM)
2000
1000
500
200
100
50
20
10
1
2
5
10
20
50
100
200
500
1000
2000
TREND 1
TREND 2
TREND 3
SR
BA
BIO
50
20
HBDE
OPX
KSPR
10
PLAG

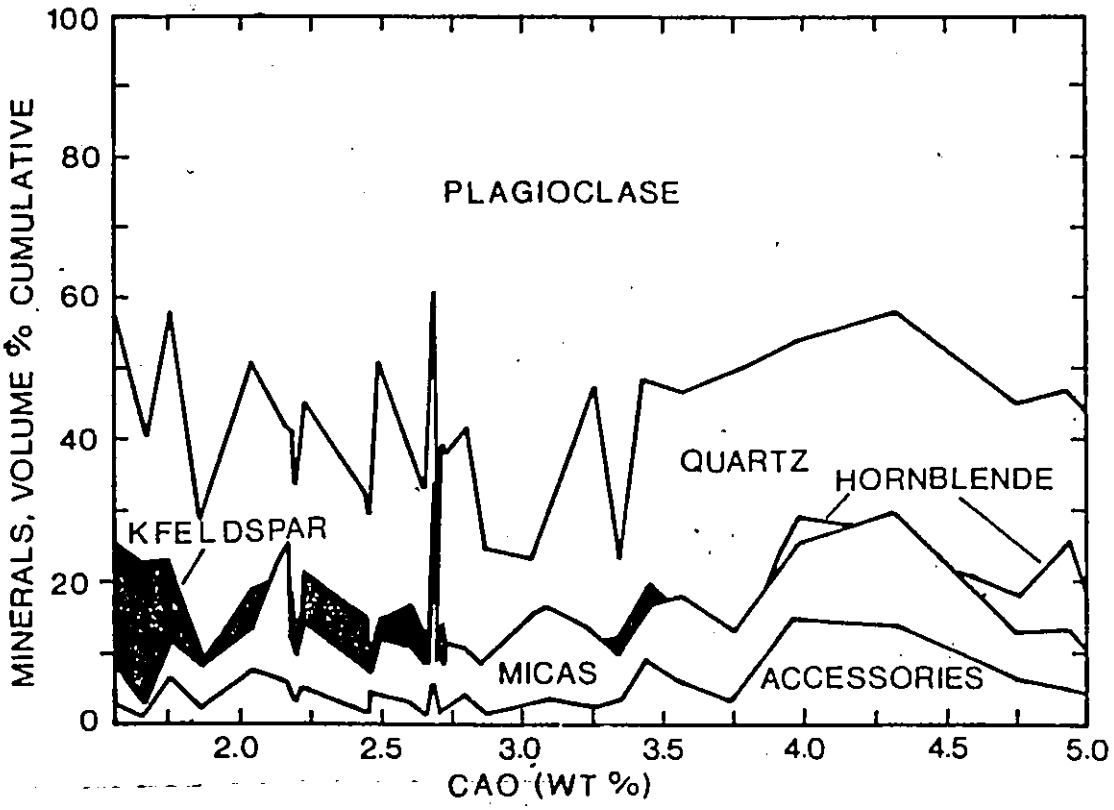

Fig. 19. Relationship between CaO content (whole rock) and mineralogy from the Round Lake Batholith older phase (map-units 8A, B, D, E).

it best describes the composition of an evolving melt and of the instantaneous solids crystallized from the melt; by definition, the total solid is never in equilibrium with the melt (except for the first infinitesimal increment of crystallization) (McCarthy and Hasty, 1976; Cox et al., 1979). This agrees with the nature of zoned plagioclase within the older phase. Zoning implies crystal growth at a faster rate than re-equilibration with the changing melt composition. Thus, total equilibrium was never attained between solids and melt.

The direction of (and annotation on) each vector in Fig. 18 represents the path (and amount of fractionation) taken by the melt as either plagioclase (PLAG), K-feldspar (KSPR), biotite (BIO), hornblende (HBDE) or orthopyroxene (OPX) is crystallizing, involving up to 50% crystallization. An example of mineral phases involved in differentiation is shown in the inset plot of Fig. 18, and is taken from the Silurian Loch Doon Pluton of Scotland (Tindle and Pearce, 1981). There are three differentiation trends exhibited by the diorite to granite pluton. The first involves a decrease in Sr with increasing Ba (trend 1); the second, decreasing Sr with decreasing Ba (trend 2); and the third, minimal decrease in Sr with a strong depletion in Ba (trend 3). From the vectors, trend 1 could be controlled by plagioclase, orthopyroxene and hornblende fractionation; plagioclase and K-feldspar would enable trend 2

to be modelled, whereas mostly K-feldspar could control trend 3. Overall, these trends indicate differentiation with pure melts and solids of cumulate nature rather than crystal-liquid mushes with imperfect separation of melt and solid phases.

No clear single mineral phase emerges for the older phase of the Round Lake Batholith. This is contrary to the field evidence; plagioclase should emerge as the mineral phase controlling the crystallization history. Partition coefficients for Sr and, less so, Ba are compatible with plagioclase fractionation (K_D^{Sr} is 4.12, K_D^{Ba} is 1.21; Table 5). Thus, plagioclase fractionation should deplete both Sr and Ba in the residual melt. Of all the other minerals, quartz and K-feldspar are solely residual melt minerals, since they occur as groundmass minerals surrounding plagioclase. Biotite, muscovite and hornblende are late stage metamorphic/alteration minerals.

The lack of clear melt (and solid) trends as shown by Sr and Ba from the older phase during its crystallization history is a possible indication that the cluster of data points represents mixtures between pure melts and solid/crystal portions. Rayleigh Fractionation curves calculated for melts and crystals with intercumulus melt could be constructed allowing for crystal-liquid mushes, rather than pure melts and crystals of cumulate nature. Curves could be based on the removal of a

constant modal mineralogy from a parent magma/melt containing an initial Ba and Sr content corresponding to an older phase average compositions. Homogeneity within the older phase allows for the removal of a constant mineralogy during fractionation, and because of the possibility of solid-melt mixing, the chemical composition of the parent melt should approximate the average of the older phase.

Crystal-liquid mixing can not be solely responsible for the behaviour of both Ba and Sr within the older phase. Recalculating the modal mineralogy of the older phase in order to exclude either alteration or late growth minerals, plagioclase would constitute roughly 90% of the mineral assemblage used in the mixing model. The resulting curve would closely approximate that of the plagioclase (PLAG) vector in Fig. 18. The accompanying solid and solid with intercumulus melt curves would be subparallel to the PLAG melt curve. The cluster of points from the least to intermediate to the most differentiated subphases roughly trend parallel to the K-feldspar (KSPR), hornblende (HBDE), and orthopyroxene (OPX) vectors. Accordingly, plagioclase could not produce the observed patterns. However, K-feldspar would also have to be excluded, since the feldspar can not be a fractionating phase within a tonalitic melt. K-feldspar crystallizes at low temperatures when compared to the 1000^{o}C plus temperatures of tonalitic melts. K-feldspar is strictly a late stage mineral. In addition, hornblende and

orthopyroxene could not exceed 10% of the fractionating mineralogy. This is insufficient to deplete either Ba or Sr, as the feldspars, since both K_D^{Ba} and K_D^{Sr} approach zero (Table 5). Fractionation of appreciable amounts of hornblende and orthopyroxene would enrich the residual melt in Ba and Sr, again akin to the observed trends. This is not feasible, since neither hornblendites or gabbros occur within the older phase, nor are they expected to be present at depth. The substantial negative gravity anomaly corresponding to the batholith precludes the existence of basic rocks directly underlying the Round Lake Batholith.

The role of intercumulus melt during the crystallization of the older phase cannot be rejected in view of the inconclusive results from the present modelling. Chemical differentiation has taken place, indicated by the zoned plagioclase, whereas residual melt was preserved as groundmass quartz and K-feldspar, some of which forms the granodiorite subphase located at the eastern margin of the batholith. There is a differentiation mechanism which could link the older phase's Sr enriched main tonalite (according to Fig. 18, CaO values greater than 2.25% are mostly Sr enriched tonalite) to the more Sr depleted granodiorite. This link is based on the premise that both subphases are gradational in the field. The mechanism is filter pressing, whereby some of the residual melt (depleted in Sr) was squeezed out of the enclosing semi-

crystalline tonalite magma, inducing differentiation, and forming the granodiorite. Filter pressing (also termed filter differentiation; Propach, 1976) may explain the marked shift of data points, in Fig. 18, away from the main cluster, occupied mostly by tonalite, towards the Sr depleted granodiorite cluster. The process would allow for marked deviations in the concentration of elements even at the end stages of crystallization, which may explain the overlap of data points between samples with less than 2.25% CaO and the remainder of the older phase. The scenario would have residual melt removal by filter pressing late in the crystallization sequence of the tonalite. Prior and during melt removal, the magma viscosity would have increased several orders of magnitude when compared to the original tonalite melt. The melt would retain some trace element vestiges of the crystalline portion via remnant plagioclase from which it separated, because of incomplete crystal-liquid separation due to a high viscosity.

4) Petrogenesis of the Round Lake Batholith: magma source and crystallization history

Geochemical modelling of Archean tonalite/trondhjemite suites, encompassing the compositional homogeneity and voluminous nature of these rocks, suggests that tonalites are derived via 5 to 35% partial melting of basaltic or gabbroic materials from the lower crust (/upper mantle). Glikson (1979) suggested that the sinking Archean ultramafic-mafic greenstone pile provided the source material, upon melting, to

generate tonalite/trondhjemite melts.

A Batch Melting model will be tested for the Round Lake Batholith in an attempt to impose constraints on source region mineralogy. The model will encompass mainly the LiL and RE elements (partition coefficients listed in Table 5 under K_D values for basic and intermediate compositions). The source rock will be one having the composition of the Abitibi supracrustal pile, with the exception of Ba and Sr, which was inferred from Condie's (1976) average depleted Archean tholeiite: Ba at 80 ppm, Sr at 100 ppm, Rb at 4 ppm, La at 4 ppm, Sm at 2 ppm, Eu at 0.2 ppm, Tb at 0.5 ppm, Yb at 1.8 ppm. The nature of the melting will be non-modal equilibrium melting as Batch Melting[2].

Modelling will involve leaving single mineral residue of plagioclase (PLAG), biotite (BIO), garnet (GT), hornblende (HBDE), orthopyroxene (OPX), clinopyroxene (CPX), and the accessories apatite-sphene-allanite, over the 0 to 90% melting interval in order to evaluate potential source mineral. Results

---

[2]Batch Melting equation:

$$C_l/C_o = \frac{1}{F+D_i(1-F)}$$

where C_o = concentration of element i in the solid.
C_l = concentration of element i in the melt.
F = weight proportion of melt formed.
D_i = bulk partition coefficient of the element i for the residual solids at the moment when the melt is removed from the system.

are given as Ba, Sr and Rb variation diagrams, and La/Yb and Eu/Eu* vs Yb plots in Figs. 21 and 22, respectively.

Figure 20 illustrates the chondrite-normalized REE patterns of Arth and Hanson (1975), for 5, 20 and 35% batch melting of a tholeiite. Patterns are shown in comparison with the Round Lake Batholith older phase field (the younger phase curve is located near the upper boundary of the field, whereas the hornblende tonalite consist of higher normalized values). The model itself is based on a garnet-pyroxene residue, although hornblende (and garnet) in the residue would also produce a similar pattern. The older phase pattern is one of slightly higher REE values than the modelled curves, and 5 times chondrites. Modelled HREE's average near chondrite values, and show a distinct upturn in Yb and Lu contrary to the older phase trend.

The difference between the modelled and observed patterns suggest that the tholeiite may not be adequate to produce tonalitic melts, since the source would require generally higher REE values to impart an older phase trend. Secondly, there may be an involvement of accessory mineral phases, such as allanite, sphene and/or apatite, in addition to garnet and hornblende (and/or pyroxene) which would decrease or increase (depending if the accessory is residual or not) the overall REE content in the tonalitic melt (allanite and sphene exhibit K_D increases over those of garnet and hornblende by factors of

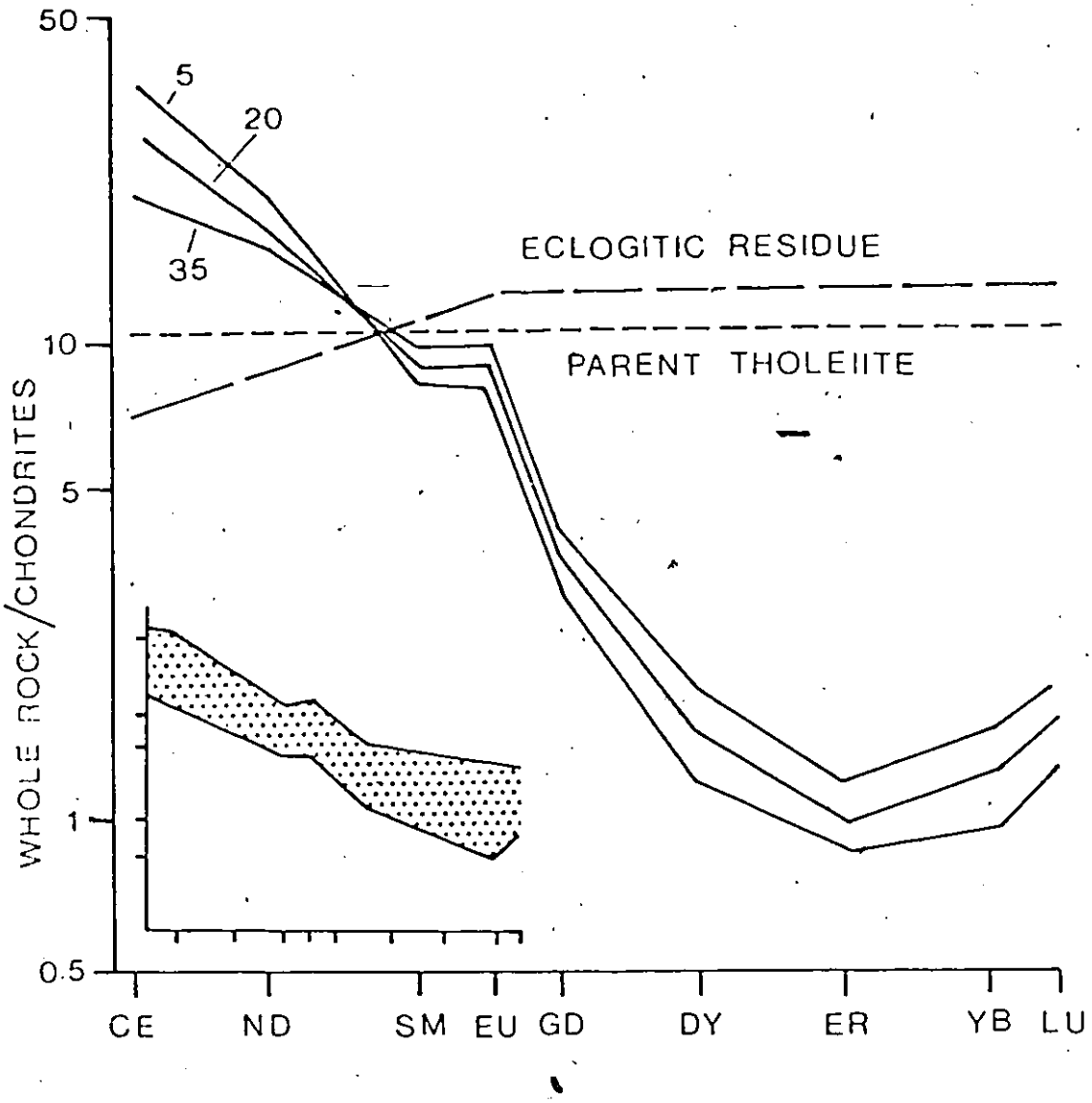

Fig. 20. Chondrite-nomalized REE plot showing patterns predicted for 5, 20 and 35% melting of tholeiite, leaving an eclogitic residue (Arth and Hanson, 1975). Inset: older phase field of the Round Lake Batholith (taken from Figure 13).

10 to 1000).

Vectors in Figures 21 and 22 demonstrate that extensive batch melting of a depleted tholeiite produces a melt of tonalitic composition (at least plagioclase-rich) akin to the older and younger phases of the Round Lake Batholith. The residue would contain garnet, hornblende and clinopyroxene ($\pm$orthopyroxene, $\pm$accessory minerals), which is consistent with Barker and Arth's (1976) model. Choosing of a different source material with Ba and Sr values closer to the known Abitibi pile (Ba: 162 ppm, Sr: 184 ppm) and REE values from average enriched Archean tholeiites (Yb: 2.4 ppm, La/Yb: 5 to 6, Eu/Eu*: 0.9; from Condie, 1976), which exclude komatiitic tholeiites, would not modify the residual mineralogy that greatly.

One interesting feature of the La/Yb vs Yb graph is the marked separation between the main tonalite of the older phase and the granodiorite portion. REE's of the main tonalite mass appear to indicate derivation from partial melting of tholeiite leaving a garnet-hornblende residue, whereas REE's of the granodiorite and cataclastic granodiorite-tonalite were possibly influenced by a residue containing accessory minerals. The younger phase unit and hornblende tonalite are probably partial melt products of the same source as the older phase main tonalite mass, although the possibility of accessory minerals in the residue curbed any La/Yb increase in the younger phase melt.

The concept of two partial melting episodes rekindles

Fig. 21. Sr-Ba, Rb-Ba and Sr-Rb for the Round Lake Batholith with vectors showing the theoretical effects on melt composition from single mineral residue (assuming batch melting). Vectors are annotated according to the melt fraction (in per cent). Field corresponds to the older phase tonalite (map-unit 8A), granodiorite (map-unit 8B), and cataclastic granodiorite-tonalite (map-units 8D, E); ◇ : younger phase granodiorite-tonalite (map-unit 9).

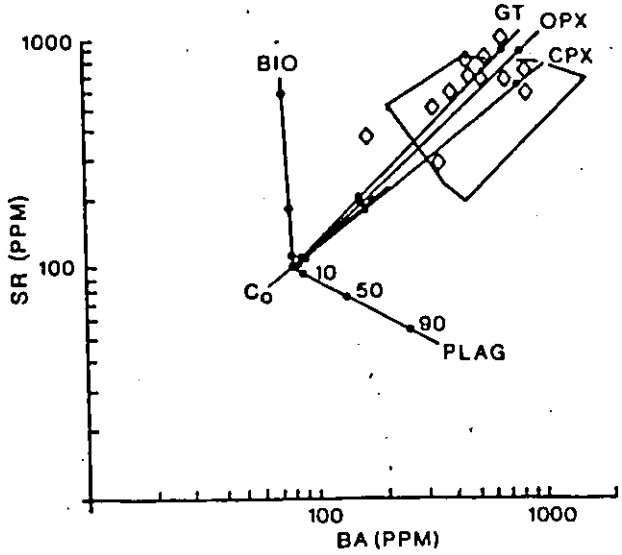
1000
100
SR (PPM)
BIO
GT
OPX
CPX
C_o
10
50
90
PLAG
100
1000
BA (PPM)

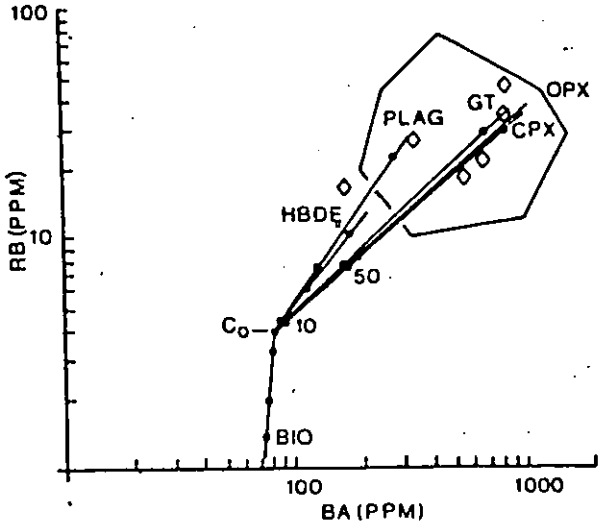
100
10
RB (PPM)
PLAG
GT
OPX
CPX
HBDE
50
C_o
10
BIO
100
1000
BA (PPM)

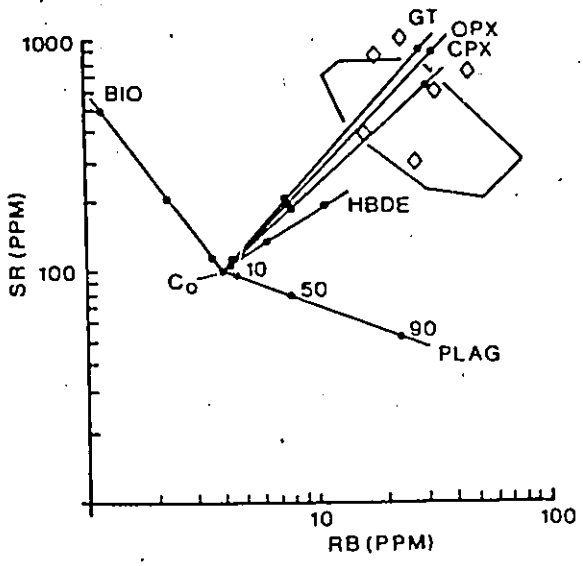
1000
100
SR (PPM)
BIO
GT
OPX
CPX
HBDE
C_o
10
50
90
PLAG
10
100
RB (PPM)

Fig. 22. La/Yb and Eu/Eu* vs Yb for the Round Lake Batholith. Vectors show the theoretical effects on melt compositions from single mineral residue (assuming batch melting), and are annotated according to the melt fraction (in per cent). Field corresponds to apatite-sphene-allanite residuum. The clinopyroxene vector is not included in the Eu/Eu* diagram since its effect is minimal. Map-unit symbols are: Tonalite (map-unit 8A), ▲ ; Granodiorite (map-unit 8B), ● ; Cataclastic granodiorite (map-unit 8E), ■ ; Hornblende tonalite (map-unit 8C), ◆ ; Granodiorite-tonalite (map-unit 9), ◆ .

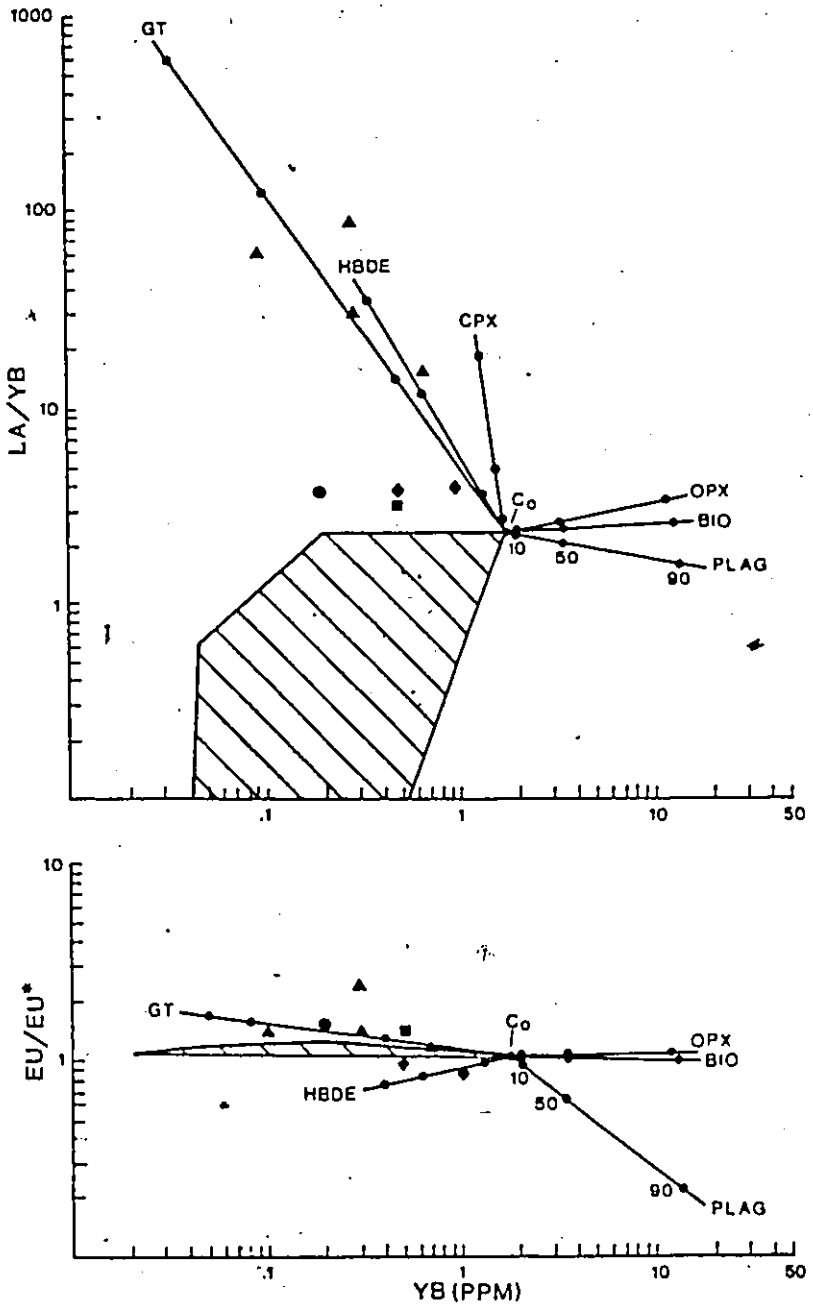
1000
100
10
1
LA/YB
GT
HBDE
CPX
Co
OPX
BIO
PLAG
10
50
90
.1
1
10
50
10
1
EU/EU*
GT
Co
OPX
BIO
HBDE
10
50
90
PLAG
.1
1
10
50
YB (PPM)

the possibility of the older phase consisting of several partial melt pulses from the same source. Each pulse would produce melts of slightly variable major and trace element character. Pulses ranging from tonalite to granodiorite; each producing separate clusters of data points in Harker, ternary and trace element plots, giving an overall false notion of differentiation. on a gradational scale. Again, this is feasible for the older phase. However, the difficulty in recognizing one separate pulse from another must be surmounted; clearcut internal contacts are needed to give creedance to the multiple pulse scenario. At present, the model will consist of one major partial melt episode producing a tonalitic melt, the older phase, which underwent internal chemical differentiation and limited physical differentiation (process of P. 109-110).

In any event the major source assemblage for the tonalite-granodiorite rocks of the Round Lake Batholith may actually approximate either an enriched tholeiite, or even a granulite facies tonalitic gneiss (mafic gneiss with tonalitic leucosome) with an assemblage consisting of garnet, clinopyroxene ($\pm$orthopyroxene), hornblende, plagioclase, quartz, opaques and minor accessories (Drury, 1978; Percival and Card, 1983).

Typical granulite facies tonalitic and basic gneisses from the well studied Archean Lewisian complex of northwest Scotland give Ba concentrations of 208 and 1209 ppm for the basic and tonalitic gneisses respectively, 215 and 894 ppm for

Sr, 8 and 30 ppm for Rb; a mean of 1.79 ppm for the combined Yb (18 analyses), 19 for La/Yb, and 1.12 for Eu/Eu* (19 analyses) (Drury, 1978; Pride and Muecke, 1980). Partial melting of granulites, with the mineralogy and trace element chemistry listed above, would yield mineral fractions in the residue comparable to the melting of either depleted or enriched tholeiites.

High grade gneisses are plausible source rocks for the bulk of the Round Lake Batholith magma (with the exception of the hornblende tonalite) when considering that various tonalitic gneisses with amphibolite to granulite facies assemblages underlie, as sill complexes, and are basement to the supracrustal pile of the Abitibi Supergroup in the western portion of the Abitibi Belt (Percival and Card, 1983) (and possibly the belt in its entirety). Percival and Card (1983) designated the gneisses as being part of domal structures occurring at depths between 10 and 15 km, and are analogous to massive and foliated tonalites (and granites) at higher levels that probably bear similarity to the Round Lake Batholith. The gneisses are believed to have been initially emplaced as voluminous, interplated tonalitic sheets (Percival and Card, 1983). Emplacement was accompanied by a heating event (Percival and Card, 1983) which may have contributed to the melting of the volcanic pile and some of the underlying gneisses, at around the 10 to 15 km depth in the upper crust (estimated from Fig.

3, p. 325; Percival and Card, 1983), to produce the higher level tonalites.

Assuming the average Archean geothermal gradient is 40°C/km (averaging of 30 to 35°C/km from Baer, 1977, and 40 to 50°C/km from Glikson, 1979), an estimate of temperature at the 10 to 15 km reported above would range between 400 and 600°C under normal regional metamorphic conditions. In order to produce tonalitic magma from the melting of tholeiites and/or granulite facies tonalitic gneisses, temperatures required must exceed 1000°C under normal regional metamorphism at lower crustal level (Glikson, 1979, postulated that temperatures of this nature would be attained at depths beyond 35 km for a 40 to 50°C/km Archean geotherm). Therefore, the underplating mechanism occurring at intermediate crustal levels, envisaged by Percival and Card (1983) for the Abitibi Belt (possibly accompanied by a regional metamorphism) would have to generate temperatures greater than 1000°C at depths of 10 to 15 km in the Archean crust of the Kirkland Lake-Timmins area.

Amphibolite inclusions within both older and younger phases of the Round Lake Batholith give some indications as to the probably source of the batholith's magma. White and Chappell (1977) pointed out that xenoliths (and xenocrysts) in granitoid bodies can represent solid residual material from the region of melting where the granitoid melt was produced. Xenoliths from the batholith are mostly amphibolitic in composition, and

are located throughout the younger phase, and in the older phase along the northern and southern contact zones with the supracrustal units from the Otto Stock to the Matachewan area and from Robillard Lake to the Penassi Lake area. In most cases, field evidence, petrography and chemical analyses demonstrate that the xenoliths are probably of local derivation, akin to the surrounding supracrustal rocks.

The only possible direct field evidence of tonalitic magma being generated by the melting of basic supracrustal rocks, on a local scale, is seen within the older phase hornblende tonalite unit. Here, amphibolitized and texturally varied supracrustal rocks are permeated by tonalitic magma rich in what appears to be xenocrystic amphibole and minute to large xenoliths of remnant volcanic material. Contacts between the tonalite and inclusions, even in a single outcrop, vary from sharp to diffuse, whereas the inclusions themselves can either be well preserved or ghost-like. Assimilation has taken place with the fracturing, transporting and mixing of fragments as the tonalite was injected; although granitization, shown by in-situ amphibolitized ghost fragments adjacent to and gradational with either finer grained amphibolite or aphanitic volcanic remnants, is also common, which tends to support the melting hypothesis.

The younger phase granodiorite-tonalite contains a diverse collection of amphibolitic xenoliths, with lesser granitized

hornfelsic and foliated tonalitic inclusions, that includes probable autoliths of intermediate composition. The variety of inclusions must reflect materials derived from a combination of source regions: these would include rocks similar to the surrounding supracrustal pile, older phase (?) tonalite-granodiorite, and possibly a precursor plutonic host.

The evidence presented here suggests that the Round Lake Batholith was derived from essentially two extensive partial melting events producing both the older and younger phase magmas. Source rocks either included or approximated in composition an average enriched tholeiite (more specifically, a komatiitic depleted-tholeiitic assemblage according to Condie, 1976), or tonalitic and basic gneisses (and, for the younger phase, a contribution from a precursor host of intermediate composition and possible the older phase). Based on xenolith types and distribution, there was a definite contribution from a volcanic source for both magmas. One scenario would have the gneisses tectonically emplaced below the ultramafic-mafic supracrustal pile. The heat generated during the emplacement would produce melting of the gneisses and the lower supracrustal pile at intermediate and upper crustal levels, producing tonalitic melts, which were then emplaced in the upper Archean crust.

In conclusion, the crystallization history of the Round Lake Batholith is schematically summarized in Figure 23. The

Fig. 23. Schematic diagram showing stages in the development of the Round Lake Batholith: partial melting and crystallization history.

A. Partial melting of intermediate and upper crusts; melting of either the ultramafic-mafic supracrustal upper crust or the tonalitic and basic gneisses, or both.

B. Diapiric mobilization of the Round Lake Batholith tonalitic melt.

C. Round Lake Batholith magma chamber: convection and differentiation in the older phase.

D. Advanced stage in the development of the Round Lake Batholith: continued differentiation in the older phase granodiorite, emplacement of the younger phase.

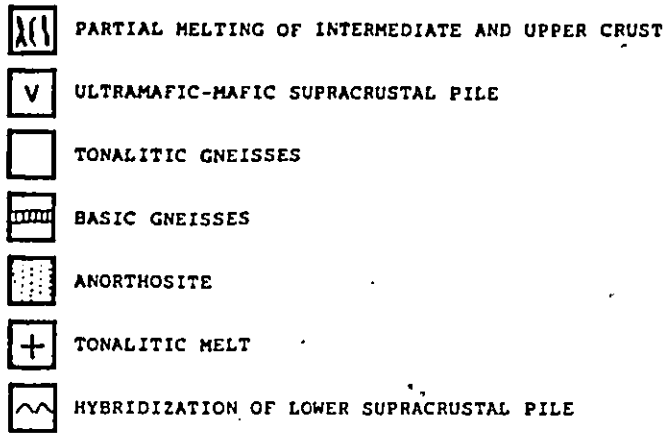
PARTIAL MELTING OF INTERMEDIATE AND UPPER CRUST
ULTRAMAFIC-MAFIC SUPRACRUSTAL PILE
TONALITIC GNEISSES
BASIC GNEISSES
ANORTHOSITE
TONALITIC MELT
HYBRIDIZATION OF LOWER SUPRACRUSTAL PILE

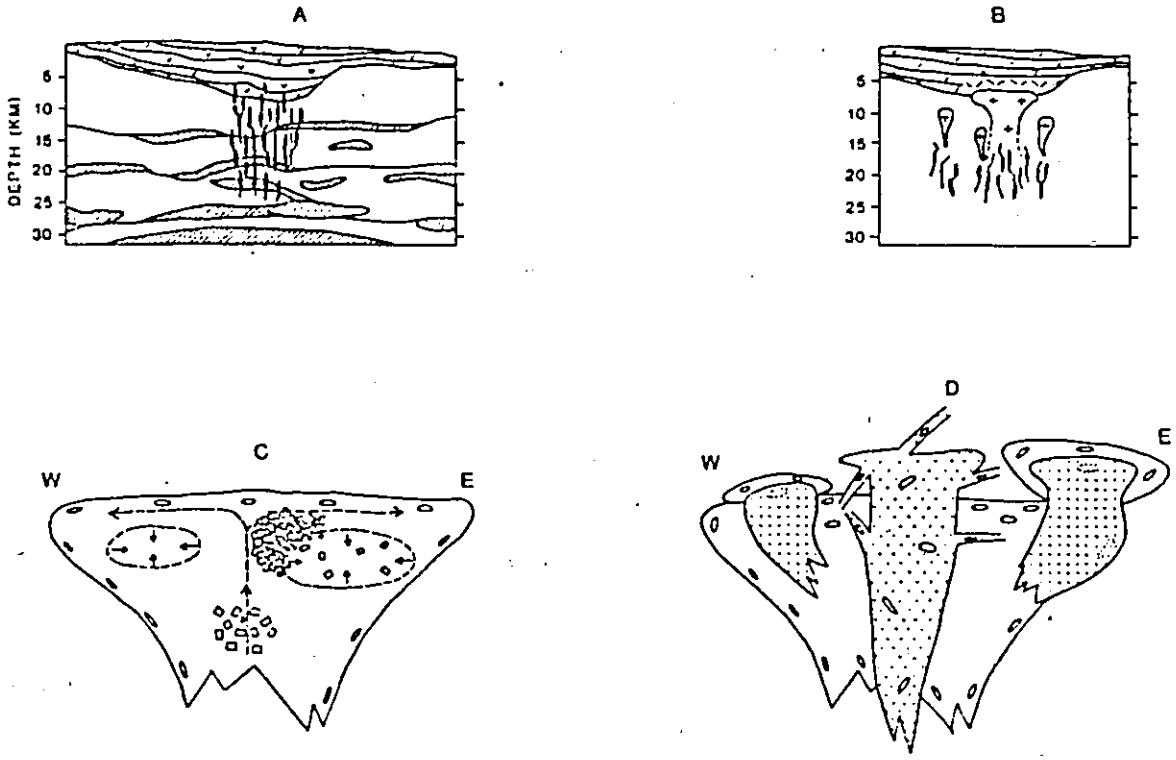
A
B
C
D
E
W
DEPTH (KM)
5
10
15
20
25
30

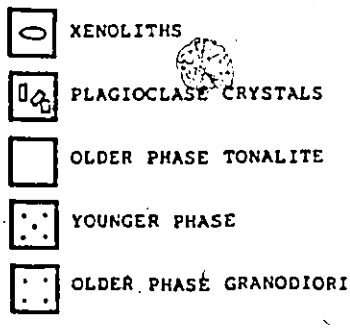
XENOLITHS
PLAGIOCLASE CRYSTALS
OLDER PHASE TONALITE
YOUNGER PHASE
OLDER PHASE GRANODIORITE

model incorporates field evidence, chemistry and several principles and evaluations reviewed earlier in this chapter concerning Archean tonalite/trondhjemite suites and the systematics of differentiation in granitoid systems. The stages envisaged in the partial melting - crystallization evolution of the Round Lake Batholith are as follows:

A) Heat generated during the emplacement of tonalitic and basic gneisses, caused widespread partial melting, at intermediate and upper crustal levels, of the ultramafic-mafic supracrustal pile and high grade tonalitic and basic gneisses (Fig. 25A). Source region mineral assemblage consisted of hornblende, garnet, plagioclase, clinopyroxene, and minor accessories. ($\pm$orthopyroxene, $\pm$quartz). The residue after melting would contain hornblende, garnet and clinopyroxene ($\pm$orthopyroxene, $\pm$accessories).

B) Partial melting was accompanied by major and subordinate tonalitic melt mobilization along a rising (diapiric) nuclei (Fig. 25B); the Round Lake Batholith older and younger phases representing the largest and subordinate nuclei respectively. Crystallization of the batholithic melt probably began early in the mobilization period with the development and accumulation of plagioclase crystals. Both major and

subordinate nuclei also incorporated marginal xenoliths, and retained restite material from the source region of which few have not been totally assimilated in the older phase.

B) Probable convection within the older phase magma chamber contributed to the upward and outward accumulation of plagioclase crystals (Fig. 25C). The granodiorite distribution and convection mechanics in a thermogravitational column suggest that two convecting cells operated and enabled minor differentiation to occur within the older phase. Filter pressing (during magma ascent) may have controlled the segregation of residual melt towards and into the convecting cells: each to become the western and prominent eastern granodiorite sites. Plagioclase accumulation brought about a Sr enrichment in the main tonalite.

D) Differentiation within the older phase, based on structural evidence, culminated with the granodiorite melt rising and probably breaking through its outer, solid granitoid envelope creating new centres of crystallization (Fig. 25D). A single (or a series) of subordinate tonalitic melt body(-ies), now termed the older phase hornblende tonalite and younger phase granodiorite-tonalite, ascended through the older

phase and crystallized with minimal internal diferentiation. The ascent took place along established weakness zones such as the main older phase core (representing the ascending portion between both convecting cells in the column) and contact zones between the main older phase and surrounding supracrustal rocks.

CHAPTER V: ECONOMIC GEOLOGY OF THE ROUND LAKE BATHOLITH

There are twelve major types of mineralization associated with four rock assemblages of different ages in the Round Lake Batholith area (Fig. 24; for a complete distribution see Pyke et al., 1973). Mineralizations are grouped as follows:

1) Au-Cu and Cu-Pb-Zn associations in volcanic and volcaniclastic rocks, from Cycles I and II of the Abitibi Supergroup, in the vicinity of the eastern and southern Round Lake Batholith contact zone (Boston Creek to the Hope Lake Stock), and within the Larder Lake Group of the Matachewan area. Many of the showings occur along shear zones accompanied by either quartz and/or quartz-carbonate veining. In addition, some showings are linked to a major quartz-feldspar porphyry body located at the base of the Skead Group (Cycle I), east of the Hope Lake Stock. Ultramafic rocks of the Larder Lake Group from the Matachewan contain asbestos.

2) Au(-Ag) in association with Fe-Cu(-Pb-Zn) sulphides from the Round Lake Batholith contact zone northeast of Charlton and southwest of Robillard Lake. Gold has more recently been recognized along a major northeast trending structure in the Hough Lake-South Mindoka area of the batholith.

3) Syenitic rocks from the major alkaline stocks north

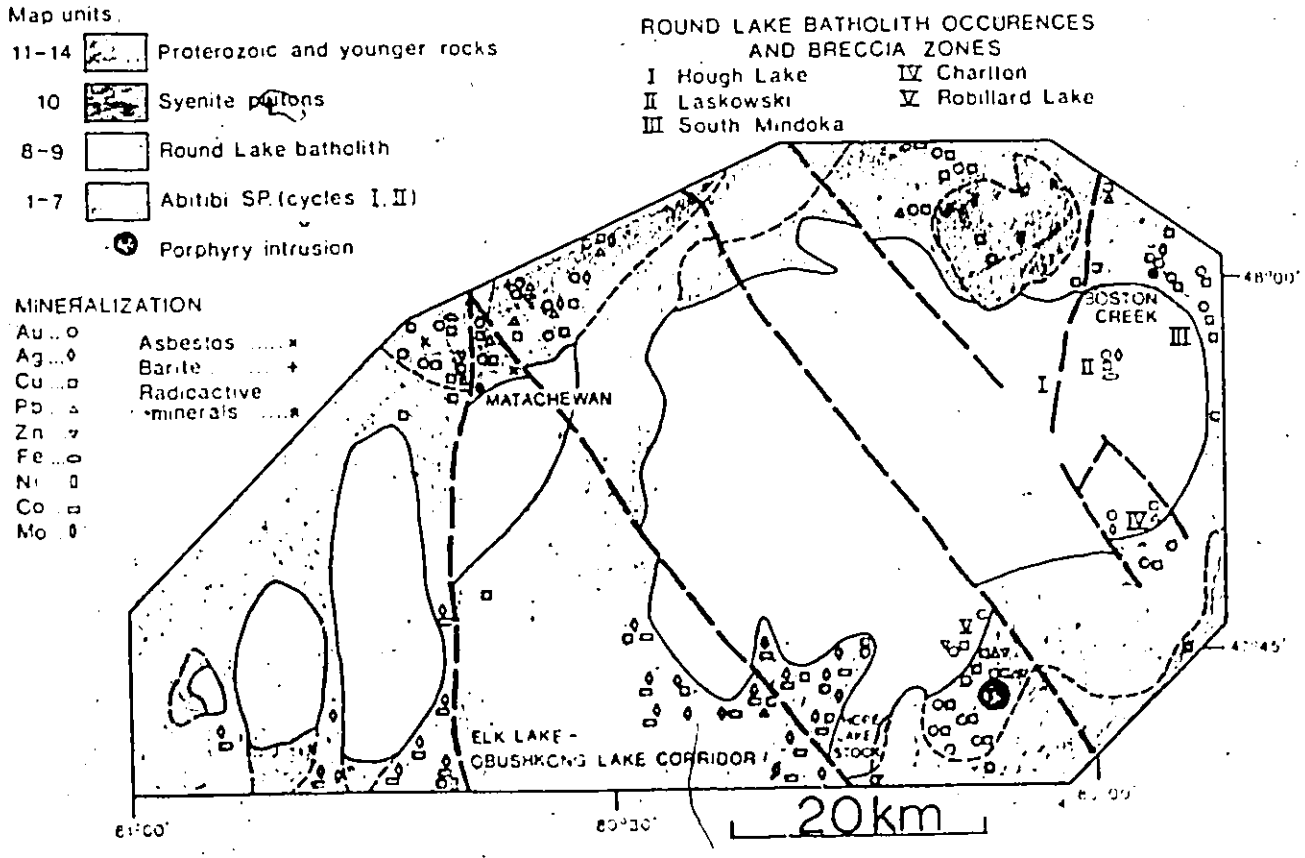

Fig. 24. Generalized geologic map of the Round Lake Batholith area showing types of mineralization (from Pyke et al., 1973; Sinclair, 1979; I, II and III were added by the author). Dashed, heavy lines represent faults.

of the batholith contain one or more of the following mineralizations: Au-Cu(-Pb-Zn), Mo, barite and radioactive minerals.

4) Ag-Co(Cu-Ni) association in gabbro-diabase of the Nipissing Diabase from Elk Lake to Obushkong Lake in the Gowganda area.

Gold within the Round Lake Batholith occurs along narrow (generally less than 100 m wide) northeast-trending brecciated and quartz veined shear zones in older phase tonalite, granodiorite and foliated to gneissic cataclastic peripheral tonalite and granodiorite. The longest zone, some 12 km in length, is located in the Hough Lake-South Mindoka corridor; a second, less prominent zone intersects the batholith periphery northeast of Charlton. A third zone, part of the southwest Robillard Lake occurrences, was not reconnoitred. Three major outcrops of breccia and/or quartz veining outline the first linear shear zone: these are the Hough Lake, South Mindoka and Laskowski subzones.

In the Hough Lake area, hematite-stained and brecciated tonalite is crosscut by a stockwork of quartz and hematite. Individual quartz veins are locally present and have consistent northeast trends of 075°. Hand specimens are barren of sulphide mineralization. The South Mindoka subzone crosscuts

weakly foliated and gneissic granodiorite outcrops from southwest of the railway track, northeastward, to the batholith contact. This zone is over 500 m wide, and consists of sporadic barren quartz veins that trend 030° and average less than 50 cm in width. The host granodiorite is locally brecciated and slightly hematitized. The Laskowski subzone is located on the west side of Highway 11 about 2 km south of the junction with Highway 573. It consists of a 100 m wide mineralized quartz stockwork crosscutting granodiorite. The surrounding granodiorite is uniform in modal and chemical composition, and texture (Pantalone, 1981). Approaching the stockwork, single quartz veins appear and the granodiorite becomes schistose with a greenish white color (sericitization). In the stockwork, granodiorite fragments (up to 1 m in size) are white (due to albitization) and are coated with chlorite and sericite. The stockwork consists of coarsely crystalline milky quartz (up to 15 cm wide) and minor carbonate, and is accompanied by chlorite-rich fractures trending north to northeast with moderate to steep westerly dips. Outlying quartz veins generally trend 025 to 040° and dip 55 to 60° to the northwest. The quartz contains occasional pyrite and chalcopyrite blebs (up to 2 cm wide). Numerous limonite-stained vugs throughout the quartz attest to the leaching of additional sulphides. The main metallic minerals include pyrite, chalcopyrite, covellite, a silver telluride and gold (Pantalone,

Plate XVI, Fig. 1

Quartz stockwork in marginal older phase foliated, cataclastic tonalite (map-unit 8D) outcrop. Veins are subparallel to the batholith contact (northeast trending). Locality, 4.5 km northeast of Charlton. Field of view 4 m across.

Plate XVI, Fig. 2

Close-up of veinlets from Fig. 1. Note tightly folded quartz veinlets (Q). Axial planes subparallel to foliation in host. Fold axes plunge southwesterly (to the right). Magnet is 2.5 cm across.

PLATE XVI

1

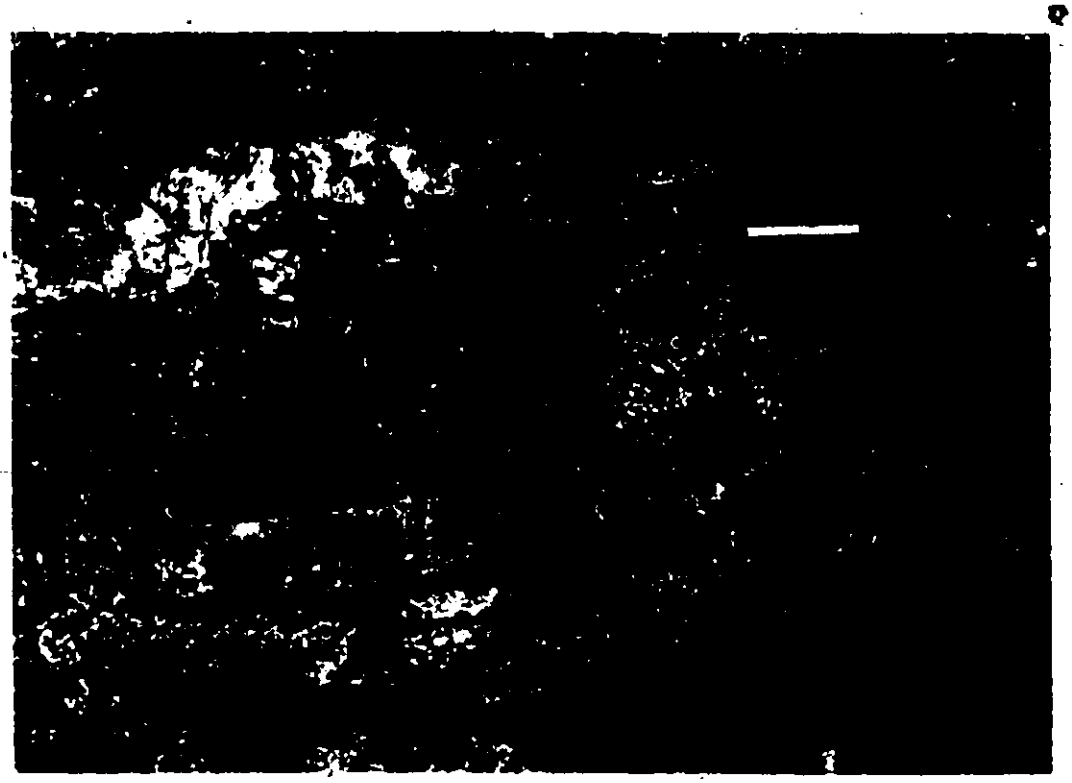

2

1981). Assays indicated gold concentrations of trace amounts to 0.771 ounces per ton, with silver values normally averaging 6 times that of gold (Pantalone, 1981).

The shear zone and reported gold occurrence, northeast of Charlton, consists of multiple and parallel quartz vein ranging in width from 3 mm to 50 cm, trending 075°, and dipping 70° northwesterly in foliated and cataclastic tonalite of the batholith's periphery. The main outcrop surface is barren of sulphide mineralization. One significant feature of the quartz veins is their subparallel orientation with respect to the cataclastic fabric and batholith-supracrustal contact. In addition, numerous veins appear to have been (tightly) folded (Plate XVI, Figs. 1 and 2) about axial planes subparallel to the fabric with southwest plunging fold axes. Consequently, vein emplacement did not postdate the deformation which produced the batholith's cataclastic periphery such that vein parallelism was a structurally induced phenomenon as a result of shortening perpendicular to the contact. Shortening probably occurred during the emplacement of the batholith.

CHAPTER VI: GEOCHRONOLOGY OF THE ROUND LAKE BATHOLITH

Absolute ages from all the geochronological investigations (Table 6) lend a quantitative aspect to the igneous history of the Round Lake Batholith area, and generally support the established stratigraphy.

Deposition of part of the Archean supracrustal sequence in the Kirkland Lake area, as indicated by the ages from the top of the first (Hunter Mine Group, equivalent to the Skead Group) and second (Blake River Group, above the Kinojevis Group) cycles, took place within a relatively short time span between 2.710 and 2.703 Ga (Nunes and Jensen, 1980).

The older phase tonalite (map-unit 8a) of the batholith gives an average crystallization age of 2.688 Ga (R.K. Wanless, pers. comm., 1979; based on two discordant zircon ages of 2.662 and 2.713 Ga), which correlates well with ages from other post-Abitibi Supergroup batholiths (ca. 2.680 Ga) from the central part of the Wawa-Abitibi Subprovince (Krogh et al., 1982). The younger mineral K-Ar (2.518, 2.534, 2.555, 2.557, 2.589, 2.624 and 2.684 Ga) and possibly the whole-rock and mineral Rb-Sr (2.390 and 2.550 Ga) ages (Aldrich and Wetherill, 1960; Lowdon et al., 1963; Purdy and York, 1968; Stevens et al., 1982) from the older phase may represent either primary crystallization or secondary metamorphic cooling ages (average 2.580 Ga). The low initial Sr^{87}/Sr^{86} of 0.7009 (Purdy and York, 1968) suggest any major contamination and suggests

Table 6. Summary of age determinations from the Round Lake Batholith area.

Rock/Map Unit	Rock Type	Method	min./wh. rock	Age-Ga (ratio*)	Reference*
Abitibi Dyke Swarm	diabase	Rb-Sr	wh. rock	2.197(.7048)	1
Nipissing Diabase	diabase	Rb-Sr	wh. rock	2.162(.7061)	2
Gowganda Fm.	matrix	Rb-Sr	wh. rock	2.288(.7063)	2
Matachewan Dyke Swarm	diabase	Rb-Sr	wh. rock	2.633(.7000)	1
Otto Stock	lamprophyre dyke	K-Ar	biotite	2.435	3
	syenite (2 localities)	K-Ar	hornblende	2.239, 2.552	3
	quartz syenite	U-Pb	zircon	2.493	4
	mafic inclusions	K-Ar Rb-Sr	biotite in both cases	2.506 2.470	5
	syenite	Rb-Sr	wh. rock	2.160(.7015)	6
	syenite	Rb-Sr	wh. rock	1.730(.7046)	7
Round Lake batholith					
Younger Phase	granodiorite	K-Ar	hornblende	2.469	7
	granodiorite	K-Ar	hornblende	2.564	3
Older Phase	granodiorite	Rb-Sr	wh. rock	2.390(.7009)	7
	tonalite (2 localities)	K-Ar	biotite	2.518, 2.557	3
	tonalite (2 localities)	K-Ar	hornblende	2.539, 2.684	3
	tonalite	K-Ar	muscovite	2.624	3
	granodiorite/ tonalite	K-Ar Rb-Sr	biotite in both cases	2.555 2.550	5
	tonalite	K-Ar	biotite	2.589	8
	tonalite	U-Pb	zircon	2.688†	4
Abitibi Supergroup Blake River Gp. Top cycle II	quartz-feldspar porphyry	U-Pb	zircon	2.703	9
Hunter Mine Gp. Top cycle I	dacite	U-Pb	zircon	2.710	9

Legend

Decay

λ^{87}_{Rb}: $1.42 \times 10^{-11}\ yr^{-1}$

$\lambda^{40}_{B}K$: $4.961 \times 10^{-10}\ yr^{-1}$

$\lambda^{40}_{e}K$: $0.581 \times 10^{-10}\ yr^{-1}$

λ^{235}_{U}: $9.8485 \times 10^{-10}\ yr^{-1}$

λ^{238}_{U}: $1.55125 \times 10^{-10}\ yr^{-1}$

* Isotopic ratio: Sr^{87}/Sr^{86} (initial)

† average of two discordant ages: 2.663 and 2.713 Ga

* reference list

1 Gates and Hurley, 1973
2 Fairbairn et al., 1969
3 Stevens et al., 1982
4 Wanless, pers. comm., 1979
5 Aldrich and Wetherill, 1960
6 Bell and Blenkinsop, 1976
7 Purdy and York, 1968
8 Lowdon et al., 1963
9 Nunes and Jensen, 1980

that the older phase was not primarily derived from reworked sialic crustal material, although it may have been short-lived, since ratios for these rocks tend to exceed 0.708 (Chappell and White , 1974). The isotopic ratio supports the evidence from the major and minor element chemistry that the older phase was derived from a mafic parent: a single source of either (or a mixture between) ultramafic-mafic supracrustal rocks and/or granulite facies tonalitic and basic gneisses, both having generally low Archean initial Sr^{87}/Sr^{86}.

Hornblende K-Ar ages of 2.469 and 2.564 Ga (Purdy and York, 1968; Stevens et al., 1982) for granodiorite of the younger phase (map-unit 9) are compatible with the older phase K-Ar and Rb-Sr ages, and since intrusive relationships have been established between both phases, all the ages must date the late Archean cooling stages of metamorphism (ca. 2.500-2.600 Ga).

The Otto Stock yields a wide span of K-Ar, Rb-Sr and U-Pb ages ranging from 1.730 to 2.552 Ga (Aldrich and Wetherill, 1960; Purdy and York, 1968; Bell and Blenkinsop, 1976; R.K. Wanless, pers. comm., 1979; Stevens et al., 1982), even though previously outlined field evidence suggests a relative age of late Archean or early Proterozoic for the intrusion. Whether the Gowganda Formation (contains cobbles of Otto Stock syenite) age of 2.288 Ga (Rb-Sr method on the matrix; Fairbairn et al., 1969) is correct or not, the stock predates the

emplacement of the Nipissing Diabase (whole-rock Rb-Sr age of 2.162 Ga; Fairbairn et al., 1969, since the Diabase crosscuts Huronian Supergroup rocks in the area, and postdates the Round Lake Batholith older phase (zircon U-Pb age of 2.688 Ga). Thus, the U-Pb zircon date of 2.493 Ga (R.K. Wanless, pers. comm., 1979) on the quartz syenite (map-unit 10c) seems to be a plausible crystallization age, whereas the hornblende K-Ar age 2.234 Ga (Stevens et al., 1982) may well represent a primary cooling age. The second hornblende K-Ar age of 2.552 Ga (Stevens et al., 1982) is not only compatible with two other biotite K-Ar and Rb-Sr ages of 2.506 and 2.470 respectively (Aldrich and Wetherill, 1960), from two different mafic supracrustal xenoliths, but the similarity tends to suggest that the hornblende is a xenocryst remnant from hornblende-biotite-rich xenoliths commonly found throughout the stock. Along the northeastern margin of the stock, a crosscutting lamprophyre dyke gives a biotite K-Ar age of 2.435 Ga (R.K. Wanless, pers. comm., 1979).

Two major diabase dyke swarms, the Matachewan and Abitibi, crosscut the Round Lake Batholith, and give whole-rock Rb-Sr ages of 2.633 and 2.147 Ga respectively (Gates and Hurley, 1973).

CHAPTER VII: TECTONIC EVOLUTION OF THE ROUND LAKE BATHOLITH

1) Review of Archean "granite-greenstone belt" evolution

Granite-greenstone belts consist of volcanic-sedimentary rock successions (supracrustal sequences), and granitoids which surround and intrude the greenstone belts (Anhaeusser et al., 1969). The volcanic phase consists mainly of ultramafic to mafic lava flows and sills, intercalated with a variety of felsic pyroclastics, and volcaniclastic and chemical sediments. The supracrustal rocks are highly deformed and faulted with large scale synformal folds developed subparallel to the usually elongated greenstone belt. Major faults are generally inconspicuous, since they trend parallel to the bedding and/or foliation surfaces. Metamorphism within the supracrustal rocks is of the low grade greenschist facies, with local increases in grade to amphibolite facies at the edges of the belt and around intrusive granitoids within the belt. The granitoids can be subdivided into three categories based on compositional, textural and structural grounds: migmatites and banded gneisses, circular to elliptical diapiric bodies, and late crosscutting granitoids. The complex array of migmatites and gneisses which surround the greenstone belts contain homogeneous massive granitic phases and enclaves of contorted, granitized greenstone. It is believed that the gneisses may be in part older and basement to the greenstone belts (Baragar and McGlynn, 1976). Possibly transitional to

the gneiss are sodic-rich diapiric granitoid bodies (granodiorite-tonalite); whereas younger potassic-rich granitoids (syenite-monzonite), of upper mantle origin, occur in both the supracrustal succession and gneissic to diapiric granitoids.

Some granite-greenstone belt evolutionary models (Anhaeusser et al., 1969; Baragar and McGlynn, 1976; Archibald et al., 1978; Gorman et al., 1978), consistent with Archean stratigraphy of the Canadian Shield, propose that the supracrustal rocks were deposited on a thin, older, sialic crust of gneissic and migmatitic affinities. The volcanic portions were erupted through faults which probably remained active during the entire sequence of development of the belts. Contemporaneous sedimentation from granitoid and volcanic sources during the eruptive cycle was concentrated near belt margins and continued beyond the end of volcanism. With subsequent thickening and subsidence of the supracrustal piles, the underlying sialic crust began melting (due to a high geothermal gradient) and, because of the density inversion (heavy basaltic material above lighter granitoid material), granitoid magma rose through the crust and eventually through the volcanic-sedimentary rocks. Crustal bulging at the margins of the belt and the internal emplacement of plutons contributed to the deformation of the supracrustal rocks, which is marked by isoclinal folding, thrusting and longitudinal strike-slip faulting.

Greenstone belts are usually affected by more than one period of deformation (Coward and James, 1974; Archibald et al., 1978; Fyson et al., 1978; Fyson and Frith, 1979) which cannot be accounted for solely be the diapiric rise of granitoid material as proposed by Anhaeusser et al. (1969) and others. The previous authors concluded that both diapiric emplacement (vertical tectonics) and lateral compression (or shortening) on a regional scale (horizontal tectonics) played major roles in the deformational sequence of greenstone belts. Field evidence depicts early deformational structures in greenstone belts being formed in response to diapiric uplift of granitoid bodies, whereas later structures were due to regional compression imposed across granite-greenstone terrains. Diapirism[1] is commonly initiated prior to D_1 deformation, and diapirs are emplaced, at their present levels, during or slightly after D_1, with two or more post-emplacement deformational episodes (see examples by Coward and James, 1974; Fyson et al., 1978).

Criteria for diapirism in Archean granitoid batholiths (Clifford, 1972; Stephansson, 1977) must include:

1) conformable structures in the diapir (assumed to be a granitoid body) and surrounding supracrustal units. Stratigraphy within the supracrustals should be concordant to the diapir's contact.
2) development of local shear/mylonite zones along the

diapir-supracrustal contact. Formation of a foliation (cataclasis) in the marginal parts of the diapir and adjacent supracrustal rocks (Fyson et al., 1978).

3) semicircular to oval shape of the diapir. Diapir should contain subvertical lineations (displayed by minerals and/or slickensides) to be conformable with moderate to steep outward (or inward)-dipping foliation and mineral lineation in the supracrustals around the diapir.

4) lack of a ghost stratigraphy of supracrustal remnants within the diapir. Rare dykes emanating from the diapir into the supracrustal cover (also indicating near solid-state emplacement).

5) radial and tangential fracture patterns about the diapir into the supracrustals.

6) strong compression normal to the bedding and/or schistosity in the supracrustal rocks (with extension in the plane of schistosity) parallel to the tectonic transport caused by the diapir. Deformational mode is one of severe flattening illustrated by fabrics in pillows, buckled dykes and layered volcano-sedimentary units, and bending of previously folded supracrustals into concordance with the diapir contact. Scenario is such that a gradation exists from generally undeformed pillows with axial ratios

($Y':Z'$, where Y'=intermediate pillow axis in plan view, Z'=long axis in third dimension) of 1:1 to 4:1, to flattened pillows with ratios of up to 50:1 at the diapir contact. Observed deformation implies that the diapir underwent a balloon-like inflation with an axially symmetric stress field at all points on the expanding diapir surface.

Post-diapir structures consist of pervasive schistosities (accompanying tight isoclinal folding in the supracrustal succession) that passes from the supracrustals into the diapir with little deflection. In addition, a granitoid diapir would also act as a relatively rigid massif during regional compression. Pressure shadows would then develop in the supracrustal terrain adjacent to the diapir. Pressure shadows would lack schistosity and any extensional features, such as pillow and pyroclastic or clastic fragment elongations that typify diapirism.

2) Structural evolution of the Abitibi Greenstone Belt

The central part of the Abitibi Belt consists of an extensive succession of volcanic and sedimentary rocks crosscut (and possibly underlain) by a variety of gneissic, foliated to massive granitoids and mafic intrusives. The volanics are subdivided in the Kirkland Lake-Timmins Area into a lower and upper cycle, each composed of komatiitic, tholeiitic and calc-alkaline volcanic rocks, capped by clastic sediments and

alkaline volcanics. Three volcanic edifices (or domes), characterized by the circular arrangement of felsic units, occupy the thickest part of the supracrustal pile at approximately the same latitude. The Round Lake Batholith is one of five major granitoid masses in the area. Two major easterly and northwesterly trending fault systems crosscut the Belt. The easterly trending Larder Lake and Porcupine-Destor Faults controlled sedimentation and volcanism within a graben-type structure of late Archean age (Jensen, 1978).

Pyke (1980) provided a working model for the origin of the volcanic-plutonic pattern exhibited in the Kirkland Lake-Timmins area. Salient features of Pyke's model, which is based primarily on the paleogeographic setting of Abitibi Supergroup cycles and the major batholithic complexes, are:

1) initial buildup of shield volcanic complexes producing the lower cycle sequence (consisting of the Wawbewawa, Catharine and Skead Groups, map-units 2, 3 and 4). The primordial crust is postulated to have been ultramafic to mafic in composition. Subsequent rifting and outpouring of ultramafic lavas marked the beginning of the upper cycle, along with clastic sediment accumulation within and adjacent to the main rift zones (ultramafic lavas and sediments form the Larder Lake Group, map-unit 5) of the Larder Lake Fault in Kirkland Lake. Partial melting in the downwarped

central portions of the lower cycle volcanic complexes produced tonalite/trondhjemite melts (for example, the Round Lake Batholith) which eventually intruded the overlying volcanic ejecta.

2) outpouring of tholeiitic basalts (Kinojevis Group, map-unit 6). Downwarping of upper cycle komatiites, sediments, and tholeiites gave rise to partial melting, providing calc-alkaline volcanism for the top of the cycle (Blake River Group).

3) renewed activity along the Larder Lake Fault zone led to minor extrusions of alkaline volcanics, and further sedimentation (Timiskaming Group, map-unit 7).

The above model provides a conceptual example of how the volcanic-sedimentary-intrusive association may have developed without incorporating any structural details. A more comprehensive geotectonic model was formulated by Dimroth et al. (1983a, b), in which the authors summarized the stratigraphic, paleogeographic and tectonic evolution of the southern segment of the Abitibi Belt, overlapping the Kirkland Lake area. Dimroth's model evokes a similar supracrustal evolution to the above scenario, but with the addition of a correlation between deformational episodes and emplacement of batholithic complexes. The generation of abundant granitoid magma (major tonalite/trondhjemite batholiths) began, during and/or after the deposition of the upper cycle, simultaneously with major folding

as the Abitibi Belt was shortened in a north-south direction. Folding developed from an early stage of buckling (flexure folds) with subvertical axial plane trending easterly, accompanied by (and probably resulting in part from) granitoid diapirism. This event was succeeded by isoclinal folding, in the same general direction, with a strong east-west penetrative schistosity. The penetrative deformation reportedly did not affect the major synvolcanic batholiths, since these areas were stiffened by the rigid massifs. Folding terminated with strike-slip faulting (for example, along the Larder Lake Fault), and the formation of sporadic kink bands and conjugate fracture sets related to continued north-south shortening.

3) Structures of the Round Lake Batholith

Even though Lawton (1954) suggested that solid state deformation contributed to the development of fabrics in the older phase granodiorite-tonalite, speculation on the actual mechanics of emplacement for the batholith as a whole, can only be resolved from detailed examinations of external contact zones (in relation to regional structures). Such a study was undertaken in three areas (Boston Creek, Charlton and Hope Lake Stock) along the eastern perimeter of the batholith, where structures strictly ascribed to the emplacement of the older and younger phases were distinguished from those produced on a regional extent.

A) The Round Lake Batholith contact zones

Boston Creek (northeast portion of the Round Lake Batholith)

The supracrustal sequence of the Boston Creek area is subdivided into the Pacaud Tuffs (map-unit 1), Wawbewawa (map-unit 2) and Catharine (map-unit 3) Groups. The supracrustal rocks show distinct structural elements (Fig. 25):

1) primary structures such as graded bedding in tuffaceous layers, pillows and an accompanying stratiform foliaton indicate younging away from, and general conformity to, the Round Lake Batholith contact (A; see Fig. 25; Plate XVII, Fig. 1).
2) the S_0-S_1 fabric tends to dip vertically, although south and west of Boston Creek, the fabric and mineral lineations in the marginal granodiorite facies of the batholith are inward dipping (Plate XVII, Fig. 2).
3) the S_0-S_1 fabric is also accentuated by a strong subparallel schistosity and boudinage of competent tuffaceous layers in the immediate batholith contact zone. One set of quartz veins tend to subparallel the stratiform foliation. In addition, outcrops of tuffaceous sediments adjacent to the batholith appear silicified with a conchoidal like fracture.
4) minor folds in tuffaceous rocks southeast of Boston Creek (Plate XVII, Fig. 3) have an array of axial plane orientations from subparallel to the batholith

Fig. 25. Schematic structural description of the Boston Creek area (northeast portion of the Round Lake Batholith). Location on Map 1. Geology modified from Lawton (1957).

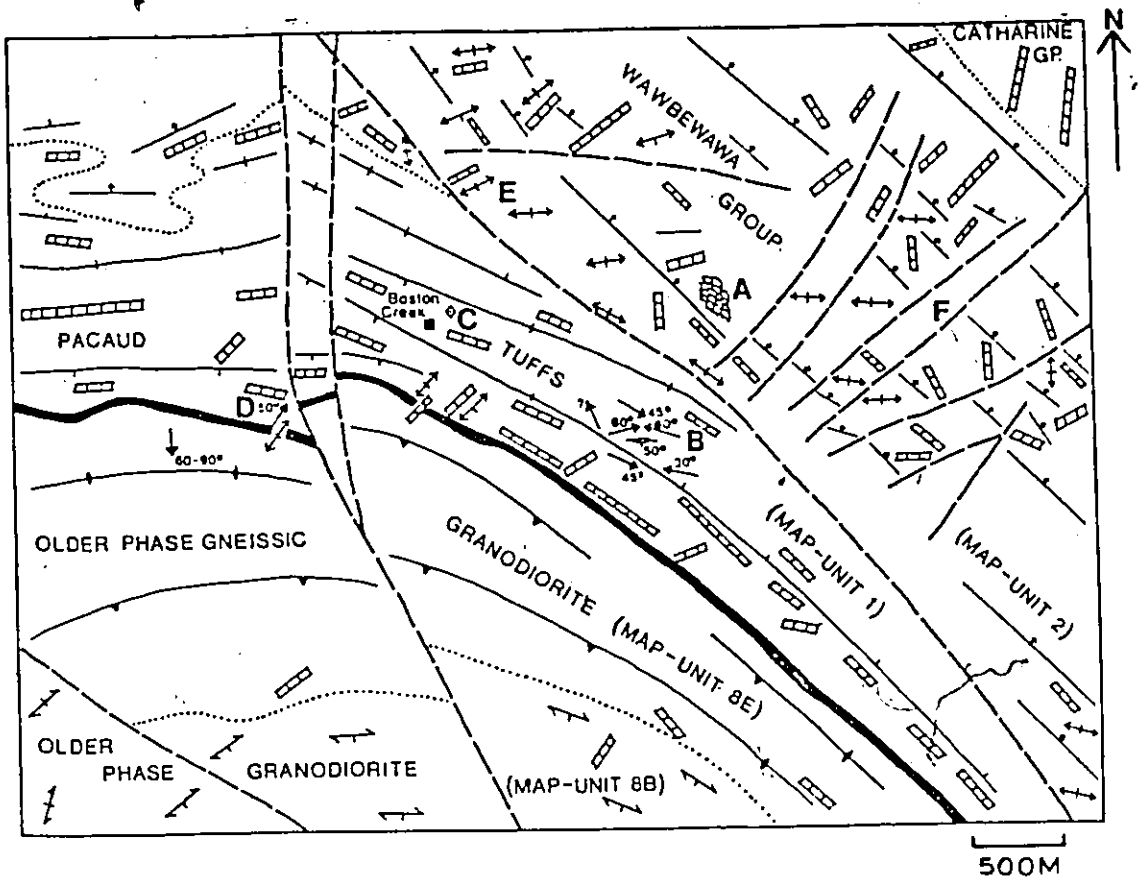

LEGEND

- GEOLOGICAL CONTACT
- METAMORPHIC AUREOLE
- FAULT-LINEAMENT
- BEDDING (TOPS KNOWN)
- BEDDING (TOPS UNKNOWN, INCLINED, VERTICAL)
- FOLIATION (INCLINED, VERTICAL) - BATHOLITH
- SCHISTOSITY (INCLINED, VERTICAL) - COUNTRY ROCKS
- GNEISSOSSITY (INCLINED, VERTICAL) - BATHOLITH
- AXIAL PLANE OF MINOR FOLD (INCLINED)
- 50° LINEATION (PLUNGE, VERTICAL)
- PILLOWS (UNDEFORMED)
- QUARTZ VEINS

Plate XVII, Fig. 1

Well preserved pillows in tholeiitic basalt outcrop from the Wawbewawa Group (map-unit 2). Younging direction towards top of figure, to the northeast. Round Lake Batholith contact to the southwest. Locality, 2 km northeast of Boston Creek. Pen is 15 cm long.

Plate XVII. Fig. 2

S_0-S_1 foliation in basalt outcrop from the Pacaud Tuffs (map-unit 1). The foliation and batholith gneissossity face southerly suggesting an inward dipping Round Lake Batholith contact. Locality, 650 m southwest of Boston Creek. Pen is 15 cm long.

Plate XVII, Fig. 3

Minor folds in tuffaceous volcanics outcrop from the Pacaud Tuffs (map-unit 1). Axial planes here are oriented in an east-west direction with westerly plunging fold axes. Locality, 1.5 km southeast of Boston Creek. Pen is 15 cm long.

1

2

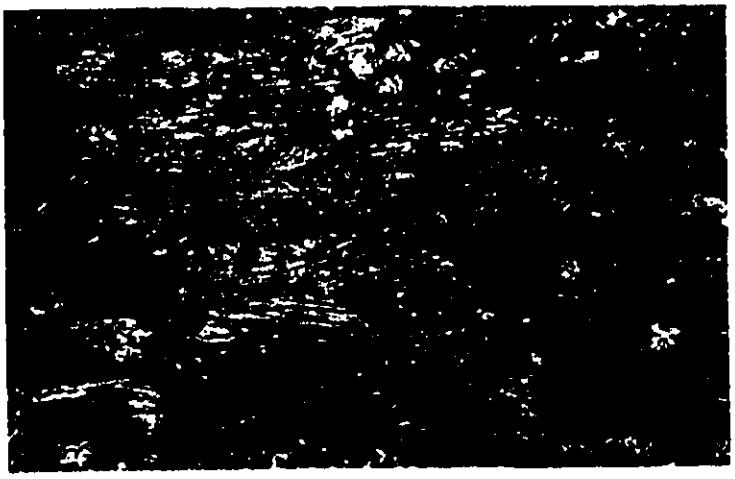

3

to easterly with moderate plunging axes in no consistent direction (B). However, a conglomeratic outcrop at Boston Creek has pebbles elongated vertically (C).

5) several sets of disconformable structures were discerned, all of which are inherent to the eastern internal-external contact zone of the batholith.

5 a) radially distributed lineament and schistosities transect both the batholith and supracrustal rocks between Round Lake and Charlton (D). Schistosities are axial plane cleavages associated with small scale en echelon kink bands (Plate XVIII, Fig. 1). Kink folding was accompanied by ductile shearing with the shear sense being partly defined in the northeast by the plastically deformed gneissic granodiorite (Plate XVIII, Fig. 2). Sinistral strike-slip movement produced the observed rotation of the fabric.

5 b) easterly trending shear structures (E) accompanied by a strong penetrative schistosity, brecciation and quartz-carbonate stockwork development.

5 c) northeast trending lineaments (F) occurring east of Boston Creek form part of a regional shear system that transects the batholith in

Plate XVIII, Fig. 1

En-echelon kink folds accompanied by shearing in tuffaceous volcanics outcrop from the Pacaud Tuffs (map-unit 1). Direction of shear is to the northeast, radial to the batholith contact which is located a few meters from the bottom of the figure. Locality, 650 m southwest of Boston Creek. Pen is 15 cm across.

Plate XVIII, Fig. 2

Ductile shear in the marginal older phase gneissic granodiorite (map-unit 8E) outcrop. The shear is a continuation of the structure shown in Fig. 1. Sinistral strike-slip movement along the shear produced the observed rotation of the fabric. Camera lens cap is 5 cm in diameter.

PLATE XVIII

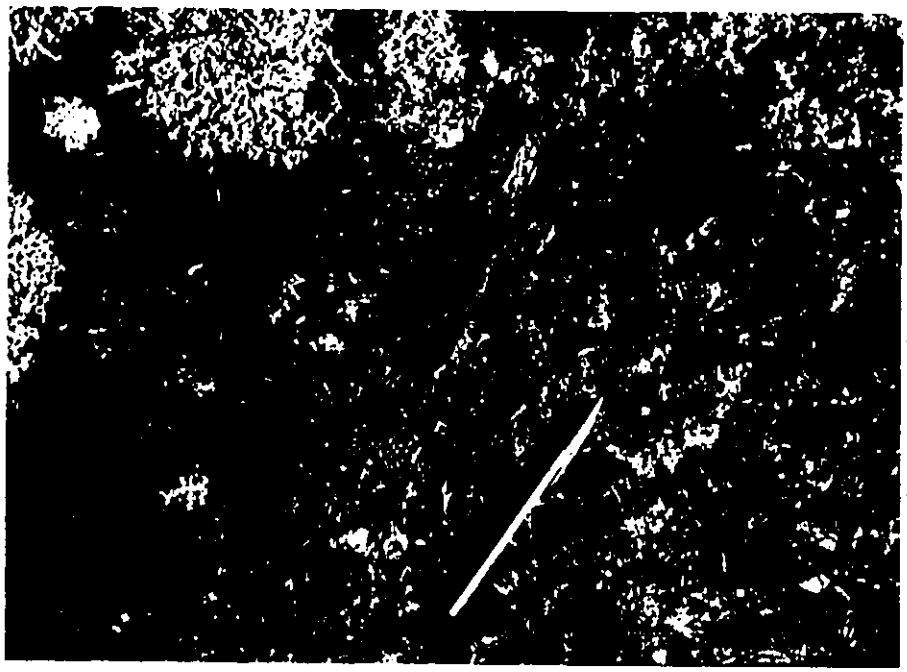

1

2

Plate XIX, Fig. 1

Photomicrograph from the amphibolite facies metamorphic aureole contact rock (recrystallized mafic tuffs) within the Pacaud Tuffs (map-unit 1) adjacent to the Round Lake Batholith. Note hornblende porphyroblasts (H) set in a fine-grained groundmass of hornblende, biotite/chlorite and feldspar/quartz. Fabric conforms to the S_0-S_1 stratiform foliation. Locality, Boston Creek. Field of view is 1 cm across.

PLATE XIX

Plate XX, Fig. 1

Crosscutting tonalitic dykes (D) from the Round Lake Batholith in tuffaceous volcanics outcrop from the Pacaud Tuffs (map-unit 1). Locality 1 km east of Tarzwell. Hammer is 30 cm long.

Plate XX, Fig. 2

Crumpled S_0-S_1 foliation in tuffaceous volcanics outcrop from the Pacaud Tuffs (map-unit 1). Axial planes are perpendicular to the Round Lake Batholith contact. Same locality as Fig. 1. Pen is 15 cm long.

Plate XX, Fig. 3

Conjugate kink folds in tuffaceous volcanics outcrop from the Pacaud Tuffs (map-unit 1) near the Round Lake Batholith contact. Folding (KF) resulted from shortening parallel to the S_0-S_1 foliation along the dip direction. Same locality as Fig. 1. Field of view is 40 cm across.

1

2

3

the Hough Lake-South Mindoka and Boston Creek areas, to beyond the McElroy Stock near the Larder Lake-Cadillac Fault. The shear system consists of brecciation and gold-sulphide bearing quartz-carbonate stockworks.

6) a narrow metamorphic aureole of amphibolite facies at the batholith contact is well foliated, with schistosity conforming to the S_0-S_1 fabric (Plate XIX, Fig. 1).

The contact zone due east of Highway 112 at Tarzwell reveals two sets of intersecting structures, in the supracrustal rocks, within 30 m of the batholith. The contact can be described as follows: narrow agmatitic section between the gneissic granodiorite-tonalite and conformable supracrustal tuffaceous rocks, tonalitic dykes (apparently from the batholith) crosscutting the tuffs conformably and disconformably (Plate XX, Fig. 1), and finally, crumpled tuff layers (Plate XX, Fig. 2) containing minor folds with north-south and N40^{o}E axial planes. The supracrustal rocks are inward dipping towards the batholith and show evidence of shortening, marked by conjugate kink folds (flowage folds), parallel to the S_0-S_1 fabric along the dip direction (Plate XX, Fig. 3). The dykes incorporate previously deformed xenoliths and crosscut these early formed conjugate kink folds developed in the foliation plane.

Charlton (southeast portion of the Round Lake Batholith)

The Charlton and Boston Creek areas have similar

structural settings, since both are located on opposite corners of the eastern perimeter of the Round Lake Batholith. Similarities between both settings include conformity (and overturning) of the supracrustal S_0-S_1 fabric to the batholith outline and axial planes of minor folds within the supracrustals lie roughly perpendicular to the batholith contact. These and additional structures warrant separate descriptions.

The geology of the Charlton section (Fig. 26) is subdivided into the batholith's cataclastically foliated tonalite (map-unit 8D), and Wawbewawa and Catharine Groups(map-units 2 and 3). Two major northwest-southeast trending faults, part of the Timiskaming System, crosscut the area. The tonalite is devoid of a gneissic fabric, implying weaker cataclasis in comparison to the northeast margin where the gneissic fabric overprinted the cataclastic foliation. In addition, there is little evidence suggesting that the Pacaud Tuffs (map-unit 1) are found in the Charlton area, since volcaniclastic rocks similar to those in Boston Creek are lacking. However, there are minor, thin horizons of argillite intermixed in the ultramafic and basaltic succession.

There are four important structural features that give additional insights as to the nature and timing of emplacement of the batholith, with respect to regional structures. These are:

1) conformity of the east-west cataclastic fabric of the

Fig. 26. Schematic structural description of the Charlton area. Location given on Map 1. Geology modified from Moorhouse (1944).

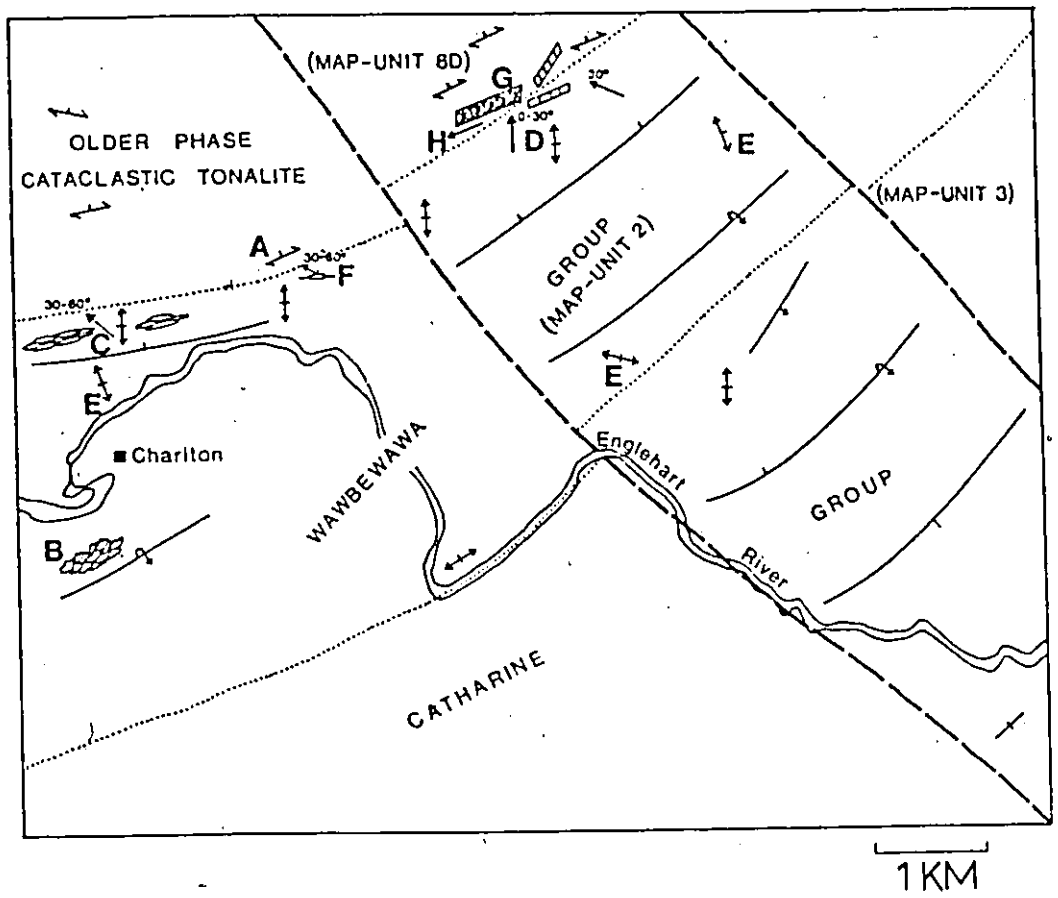

LEGEND

- GEOLOGICAL CONTACT
- FAULT
- FOLIATION (INCLINED, VERTICAL) - BATHOLITH
- SCHISTOSITY (INCLINED, VERTICAL) - COUNTRY ROCKS
- BEDDING (INCLINED, VERTICAL, TOPS DEFINED-OVERTURNED)
- AXIAL PLANE OF MINOR FOLD (INCLINED)
- 30° LINEATION (PLUNGE)
- PILLOWS 1) UNDEFORMED
  2) FOLIATED (TABULAR)
- QUARTZ STOCKWORK
- QUARTZ VEIN

Round Lake Batholith granodiorite-tonalite as the contact and more intense cataclasis is approached to the south and east (A; see Fig. 26)

2) the flattening of pillows into conformity with the batholith contact. Basalts due south of Charlton trend somewhat oblique to the batholith contact (B). Pillow shapes and top directions indicate a south facing and overturned sequence (Plate XXI, Fig.1). Interpillow sediments, pillow selvages and amygdules are easily recognizable primary features. Basalts due north of Charlton consist of highly stretched pillows that have been elongated in conformity to the batholith contact (C Plate XXI, Fig. 2). Selvages are the only recognizable remnant aiding in identification of pillows. Pillows are generally several metres in length and less than 10 cm wide. Flattening is consistent with a compression directed perpendicular to the stretching; here, perpendicular to the batholith contact. The apparent layering produced by alternating massive, basaltic pillow cores and selvages can easily be erroneously interpreted as tuffs. Anastomosing thin layers in a basaltic section, akin to tuffaceous layering, may be a subtle indication of highly deformed pillows.

3) two direction of minor folding in the supracrustal

Plate XXI, Fig. 1

Well preserved pillows in tholeiitic basalt outcrop from the Wawbewawa Group (map-unit 2). North is to the right. Pillow sequence dips to the north and youngs southwards. Locality, roadcut Highway 560, Charlton. Hammer is 40 cm long.

Plate XXI, Fig. 2

Stretched pillows (outlined in black) in tholeiitic basalt outcrop from the Wawbewawa Group (map-unit 2). Stretching direction is parallel to the Round Lake Batholith contact, a few metres from the bottom of the figure. Locality, 2.5 km north of Charlton. Magnet is 2.5 cm across.

PLATE XXI

1

2

sequence. Rare mafic volcaniclastics-argillaceous units, interspersed within the recognizable but highly deformed pillow basalts in the contact zone, are folded with north-south subvertical axial planes and north to northwest shallow to moderate dipping axes (D). Axial plane surfaces are oblique and roughly perpendicular to the batholith contact. Traces of axial planes are discerned throughout the supracrustal sequence due to a strong axial planar cleavage (E). Axial planes and cleavages are inferred as being partly radial to the batholith. However, these structures more than likely postdate the deformation of the pillows north of Charlton. The pillows were deformed during emplacement of the batholith, whereas later east-west compression produced folds with north-south axial plane orientation. In addition, some folds are either buckle folds produced during emplacement of the batholith or early folds subsequently reoriented into conformity with the batholith (F). Axial planes are inward dipping, and plunge, towards the batholith, mimicking the overturned basaltic sequence.

4) quartz stockwork and veining in the cataclastic tonalite of the marginal phase (G). There is evidence suggesting quartz veining was completed prior to the

final emplacement of the batholith. Veins were compressed with axial planes and fold axes parallel to the batholith margin (H).

Hope Lake Stock

The younger phase Hope Lake Stock (map-unit 9) is bounded to the north by the older phase tonalite (map-unit 8A) to the east by pillowed basaltic rocks of the Catharine Group (map-unit 3), and Proterozoic cover rocks (conglomerate, quartzite and diabase), and to the south and west by the Montreal River Fault (Fig. 27). The area of structural interest is the well exposed eastern contact zone. Structures are summarized as follows:

1) the Hope Lake Stock contact is transitional with the host basalts, producing an agmatite zone several hundred metres wide. Xenoliths are amphibolitic, generally massive and unfoliated with few recognizable pillow structures. Undeformed tonalitic dykes commonly crosscut the basaltic sequence, (Plate XXII, Fig. 1), and appear radially distributed about the stock margin.

2) the earlier east-northeast S_0-S_1 fabric in the basalts (A; Fig. 27) has been deflected and rotated into conformity with the younger phase intrusive. Evidence suggest folding and other structures are related to the emplacement of the stock:

Fig. 27. Schematic structural description of the Hope Lake Stock contact zone. Location given on Map 1. Geology modified from Moorhouse (1944).

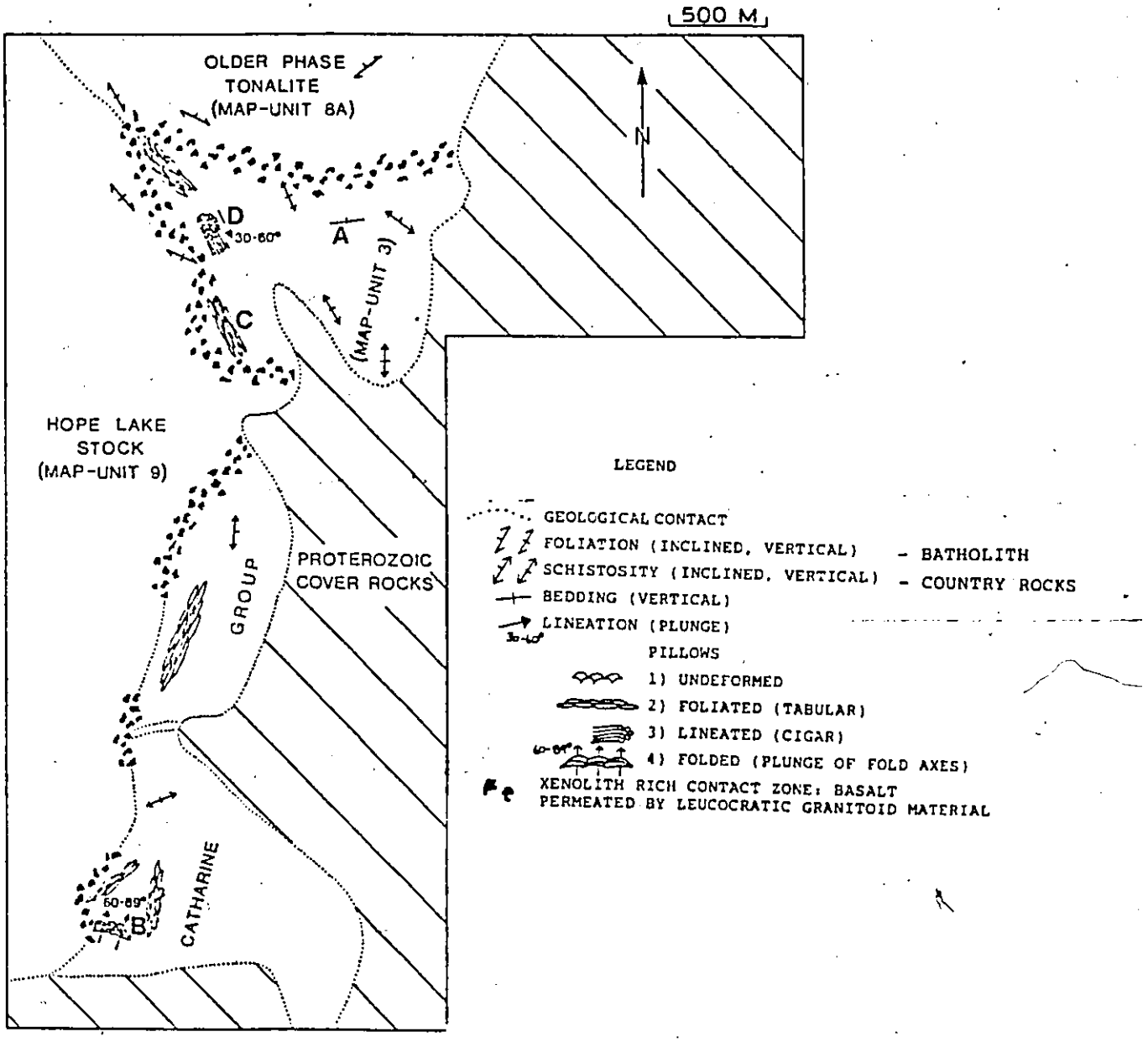

Plate XXII, Fig. 1

Undeformed tonalitic dykes (D) emanating from the Hope Lake Stock, intruding an amphibolite outcrop of volcanic origin from the Wawbewawa Group (map-unit 2). Locality, east contact zone of the Hope Lake Stock. Magnet is 2.5 cm across.

Plate XXII, Fig. 2

Buckled pillows in basalt from the Wawbewawa Group (map-unit 2). Pen is parallel to axial planes which are parallel to the Hope Lake Stock contact to the left. Buckling resulted from compression direction perpendicular to the stock. Locality, southeast contact zone of Hope Lake Stock. Pen is 15 cm long.

Plate XXII, Fig. 3

Pillow elongation in basalt from the Wawbewawa Group (map-unit 2). The unidirectional extension is subparallel to the Hope Lake Stock. The deformation is analogous to "die-drawing" extension. Pillow cores are epidotized (E). Locality, northeast contact zone of Hope Lake Stock. Hammer is 40 cm long.

PLATE XXII


1

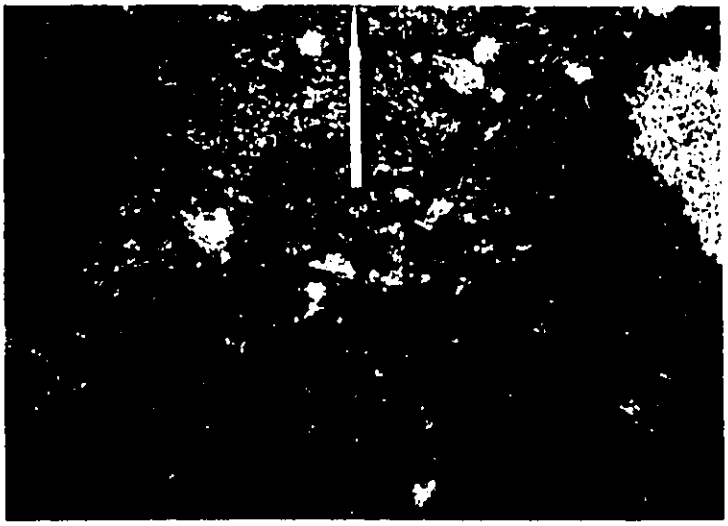
2


3

2 a) in area annotated B, pillows are buckled (Plate XXII, Fig. 2) with the compression direction having been perpendicular to the stock. Axial planes trend northerly conforming to the stock margin.

2 b) elsewhere, flattened pillows (in all three dimensions) and a pronounced schistosity, possibly an axial plane cleavage, generally conform to the contact (C and D).

3) Pillows also depict unidirectional extensions on moderately dipping axes subparallel to the stock (D; Plate XXII, Fig. 3), suggesting that the flattening mode in proximity to the stock was accompanied by a "die drawing" extensional deformation (see Clifford, 1972). This unidirectional strain fabric is located within the supracrustal wedge at the junction of the stock with the older phase tonalite.

Deformation resulting from emplacement of the stock can be implied from the close proximity of structures to, and uniformity of deformation about, the eastern margin of the stock (structures tend to follow curvatures in the contact). Structures in the southern supracrustal pile are conformable to the main batholith from Charlton to the Hope Lake Stock, such that folding near the intrusive implicates, either directly or indirectly, the stock in a post-older phase

deformation. Finally, regional deformation would not be expected to produce flattening and extensional structures in a supracrustal wedge between two rigid granitoid bodies of the type described here. The wedge would remain an area of low strain, possibly devoid of L-S fabrics.

The simplest way to account for the L-S fabrics would be to hypothize that the tonalite stock at an early stage underwent a balloon-like inflation. During expansion, the surrounding east-northeast trending basaltic pile adjacent the stock was compressed producing folds with northerly axial planes. Compression in a plane parallel to the stock margin included pillow flattening, ie, extension of pillows in all directions parallel to the stock. The older phase tonalite acted as a rigid body to the north which constricted flattening in the supracrustal wedge between the rising younger phase stock and somewhat stationary tonalite. Consequently, deformation within the wedge was a flattening mode in one direction (in this case, any volume change would be unidirectional probably parallel to the rising plutonic body), which was accompanied by a unidirectional extension producing cigar-shaped pillows. Tonalitic dykes were then injected into an already deformed volcanic sequence at the younger phase margin, and did not noticeably participate in the non-rupturing extensional strain.

4) Emplacement history of the Round Lake Batholith and tectonic evolution of the Kirkland Lake segment of the Abitibi Greenstone Belt

In summary, regional structures consist of easterly trending shears accompanied by a strong penetrative schistosity that appears to overprint conformable S_0-S_1 stratiform foliation about the northeast margin of the Round Lake Batholith. The easterly trending fabric does not penetrate the batholith's eastern cataclastic margin and adjacent unfoliated granodiorite subphase, although the fabric becomes pervasive throughout the main older phase tonalite, and is weak in the younger phase Indian Chute Stock. Folds with north-south axial planes in the Tarzwell area, adjacent the batholith's east-west trending contact, postdate the development of S_0-S_1 structures. Emplacement of the later Archean-early Proterozoic Otto Stock, northwest of Tarzwell, may have contributed to the buckling of the east-west S_0-S_1 fabric; although, it is unlikely, based on evidence from the Charlton area.

Nevertheless, it is quite apparent that these folds and the array of minor folds southeast of Boston Creek were not produced by the emplacement of the Round Lake Batholith. The S_0-S_1 was uniquely developed during the emplacement of the batholith. In addition, conformable flowage folds (depicted by conformable axial planes to the S_0-S_1 fabric, and horizontal fold axes) parallel to the batholith margin result from vertical movement most probably associated with ascension of the batholith. All other obliques and perpendicular folds located in the supracrustal S_0-S_1 fabric adjacent the batholith were formed during post-batholith deformation, either from regional north-

south and east-west compressions or, as previously stated, localized shortening during intrusion of post-batholith/older phase stocks similar to the post S_0-S_1 structures about the younger phase Hope Lake Stock.

In the Charlton area, there was no significant post S_0-S_1 intrusions in order to bring about shortening. Therefore it is proposed that the shortening producing the north-south oriented folds, normal to the batholith contact in the Tarzwell and Charlton areas, was part of an east-west compressional event.

Most of the other structures about the eastern portion of the batholith are related to emplacement and comply with diapirism at the present level of exposure. The structures not only include the conformable S_0-S_1 fabric, but also stratigraphic younging away from the batholith, mylonitization (?) of supracrustals adjacent the batholith, cataclasis in the marginal parts of the batholith, rounded shape of the eastern portion of the batholith, subvertical lineations in the batholith and adjacent supracrustals, subradial to radial lineaments about the margin, and a steeply outward and inward dipping S_0-S_1 fabric, along the eastern margin, which is accompanied by flowage folds with subhorizontal fold axes. The eastern portion of the batholith has also criteria for a highly viscous-near solid emplacement of the tonalitic-granodiorite magma of the older phase in the late stages of intrusion.

This is indicated by acute cataclasis and lack of xenoliths along the batholith margin compared to the generally agmatitic contacts elsewhere in the older phase. Continued ascension of a crystallized margin during diapirism would induce cataclasis (termed protoclasis) obliterating any evidence of previously incorporated xenoliths; whereas the high viscosity of the magma eliminated further stoping.

Any emplacement model for the Round Lake Batholith must take into account contrasting geological settings for the major portion of the batholith's older phase tonalite and eastern margin granodiorite phase, both of which display two distinct emplacement features, stoping and protocataclasis. Both are probably transitional events during diapirism: initial stoping involving the older phase tonalitic melt, progressing to protocataclasis after minor differentiation produced the granodiorite and was subsequently "brecciated", during ascension, once crystallization was at an advanced stage. The events are termed early and late diapirism.

Early diapirism would incorporate partial melting of the lower crust-upper mantle (basic in character) producing the tonalitic melt of the Round Lake Batholith. Due to the melt's relatively less dense and viscous character, the buoyant melt would rise as a diapir (mushroom or inverted droplet shape) through the crust, crystallizing, and subjected to some differentiation involving feldspar crystal settling and

convection. Ascension of the melt through the crust was effected by stoping and pervasive assimilation of the predominantly mafic crust. Exposed remnants of this episode would include agmatite zones, and tonalitic dykes intrusive into the country rocks ($\pm$ hornblende tonalite subphase).

The earliest structural feature possibly indicating the presence of the Round Lake diapir would have been doming of the supracrustal pile. Superimposed folding would enhance the dome into a large scale antiformal structure. Supracrustal rocks would be tilted, facing away from the domal centre. Tilting would approach the vertical during continued ascension, as the supracrustals would be eventually squeezed under the inverted tear drop-shaped diapir producing an inward facing and overturned stratigraphy. At this advanced stage of emplacement and because of faster cooling rates at the margin, the diapir would consist of an outer crystallized shell. The crystalline margin would therefore be subjected to cataclasis as the diapir rose to higher levels in the crust. Deformation in the supracrustal pile close to, and accompanying the emplacement of, the diapir would be flattening in all three dimensions. This is indicated by flattened pillows (and probably boundinaged S_0-S_1 layers), implying extension in all directions parallel to the diapir margin and a marked compression on horizontal axes normal to the diapir margin.

Late diapirism denotes continuing ascension of the (diapir

and) tonalitic melt in segregrated parts of the batholith. Minor differentiation within the older phase, as indicated in the previous chapter, probably resulted from filter pressing, whereby the granodioritic melt was squeezed out of the surrounding crystalline framework consisting primarily of plagioclase. The differentiate migrated upwards and laterally towards the eastern margin. Factors permitting filter pressing may have included loading from the overlying supracrustal pile and/or squeezing of the diapir via regional compression. Whichever the event, vertical loading or horizontal compression, the remaining melt likely migrated towards low pressure extremities within the diapir. At this stage, the differentiate possibly broke through the largely crystalline diapir, and continued its ascension with the surrounding crystalline shell producing a second smaller scale diapir. This smaller diapir would be represented by outcroppings of mostly granodiorite along the eastern portion of the batholith, and its contact zone with the supracrustals became the site of extensive protocataclasis.

Several sections of the remaining contact facies of the older phase also show evidence of emplacement deformation. Xenoliths and dykes are flattened-elongated parallel to the batholith margin. Dykes are buckled, having axial planes parallel to the margin; whereas amphibolitized xenoliths are elongated, apparently deformed into conformity with the margin. This is substantiated by the conformable internal foliation in

xenoliths defined by amphibole and platy minerals. Flattening is largely ascribed to dispirism, and possibly a late expansion of the diapir due to the arrival of the younger phase granodioritic-tonalitic Indian Chute Stock at the core of the older phase. The deformation never proceeded beyond minor cataclasis when compared to the pervasive and intense brecciation along the eastern margin.

An additional feature related to the eastern portion of the older phase pertains to the temperature of emplacement. Metamorphism in the supracrustal pile in the Round Lake Batholith area is mainly greenschist-subgreenschist facies with few areas of amphibolite facies abutting against the batholith, including a narrow contact aureole. Elsewhere, xenoliths along the older phase contact (and younger phase Hope Lake and Crooked Cree Stocks) are amphibolitized, although amphibolitization decreases rapidly outside the confines of the contact. This lack of increased temperature (in the supracrustals) with proximity to the batholith is not fortuitous. At present levels, much of the batholith was crystallized during emplacement, thus allowing minimal heat transfer to the supracrustal host. A near solid emplacement of the eastern portion would produce radial and conformable stress regimes producing structures in the surrounding supracrustal pile that would include radial lineaments and schistosity development parallel to the batholith margin. Both structural features can be recognized along the

eastern margin.

One query remains, and it concerns the role of the Round Lake Batholith in the tectonic framework of the Kirkland Lake segment of the Abitibi Belt. The geotectonic model for the southern segment of the Abitibi Belt, produced by Dimroth et al. (1983a, b), recognizes three major deformational episodes. A D_1 event consisting of large scale flexure folding. Synclinoria were formed at zones of pre-orogenic subsidence , ie., zones of thickest volcanic accumulation, whereas anticlinoria nucleated at less subsident zones, in part from diapirism in the crust. F_1 were open folds, generally easterly trending with subvertical axial surfaces and a weak S_1 fabric in the supracrustals. The S_1 (and subparallel S_0 primary fabric) conforms to the outline of domal structures where diapirism occurred. F_2 folding was isoclinal with a penetrative vertical S_2 fabric trending east-west. D_2 originated from a north-south compression. Late northeast-southwest and northwest-southeast schistosities belonged to conjugate shear planes, manifested by strike-slip faulting related to continuing north-south shortening.

Dimroth's scheme can be applied to structures in the Round Lake Batholith area. S_0 primary fabric and S_1 stratiform foliation are subparallel and conform to the elliptical shape of the batholith. Vertical tectonics related to diapirism was the mechanism producing the S_1 fabric. S_2 developed from north-south horizontal compression and is represented by the

internal cataclastic east-west fabric within the batholith and crosscutting east-west shears and schistosities in the supracrustal pile. Pervasiveness of S_2 supports a stronger penetrative plastic rock strain during D_2 than in D_1. Additional folds with north-south axial surfaces in the supracrustal rocks adjacent the batholith's north and south contacts east of the Cross Lake Fault could depict a D_3 deformation resulting from an east-west compression. The north-south trending fold structures deflecting the S_0-S_1 fabric and accompanying the emplacement of the younger phase Hope Lake Stock also qualifies as a D_3 fabric. There is no evidence to suggest that emplacement of the Hope Lake Stock and the other younger phase stocks was not synchronous with east-west compression in the Belt. Current field evidence indicates that the younger phase Indian Chute Stock, at the core of the older phase, contains a weak east-west foliation subparallel to S_2, suggesting a late D_2 emplacement possibly extending into D_3. Recognition of an east-west compression in the Round Lake Batholith area is significant, since it has been overlooked by previous workers. However, relative timing of the D_3 event with emplacement of younger phase stocks remains ambiguous.

Timing of the development of the older phase marginal diapir is also vague. The smaller diapir must either postdate D_2

deformation, since S_2 did not penetrate the granodioritic core and cataclastic margin, or was not affected by D_2. If emplacement of the smaller diapir did accentuate the S_0-S_1 fabric in the supracrustals, then the east-west schistosities and shears adjacent the batholith, and believed to be D_2 deformation, must postdate this second diapir. This is not the case here.

Allowing that the north-south compression promoted filter pressing and differentiation in the older phase which led to the development of the marginal diapir, it may be concluded that the compressive stresses producing the east-west cataclasis elsewhere in the batholith and schistosities in the surrounding supracrustals were not of sufficient intensity to exceed expansive stresses accompanying the smaller diapir. Thus, the only structures formed were those derived from the emplacement of the smaller diapir. In addition, the deformation associated with the smaller diapir appears to be restricted to the immediate contact zone along the eastern margin. Diapirism of the older phase as a whole produced the large scale conformity of the supracrustal pile surrounding the batholith. Subsequent north-south compression induced development of the second diapir, and produced on S_2 cataclasis in the batholith and an S_2 schistosity overprinting an S_0-S_1 stratiform foliation away from the batholith. The smaller diapir and marginal supracrustals were not affected by D_2 for two reasons. The

diapir's magma at the core was probably less viscous than the remainder of the batholith which underwent brittle deformation. Secondly, the crystalline margin of the smaller diapir and adjoining supracrustals were subjected to intense vertical deformation brought forth by cataclasis, never allowing any D_2 fabric to develop. Ascension of the smaller diapir was accompanied by an intense stress field which led to the marginal cataclasis, and was probably responsible for the development of near radial lineaments about the eastern margin.

The late northeast trending shear zones which crosscut the batholith from Hough to South Mindoka and the supracrustals from Boston Creek to the Larder Lake Fault, would represent remnants from the last structural episode.

The proximity of, and ambiguity between, structural events in the Round Lake Batholith area can only be resolved by additional detailed structural studies where crosscutting structures ascribed to both diapiric and regional deformation can be identified. Structural interpretations offered here are based on field evidence supplemented by general Archean structural concepts (vertical and horizontal tectonics) and Dimroth's et al. (1983a, b) studies in the Abitibi Belt. Nevertheless, a comprehensive model for the tectonic evolution of the Round Lake Batholith, incorporating the Kirkland Lake segment of the Abitibi Belt, can now be formulated using petrochemical and structural constraints already discussed.

The model follows previous models for the western and southern Abitibi Belt devised by Pyke (1982) and Dimroth et al.(1983a, b), and is summarized in Figure 28.

Phase 1 ((a) in Fig. 28)

The initial stage in the development of the volcanic pile began with the presence of (at least) two large shield volcanic complexes: the Lake Abitibi and Round Lake Complexes (A). Both were responsible for the deposition of Cycle 1 volcanics (Wawbewawa, Catharine and Skead Groups and equivalent rocks, map-units 2, 3 and 4; may or may not have included the Pacaud Tuffs, map-unit 1). The tonalitic-granodioritic rocks of the Round Lake Batholith appear to be geochemically incompatible with the Cycle 1 supracrustal sequence. It is postulated that the present site of the batholith has remained an active geothermal hot spot during the late Archean. The site evolved from an early mantle derived volcanism, and progressed to a deep seated (crustal) partial melting episode which produced a tonalitic melt. The central part of the Belt consisted of an extensive east-west trending rift structure(B). Cycle 2 komatiitic and tholeiitic volcanic rocks (Larder Lake and Kinojevis Groups and equivalent rocks, map-units 5 and 6) eminated from this rift.

Phase 2 ((b) in Fig. 28)

Cycle 2 volcanism terminated with the volcanic rocks of the calc-alkaline Blake River Group encompassing four major

volcanic complexes(C): from east to west, these are the Lac Dufault, Ben Nevis, Watabeag and Shaw Complexes. The Belt also experienced the beginnings of a north-south compression (of unknown origin)(D). Two major fault (-rift) structures, the Larder Lake(E) and Porcupine-Destor(F) Faults, were present early in the evolution of the Belt. Both were active as normal faults during subsidence of the dense Cycle 2 volcanics, and were later to become zones of prominent alkaline volcanism and fluviatile sedimentation (the Timiskaming Group of Cycle 3, map-unit 7). The supracrustals were moderately affected by a low-grade burial metamorphism of subgreenschist prehnite-pumpellyite facies. Extensive partial melting of Cycle 1 ultramafic-mafic supracrustals and tonalitic gneisses in the lower crust, with the possible addition of upper mantle basic material, generated tonalitic melts at the present sites of the Round Lake and Lake Abitibi Batholiths(A). Ascension of melts and xenoliths via stoping and eventually diapirism caused upwelling in the upper crust, resulting in domal structures that were to eventually accomodate both the Round Lake and Lake Abitibi diapirs.

Early Diapirism ((c) in Fig. 28)

D_1 structures (F_1 flexure folds-G and S_1 stratiform foliation-H) were initiated due to diapirism and the continued sinking of the dense volcanic pile. A synclinoria developed between the Round Lake and Lake Abitibi diapirs(A). Supracrustal rocks became tilted away from the domal centres. Tilting

approached the vertical as ascension and expansion of the diapirs proceeded. Supracrustals were eventually squeezed under the inverted tear-shaped diapir producing an inward facing foliation (facing the diapirs) and overturned stratigraphy. Deformation in the supracrustal pile, accompanying the emplacement of diapirs, is one of extreme flattening: extension in all directions parallel to the diapir margin and compression normal to the margin.

Sinking of Cycle 2 supracrustals allowed partial melting at depth with the production of granodioritic to monzonitic melts(I). The melts rose, as smaller scale diapirs along the initial rift structure, at the former sites of Cycle 2 volcanic complexes, between the Larder Lake(E) and Porcupine-Destor Faults(F).

North-south compression(D) intensified throughout the Belt, initiating the regional isoclinal folding in the supracrustals with east-west trending axial planes.

Folding ((d) in Fig. 28)

North-south compression(D) culminated with the development of F_2 east-west trending isoclinal folds(J) and S_2 penetrative schistosity(K), subparallel to D_1 structures, which affected both the supracrustal and granitoid rocks. S_1 stratiform foliation, conforming to the Round Lake diapir's circular to elliptical outline, was transected by S_2 shear zones and schistosities(L).

Filter pressing within the Round Lake diapir probably occurred during the peak of north-south compression, and resulted in the physical separation of the granodiorite melt fraction from the crystallized tonalite of the older phase(M).

All major granitoid bodies in the Belt were emplaced in the upper crust by the end stages of D_2.

Late Diapirism ((e) in Fig. 27)

North-south D_2 compression(D) was in the waning stages as the second smaller granodiorite diapir along the eastern portion of the Round Lake Batholith, continued its ascension through the crust(N). Here, diapirism produced extensive cataclasis along the eastern margin of the batholith; boudinage of S_1 layering in the supracrustals and radial lineaments about the eastern margin. In all, diapirism altered the ellipticity of the batholith bringing about a more rounded eastern perimeter. However, the ellipticity of the batholith as a whole was somewhat modified due to the incoming younger phase granodioritic-tonalitic melt. Emplacement of the younger phase(O) brought about variable expansion of the older phase as melts rose through the core and north and south central margins of the older phase. The space problem created by the younger phase neccessitated adjustments in the shape and size of the batholith, most of which occurred between the Cross Lake and Motreal River Faults.

Emplacement of the Hope Lake Stock(P) folded the S_1

easterly trending fabric into northerly oriented folds and accompanying schistosity. This was possibly synchronous with an east-west compression (D_3 event) which produced north-south schistosities throughout the supracrustals adjacent the batholith.

The prominent Hough Lake-South Mindoka, northeast Charlton, and Boston Creek-McElroy shear and breccia zones (all towards the eastern margin of the batholith) were probably initiated at this stage. Movement along the Larder Lake(E) and Porcupine-Destor(F) Faults activated strike-slip faulting which may have produced conjugate sets of faults oblique to the main east-west system of fractures. The shear-breccia zones would therefore be remnants of these subsidiary faults.

Final Stage ((f) in Fig. 27)

The sketch represents the current level of exposure for the Round Lake Batholith, and outlines all of the structures related to diapirism and regional compression (refer to sketch for a complete summary).

Fig. 28. Diagrammatic illustration of model for the evolution of the Round Lake Batholith and central Abitibi Belt. Keyed to summary.

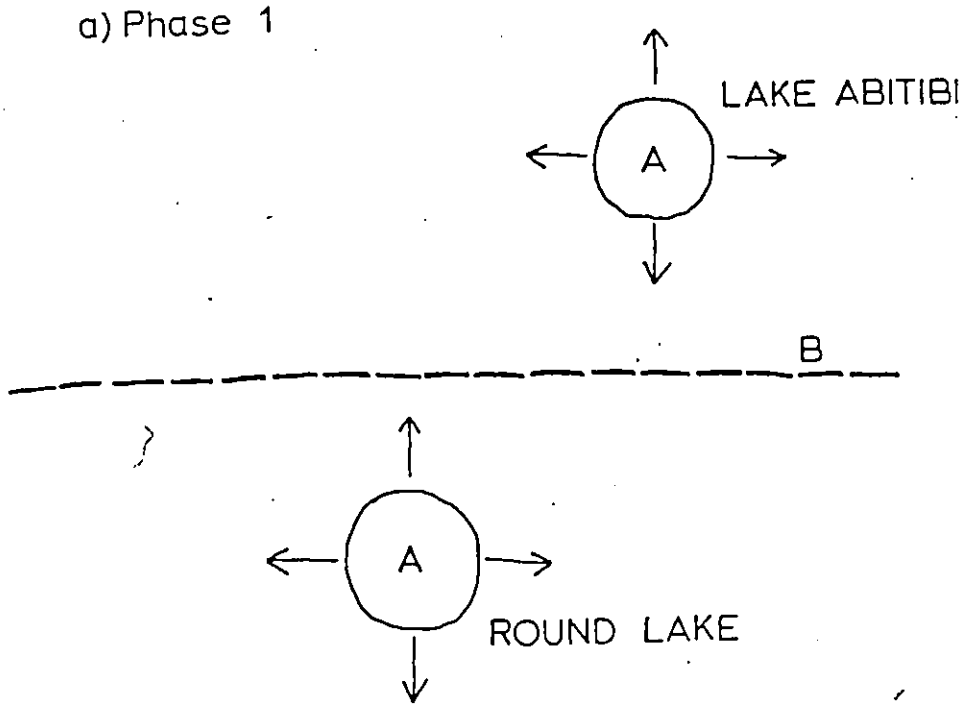

b) Phase 2

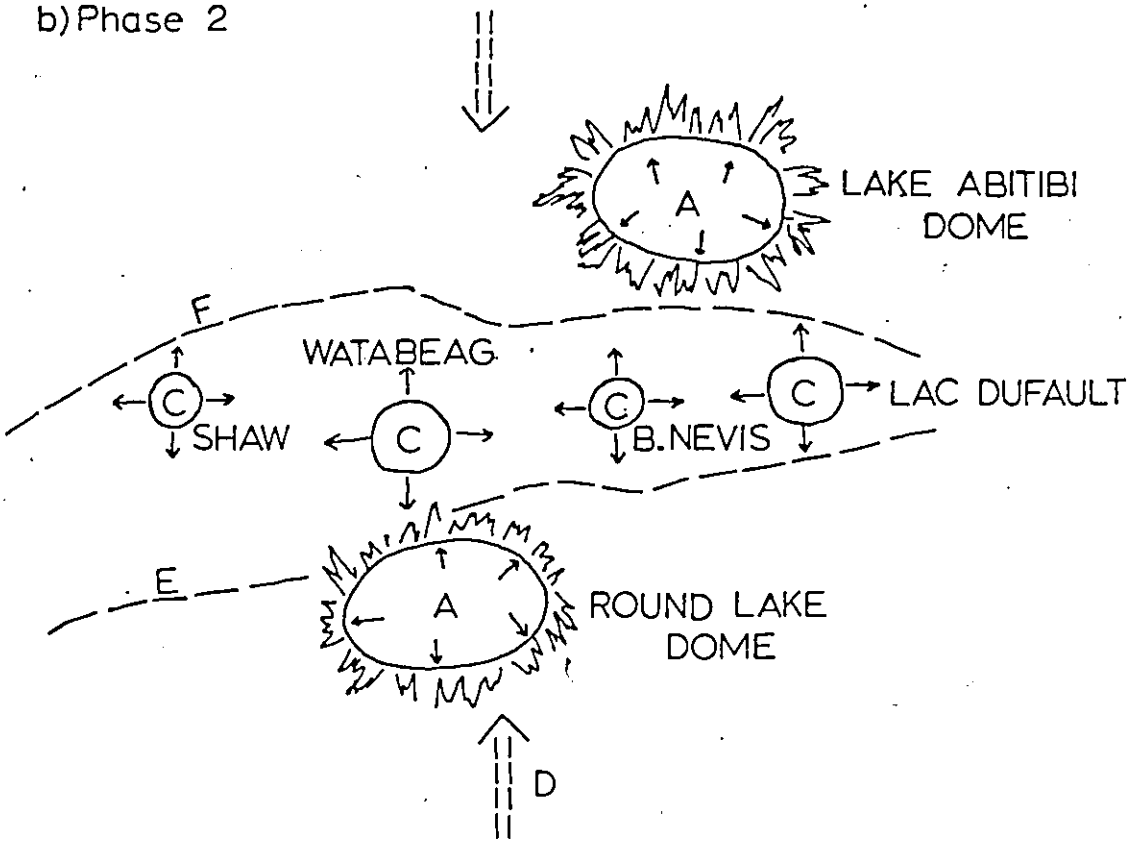
LAKE ABITIBI
DOME
A
F
WATABEAG
C
SHAW
B.NEVIS
LAC DUFAULT
E
ROUND LAKE
DOME
D

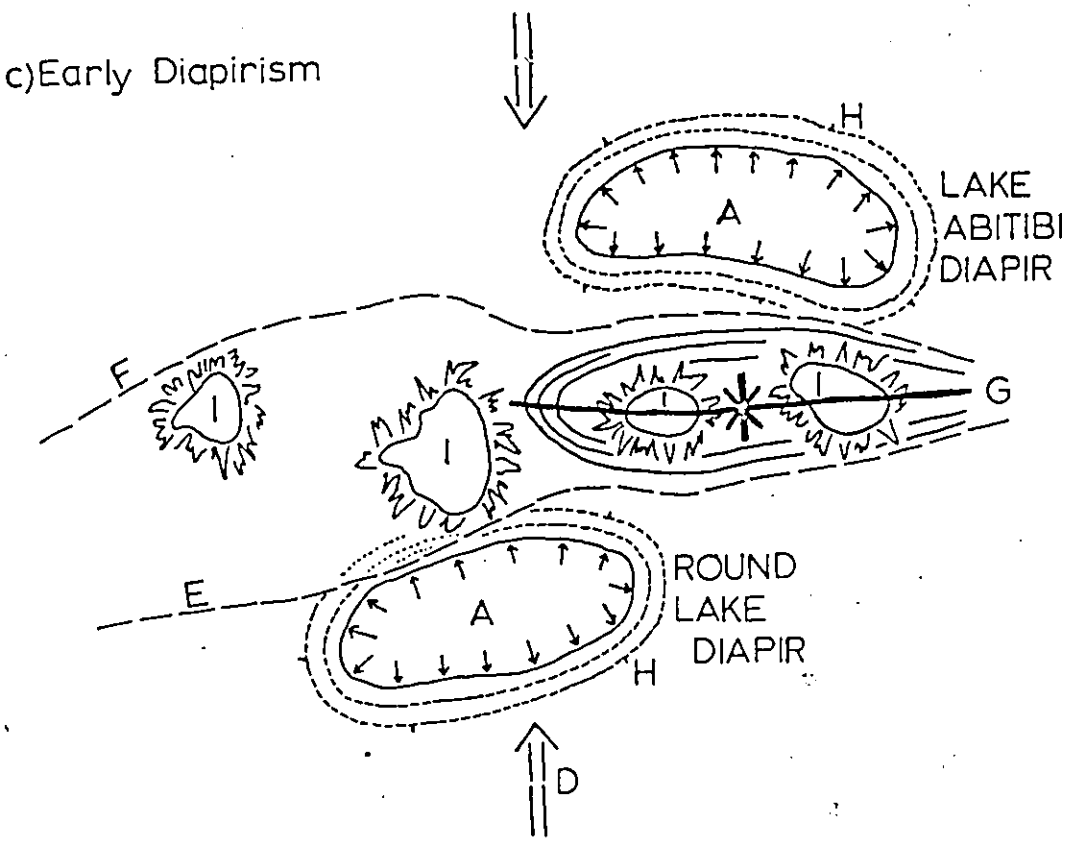
c)Early Diapirism
H
A
LAKE
ABITIBI
DIAPIR
F
G
E
A
ROUND
LAKE
DIAPIR
H
D

d) Folding

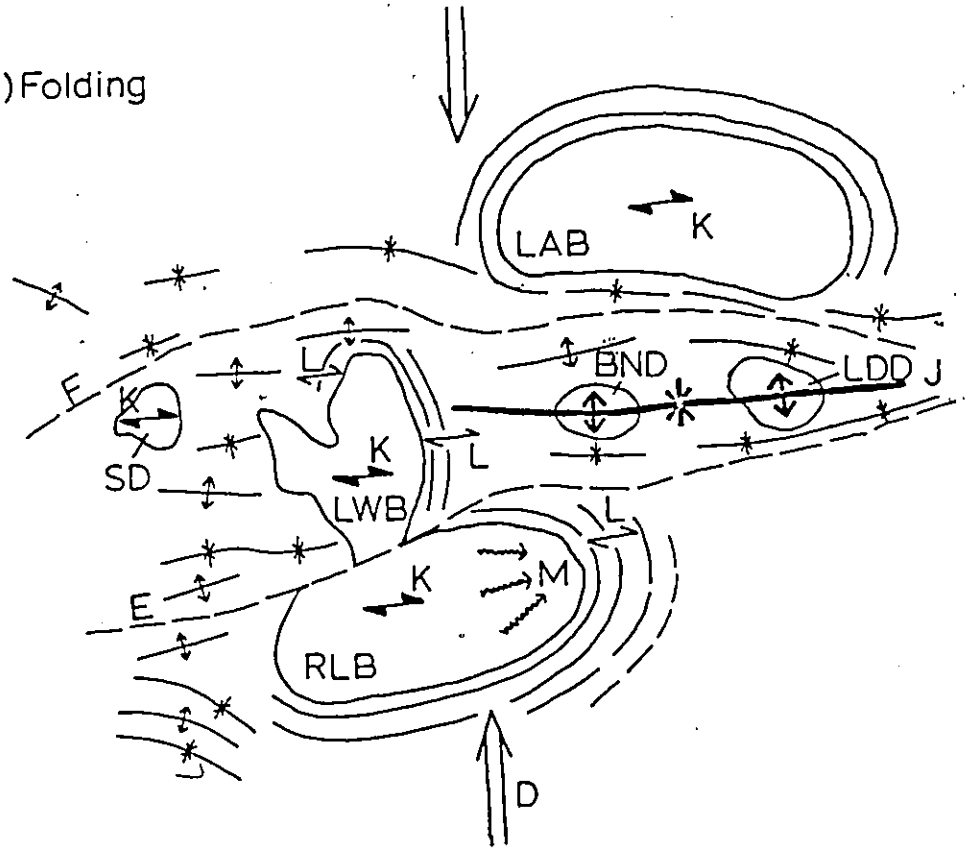

RLB - Round Lake Batholith
LAB - Lake Abitibi Batholith
LWB - Lake Watabeag Batholith
SD - Shaw Dome
BND - Ben Nevis Dome
LDD - Lac Dufault Dome

e) Late Diapirism

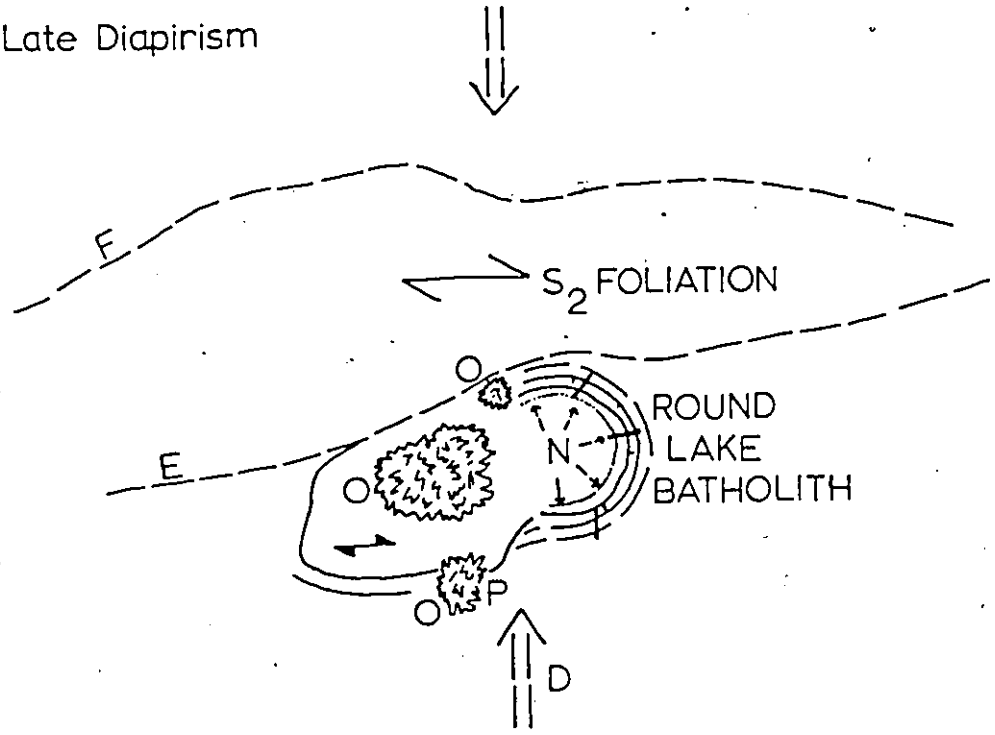

f) Final Stage

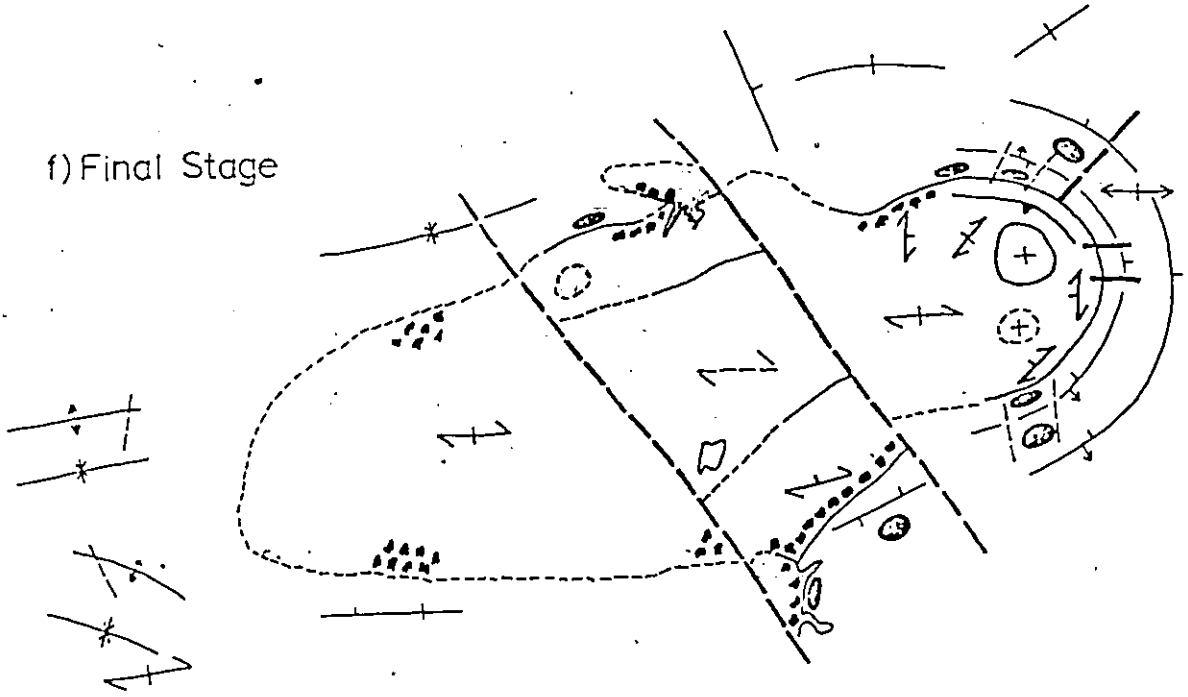

Younger phase

Older phase

Older phase granodiorite cores (diapiric feature)

Xenolith

1 Strain ellipsoid
1 undeformed
2 2 flattening mode

Bedding (tops known, inclined, vertical)

Foliation (inclined, vertical); weak foliation

Schistosity (S_3)

Gneissosity

Fold (antiform, synform)

Lineament

CHAPTER VIII: SUMMARY AND CONCLUSIONS

Two origins have previously been outlined for the Round Lake Batholith. The batholith is a magmatic intrusion, differentiated from a mafic parent, and younger than the surrounding supracrustal pile. Alternatively, it has been suggested that the batholith represents in part a diapir of remobilized pre-greenstone sialic basement. The main purpose of this thesis was to resolve the ambiguity between the two contrasting interpretations by defining the lithological, chemical and structural characteristics of the batholith and to hopefully determine not only its origin, but also mechanism of emplacement, and relationship to the tectonic evolution of the region.

The Round Lake Batholith is crudely an elliptical body, elongated in an east-west direction, and consists of an older cataclastically foliated, in places marginally gneissic, biotite (-hornblende) tonalite (-granodiorite), compositionally variable from tonalite and quartz diorite to granodiorite and monzodiorite, and a younger unfoliated to weakly foliated hornblende (-biotite) granodiorite-tonalite, with minor quartz monzodiorite. Agmatite zones along the margin of, and within the older phase, contain amphibolitic fragments permeated by leucocratic and unfoliated hornblende tonalite. The hornblende tonalite forms distinct plutons along the western margin of the batholith.

Planar fabrics in both older and younger phases are generally

east-west trending, except at the eastern periphery of the older phase, where they curve parallel to the batholith outline.

Field and chemical evidence demonstrate spatial and genetic relationships between the older phase units: main tonalite (map-unit 8A), eastern granodiorite (map-unit 8B), and marginal cataclastic granodiorite-tonalite (map-units 8D, E). Chemically, in terms of major oxides and trace element data, there is minor variation across the older phase considering its large dimensions (exceeding 3200 km^2). Concentrations from the younger phase granodiorite-tonalite (map-unit 9) resembles that of the older phase tonalite. On this basis, both phases are believed to have a common origin, probably the same parent, although their age difference promotes two distinct evolutionary lines. The batholith displays an overall calc-alkaline affinity of the tonalite-trondhjemite series which is consistent with other Archean tonalite-trondhjemite suites.

One of three processes may have contributed to the mineralogical and chemical homogeneity of the older phase of the batholith. These are alteration from either regional metamorphism or autometamorphism; partial melting of a chemically homogeneous parent and rapid crystallization without differentiation; and partial melting with a single pulse of tonalitic melting subjected to chemical differentiation inhibited by a lack of physical separation between crystals and residual melt.

The apparent eastward gradation of subphases from tonalite to granodiorite coupled with a minor variability in major elements, would exclude significant modifications brought upon by alteration. Ubiquitous zoning of plagioclase throughout the older phase, in addition to both gradation and major element variability, attest to a chemical and physical differentiation, however minor it may be, which would exclude the second process. Hence, chemical with minimal physical differentiation does appear as the most likely process.

The LiL elements Ba and Sr from the older phase are modelled using Rayleigh Fractionation, in an attempt to outline a crystallization sequence within the older phase. Assuming normal differentiation of a tonalitic melt, both Ba and Sr should decrease in the residual melt involving plagioclase crystallization ($K_D^{Ba,Sr}$ much greater than one). The effect of having intercumulus melt during crystallization would impart a melt character to the crystallized portions, suppressing the degree of depletion (or enrichment) in the late solids and melts. A clustering of chemical elements would then result (as observed in the Sr vs Ba plot of P.117) instead of normal liquid lines of ascent and descent.

Modelling from the older phase indicate a lack of clear melt (and solid) trends during the crystallization history. Clustering of Ba and Sr appears to support the premise of mixtures between pure melts and crystal portions. The intercumulus residual melt would be preserved as quartz and K

feldspar, whereas plagioclase is the crystalline portion.

It is suggested that minor differentiation proceeded by filter pressing, whereby some of the residual melt was squeezed out of the enclosing semi-crystalline tonalite magma to form the granodiorite.

The major source assemblage for the Round Lake Batholith approximates either an enriched tholeiite or a granulite facies tonalitic gneiss, with a mineralogy consisting of garnet, clinopyroxene ($\pm$ orthopyroxene), hornblende. plagioclase, quartz, opaques and accessories. Two episodes of extensive batch melting in the order of 5 to 35% melting of either, or a combination of both, sources would produce fairly homogeneous melts of tonalitic composition, one for the older and another for the younger phase.

Partial melting may also apply to the generation of the older phase tonalite and granodiorite as two separate episodes, accounting for the slightly variable clusters in the chemistry. Partial melt pulses would produce melts of slightly different major and trace element character, each producing separate clusters of data points in any variation diagram; thus giving an overall false notion of differentiation on a gradational scale. The difficulty in recognizing one separate tonalite pulse from the other more granodiorite one in the older phase must be surmounted, since clearcut internal intrusive contacts are not to be found.

The crystallization history of the Round Lake Batholith

can be summarized in four stages. (A) Heat generated during the emplacement of tonalitic and basic gneisses in the lower crust caused widespread partial melting of the ultramafic-mafic supracrustal greenstone pile and the high grade tonalitic and basic gneisses. (B) Melting was accompanied by tonalitic melt mobilization along a rising diapiric nuclei, eventually to become the older phase. (C) Filter pressing during magma ascent may have controlled the segregation of residual melt, from the crystallized plaigoclase bearing nuclei, towards the eastern margin of the batholith. (D) A single (or a series of) subordinate tonalitic melt body(ies), ascended through the older phase and crystallized with minimal internal differentiation, producing the younger phase.

Detailed examinations of external contact zones along the northern, eastern and southern margin of the Round Lake Batholith was undertaken to resolve emplacement structures from both older and younger phases of the batholith, and regional structures.

Structures such as conformable S_0-S_1 fabric from the supracrustals along the older phase margin, mylonitization of supracrustals adjacent the older phase, pillow flattening in the vicinity of the contact only, cataclasis in the marginal parts of the batholith, rounded shape of the eastern portion of the batholith, subvertical lineations in the batholith and adjacent supracrustals, subradial to radial lineaments

about the margin, and a steeply outward and inward dipping S_0-S_1 fabric, along the eastern margin, accompanied by flowage folds with subhorizontal fold axes in the supracrustals, are all indicative of diapirism as a mode of emplacement for the older phase. Structures at present erosional levels suggest a small viscosity contrast between a mostly crystalline older phase and host supracrustals during emplacement.

The younger phase Hope Lake Stock at the southcentral margin of the batholith also deflected the conformable east-northeast S_0-S_1 fabric in the supracrustals. Emplacement features here mimic those of the older phase.

Regional structures consist of easterly trending shears accompanied by a strong penetrative schistosity that overprinted the conformable S_0-S_1 fabric about the eastern margin of the older phase. Folds with north-south axial planes adjacent the older phase's east-west trending contact postdate the development of S_0-S_1 structures. Both structural fabrics can be attributed to north-south and subsequent east-west compression. The last regional event was the development of northeast-southwest trending shear zone of large extent, such as the breccia-quartz vein bearing structure of the Hough Lake-Laskowski-South Mindoka zone.

The structural evolution of the Round Lake Batholith has been subdivided into episodes of partial melting, and early and late diapirism, which incorporate tectonic events from the Kirkland Lake segment of the Abitibi Greenstone Belt.

Deposition of the supracrustal pile (Abitibi Supergroup)

in the Kirkland Lake area occurred prior to 2.703 Ga. Partial melting of the sinking ultramafic-mafic upper crust and tonalitic gneisses in the lower crust (with the possible addition of upper mantle basic material) generate tonalitic melts. These melts eventually nucleated and rose to the upper crust and became the Round Lake Batholith. Ascension of the older phase tonalitic melt proceeded by initial stoping and hybridization, and later strictly diapirism without assimilation (early diapirism).

Combined diapirism and sinking of the dense volcanic pile produced F_1 flexure folds and S_1 stratiform foliation (subparallel to S_0 bedding in the supracrustals). Synchronous north-south compression in the Belt culminated with the development of F_2 east-west trending isoclinal folds and S_2 penetrative schistosity (subparallel to D_1 structures), affecting both the supracrustal and granitoid rocks. The S_2 fabric transects the S_1 foliation at the north-south trending margin of the Round Lake Batholith.

Filter pressing with the older phase may have occurred during the peak of north-south compression, and resulted in the physical separation of residual melt, later to crystallize as the granodiorite at the eastern portion of the older phase. The granodiorite developed as a second smaller diapir, and continued its ascension through the crust producing extensive cataclasis along the entire length of the eastern margin (late diapirism).

The ellipticity of the batholith was further modified

by the emplacement of the younger phase as a granodiorite-tonalite melt ascended through the core and north and south central margins of the older phase late in the D_2 event. Emplacement of one of the younger phase plutons, the Hope Lake Stock, folded the S_1 easterly trending fabric into northerly oriented folds. This may have been closely followed by an east-west compression (D_3 event) which produced north-south schistosities throughout the supracrustals adjacent the batholith's north and south contacts.

The main older phase tonalite was emplaced prior to the 2.688 Ga crystallization age based on zircon geochronology. Eleven K-Ar and Rb-Sr ages from the older and younger phases average 2.549 Ga, and probably dates the cooling stages of Archean metamorphism and the last episode of structural deformation. Archean metamorphism and deformation did not affect the Otto Stock, and must therefore predate the 2.493 Ga crystallization age of the Stock (which is intrusive into the Round Lake Batholith). This implies that the metamorphism, deformation and plutonism within the Abitibi Belt of the Kirkland Lake area took place over a 200 million year interval spanning the deposition of the Abitibi Supergroup, circa 2.700 Ga, to the intrusion of the Otto Stock, circa 2.500 Ga.

Both Lawton's and Ridler's original interpretations have credibility based on results from this study, although neither one by itself is entirely valid: the Round Lake Batholith *is a magmatic body* derived via partial melting from

a *mafic parent* (either, or a combination of, ensialic greenstone and/or *sialic "basement"*); *diapirically mobilized*, slightly *differentiated*; and *intruded into (thus younger than) the surrounding supracrustal country rocks.*

REFERENCES

Abbey, S.
1977: Studies in standard samples for use in the general analysis of silicate rocks and minerals; Geological Survey of Canada, Paper 77-34, 31 pages.

Abbey, S.
1979: Reference Materials-Rock samples SY-2, SY-3, MRG-1; Canada Centre for Mineral and Energy Technology, Mineral Sciences Laboratories, Energy, Mines and Resources Report 79-35, 66 pages.

Abraham, E.M.
1951: Geology of McElroy and Part of Boston Townships; Ontario Department of Mines, Vol. LIX, Part 6, pp. 1-66. Geological Map No. 1950-3, scale 1 inch to 1000 feet.

Aldrich, L.T. and Wetherill, G.W.
1960: Rb-Sr and K-Ar ages of rocks in Ontario and northern Minnesota; Journal of Geophysical Research, Vol. 65, no. 1, pp. 337-340.

Allègre, C.J., Treuil, M., Minster, J.F., Minster, B., and Albarede, F.
1977: Systematic use of trace elements in igneous processes. Part I: fractional crystallization processes in volcanic suites; Contributions to Mineralogy and Petrology, v. 62, pp. 57-75.

Anhaeusser, C.R.
1974: Early Precambrian rocks in the vicinity of the Bosmanskop syenite pluton, Barbeton Mountain Land, South Africa (abstract); in Geology and Geochemistry of the oldest Precambrian rocks, Symposium University of Illinois.

Anhaeusser C.R., Mason, R., Viljoen, M.J. and Viljoen, R.P.
1969: A reappraisal of some aspects of Precambrian shield geology; Geological Society of America Bulletin, vol. 80, pp. 2175-2200.

Archibald, N.J., Bettenay, L.F., Binns, R.A., Groves, D.I., and Gunthorpe, R.J.
1978: The evolution of Archean greenstone terrains, Eastern Goldfields Province, Western Australia; Precambrian Research, vol. 6, pp. 103-131.

Arth, J.G., Barker, F., Peterman, Z.E., and Friedman, I.
1978: Geochemistry of the Gabbro-Diorite-Tonalite-Trondhjemite suite of southwest Finland and its implications for the origin of tonalitic and trondhjemitic magmas; Journal of Petrology, vol. 19, Part 2, pp. 289-316.

Arth, J.G. and Hanson, G.N.
1972: Quartz diorites derived by partial melting of eclogite or amphibolite at mantle depths; Contributions to Mineralogy and Petrology, vo. 37, pp. 161-174.

Arth, J.G. and Hanson, G.N.
1975: Geochemistry and origin of the early Precambrian crust of northeastern Minnesota; Geochimica et Cosmochimica Acta, vol. 39, pp. 325-362.

Baer, A.J.
1977: Speculations on the evolution of the lithosphere; Precambrian Research, vol. 5, pp. 249-260.

Baragar, W.R.A. and McGlynn, J.C.
1976: Early Archean basement in the Canadian Shield: a review of the evidence; Geological Survey of Canada Paper 76-14, 20 pages.

Barker, F.
1979: Trondhjemite: definition, environment and hypotheses of origin; in Trondhjemites, Dacites, and Related Rocks (F. Barker, editor), Developments in Petrology Series, Elsevier Publication, pp. 1-12.

Barker, R. and Arth, J.G.
1976: Generation of trondhjemitic-tonalitic liquids and Archean bimodal trondhjemite-basalt suites; Geology, vol. 4, no. 10, pp. 596-600.

Bateman, P.C., Clark, L.D., Huber, N.K., Moore, J.G., and Rinehart, C.D.
1963: The Sierra Nevada Batholith-a synthesis of recent work across the central part; U.S. Geological Survey Professional Paper 414-D, 46 pages.

Bell, K., and Blenkinsop, J.
1976: A Rb-Sr whole rock isochron from the Otto Stock, Ontario; Canadian Journal of Earth Sciences, vol. 13, pp. 998-1002.

Bell, L.V.
1929: The Boston-Skead Gold-Copper areas; Ontario Department of Mines, vol. XXXVIII, Part 6, pp. 86-113. Geological map 38d, scale 1 inch to 800 feet.

Burrows, A.G. and Hopkins, P.E.
1922a: Boston-Skead Gold Area: Ontario Department of Mines, vol. XXX, Part 6, pp. 1-26. Geological map 30d, scale 1 inch to 3/4 mile.

Burrows, A.G. and Hopkins, P.E.
1922b: Blanche River Area, Timiskaming District, Ontario; Ontario Department of Mines, vol. XXXI, Part 3, pp. 1-22. Geological map 31b, scale 1 inch to 1 mile.

Chappell, B.W. and White, A.J.R.
1974: Two contrasting granite types; Pacific Geology, vol. 8, pp. 173-174.

Clifford, P.M.
1972: Behavior of an Archean granitic batholith; Canadian Journal of Earth Sciences, vol. 9, pp. 71-77.

Collins, W.H.
1913: The Geology of Gowganda Mining Division; Geological Survey of Canada, Memoir 33, 121 pages. Geological map 1076, scale 1 inch to 1 mile.

Condie, K.C.
1976: Trace element geochemistry of Archean Greenstone Belts; Earth Science Reviews, vol. 12, pp. 393-417.

Condie, K.C. and Hunter, D.R.
1976: Trace element geochemistry of Archean granitic rocks from the Barbeton region, South Africa; Earth and Planetary Science Letters, vol. 29, pp. 389-400.

Cooke, D.L. and Moorhouse, W.W.
1969: Timiskaming volcanism in the Kirkland Lake area, Ontario; Canadian Journal of Earth Sciences, vol. 6, pp. 117-132.

Cooke, H.C.
1922: Kenogami, Round and Larder Lake areas, Timiskaming District , Ontario; Geological Survey of Canada, Memoir 131, 64 pages. Geological maps 1926-1927, scales 1 inch to 1 mile.

Cooper, J.A., Nesbitt, R.W., Platt, J.P., and Mortimer, G.E.
1978: Crustal development in the Agnew region, Western Australia, as shown by Rb/Sr isotopic and geochemical studies; Precambrian Research, vol. 7, pp. 31-59.

Coward, M.P. and James, P.R.
1974: The deformation patterns of two Archean greenstone belts in Rhodesia and Botswana; Precambrian Research, vol. 1, pp. 235-258.

Cox, K.G., Bell, J.D., and Pankhurst, R.J.
1979: The interpretation of igneous rocks; George Allen and Unwin Ltd., London, 450 pages.

DeJongh, W.K.
1973: X-ray fluorescence analysis applying theoretical matrix correction; X-ray Spectrometry, vol. 2, pp. 151-158.

Dimroth, E., Imreh, L., Goulet, N. and Rocheleau, M.
1983a: Evolution of the south-central segment of the Archean Abitibi Belt, Quebec. Part II: Tectonic evolution and geomechanical model; Canadian Journal of Earth Sciences, vol. 20, pp. 1355-1373.

Dimroth, E., Imreh, L., Goulet, N. and Rocheleau, M.
1983b: Evolution of the south-central segment of the Archean Abitibi Belt, Quebec. Part III: Plutonic and metamorphic evolution and geotectonic model; Canadian Journal of Earth Sciences, vol. 20, pp. 1374-1388.

Dominion Observatories Branch.
1966: Timmins-Senneterre, Quebec-Ontario (Gravity Map); Department of Energy, Mines and Resources, Gravity Map Series No. 58, scale 1:500,000.

Douglas, R.J.W.
1979: Geology of Eastern Canada and adjacent areas; Geological Survey of Canada, Map 1401 A (S.W.), scale 1:2,000,000.

Drury, S.A.
1978: REE distribution in a high-grade Archean gneiss complex in Scotland: implications for the genesis of ancient sialic crust: Precambrian Research, vol. 7, pp. 237-257.

Dyer, W.S.
1936: The Matachewan-Kenogami Area; Ontario Department of Mines, vol. XLIV, Part 2, pp. 1-55 (1935). Geological map No. 44b, scale 1 inch to 1 mile.

Ermanovics, I.F., McRitchie, W.D., and Houston, W.N.
1979: Petrochemistry and tectonic setting of plutonic rocks of the Superior Province of Manitoba; in Trondhjemites, Dacites, and Related Rocks (F. Barker, editor), Developments in Petrology Series, Elsevier Publication, pp. 323-362.

Fairbairn H.W., Hurley, P.M., Card, K.D. and Knight, C.J.
1969: Correlation or radiometric ages of Nipissing Diabase and Huronian metasediments with Proterozoic orogenic events in Ontario; Canadian Journal of Earth Sciences, vol. 6, pp. 489-497.

Flanagan, F.J.
1973: 1972 values for international geochemical reference samples; Geochimica et Cosmochimica Acta, vol. 37, pp. 1189-1200.

Fyson, W.K. and Frith, R.A.
1979: Regional deformations and emplacement of granitoid plutons in the Hackett River Greenstone Belt, Slave Province, NWT; Canadian Journal of Earth Sciences, vol. 16, pp. 1187-1195.

Fyson, W.K., Herd, R.K. and Ermanovics, I.F.
1978: Diapiric structures and regional compression in an Archean greenstone belt, Island Lake, Manitoba; Canadian Journal of Earth Sciences, vol. 15, pp. 1817-1825.

Gates, T.M. and Hurley, P.M.
1973: Evaluation of Rb-Sr dating methods applied to the Matachewan, Abitibi, MacKenzie, and Sudbury Dyke Swarms in Canada; Canadian Journal of Earth Sciences, vol. 10, pp. 900-919.

Geological Survey of Canada.
1965: Ville-Marie, Quebec-Ontario; Aeromagnetic Map No. 7075G., Aeromagnetic Series, scale 1:253,440.

Geological Survey of Canada.
1981: Noranda-Rouyn, Quebec-Ontario; Aeromagnetic Map No. 7084G, Geophysical Series, scale 1;250,000.

Geological Survey of Canada and Ontario Department of Mines.
1970a: Gogama, Nipissing-Timiskaming-Sudbury Districts, Ontario; Aeromagnetic Map No. 7076G, Aeromagnetic Series, scale 1:250,000.

Geological Survey of Canada and Ontario Department of Mines.
1970b: Timmins, Cochrane-Timiskaming-Sudbury Districts; Aeromagnetic Map No. 7085G, Aeromagnetic Series, scale 1:250,000.

Gibb, R.A. and vanBoeckel, J.
1970: Three-dimensional gravity interpretation of the Round Lake Batholith, northeastern Ontario; Canadian Journal of Earth Sciences, vol. 7, pp. 156-173.

Gibson, I.L. and Jagam, P.
1980: Instrumental neutron activation analysis of rocks and minerals; in Short Course in Neutron Activation Analysis in the Geosciences (G.K. Muecke, editor), Mineralogical Association of Canada Short Course Handbook, vol. 5, pp. 109-131.

Glikson, A.Y.
1976: Trace element geochemistry and origin of early Precambrian acid igneous series, Barbeton Mountain Land, Transvaal; Geochimica et Cosmochimica Acta, vol. 40, pp. 1261-1280.

Glikson, A.Y.
1979: Early Precambrian tonalite-trondhjemite sialic nuclei; Earth Science Reviews, vol. 15, pp. 1-73.

Goodwin, A.M.
1972: The Superior Province; in Variations in Tectonic Styles in Canada, Geological Association of Canada, Special Paper 11, pp. 527-623.

Goodwin, A.M.
1978: Archean crust in the Superior geotraverse area: geologic overview; in Proceedings of the 1978 Archean Geochemistry Conference (I.E.M. Smith and J.G. Williams, editors), University of Toronto, pp. 73-106.

Goodwin, A.M.
1979: Archean volcanic studies in the Timmins-Kirkland Lake-Noranda region of Ontario and Quebec; Geological Survey of Canada, Bulletin 278, 49 pages.

Goodwin, A.M. and Ridler, R.H.
1970: The Abitibi Orogenic Belt; in Symposium on Basins and Geosynclines of the Canadian Shield (A.J. Baer, editor), Geological Survey of Canada, Paper 70-40, pp. 1-31.

Gordon, G.E., Randle, K., Goles, G.G., Corliss, J.B., Beeson, M.H., and Oxley, S.S.
1968: Instrumental activation analysis of standard rocks with high resolution gamma ray detectors; Geochimica et Cosmochimica Acta, vol. 32, pp. 369-396.

Gorman, B.E., Pearce, T.H. and Birkett, T.C.
1978: On the structure of Archean greenstone belts: Precambrian Research, vol. 6, pp. 23-41.

Gower, C.F., Paul, D.K., and Crocket, J.H.
1982: Protoliths and petrogenesis of Archean gneisses from the Kenora area, English River Subprovince, Northwest Ontario; Precambrian Research, vol. 17, pp. 245-274.

Grant, J.A.
1963: Geology of Catharine and Marter Townships, District of Timiskaming; Ontario Department of Mines, Geological Report 18, 20 pages. Geological map 2043, scale 1 inch to 1/2 mile.

Gupta, V.K. and Wadge, D.R.
1977: Gravity and magnetic susceptibility surveys of the North Bay-Cobalt and Englehart-Elk Lake areas, District of Nipissing and Timiskaming; in Summary of Field Work, 1977, by the Geological Branch (V.G. Milne and others, editors), Ontario Geological Survey, Miscellaneous Paper 75, pp. 172-173.

Gupta, V.K. and Wadge, D.R.
1979: A gravity survey of the Gowganda, Shining Tree and Gogama areas, Districts of Timiskaming and Sudbury; in Summary of Field Work, 1979, by the Ontario Geological Survey (V.G. Milne and others, editors), Ontario Geological Survey, Miscellaneous Paper 90, pp. 167-168.

Hanson, G.N.
1980: Rare earth elements in petrogenetic studies of igneous systems; Annual Reviews of Earth and Planetary Sciences, vol. 8, pp. 371-404.

Haskin, L.A., Haskin, M.A., Frey, F.A., and Wildeman, T.R.
1968: Relative and absolute terrestrial abundances of the rare earths; in Origin and Distribution of the Elements 1. (L.H. Ahrens, editor), Pergamon, New York, pp. 889-912.

Hunter, D.R., Barker, F., and Millard, Jr, H.T.
1978: The geochemical nature of the Archean Ancient Gneiss Complex and Granodiorite Suite, Swaziland: a preliminary study; Precambrian Research, vol. 7, pp. 105-127.

Hyndman, D.W.
1984: A petrographic and chemical section through the northern Idaho Batholith; Journal of Geology, vol. 92, pp. 83-102.

Irvine, T.N. and Baragar, W.R.A.
1971: A guide to the chemical classification of the common volcanic rocks; Canadian Journal of Earth Sciences, vo. 8, pp. 523-548.

Jensen, L.S.
1978: Archean komatiitic, tholeiitic, calc-alkalic and alkalic volcanic sequences in the Kirkland Lake area; in Toronto '78 Field Trip Guidebook (A.L. Currie and W.O. Mckasey, editors), Geological Association of Canada, pp.237-259.

Jensen, L.S.
1980: Kirkland Lake-Larder Lake Synoptic Mapping Project, Districts of Cochrane and Timiskaming; in Summary of Field Work, 1980, by the Ontario Geological Survey (V.G. Milne and others, editors); Ontario Geological Survey, Miscellaneous Paper 96, pp. 55-60.

Johns, G.W.
1980: Hill Lake Area, District of Timiskaming; in Summary of Field Work, 1980, Ontario Geological Survey (V.G. Milne and others, editors), Miscellaneous Paper 96, pp. 89-91.

Johns, G.W., Hoyle, Warren, and Good, David
1981a, b, c: Precambrian Geology of the Hill Lake Area, Bryce-Robillard Townships (1981a), Beauchamp and Dack Townships (1981b), Tudhope and part of Truax Townships (1981c), Timiskaming District; Ontario Geological Survey Preliminary. Maps P.2415 (1981a), P.2416 (1981b), P.2414 (1981c), Geological Series, scales 1:15,840 or 1 inch to 1/4 mile.

Jolly, W.T.
1974: Regional metamorphic zonation as an aid in the study of Archean terrains; Canadian Mineralogist, Vol. 5, p. 499-508.

Jolly, W.T.
1978: Metamorphic history of the Archean Abitibi Belt; in Metamorphism in the Canadian Shield (J.A. Fraser and W.W. Heywood, editors); Geological Survey of Canada, Paper 78-10, pp. 63-78.

Jolly, W.T.
1980: Development and degradation of Archean lavas, Abitibi area, Canada, in light of major element geochemistry; Journal of Petrology, vol. 21, part 2, pp. 323-363.

Knight, C.W.
1907: Report on part of the Montreal River and Timagami Forest Reserve; Ontario Bureau of Mines, vol. XVI, Part 2, pp. 117-128.

Krogh, T.E., Davis, D.W., Nunes, P.D. and Corfu, F.
1982: Archean evolution from precise U-Pb isotopic dating; in GAC-MAC Program with Abstracts, vol. 7, Joint Annual Meeting, Winnipeg, p. 61.

Lawton, K.D.
1954: The Round Lake Batholith and its satellitic intrusions in the Kirkland Lake area; PhD Thesis, University of Toronto, 182 pages.

Lawton, K.D.
1959: Geology of Boston Township and part of Pacaud Township; Ontario Department of Mines, vol. LXVI, Part 5, 55 pages (1957). Geological map 1957-4, scale 1 inch to 1000 feet.

Lee, D.E. and Christiansen, E.H.
1983: The granite problem as exposed in the southern Snake Range, Nevada; Contributions to Mineralogy and Petrology, vol. 83, pp. 99-116.

Lovell, H.L.
1964: Flavelle-Sharpe Area, District of Timiskaming; Ontario Department of Mines, Preliminary Map 264 with marginal notes.

Lovell, H.L.
1967: Geology of the Matachewan area; Ontario Department of Mines, Geological Report 51, 61 pages. Geological maps 2109-2110, scales 1 inch to 1/2 mile.

Lovell, H.L.
1972: Geology of the Eby and Otto area, District of Timiskaming; Ontario Department of Mines and Northern Affairs, Geological Report 99, 34 pages. Geological map 2239, scale 1 inch to 1/2 mile.

Lovell, H.L. and Caine, T.W.
1970: Lake Timiskaming Rift Valley; Ontario Department of Mines, Miscellaneous Paper 39, 16 pages.

Lowdon, J.A., Stockwell, C.H., Tipper, H.W. and Wanless, R.K.
1963: Age determinations and geological studies; Geological Survey of Canada, Paper 62-17, p. 91.

Mackean, B.E.
1968: Geology of the Elk Lake Area, District of Timiskaming; Ontario Department of Mines, Geological Report 62, 62 pages. Geological maps 2150-2151, scales 1 inch to 1/2 mile.

McCarthy, T.S. and Hasty, R.A.
1976: Trace element distribution patterns and their relationship to the crystallization of granitic melts; Geochimica et Cosmochimica Acta, vol. 40, pp. 1351-1358.

McIlwaine, W.H.
1978: Geology of the Gowganda Lake-Miller Lake Silver Area; District of Timiskaming; Ontario Geological Survey, Geological Report 175, 161 pages. Geological maps 2348-2349, scales 1 inch to 1/2 mile.

McOuat, W.
1873: Report of an examination of the country between Lakes Temiscaming and Abbitibbe (Temiscaming and Abitibi); in Report of Progress 1872-73, Geological Survey of Canada, pp. 112-135.

Miller, C.F. and Mittlefehldt, D.W.
1982: Depletion of light rare earth elements in felsic magmas; Geology, Vol. 10, pp. 129-133.

Mittlefehldt, D.W. and Miller, C.F.
1983: Geochemistry of the Sweetwater Wash Pluton, California: Implications for "anomalous" trace element behaviour during differentiation of felsic magmas; Geochimica et Cosmochimica Acta, vol. 47, pp. 109-124.

Moore, J.C.G.
1966: Geology of Holmes-Burt Area, District of Timiskaming; Ontario Department of Mines, Geological Report 44, 20 pages. Geological Map 2078, scale 1 inch to 1/2 mile.

Moorhouse, W.W.
1944: Geology of the Bryce-Robillard Area; Ontario Department of Mines, Vol. L, Part 4, 50 pages (1941). Geological map 50j, scale 1 inch to 1/2 mile.

Nie, N.H., Hull, C.H., Jenkins, J.G., Steinbrenner, K. and Bent, D.H.
1975: SPSS-Statistical Package for the Social Sciences, 2nd Edition; McGraw-Hill Book Company, New York, pp. 293-300.

Nockolds, S.R.
1954: Average chemical compositions of some igneous rocks; Bulletin of the Geological Society of America, vol. 65, pp. 1007-1032.

Nunes, P.D. and Jensen, L.S.
1980: Geochronology of the Abitibi Metavolcanic Belt, Kirkland Lake area- Progress Report; in Summary of Geochronology Studies 1977-1979 (E.G. Pye, editor), Ontario Geological Survey, Miscellaneous Paper 92, pp. 40-45.

Oversby, V.M.
1976: Isotopic ages and geochemistry of Archean acid igneous rocks from the Pilbara, Western Australia; Geochimica et Cosmochimica Acta, vol. 40, pp. 817-829.

Pantalone, A.D.
1981: The Laskowski Gold-Silver Occurrence in the Round Lake Batholith, Kirkland Lake, Ontario; unpublished B.Sc. Thesis, University of Ottawa, 64 pages.

Park, W.A.
1904: The Geology of a district from Lake Timiskaming northward; in Annual Report (New Series), vol. XVI, 1904 (1906 edition), Geological Survey of Canada, pp. 198-225.

Percival, J.A. and Card, K.D.
1983: Archean crust as revealed in the Kapuskasing uplift, Superior Province, Canada; Geology, vol. 11, pp. 323-326.

Pride, C. and Moore, Jr, J.M.
1983: Petrogenesis of the Elzevir Batholith and related trondhjemitic intrusions in the Grenville Province of eastern Ontario, Canada; Contributions to Mineralogy and Petrology, vol. 82, pp. 187-194.

Pride, C. and Muecke, G.K.
1980: Rare earth element geochemistry of the Scourian Complex N.W. Scotland - evidence for the granite/granulite link: Contributions to Mineralogy and Petrology, vol. 73, pp. 403-412.

Propach, G.
1976: Models of filter differentiation; Lithos, vol. 9, pp. 203-209.

Purdy, J.W. and York, D.
1968: Rb-Sr whole rock and K-Ar mineral ages of rocks from the Superior Province near Kirkland Lake, northeastern Ontario, Canada; Canadian Journal of Earth Sciences, vol. 5, pp. 699-705.

Pyke, D.R.
1980: Geology of the Timmins area, District of Cochrane; Ontario Geological Survey, Open File Report 5281, 396 pages (Ontario Geological Survey Report 219, 141 pages, 1982).

Pyke, D.R., Ayres, L.D. and Innes, D.G.
1973: Timmins-Kirkland Lake, Cochrane, Sudbury and Timiskaming Districts; Ontario Division of Mines, Geological Compilation Series, Map 2205.

Ridler, R.H.
1972: Volcanic stratigraphy of the Kirkland Lake area; in Precambrian Volcanism of the Noranda-Kirkland Lake-Timmins-Michipicoten and Mamainse Point area, Quebec-Ontario (A.M. Goodwin and others, editors), Geological Association of Canada Guidebook, pp. 33-41.

Ridler, R.H.
1975: Regional metallogeny and volcanic stratigraphy of the Superior Province; in Report of Activities, Geological Survey of Canada, Paper 75-1A, pp. 353-358.

Ridler, R.H.
1976: Regional metallogeny and volcanic stratigraphy of the Superior Province; in Report of Activities, Part A, Geological Survey of Canada, Paper 76-1A, pp. 399-405.

Ridler, R.H.
1977: Regional metallogeny and volcanic stratigraphy of the Superior Province; in Report of Activities, Part A, Geological Survey of Canada, Paper 77-1A, pp. 197-198.

Sinclair, W.D.
1979: Copper-Molybdenum occurrences of the Matachewan area, Ontario; in Current Research, Part A, Geological Survey of Canada, Paper 79-1A, pp. 253-258.

Stephansson, O.
1977: Granite diapirism in Archean rocks; Journal of the Geological Society of London, vol. 133, pp. 357-361.

Stevens, R.D., Delabio, R.N. and Lachance, G.R.
1982: Age determinations and geological studies, K-Ar isotopic ages, Report 15; Geological Survey of Canada, Paper 81-2, pp. 39-41.

Stockwell, C.H.
1970: Geology of the Canadian Shield: Introduction; in Geology and Economic Minerals of Canada (R.J.W. Douglas, editor), Geological Survey of Canada, Economic Geology Report No. 1, pp. 44-54.

Streckeisen, A.
1976: To each plutonic rock its proper name; Earth Science Reviews, vol. 12, pp. 1-33.

Sutcliffe, R.H.
1978: Geology of the Rainy Lake Granitoid Complex, Northwestern Ontario; in Proceedings of the 1978 Archean Geochemistry Conference (I.E.M. Smith and J.G. Williams, editors), University of Toronto, pp. 235-244.

Tindle, A.G. and Pearce, J.A.
1981: Petrogenetic modelling of in situ fractional crystallization in the zoned Loch Doon Pluton, Scotland; Contributions to Mineralogy and Petrology, vol. 78, pp. 196-207.

Viljoen, M.J. and Viljoen, R.P.
1969: The geochemical evolution of the granitic rocks of the Barbeton Region; in Upper Mantle Project Symposium Volume, Geological Society of South Africa, Special Publication No. 2, pp. 189-218.

White, A.J.R. and Chappell, B.W.
1977: Ultrametamorphism and granitoid genesis; Tectonophysics, vol. 43, pp. 7-22.

Winkler, H.G.F.
1975: Petrogenesis of metamorphic rocks; Springer-Verlag New York Inc., 320 pages.

Wyllie, P.J.
1979: Petrogenesis and the physics of the earth; in The Evolution of the Igneous Rocks: Fiftieth Anniversary Perspectives (H.S. Yoder, editor), Princeton University Press, pp. 483-520.

Wyllie, P.J., Huang, W.L., Stern, C.K., and Maaløe, S.
1976: Granitic magmas: possible and impossible sources, water contents, and crystallization sequences; Canadian Journal of Earth Sciences, vol. 13, pp. 1007-1019.

APPENDIX I

Geochemical sample distribution from the Round Lake Batholith and Abitibi Supergroup: by unit and laboratory facilities.

Rock Type	Map Unit	Total Samples (159)	University of Ottawa	Ontario Geological Survey	Geological Survey of Canada
Round Lake Batholith					
Tonalite	8A	29	17	7	5
Granodiorite	8B	8	6	-	2
Cataclastic granodiorite-tonalite	8D,E	8	7	-	1
Hornblende tonalite	8C	10	9	1	-
Granodiorite-tonalite	9	26	6	15	5
Dykes: porphyry		1	1	-	-
pegmatite		2	1	1	-
aplite		1	1	-	-
Xenoliths:					
from unit 8		1	-	-	1
from unit 9		2	-	-	2
Abitibi Supergroup					
Pacaud tuffs	1	19	4	-	15
Catharine-Wawbewawa Group	2,3	42	-	-	42
Skead Group	4	10	-	-	10

Appendix II

Geochemical data from the Round Lake Batholith

1 sample analysed at the Geological Survey of Canada.

2 sample analysed at the Ontario Geological Survey. Samples without suffixes 1 or 2 analysed at the University of Ottawa.

3 mean value (x_i) of oxides with accompanying standard deviation (σ_i) for the number of samples (n_i) per map-unit (i).

4 quartz-feldspar porphyry dyke.

5 pegmatite dyke.

6 aplite dyke.

7 amphibolite xenolith in map-unit 8A.

8 amphibolite xenolith in map-unit 9.

Map-unit 8A Tonalite

Sample No.	59[1]	69[1]	70[1]	125	136	140	174	195A[1]	201A	299
Oxides (weight %)										
SiO_2	66.40	64.50	66.90	70.47	71.98	71.20	70.92	70.90	69.56	71.44
Al_2O_3	16.70	16.20	16.50	15.91	15.90	16.19	16.39	16.00	16.19	15.83
FeO	1.40	2.70	1.60					0.70		
Fe_2O_3	2.10	1.70	1.90	1.04	1.31	1.32	1.47	0.90	3.08	1.22
MgO	1.42	1.96	1.55	0.44	0.47	0.55	0.53	0.49	1.03	0.64
CaO	4.49	5.01	4.75	2.19	2.42	2.72	2.30	2.68	3.25	2.45
Na_2O	4.20	3.90	4.30	5.41	5.65	5.46	5.63	5.70	4.98	5.66
K_2O	0.88	1.36	1.10	2.18	1.63	1.46	1.37	0.98	0.98	1.04
TiO_2	0.41	0.41	0.37	0.11	0.13	0.14	0.15	0.19	0.27	0.13
P_2O_5	0.13	0.15	0.14	0.02	0.03	0.03	0.03	0.06	0.08	0.03
MnO	0.04	0.07	0.05	0.01	0.01	0.01	0.01	0.02	0.03	0.01
S	0.02	0.03	0.03	0.01	0.01	0.01	0.00	0.02	0.00	0.01
Total	98.19	97.99	99.19	97.79	99.54	99.09	99.50	98.64	99.45	98.46
Trace elements (ppm)										
Ba	330	320	270	1541	532	451	993	350	364	335
Cr				0	13	20	0		6	6
Zr				96	111	102	118		144	95
Sr				716	628	684	837		464	699
Rb				30	25	25	13		20	11
Zn				0	36	2	13		36	0
Ni				5	11	36	15		19	3
K/Rb				603.25	541.26	484.81	874.86		406.78	784.88
Rb/Sr				0.04	0.04	0.04	0.02		0.04	0.02
Ca/Sr				21.86	27.34	28.42	23.91		50.06	25.05
K/Sr				25.28	21.55	17.72	13.59		17.53	12.35
K/Ba	22.14	35.28	33.82	11.74	25.44	26.87	11.45	23.24	22.35	25.77
Ba/Rb				51.37	21.28	18.04	76.38		18.20	30.45
Ba/Sr				2.15	0.85	0.66	1.19		0.78	0.48
CIPW Norms (%cation equivalents)										
Q	25.60	21.62	23.66	23.83	25.02	25.35	24.24	25.80	26.53	26.33
Or	5.32	8.25	6.58	13.08	9.62	8.66	8.09	5.83	5.84	6.20
Ab	38.55	35.92	39.05	49.23	50.62	49.18	50.45	51.48	45.04	51.25
An	21.91	23.27	22.73	10.89	11.79	13.34	13.67	12.98	15.72	12.06
Lc	0.00	0.00	0.00	0.00	0.00	0.00	0.00	0.00	0.00	0.00
Ne	0.00	0.00	0.00	0.00	0.00	0.00	0.00	0.00	0.00	0.00
Di	0.00	0.75	0.12	0.00	0.00	0.00	0.00	0.00	0.00	0.00
He	0.00	0.23	0.02	0.00	0.00	0.00	0.00	0.00	0.00	0.00
En	4.01	5.17	4.67	1.23	1.30	1.52	1.46	1.36	2.87	1.78
Fs	0.37	1.55	0.67	0.00	0.00	0.00	0.00	0.00	0.25	0.00
Fo	0.00	0.00	0.00	0.00	0.00	0.00	0.00	0.00	0.00	0.00
Fa	0.00	0.00	0.00	0.00	0.00	0.00	0.00	0.00	0.00	0.00
Mt	2.04	2.05	1.93	0.00	0.00	0.00	0.00	0.00	1.86	0.00
Ap	0.25	0.11	0.30	0.04	0.06	0.06	0.06	0.13	0.17	0.06
C	1.10	0.00	0.00	0.79	0.56	0.83	0.90	0.92	1.34	1.11

Map-unit 8A Tonalite

Sample No.	305	338	367	376	391	392	394	407	2519[2]	2522[2]	2521[2]
Oxides											
SiO_2	71.39	70.56	69.97	64.26	66.38	68.01	69.78	69.69	65.50	68.40	65.30
Al_2O_3	15.70	16.79	16.68	16.76	17.55	15.49	16.73	16.33	16.50	15.80	16.40
FeO											
Fe_2O_3	1.63	1.88	2.44	5.76	4.02	1.31	1.97	1.74	2.75	2.44	3.62
MgO	0.65	0.75	1.03	2.92	1.67	0.60	0.82	1.13	1.67	0.92	1.83
CaO	2.72	2.87	3.34	2.17	4.93	2.70	3.04	1.86	3.45	2.97	3.76
Na_2O	5.31	6.05	5.36	4.93	4.83	5.67	5.64	6.06	5.45	5.77	5.42
K_2O	0.96	0.90	1.24	2.26	0.83	0.80	0.88	1.29	1.57	1.22	1.21
TiO_2	0.18	0.23	0.31	0.58	0.44	0.16	0.24	0.21	0.37	0.33	0.44
P_2O_5	0.03	0.06	0.08	0.18	0.14	0.03	0.05	0.07	0.14	0.11	0.19
MnO	0.01	0.01	0.03	0.07	0.06	0.01	0.03	0.03	0.05	0.03	0.05
S	0.00	0.00	0.00	0.01	0.00	0.00	0.00	0.00	0.00	0.02	0.01
Total	98.78	99.80	100.68	99.90	100.85	94.78	99.18	98.41	97.45	98.01	98.43
Trace elements											
Ba	368	352	435	628	262	378	334	456			
Cr	1	13	8	28	3	0	19	12	25	7	16
Zr	107	133	123	169	169	100	130	125			
Sr	496	552	623	346	399	655	406	842			
Rb	14	18	27	66	18	15	15	28			
Zn	27	22	23	91	33	14	18	29			
Ni	14	13	15	21	8	8	12	11	15	6	13
K/Rb	569.25	415.08	381.26	284.27	382.80	442.75	487.03	382.47			
Rb/Sr	0.03	0.03	0.04	0.19	0.05	0.02	0.04	0.03			
Ca/Sr	39.19	37.16	38.32	44.82	88.31	29.46	53.51	15.79			
K/Sr	16.07	13.54	16.52	54.22	17.27	10.14	17.99	12.72			
K/Ba	21.66	21.23	23.66	29.85	26.30	17.57	21.87	23.48			
Ba/Rb	26.29	19.56	16.11	9.52	14.56	25.20	22.27	16.29			
Ba/Sr	0.74	0.64	0.70	1.82	0.66	0.58	0.82	0.54			
CIPW Norms											
Q	28.36	22.55	22.34	15.61	20.15	24.58	24.14	22.34	17.29	21.42	17.77
Or	5.74	5.28	7.25	13.35	4.87	4.95	5.21	7.66	9.44	7.31	7.23
Ab	48.15	53.92	49.33	44.20	43.04	53.25	50.73	54.61	49.74	52.49	49.15
An	13.43	13.75	15.86	9.58	23.37	13.81	14.79	8.80	16.19	13.79	17.02
Lc	0.00	0.00	0.00	0.00	0.00	0.00	0.00	0.00	0.00	0.00	0.00
Ne	0.00	0.00	0.00	0.00	0.00	0.00	0.00	0.00	0.00	0.00	0.00
Di	0.00	0.00	0.00	0.00	0.00	0.00	0.00	0.00	0.23	0.33	0.42
He	0.00	0.00	0.00	0.00	0.00	0.00	0.00	0.00	0.00	0.00	0.03
En	1.31	2.06	2.31	8.05	4.58	1.73	2.27	3.13	4.57	2.41	4.89
Fs	0.00	0.00	0.00	2.89	0.99	0.00	0.00	0.00	0.00	0.00	0.38
Fo	0.00	0.00	0.00	0.00	0.00	0.00	0.00	0.00	0.00	0.00	0.00
Fa	0.00	0.00	0.00	0.00	0.00	0.00	0.00	0.00	0.00	0.00	0.00
Mt	0.00	0.00	0.72	2.17	2.01	0.00	0.045	0.00	1.18	0.55	2.05
Ap	0.06	0.13	0.17	0.38	0.29	0.07	0.11	0.15	0.30	0.23	0.40
C	1.16	0.86	0.34	2.93	0.09	0.53	1.20	1.92	0.00	0.00	0.00

Map-unit 8A Tonalite

Sample No.	2527[2]	2520[2]	4769[2]	2526[2]	14[1]	15	311	362	X'_{8A}	σ_{8A}	n_{8A}
Oxides											
SiO_2	64.30	74.20	63.50	64.40	68.60	68.98	69.04	70.22	68.31	2.81	29
Al_2O_3	16.40	13.60	17.40	16.60	16.50	16.89	15.38	16.08	16.26	0.72	do
FeO					1.60						
Fe_2O_3	4.91	1.28	4.00	4.56	1.30	1.77	4.03	2.12	2.68	1.31	do
MgO	2.55	0.34	2.26	2.36	0.99	0.96	1.82	0.84	1.21	0.71	do
CaO	4.25	0.66	4.17	3.16	3.75	3.56	3.96	3.09	3.21	0.98	do
Na_2O	4.19	4.83	4.45	4.32	4.60	5.55	4.31	5.39	5.15	0.62	do
K_2O	1.67	3.73	1.34	1.88	1.21	0.96	1.16	1.06	1.35	0.99	do
TiO_2	0.55	0.12	0.42	0.50	0.37	0.29	0.42	0.23	0.30	0.14	do
P_2O_5	0.14	0.08	0.19	0.16	0.13	0.09	0.08	0.06	0.09	0.05	do
MnO	0.07	0.02	0.07	0.08	0.04	0.01	0.05	0.03	0.04	0.02	do
S	0.03	0.00	0.01	0.00	0.01	0.01	0.03	0.02	0.01	0.01	do
Total	99.06	98.86	97.81	98.02	99.10	99.07	100.28	99.14			
Trace elements											
Ba			290		310	200	365	361	445	286.88	23
Cr	15	8	30	19		8	42	19	13	10.69	24
Zr						152	152	132	127	24.02	17
Sr						525	237	477	464	168.43	do
Rb						21	31	19	23	12.60	do
Zn						20	12	17	23	20.90	do
Ni	18		15	17		5	27	6	14	7.57	23
K/Rb						379.50	310.64	463.14			
Rb/Sr						0.04	0.13	0.04			
Ca/Sr						48.46	119.42	46.30			
K/Sr						15.18	40.63	18.45			
K/Ba			38.36		32.40	39.85	26.38	24.38			
Ba/Rb						9.52	11.77	19.00			
Ba/Sr						0.38	1.54	0.76			
CIPW Norms											
Q	18.84	28.20	19.07	20.25	26.27	22.47	26.09	25.23			
Or	10.01	22.30	8.09	11.36	7.23	5.69	6.89	6.30			
Ab	38.11	43.83	40.80	39.64	41.74	49.92	38.88	48.64			
An	20.44	2.78	19.86	14.96	17.95	17.11	19.22	15.02			
Lc	0.00	0.00	0.00	0.00	0.00	0.00	0.00	0.00			
Ne	0.00	0.00	0.00	0.00	0.00	0.00	0.00	0.00			
Di	0.00	0.00	0.00	0.00	0.00	0.00	0.00	0.00			
He	0.00	0.00	0.00	0.00	0.00	0.00	0.00	0.00			
En	7.13	0.95	6.37	6.66	2.76	2.66	5.05	2.33			
Fs	1.78	0.00	1.04	1.60	0.00	0.00	0.97	0.00			
Fo	0.00	0.00	0.00	0.00	0.00	0.00	0.00	0.00			
Fa	0.00	0.00	0.00	0.00	0.00	0.00	0.00	0.00			
Mt	2.17	0.08	2.05	2.14	1.54	0.00	2.02	0.29			
Ap	0.30	0.17	0.41	0.34	0.28	0.19	0.17	0.13			
C	0.34	0.67	1.68	2.34	1.23	0.51	0.03	0.65			

Map-unit 8B Granodiorite

Sample No.	21	26	31	88[1]	156[1]	259	260	381B	X_{8B}	σ_{8B}	n_{8B}
Oxides											
SiO_2	70.90	70.75	72.10	72.40	72.70	76.79	73.82	71.68	72.66	1.95	8
Al_2O_3	16.55	15.87	15.86	15.90	14.50	12.79	15.45	15.48	15.30	1.17	do
FeO				0.30	.10						
Fe_2O_3	1.93	1.27	1.04	0.50	1.00	1.02	1.11	1.27	1.21	0.31	do
MgO	0.71	0.63	0.47	0.26	0.33	0.54	0.41	0.74	0.51	0.18	do
CaO	2.69	2.45	2.60	2.17	2.21	1.08	1.81	1.67	2.09	0.54	do
Na_2O	5.15	5.42	5.50	5.20	5.30	4.63	5.44	5.93	5.32	0.37	do
K_2O	1.79	1.29	1.29	2.22	1.57	1.76	2.09	2.10	1.76	0.36	do
TiO_2	0.19	0.14	0.13	0.11	0.11	0.08	0.12	0.14	0.13	0.03	do
P_2O_5	0.05	0.02	0.03	0.05	0.04	0.00	0.01	0.05	0.03	0.02	do
MnO	0.03	0.02	0.01	0.02	0.02	0.01	0.03	0.01	0.02	0.01	do
S	0.00	0.00	0.00	0.02	0.02	0.00	0.00	0.00	0.01	0.01	do
Total	99.99	97.86	99.03	99.35	98.00	98.70	100.29	99.07	99.04		
Trace elements											
Ba	375	708	526	690	420	415	245	718	512	176.59	do
Cr	21	0	0			49	0	11	13	17.52	6
Zr	119	104	106			69	92	104	99	17.02	do
Sr	589	736	759			271	415	741	594	210.76	do
Rb	37	18	18			32	49	36	32	12.01	do
Zn	43	0	8			20	0	5	13	16.59	do
Ni	15	30	8			3	12	7	13	9.52	do
K/Rb	401.62	594.95	594.95			456.59	354.59	484.26			
Rb/Sr	0.06	0.02	0.02			0.12	0.12	0.05			
Ca/Sr	32.69	22.25	24.98			25.43	31.17	16.11			
K/Sr	25.23	13.62	14.11			53.91	41.81	23.53			
K/Ba	39.31	15.21	20.36	26.71	31.03	35.21	70.52	24.28			
Ba/Rb	10.22	39.11	29.22			12.97	5.00	19.94			
Ba/Sr	0.64	0.90	0.69			1.53	0.59	0.97			
CIPW											
Q	25.31	26.49	26.96	26.64	29.03	37.77	27.32	22.76			
Or	10.56	7.75	7.66	13.14	9.44	10.61	12.27	12.40			
Ab	46.10	49.44	49.59	46.71	45.36°	42.35	45.49	53.17			
An	12.95	12.22	12.76	10.45	10.53	5.46	8.85	7.95			
Lc	0.00	0.00	0.00	0.00	0.00	0.00	0.00	0.00			
Ne	0.00	0.00	0.00	0.00	0.00	0.00	0.00	0.00			
Di	0.00	0.00	0.00	0.00	0.00	0.00	0.00	0.00			
He	0.00	0.00	0.00	0.00	0.00	0.00	0.00	0.00			
En	1.95	1.77	1.30	0.72	0.93	1.52	1.12	2.04			
Fs	0.00	0.00	0.00	0.00	0.00	0.00	0.00	0.00			
Fo	0.00	0.00	0.00	0.00	0.00	0.00	0.00	0.00			
Fe	0.00	0.00	0.00	0.00	0.00	0.00	0.00	0.00			
Mt	0.00	0.00	0.00	0.00	0.00	0.00	0.00	0.00			
Ap	0.10	0.04	0.06	0.11	0.09	0.00	0.02	0.11			
C	1.49	1.28	0.83	1.22	0.18	1.45	1.05	0.58			

Map-unit 8D,E Cataclastic granodiorite-tonalite

Sample No.	89	151	190B	204C[1]	228	267	270	271	$X_{8D,E}$	$\sigma_{8D,E}$	$n_{8D,E}$
Oxides											
SiO_2	72.40	69.47	73.36	72.90	70.58	71.53	71.78	72.78	71.85	1.31	8
Al_2O_3	15.54	15.47	14.98	13.70	15.39	15.96	15.39	14.83	15.16	0.68	do
FeO				1.20							
Fe_2O_3	0.56	2.45	1.02	0.80	2.13	1.47	1.08	1.59	1.58	0.58	do
MgO	0.35	0.96	0.32	0.80	0.83	0.41	0.43	0.38	0.59	0.25	do
CaO	1.75	3.48	1.57	2.48	2.03	1.63	1.79	2.04	2.09	0.62	do
Na_2O	5.29	4.29	4.81	4.00	4.53	5.68	5.33	4.56	4.81	0.58	do
K_2O	2.62	1.21	2.98	1.29	2.04	2.06	2.57	2.69	2.18	0.66	do
TiO_2	0.10	0.25	0.09	0.22	0.21	0.09	0.11	0.15	0.15	0.07	do
P_2O_5	0.00	0.08	0.01	0.07	0.06	0.01	0.00	0.00	0.03	0.04	do
MnO	0.01	0.04	0.02	0.04	0.03	0.03	0.02	0.05	0.03	0.01	do
S	0.00	0.00	0.03	0.03	0.01	0.01	0.01	0.01	0.01	0.01	do
Total	98.92	97.66	99.19	97.53	97.84	98.88	98.51	99.28	98.48		
Trace elements											
Ba	1178	291	539	310	380	399	533	436	508	285.41	do
Cr	0	8	4		14	32	3	7	10	10.78	7
Zr	83	121	67		105	82	82	83	89	17.95	do
Sr	538	333	317		237	495	336	207	352	123.25	do
Rb	43	23	80		42	48	57	55	50	17.41	do
Zn	3	15	16		13	21	0	19	12	7.96	do
Ni	6	7	12		4	9	13	13	9	3.63	do
K/Rb	505.82	436.74	309.23		403.22	356.28	374.30	406.02			
Rb/Sr	0.08	0.07	0.25		0.18	0.10	0.17	0.27			
Ca/Sr	23.25	73.83	35.40		61.22	23.53	38.07	70.43			
K/Sr	40.43	30.16	78.04		71.46	34.55	63.50	107.88			
K/Ba	18.46	34.52	45.90	34.55	44.57	42.86	40.03	51.22			
Ba/Rb	27.40	12.65	6.74		9.05	8.31	9.35	7.93			
Ba/Sr	2.19	0.87	1.70		1.60	0.81	1.59	2.11			
CIPW Norms											
Q	25.43	29.87	28.14	36.79	29.42	24.66	24.72	28.72			
Or	15.57	7.37	17.76	7.90	12.36	12.23	15.33	16.06			
Ab	47.73	39.68	43.51	37.16	41.67	51.18	48.27	41.33			
An	8.73	17.04	7.78	12.26	9.92	8.05	8.96	10.22			
Lc	0.00	0.00	0.00	0.00	0.00	0.00	0.00	0.00			
Ne	0.00	0.00	0.00	0.00	0.00	0.00	0.00	0.00			
Di	0.00	0.00	0.00	0.00	0.00	0.00	0.00	0.00			
He	0.00	0.00	0.00	0.00	0.00	0.00	0.00	0.00			
En	0.97	2.73	0.89	2.29	2.35	1.14	1.20	1.62			
Fs	0.00	0.00	0.00	0.00	0.00	0.00	0.00	0.00			
Fo	0.00	0.00	0.00	0.00	0.00	0.00	0.00	0.00			
Fa	0.00	0.00	0.00	0.00	0.00	0.00	0.00	0.00			
Mt	0.00	1.05	0.00	0.19	0.46	0.00	0.00	0.00			
Ap	0.00	0.17	0.02	0.15	0.13	0.02	0.00	0.00			
C	0.90	1.17	1.11	1.56	2.44	1.58	0.64	0.78			

Map-unit 8C Hornblende Tonalite

Sample No.	165	177	204A	318	357	365	374	388	390	2528[a]	X_{8C}
Oxides											
SiO_2	61.83	60.19	57.04	63.12	61.79	65.51	62.61	65.36	62.00	58.60	61.81
Al_2O_3	17.65	17.15	19.97	15.95	16.89	16.07	16.59	15.09	15.92	17.80	16.91
FeO											
Fe_2O_3	5.33	5.45	6.38	4.87	6.32	3.38	5.14	4.34	4.84	6.28	5.25
MgO	2.81	3.34	2.92	3.49	3.55	2.21	2.91	3.12	3.44	3.52	3.13
CaO	6.09	5.02	7.19	4.52	4.57	3.98	4.29	4.26	4.82	5.30	5.00
Na_2O	4.07	4.28	4.73	5.11	4.46	6.16	4.43	4.78	5.16	4.23	4.74
K_2O	1.05	1.55	1.10	1.61	1.71	1.25	1.50	2.37	1.55	1.75	1.54
TiO_2	0.65	0.51	0.68	0.47	0.59	0.46	0.58	0.46	0.49	0.63	0.55
P_2O_5	0.14	0.11	0.19	0.19	0.16	0.19	0.31	0.07	0.23	0.24	0.18
MnO	0.07	0.08	0.08	0.08	0.11	0.05	0.08	0.07	0.08	0.10	0.08
S	0.00	0.01	0.03	0.00	0.00	0.01	0.02	0.00	0.01	0.00	0.01
Total	99.89	97.69	100.31	99.41	100.15	99.27	98.46	99.92	98.54	98.45	99.20
Trace elements											
Ba	225	458	180	788	502	793	274	996	708		547
Cr	48	47	38	86	69	39	32	76	96	25	56
Zr	166	116	129	123	180	166	118	202	146		145
Sr	305	309	307	737	403	1038	466	847	726		593
Rb	22	50	8	24	48	10	43	55	34		33
Zn	37	35	49	62	95	31	34	52	59		50
Ni	39	60	13	55	44	24	26	58	69	30	42
K/Rb	396.21	257.35	1141.47	556.90	295.74	1037.70	289.59	357.72	378.46		
Rb/Sr	0.07	0.16	0.02	0.03	0.12	0.01	0.09	0.06	0.05		
Ca/Sr	142.71	116.11	101.35	43.83	81.05	27.40	65.80	35.95	47.45		
K/Sr	28.58	41.64	18.01	18.14	35.23	10.00	26.72	23.23	17.72		
K/Ba	38.74	28.09	50.73	16.96	28.28	13.09	45.45	19.75	18.17		
Ba/Rb	10.23	9.16	22.50	32.83	10.46	79.30	6.37	18.11	20.82		
Ba/Sr	0.74	1.48	0.36	1.07	1.25	0.76	0.59	1.18	0.98		
CIPW Norms											
Q	15.42	12.03	4.82	11.93	11.83	13.72	16.33	14.64	10.85	8.96	
Or	6.24	9.37	6.46	9.51	10.10	7.35	9.02	13.96	9.22	10.30	
Ab	36.74	39.26	42.15	45.79	39.99	54.96	40.41	42.75	46.60	38.54	
An	26.94	23.51	29.79	15.80	20.99	12.43	19.57	12.67	15.80	24.78	
Lc	0.00	0.00	0.00	0.00	0.00	0.00	0.00	0.00	0.00	0.00	
Ne	0.00	0.00	0.00	0.00	0.00	0.00	0.00	0.00	0.00	0.00	
Di	1.55	0.74	2.48	3.51	0.35	4.77	0.00	5.47	4.48	0.19	
He	0.47	0.22	1.03	0.76	0.13	0.00	0.00	0.88	0.92	0.07	
En	7.03	9.05	6.76	7.86	9.61	3.68	8.16	5.85	7.31	9.77	
Fs	2.14	2.68	2.80	1.71	3.65	0.00	2.05	0.94	1.50	3.54	
Fa	0.00	0.00	0.00	0.00	0.00	0.00	0.00	0.00	0.00	0.00	
Fo	0.00	0.00	0.00	0.00	0.00	0.00	0.00	0.00	0.00	0.00	
Mt	2.26	2.15	2.26	2.06	2.18	2.03	2.21	2.04	2.09	2.26	
Ap	0.30	0.24	0.40	0.40	0.34	0.40	0.82	0.15	0.48	0.51	
C	0.00	0.00	0.00	0.00	0.00	0.00	0.00	0.00	0.00	0.00	

Dykes

Sample No..	σ_{3C}	n_{3C}	233C[4]	364[5]	363[6]	1744[2,3]	35[7]	45	123[1]	182[1]
Oxides										
SiO_2	2.67	10	64.49	72.34	73.56	74.90	68.60	65.90	67.90	66.30
Al_2O_3	1.37	do	16.49	14.85	15.93	14.40	15.40	15.83	15.30	15.60
FeO						0.25	1.00		1.30	1.80
Fe_2O_3	0.96	do	4.52	0.38	1.10	0.42	1.50	3.21	1.60	1.00
MgO	0.43	do	2.53	0.20	0.42	0.00	1.70	2.39	2.06	2.18
CaO	0.98	do	3.97	1.02	2.24	0.65	2.52	3.43	2.56	2.76
Na_2O	0.62	do	5.03	4.00	5.65	4.95	5.90	5.85	6.10	5.90
K_2O	0.38	do	1.40	5.03	1.77	3.98	2.03	1.43	1.45	1.59
TiO_2	0.08	do	0.50	0.04	0.16	0.05	0.27	0.34	0.33	0.31
P_2O_5	0.07	do	0.16	0.00	0.03	0.02	0.13	0.14	0.16	0.15
MnO	0.02	do	0.06	0.00	0.01	0.01	0.04	0.04	0.05	0.04
S	0.01	do	0.02	0.02	0.00	0.00	0.02	0.00	0.01	0.03
Total			99.17	97.85	100.87	99.63	99.11	98.56	98.83	99.26
Trace elements										
Ba	289.17	5	494	3658	1112	570	590	543	400	560
Cr	24.41	10	45	0	0	5		83		
Zr	28.43	9	137	40	114	30		135		
Sr	255.98	do	603	507	837	100		855		
Rb	17.51	do	29	54	24			19		
Zr	20.20	do	73	0	7			52		
Ni	18.43	10	40	0	12			30		
K/Rb			400.77	773.28	612.24			624.80		
Rb/Sr			0.05	0.11	0.03			0.02		
Ca/Sr			47.05	10.38	19.13	46.46		28.67		
K/Sr			19.27	82.36	17.56	330.40		13.88		
K/Ba			23.53	11.42	13.21	57.97	28.56	21.86	30.09	23.57
Ba/Rb			17.03	74.74	46.33			28.58		
Ba/Sr			0.82	7.21	1.33	5.70		0.64		
CIPW Norms										
Q			16.15	25.83	26.08	27.36	17.88	15.32	17.64	16.28
Or			8.32	30.37	10.32	23.55	11.95	8.47	8.55	9.48
Ab			45.37	36.66	49.99	44.46	52.71	52.61	54.61	53.39
An			18.37	5.17	10.76	3.10	9.50	12.74	10.06	11.48
Lc			0.00	0.00	0.00	0.00	0.00	0.00	0.00	0.00
Ne			0.00	0.00	0.00	0.00	0.00	0.00	0.00	0.00
Di			0.23	0.00	0.00	0.00	1.68	2.64	1.25	1.07
He			0.05	0.00	0.00	0.00	0.00	0.05	0.00	0.00
En			6.89	0.56	1.14	0.00	3.83	5.29	5.05	5.53
Fs			1.39	0.00	0.00	0.00	0.00	0.15	0.00	0.00
Fo			0.00	0.00	0.00	0.00	0.00	0.00	0.00	0.00
Fa			0.00	0.00	0.00	0.00	0.00	0.00	0.00	0.00
Mt			2.10	0.00	0.00	0.20	1.05	1.93	1.66	1.67
Ap			0.34	0.00	0.06	0.04	0.27	0.29	0.33	0.32
C			0.00	1.08	0.77	0.89	0.00	0.00	0.00	0.00

Map-unit 9 Granodiorite, Tonalite

Sample No.	186	194[1]	205[1]	353	373	393	404	1775[2]	1773[2]	1772[2]	1743[2]
Oxides											
SiO_2	67.21	67.30	67.70	69.04	65.93	69.15	72.33	67.00	66.80	67.40	65.10
Al_2O_3	15.20	15.30	15.20	15.92	15.89	16.73	15.49	15.70	15.20	15.30	16.40
FeO		3.60	1.40					1.41	1.74	1.66	2.24
Fe_2O_3	2.91	0.00	1.30	2.10	2.79	2.51	1.68	1.43	1.67	1.36	1.26
MgO	2.01	1.91	1.88	1.29	2.16	1.43	0.93	1.92	2.19	2.09	2.57
CaO	2.79	2.87	2.56	1.34	2.80	2.72	0.97	3.13	2.73	3.13	3.61
Na_2O	5.44	5.60	5.60	7.97	5.79	6.35	7.00	5.71	5.72	5.48	5.94
K_2O	2.05	1.86	2.08	0.69	2.02	1.39	1.79	1.54	1.53	1.71	1.38
TiO_2	0.30	0.32	0.33	0.29	0.31	0.32	0.19	0.35	0.38	0.37	0.41
P_2O_5	0.11	0.16	0.15	0.11	0.11	0.10	0.06	0.14	0.14	0.14	0.16
MnO	0.04	0.05	0.04	0.04	0.04	0.03	0.02	0.05	0.05	0.06	0.05
S	0.00	0.02	0.03	0.00	0.01	0.00	0.00	0.00	0.00	0.00	0.00
Total	98.06	98.99	98.29	98.79	97.85	100.73	100.46	98.38	98.15	98.70	99.12
Trace elements											
Ba	828	690	850	163	825	645	333	670	390	320	460
Cr	54			27	33	26	16	55	75	60	100
Zr	117			108	119	145	88	100	150	150	100
Sr	607			388	744	1004	289	700	600	500	800
Rb	34			17	48	24	28				
Zn	48			24	33	41	0				
Ni	26			28	33	17	18	30	30	30	45
K/Rb	500.34			336.95	349.36	480.80	330.71				
Rb/Sr	0.06			0.04	0.06	0.02	0.10				
Ca/Sr	32.83			24.68	26.90	19.36	23.99	31.96	32.52	44.74	32.25
K/Sr	28.04			14.76	22.54	11.49	51.42	18.26	21.17	28.39	14.32
K/Ba	20.55	22.38	20.31	35.16	20.33	17.89	44.62	19.08	32.57	44.36	24.90
Ba/Rb	24.35			9.59	17.19	26.88	11.89				
Ba/Sr	1.36			0.42	1.11	0.64	1.15	0.96	0.65	0.64	0.58
CIPW Norms											
Q	18.27	17.67	18.27	14.28	14.92	17.83	19.45	17.33	17.73	15.70	13.42
Or	12.26	11.01	12.37	4.03	12.04	8.05	10.36	9.16	9.13	10.16	8.12
Ab	49.37	50.33	50.55	70.60	52.37	55.84	61.49	51.58	51.80	49.65	53.05
An	11.12	11.13	10.75	5.56	11.49	12.58	4.33	12.74	11.38	12.16	13.94
Lc	0.00	0.00	0.00	0.00	0.00	0.00	0.00	0.00	0.00	0.00	0.00
Ne	0.00	[illegible]	[illegible]	0.00	0.00	0.00	0.00	0.00	0.00	0.00	0.00
Di	1.72	[illegible]	1.23	0.24	1.43	0.00	0.00	1.57	1.01	[illegible]	2.16
He	0.00	0.23	0.00	0.00	0.00	0.00	0.00	0.00	0.08	0.09	0.11
En	4.75	4.56	4.60	3.40	5.29	3.87	2.31	4.35	5.60	4.79	5.95
Fs	0.00	0.72	0.00	0.00	0.00	0.00	0.00	0.00	0.45	0.00	0.31
Fo	0.00	0.00	0.00	0.00	0.00	0.00	0.00	0.00	0.00	0.00	0.00
Fa	0.00	0.00	0.00	0.00	0.00	0.00	0.00	0.00	0.00	0.00	0.00
Mt	1.78	1.91	1.09	0.13	1.83	0.81	0.00	1.44	1.98	1.75	1.99
Ap	0.23	0.34	0.32	0.23	0.23	0.21	0.12	0.30	0.30	0.30	0.33
C	0.00	0.00	0.00	0.00	0.00	0.05	0.65	0.00	0.00	0.00	0.00

Map-unit 9 Granodiorite, Tonalite

Sample No.	2523[2]	1741[2]	4762[2]	4761[2]	4766[2]	4770[2]	4763[2]	4764[2]	4765[2]	4768[2]	1742[2]
Oxides											
SiO_2	68.00	71.50	66.80	68.80	64.60	67.50	66.70	66.30	66.10	65.70	62.80
Al_2O_3	15.10	16.30	16.10	17.10	15.90	16.70	16.40	16.40	16.20	16.30	16.40
FeO		0.58									2.66
Fe_2O_3	2.78	0.60	3.12	2.28	3.57	2.34	2.47	3.02	3.08	3.30	1.62
MgO	2.01	0.40	2.05	0.91	2.62	1.81	2.23	2.27	2.29	2.47	3.32
CaO	2.59	2.33	3.35	3.08	3.58	2.00	2.89	2.93	2.59	3.20	3.65
Na_2O	5.56	5.81	5.38	5.59	5.52	5.81	5.94	6.05	5.72	5.82	5.56
K_2O	1.85	1.33	1.32	1.03	1.62	1.66	1.83	1.51	1.27	1.43	1.92
TiO_2	0.31	0.15	0.34	0.32	0.43	0.34	0.35	0.34	0.36	0.39	0.56
P_2O_5	0.12	0.06	0.14	0.10	0.16	0.15	0.10	0.14	0.15	0.16	0.21
MnO	0.04	0.02	0.05	0.03	0.05	0.05	0.05	0.06	0.05	0.06	0.07
S	0.00	0.00	0.00	0.02	0.02	0.00	0.00	0.00	0.00	0.00	0.01
Total	98.36	99.08	98.65	99.26	98.07	98.36	98.96	99.02	97.81	98.83	98.78
Trace elements											
Ba		510	390	300	700	810	540	530	520	490	520
Cr	40	5	75	10	140	25	70	75	65	75	85
Zr		90									200
Sr		700									700
Rb											
Zn											
Ni	27		40		50	15	35	35	35	40	45
K/Rb											
Rb/Sr											
Ca/Sr		23.79									37.27
K/Sr		15.77									22.77
K/Ba		21.65	28.10	28.50	19.21	17.01	28.13	23.65	20.23	24.23	30.65
Ba/Rb											
Ba/Sr		0.73									0.74
CIPW Norms											
Q	19.26	25.19	19.17	22.85	14.58	19.32	14.85	14.90	18.15	15.12	10.17
Cr	11.02	7.87	7.86	6.09	9.66	9.85	10.77	8.89	7.59	8.45	11.34
Ab	50.29	52.13	48.60	50.19	49.97	52.34	53.04	54.05	51.89	52.19	49.85
An	10.86	11.17	15.80	14.63	13.94	8.97	12.61	13.07	11.99	14.12	14.10
Lc	0.00	0.00	0.00	0.00	0.00	0.00	0.00	0.00	0.00	0.00	0.00
Ne	0.00	0.00	0.00	0.00	0.00	0.00	0.00	0.00	0.00	0.00	0.00
Di	1.94	0.00	0.00	0.00	2.23	0.00	0.30	0.39	0.00	0.55	1.90
He	0.00	0.00	0.00	0.00	0.10	0.00	0.00	0.00	0.00	0.01	0.19
En	5.07	1.11	5.69	2.51	6.15	5.01	5.72	6.04	6.39	6.54	8.20
Fs	0.00	0.00	0.09	0.00	0.27	0.00	0.00	0.00	0.00	0.17	0.32
Fo	0.00	0.00	0.00	0.00	0.00	0.00	0.00	0.00	0.00	0.00	0.00
Fa	0.00	0.00	0.00	0.00	0.00	0.00	0.00	0.00	0.00	0.00	0.00
Mt	1.46	0.02	1.94	0.53	2.03	0.49	0.66	1.86	1.91	1.97	2.15
Ap	0.25	0.13	0.30	0.21	0.34	0.32	0.21	0.29	0.32	0.34	0.44
C	0.00	1.32	0.07	1.56	0.00	2.27	0.00	0.00	1.18	0.00	0.00

Inclusions

Sample No.	X_g	σ_g	n_g	37[1:7]	327[1:8]	3298[1:8]
Oxides						
SiO_2	67.25	1.98	26	47.00	54.90	56.50
Al_2O_3	15.90	0.56	do	13.50	13.10	13.50
FeO				7.90	5.50	4.80
Fe_2O_3	2.85	0.64	do	3.50	3.20	2.30
MgO	1.97	0.60	do	10.10	6.77	7.31
CaO	2.77	0.63	do	9.97	7.53	7.57
Na_2O	5.89	0.54	do	1.70	4.20	4.60
K_2O	1.59	0.33	do	1.50	0.77	0.82
TiO_2	0.34	0.07	do	0.70	0.54	0.58
P_2O_5	0.13	0.03	do	0.04	0.25	0.29
MnO	0.05	0.01	do	0.21	0.15	0.14
S	0.01	0.01	do	0.13	0.08	0.16
Total	98.75				96.99	98.57
Trace elements						
Ba	543	180.06	23	220	210	840
Cr	58	32.30	21	460	330	380
Zr	125	32.48	12	45	70	73
Sr	657	198.03	do	170	630	790
Rb	28	11.43	6			
Zn	33	19.08	do			
Ni	32	9.49	19	220	120	210
K/Rb						
Rb/Sr						
Ca/Sr						
K/Sr						
K/Ba						
Ba/Rb						
Ba/Sr						
CIPW Norms						
Q				0.00	2.67	2.50
Or				9.26	4.68	4.86
Ab				15.93	38.79	41.35
An				25.37	15.03	13.79
Lc				0.00	0.00	0.00
Ne				0.00	0.00	0.00
Di				15.00	12.65	14.64
He				5.40	4.70	3.10
En				7.15	12.88	12.98
Fs				2.57	4.79	2.78
Fo				10.85	0.00	0.00
Fa				3.91	0.00	0.00
Mt				2.40	2.19	2.18
Ap				0.09	0.54	0.61
C				0.00	0.00	0.00

Appendix III

Geochemical data from the Abitibi Supergroup: Pacaud Tuffs, and Catharine-Wawbewawa-Skead Groups

1 sample analysed at the University of Ottawa.

2 sample analysed at the Geological Survey of Canada. Samples without suffixes are from Goodwin (1979; analyses from the Geological Survey).

3 mean value (x_i) of oxides with accompanying standard deviation (σ_i) for the number of samples (n_i) per map-unit (i).

4 mean (and standard deviation) chemical composition of the Abitibi Supergroup samples used in this study (71 samples).

5 mean (and standard deviation) chemical composition of the volcanic pile (regional composite) in the Kirkland Lake-Timmins-Noranda area (Table 6 in Goodwin, 1979).

Pacaud Tuffs map-unit 1

Sample No.	16[2]	104[2]	164[2]	209[2]	230[1]	231[1]	232[2]	254A[2]	272[1]	273[1]	312[2]
Oxides (weight %)											
SiO_2	48.10	65.50	48.70	49.30	44.73	49.47	64.50	69.10	42.04	50.09	50.00
Al_2O_3	15.10	14.70	13.70	16.40	13.34	14.97	15.50	16.10	11.37	14.41	14.80
FeO	7.80	2.80	8.70	6.70			3.70	7.70			7.20
Fe_2O_3	3.60	2.10	4.20	1.90	10.70	12.26	1.80	2.60	13.67	11.55	4.60
MgO	9.02	2.15	6.98	8.40	7.33	8.47	1.92	6.40	4.37	7.52	7.46
CaO	9.01	4.79	9.88	11.20	13.78	10.68	5.80	11.40	7.56	13.81	10.90
Na_2O	2.50	2.90	2.20	1.20	1.05	2.25	3.80	2.40	0.58	1.20	1.90
K_2O	0.71	1.49	1.15	0.08	0.13	0.18	0.56	0.92	3.96	0.21	0.46
TiO_2	0.78	0.50	1.13	0.37	0.55	0.72	0.51	0.64	1.38	0.59	0.80
P_2O_5	0.12	0.10	0.12	0.04	0.04	0.04	0.12	0.06	0.08	0.03	0.05
MnO	0.24	0.06	0.23	0.17	0.23	0.19	0.12	0.18	0.17	0.24	0.21
S	0.00	0.45	0.42	0.07	0.04	0.01	0.09	0.08	0.06	0.03	0.14
Total	96.98	97.54	97.41	95.83	91.92	99.24	98.42	97.58	85.24	99.68	98.52
Trace elements (ppm)											
Ba	84	200	150	20	37	51	160	140	341	55	84
Cr	310	7	200	290	399	195	52	410	71	421	170
Zr	48	99	67		43	42	120	55	73	46	52
Sr	190	210	180	62	122	99	270	160	190	165	130
Rb					4	6			104	9	
Zn					59	86			69	28	
Ni	120	11	120	55	103	113	42	160	31	117	81
CIPW Norms (%cation equivalents)											
Q	0.00	28.53	0.25	4.94	0.38	0.00	23.72	0.00	0.00	3.05	2.26
Or	4.35	9.18	7.12	0.50	0.86	1.09	3.41	5.64	28.80	1.28	2.81
Ab	23.26	27.11	20.67	11.34	10.48	20.63	35.15	35.92	6.40	11.07	17.64
An	28.90	23.63	25.24	41.18	34.82	30.87	24.30	31.54	20.56	34.24	31.54
Lc	0.00	0.00	0.00	0.00	0.00	0.00	0.00	0.00	0.00	0.00	0.00
Ne	0.00	0.00	0.00	0.00	0.00	0.00	0.00	0.00	0.00	0.00	0.00
Di	9.41	0.52	13.45	10.30	21.97	12.31	2.44	14.20	10.43	18.81	12.86
He	3.35	0.02	6.74	3.32	10.78	6.08	1.19	7.12	9.31	9.97	6.35
En	11.17	6.02	13.44	19.25	11.52	14.99	4.24	7.60	8.30	11.93	14.87
Fs	4.61	0.45	6.73	6.19	5.65	7.41	2.06	3.81	7.57	6.33	7.38
Fo	7.44	0.00	0.00	0.00	0.00	2.05	0.00	2.70	0.99	0.00	0.00
Fa	3.07	0.00	0.00	0.00	0.00	1.01	0.00	1.35	0.90	0.00	0.00
Mt	2.47	2.18	2.88	2.06	2.38	2.37	2.17	2.32	3.70	2.25	2.49
Ap	0.26	0.22	0.26	0.09	0.09	0.09	0.26	0.13	0.21	0.07	0.11
C	0.00	0.00	0.00	0.00	0.00	0.00	0.00	0.00	0.00	0.00	0.00

Pacaud Tuffs map-unit 1

Sample No.	962	964	965	966	968	969	973	1001	X_1^3	σ_1	n_1
Oxides											
SiO_2	47.40	48.70	47.20	48.30	62.20	48.80	49.90	52.50	50.87	6.28	19
Al_2O_3	13.40	14.30	11.70	12.00	14.80	11.30	14.70	13.10	13.98	1.53	do
FeO	11.80	5.60	9.70	9.80	4.20	10.00	7.50	8.20			
Fe_2O_3	5.50	4.10	4.20	5.60	1.30	5.10	3.90	2.50	11.19	3.36	do
MgO	6.10	4.40	7.90	5.20	2.20	6.50	6.40	6.00	6.04	2.16	do
CaO	5.90	15.00	11.10	11.90	4.70	10.00	8.40	10.30	9.81	3.00	do
Na_2O	3.20	0.30	2.50	2.10	3.60	2.00	3.90	1.90	2.18	1.03	do
K_2O	0.30	0.10	0.10	0.20	0.70	0.20	0.89	0.10	0.66	0.90	do
TiO_2	1.63	0.74	0.99	1.28	0.49	1.40	1.36	0.70	0.87	0.38	do
P_2O_5				0.10				0.05			
MnO	0.38	0.17	0.24	0.26	0.08	0.23	0.19	0.19	0.20	0.06	19
S											
Total	95.56	93.41	95.63	96.74	94.27	95.53	97.14	95.89			
Trace elements											
Ba	120			42	170	34	130	48	110	81.43	17
Cr		95	88	320		110	200	250	211	131.33	do
Zr	100			86	110	110	70		75	27.22	15
Sr	180	74	100	170	160	120	220	110	134	53.14	19
Rb									31	48.83	4
Zn									56	26.72	do
Ni	220	160	130	180	160	190		230	124	62.90	18
CIPW Norms											
Q	0.00	11.94	0.00	2.45	23.84	4.30	0.00	9.34			
Or	1.92	0.66	0.63	1.28	4.45	1.29	5.45	0.63			
Ab	31.10	3.00	24.00	20.34	34.72	19.54	36.25	18.28			
An	23.08	41.67	21.83	24.53	23.81	23.15	20.89	25.85			
Lc	0.00	0.00	0.00	0.00	0.00	0.00	0.00	0.00			
Ne	0.00	0.00	0.00	0.00	0.00	0.00	0.00	0.00			
Di	3.58	19.94	18.58	15.54	0.68	14.21	12.21	13.45			
He	3.31	13.10	11.08	15.24	0.32	10.48	5.77	7.85			
En	14.85	3.57	7.04	7.72	6.18	12.83	2.93	11.02			
Fs	13.69	2.33	4.20	7.57	2.87	9.16	1.39	6.83			
Fo	1.19	0.00	5.25	0.00	0.00	0.00	6.94	0.00			
Fa	1.10	0.00	3.13	0.00	0.00	0.00	3.28	0.00			
Mt	3.54	2.61	2.78	3.14	2.24	3.30	3.10	2.46			
Ap	0.00	0.00	0.00	0.23	0.00	0.00	0.00	0.11			
C	0.00	0.00	0.00	0.00	0.00	0.00	0.00	0.00			

Catharine-Wawbewawa Groups map-units 2-3

Sample No.	954	955	956	957	958	959	960	970
Oxides								
SiO_2	42.20	46.20	45.30	43.60	46.80	47.80	48.00	48.90
Al_2O_3	12.10	14.30	15.00	14.00	14.20	15.20	12.10	16.00
FeO	11.80	12.50	10.60	5.60	10.80	11.40	9.00	9.30
Fe_2O_3	5.70	5.00	4.30	7.60	3.70	3.40	3.30	3.00
MgO	4.50	3.00	6.90	7.00	5.40	6.90	8.60	5.60
CaO	11.50	10.40	8.80	11.40	8.60	8.70	12.40	9.20
Na_2O	2.40	3.00	3.00	2.50	3.40	2.90	1.60	2.50
K_2O	0.30	0.30	0.80	0.40	0.40	0.50	0.10	0.85
TiO_2	1.18	1.36	1.22	1.01	1.16	1.19	0.89	1.26
P_2O_5		0.08			0.09			
MnO	0.31	0.43	0.28	0.21	0.24	0.23	0.20	0.21
S								
Total	91.99	98.57	96.20	93.32	94.79	98.22	96.19	96.82
Trace elements								
Ba	95	130	140	59	160	79		290
Cr		82		500	140	130	280	80
Zr	92	130	93		93	97	70	
Sr	260	130	180	180	150	140	95	96
Rb								
Zn								
Ni	220	220	210	240	220	200	270	
CIPW Norms								
Q	0.00	0.00	0.00	0.00	0.00	0.00	0.69	1.02
Or	2.02	1.86	5.01	2.58	2.56	3.08	0.63	5.31
Ab	19.96	24.91	26.39	19.41	32.99	27.10	15.26	23.69
An	24.32	16.41	26.39	28.15	24.11	28.09	27.13	31.39
Lc	0.00	0.00	0.00	0.00	0.00	0.00	0.00	0.00
Ne	2.74	13.21	1.28	3.05	0.00	0.00	0.00	0.00
Di	13.57	9.69	9.19	16.62	9.05	7.87	20.84	8.06
He	18.94	19.90	6.54	10.23	8.05	5.60	9.73	5.21
En	0.00	0.00	0.00	0.00	3.92	7.49	14.79	12.28
Fs	0.00	0.00	0.00	0.00	3.49	5.32	6.91	7.93
Fo	5.52	2.86	11.69	9.58	5.75	6.30	0.00	0.00
Fa	7.70	5.87	8.32	5.90	5.11	4.48	0.00	0.00
Mt	3.19	3.13	3.01	2.86	3.01	2.93	2.65	3.05
Ap	0.00	0.18	0.00	0.00	0.20	0.00	0.00	0.00
C	0.00	0.00	0.00	0.00	0.00	0.00	0.00	0.00

Catharine-Wawbewawa Groups map-units 2-3

Sample No.	971	972	985	986	987	988	989	992	1000	1002	1003
Oxides											
SiO_2	50.50	47.10	46.90	48.90	48.10	46.50	48.40	46.50	52.50	53.80	49.10
Al_2O_3	15.70	15.50	10.20	13.00	13.10	11.60	12.40	14.10	12.90	12.90	14.30
FeO	6.40	7.30	10.20	8.60	6.60	11.10	8.30	12.60	7.40	7.20	10.10
Fe_2O_3	4.60	3.00	4.60	12.20	11.30	4.60	3.70	2.30	2.00	4.50	1.50
MgO	6.80	7.90	4.80	5.00	5.80	3.40	8.80	5.00	7.90	5.60	5.60
CaO	11.80	9.40	10.20	8.90	8.90	11.30	12.50	9.20	10.30	9.70	8.90
Na_2O	2.60	3.40	2.40	1.90	2.40	4.00	3.90	3.30	1.30	1.20	4.00
K_2O	0.29	0.83	0.10	0.10	0.10	0.40	0.20	0.20	0.10	0.10	0.40
TiO_2	0.96	0.85	1.16	1.29	1.31	1.23	0.80	1.24	0.47	0.81	1.04
P_2O_5	0.06		0.08	0.09	0.10						0.09
MnO	0.21	0.19	0.29	0.25	0.25	0.34	0.20	0.27	0.21	0.22	0.22
S											
Total	99.92	95.47	90.93	96.13	97.96	94.67	99.20	94.91	95.28	96.03	95.25
Trace elements											
Ba	100	130	91	37	39	92	52	41		32	100
Cr	200	370					240		280		140
Zr	80			94	97			89			110
Sr	160	130	110	280	110	100	140	170		130	300
Rb											
Zn											
Ni	100		150	240	170	150	200	220	220	190	240
CIPW Norms											
Q	0.13	0.00	0.00	6.45	1.02	0.00	0.00	0.00	10.27	15.69	0.00
Or	1.78	5.12	0.65	0.65	0.63	2.58	1.19	1.28	0.63	0.64	2.51
Ab	23.69	27.49	23.69	18.63	22.98	27.49	20.45	33.97	12.52	11.65	38.07
An	30.77	25.65	18.40	29.12	26.32	13.67	15.87	23.98	31.18	31.92	21.09
Lc	0.00	0.00	0.00	0.00	0.00	0.00	0.00	0.00	0.00	0.00	0.00
Ne	0.00	2.64	0.00	0.00	0.00	7.04	8.91	0.00	0.00	0.00	0.00
Di	15.25	13.21	22.99	6.67	7.71	15.15	25.71	10.27	14.19	9.59	12.37
He	7.35	5.20	23.67	7.68	8.35	23.76	11.62	10.03	5.57	6.50	7.72
En	11.43	0.00	1.67	11.74	13.22	0.00	0.00	1.68	16.30	11.92	3.06
Fs	5.51	0.00	1.72	13.53	14.31	0.00	0.00	1.64	6.39	8.08	1.91
Fo	0.00	12.11	1.03	0.00	0.00	2.01	8.73	6.08	0.00	0.00	5.36
Fa	0.00	4.77	1.25	0.00	0.00	3.14	3.94	5.94	0.00	0.00	3.34
Mt	2.61	2.56	3.05	3.19	3.13	3.12	2.42	3.10	2.21	2.61	2.82
Ap	0.13	0.00	0.18	0.21	0.22	0.00	0.00	0.00	0.00	0.00	0.20
C	0.00	0.00	0.00	0.00	0.00	0.00	0.00	0.00	0.00	0.00	0.00

Catharine–Wawbewawa Groups map-units 2-3

Sample No.	1004	1005	1006	1007	1008	1009	1010	1011	1012	1013	1014
Oxides											
SiO_2	46.90	48.30	49.30	49.60	48.30	43.50	48.00	52.00	50.00	48.70	46.60
Al_2O_3	14.20	14.20	13.00	13.10	13.60	10.00	13.60	12.70	13.50	13.00	12.60
FeO	9.60	8.90	10.40	12.70	10.20	13.80	12.20	10.80	10.70	10.80	11.80
Fe_2O_3	1.30	1.90	3.20	2.00	2.40	0.60	2.40	2.40	2.40	3.00	2.10
MgO	6.70	6.30	6.40	5.00	7.10	8.70	4.60	4.20	5.30	5.40	5.60
CaO	12.10	10.60	8.80	7.50	8.10	11.10	9.60	8.60	10.40	9.50	9.80
Na_2O	2.10	2.40	1.90	2.70	2.50	2.30	3.10	3.20	2.60	3.30	3.70
K_2O	0.30	0.20	0.10	0.10	0.00	0.20	0.20	0.10	0.30	0.20	0.20
TiO_2	0.93	0.97	1.13	1.20	1.08	1.39	1.44	1.40	1.09	1.29	1.25
P_2O_5		0.07	0.09	0.09	0.15	0.09	0.11	0.10	0.08	0.09	
MnO	0.19	0.20	0.21	0.27	0.21	0.25	0.24	0.26	0.22	0.28	0.29
S											
Total	94.32	94.04	94.53	94.26	93.64	91.93	95.49	95.76	96.59	93.56	91.94
Trace elements											
Ba	390	35	44	52	32		30	48	36	49	48
Cr	310	300	160	140	200	310					
Zr	99	89	120	82	98	110	97	85	86	85	91
Sr	100	960	170		93		140	84	140	12	78
Rb											
Zn											
Ni	290	270	220	200	230	320	170	210	220	200	160
CIPW Norms											
Q	0.00	2.30	6.85	5.97	3.29	0.00	0.69	7.68	3.33	2.98	0.00
Or	1.91	1.23	0.65	0.65	0.00	1.32	1.28	0.64	1.89	1.31	1.32
Ab	20.34	23.32	18.66	26.63	24.48	22.98	30.10	30.98	24.87	32.76	37.19
An	30.68	29.64	29.16	25.69	28.24	18.22	24.45	21.57	25.87	22.20	19.24
Lc	0.00	0.00	0.00	0.00	0.00	0.00	0.00	0.00	0.00	0.00	0.00
Ne	0.00	0.00	0.00	0.00	0.00	0.00	0.00	0.00	0.00	0.00	0.00
Di	18.34	14.26	8.54	5.93	7.48	22.43	10.67	9.94	12.81	10.37	12.71
He	8.93	7.17	5.83	5.77	4.14	11.50	10.35	9.06	10.02	13.05	15.46
En	9.66	11.69	15.06	12.23	17.64	0.36	8.40	7.54	9.18	5.19	1.42
Fs	4.70	5.85	10.29	11.90	9.77	0.19	8.15	6.87	7.18	6.53	1.73
Fo	0.34	0.00	0.00	0.00	0.00	11.36	0.00	0.00	0.00	0.00	2.31
Fa	0.41	0.00	0.00	0.00	0.00	5.83	0.00	0.00	0.00	0.00	3.06
Mt	2.74	2.80	3.01	3.11	2.94	3.36	3.32	3.27	2.88	3.23	3.22
Ap	0.00	0.16	0.21	0.21	0.34	0.21	0.25	0.23	0.18	0.21	0.00
C	0.00	0.00	0.00	0.00	0.00	0.00	0.00	0.00	0.00	0.00	0.00

Skead Group and equivalent rocks

Sample No.	401[2]	$x_{z,s}$	$\sigma_{z,s}$	$n_{z,s}$	974	975	976	977	990	991
Oxides										
SiO_2	74.90	48.58	4.75	42	61.00	61.50	57.30	53.30	56.00	46.40
Al_2O_3	11.50	13.42	1.36	do	15.30	15.50	15.20	14.40	12.60	11.60
FeO	4.10				3.00	3.80	5.30	4.80	5.50	5.90
Fe_2O_3	2.10	13.85	2.77	do	2.50	1.30	0.60	2.40	0.80	1.90
MgO	0.66	5.71	1.79	do	3.80	4.50	5.70	5.20	6.40	7.30
CaO	2.12	9.69	2.00	do	7.90	4.70	5.70	8.30	5.80	7.50
Na_2O	2.50	2.69	0.83	do	0.10	2.80	4.30	4.20	4.30	1.70
K_2O	1.16	0.35	0.30	do	4.10	0.50	0.90	1.00	0.50	0.80
TiO_2	0.30	1.18	0.38	do	0.47	0.38	0.60	0.64	0.59	0.54
P_2O_5	0.05	0.10	0.02	28		0.11			0.17	
MnO	0.11	0.25	0.06	42	0.37	0.09	0.13	0.12	0.16	0.14
S	0.35	0.25	0.20	10						
Total	99.35	96.07			98.54	95.18	95.73	94.36	92.82	83.78
Trace elements										
Ba	210	91	76.34	39	270	130	240	200	210	240
Cr	8	195	140.36	28	230	130	330	180	200	210
Zr	540	106	79.98	34	93		120	120	84	
Sr	140	163	140.70	39	160	310	440	750	330	270
Rb				0						
Zn				0						
Ni		182	69.55	39	230	190	290	200	210	130
CIPW Norms										
Q	46.85				21.68	24.87	7.97	1.95	8.89	7.38
Or	7.14				25.32	3.13	5.31	6.24	3.16	5.70
Ab	23.35				0.94	26.64	39.95	39.78	41.25	18.37
An	10.60				30.47	23.95	20.20	18.45	14.58	26.08
Lc	0.00				0.00	0.00	0.00	0.00	0.00	0.00
Ne	0.00				0.00	0.00	0.00	0.00	0.00	0.00
Di	0.00				6.30	0.00	6.04	14.99	9.89	11.55
He	0.00				2.07	0.00	1.21	5.01	2.13	3.43
En	1.90				7.80	13.17	13.26	7.65	13.93	18.49
Fs	3.68				2.56	2.93	2.67	2.56	2.99	5.50
Fo	0.00				0.00	0.00	0.00	0.00	0.00	0.00
Fa	0.00				0.00	0.00	0.00	0.00	0.00	0.00
Mt	1.96				2.15	2.08	2.27	2.36	2.34	2.37
Ap	0.11				0.00	0.24	0.00	0.00	0.35	0.00
C	2.72				0.00	2.40	0.00	0.00	0.00	0.00

Skéad Group and equivalent rocks

Sample No.	993	994	995	996	X_n	σ_n	n_n	X^*_{AS}	σ_{AS}	N_{AS}
Oxides										
SiO_2	61.60	61.90	54.50	55.90	56.94	4.90	10	50.37	5.88	71
Al_2O_3	15.00	15.30	13.70	16.50	14.51	1.48	do	13.72	1.46	do
FeO	5.90	3.80	5.30	3.90						
Fe_2O_3	1.10	1.10	0.50	1.40	5.88	0.97	do	12.02	3.88	do
MgO	5.10	4.50	4.40	3.50	5.04	1.17	do	5.70	1.83	do
CaO	4.30	4.20	6.30	5.00	5.97	1.50	do	9.20	2.59	do
Na_2O	5.00	3.90	3.20	0.70	3.02	1.67	do	2.60	1.05	do
K_2O	1.50	1.50	2.80	5.20	1.88	1.63	do	0.65	0.93	do
TiO_2	0.39	0.40	0.56	0.45	0.50	0.10	do	1.00	0.43	do
P_2O_5							2	0.07	0.04	43
MnO	0.10	0.11	0.37	1.24	0.28	0.35	do	0.24	0.14	71
S								0.19	0.22	21
Total	97.99	96.71	91.63	93.79	94.02			95.76		
Trace elements										
Ba	180	250	630	2900	525	845.53	do	162	357.81	66
Cr			180	110	196	67.18	8	202	127.23	53
Zr			72	80	95	20.63	6	96	65.76	53
Sr	330	160	200	310	326	172.35	10	184	139.70	68
Rb							0	31	48.83	4
Zn							0	56	26.72	do
Ni	170	130	180	250	202	44.67	10	170	70.09	67
CIPW Norms										
A	9.48	15.95	6.84	13.55						
Or	8.92	9.14	18.09	33.44						
Ab	45.15	36.07	31.38	6.83						
An	14.19	20.41	16.11	26.97						
Lc	0.00	0.00	0.00	0.00						
Ne	0.00	0.00	0.00	0.00						
Di	4.97	0.71	11.18	0.00						
He	0.89	0.13	3.25	0.00						
En	11.68	12.44	7.68	10.51						
Fs	2.08	2.35	2.24	5.02						
Fo	0.00	0.00	0.00	0.00						
Fa	0.00	0.00	0.00	0.00						
Mt	1.99	2.05	2.35	2.22						
Ap	0.00	0.00	0.00	0.00						
C	0.00	0.00	0.00	0.74						

Sample No.	X^{t}_{KTN}	n_{KTN}
Oxides		
SiO_2	53.20	1066
Al_2O_3	14.90	do
FeO		
Fe_2O_3	9.30	do
MgO	5.30	do
CaO	7.10	do
Na_2O	3.20	do
K_2O	0.80	do
TiO_2	1.01	do
P_2O_5	0.16	410
MnO	0.19	1066
S		
	95.16	
Trace elements		
Ba	236	1012
Cr	183	984
Zr	100	1008
Sr	172	993
Rb		
Zn	75	1002
Ni	154	987
CIPW Norms		
Q		
Or		
Ab		
An		
Lc		
Ne		
Di		
He		
En		
Fs		
Fo		
Fa		
Mt		
Ap		
C		

Appendix IV

Compilation of geochemical data from Archean trondhjemite/tonalite suites (world wide occurrences) and the Proterozoic gabbro-tondhjemite differentiation suite of southwest Finland.

Group	1	gabbro to trondhjemite suite of southwest Finland.
	2	Saganaga tonalite of northeastern Minnesota.
	3	Giants Range Batholith of northeastern Minnesota.
	4	Vermilion Granite of northeastern Minnesota.
	5	Theespruit Pluton of the Barbeton Region, South Africa.
	6	Nelshoogte Pluton of the Barbeton Region, South Africa.
	7	Dalmein Pluton of the Barbeton Region, South Africa.
	8	Kaap Valley Pluton of the Barbeton Region, South Africa.
	9	Stolzburg Pluton of the Barbeton Region, South Africa.
	10	Swaziland Granodiorite Suite, Ancient Gneiss Complex, Africa.
	11	Pilbara Granites, Western Australia.
	12	Yilgarn granitoids, Western Australia.
	13	Average trondhjemite/tonalite, Superior Province of Manitoba.
	14	Lawlers Tonalite, Western Australia (Yilgarn Block).
	15	Mount Edgar Batholith, Western Australia (Pilbara Block).
	16	Rainy Lake Granitoid Complex, Superior Province of Ontario.
	17	Average granodiorite (III) and tonalite (V).

	GROUP 1																	GROUP 2	
Sample No.	UK-1	UK-2	UK-3	UK-9	UK-4	UK-5	UK-6	UK-7	UK-10	UK-11	UK-8	UK-14	UK-18	UK-15	UK-17	UK-12	UK-13	UK-16	DDH-9	SM-63
Oxides (wt %)																				
SiO_2	41.18	48.92	50.85	51.44	54.47	56.81	57.36	59.50	60.43	62.75	69.31	69.96	70.06	70.35	71.88	72.39	72.40	72.58	63.30	67.30
Al_2O_3	15.84	13.91	14.32	17.07	16.17	16.62	17.41	16.28	16.33	15.50	16.12	16.55	16.36	16.34	16.00	15.51	15.73	15.46	19.40	17.30
Fe_2O_3	12.33	9.51	8.77	10.07	9.20	7.01	7.77	6.01	5.69	7.55	2.66	2.10	2.18	1.96	1.33	1.61	1.24	1.23	2.43	1.98
MgO	10.13	10.87	10.73	4.78	5.16	4.88	3.07	4.55	4.06	1.88	1.36	0.94	0.75	0.74	0.57	0.63	0.67	0.46	1.85	1.39
CaO	12.75	10.00	9.74	8.07	7.89	5.96	5.64	5.16	4.86	3.96	2.60	2.71	2.51	2.77	2.05	2.11	1.85	1.98	5.30	3.45
Na_2O	1.88	2.02	2.72	3.11	3.11	3.67	3.55	3.05	3.36	3.01	4.75	5.40	5.08	5.23	5.46	5.00	5.28	5.56	6.12	6.05
K_2O	0.78	0.74	0.17	1.69	1.37	2.03	2.00	2.52	2.32	2.29	1.86	1.41	2.09	1.56	1.97	1.78	2.43	2.02	0.90	1.08
TiO_2	1.48	1.41	0.81	1.43	0.92	0.89	1.10	0.76	0.72	1.22	0.37	0.31	0.35	0.30	0.19	0.23	0.19	0.20	0.28	0.22
Trace elements (ppm)																				
Ba	90	131	57	395	199	390	471	629	655	711	255	292	451	377	240	209	356	460	805	604
Sr	629	301	401	636	460	766	853	1112	1101	428	872	609	670	635	914	387	727	920	1127	1102
Rb	21	23	2	70	60	61	63	116	147	123	132	57	51	49	75	66	65	39	12	16
La																				
Ce	73.10	27.00	4.42	80.90	36.60	81.70	86.90	119.00	119.00		17.30	10.70		9.81	7.90	14.70		21.30	15.60	11.40
Sm	11.10	3.95	0.950	7.22	3.93	6.21	7.24	10.60	9.86		1.67	1.28		1.10	0.763	0.727		1.78	1.68	
Eu	2.98	1.17	0.317	2.00	1.19	2.03	2.05	2.98	2.77		0.916	0.662		0.591	0.567	0.489		0.553	0.642	0.556
Gd	8.10	3.98	1.04	5.55	3.34	4.49	5.76	7.29	6.68		1.78	0.997		0.990	0.664	0.755		1.25	1.53	
Tb																				
Yb	1.53	1.84	0.590	1.57	1.87	1.13	1.73	1.82	1.69		0.595	0.239		0.232	0.239	0.171		0.159	0.253	0.215
Lu	0.225	0.309	0.099	0.262	0.309	0.177	0.317	0.304	0.276		0.104	0.038		0.040	0.040	0.030		0.026	0.042	
ΣREE	97.04	38.25	7.62	97.30	47.44	95.76	104.00	141.79	140.28		22.37	13.92		12.36	10.13	16.87		25.07	19.75	
La/Yb*	0.92	0.90	1.39	0.93	0.96	1.13	0.94	1.00	0.99		1.62	1.73		1.71	2.30	2.01		1.08	1.21	
La/Sm																				
CIPW (% cation equivalents)																				
Q	0.00	0.00	0.00	2.69	5.76	7.20	10.92	13.52	14.64	23.74	25.58	24.22	24.20	25.23	25.42	29.08	25.77	25.64	10.69	17.15
Or	4.76	4.48	1.01	10.29	8.31	12.22	12.16	15.20	14.01	14.07	11.08	8.34	12.40	9.26	11.64	10.59	14.36	11.93	5.26	6.37
Ab	6.99	18.57	24.64	28.73	28.63	33.34	32.77	27.93	30.51	28.08	42.97	48.50	45.76	47.12	48.92	45.17	47.35	49.86	54.33	54.17
An	33.51	27.34	26.61	28.45	26.78	23.29	25.99	23.05	22.02	17.56	11.94	12.99	12.43	13.27	9.53	10.16	8.84	9.49	22.56	16.82

2		GROUP 3					GROUP 4				GROUP 5			GROUP 6				GROUP 7	
Sample No. Oxides	SH-83	DL-7	MN-28A	DLNW-30	DLSE-6	DLNW-10	KA-2A	KA-2B	V-5	VG-18	THEES	106	TR1	VI7	117	118	NELSH	VG1C	VD19
SiO_2	64.10	74.20	73.90	71.90	71.00	73.80	71.10	73.80	74.00	70.77	71.30	70.63	70.60	72.55	68.93	70.63	71.00	69.76	69.40
Al_2O_3	16.10	14.00	15.00	15.10	15.30	14.90	14.80	14.60	13.80	14.68	14.00	14.98	15.33	14.82	16.21	15.29	14.70	13.90	15.05
Fe_2O_3	3.32	1.76	1.02	1.99	1.94	1.07	2.09	0.92	1.66	1.97	2.49	1.65	2.08	1.72	2.34	2.25	2.15	2.64	2.24
MgO	2.62	0.50	0.26	0.65	0.76	0.26	0.56	0.20	0.30	1.08	1.16	1.06	1.18	0.37	1.22	1.06	0.80	1.05	1.15
CaO	4.21	1.28	0.77	1.64	0.86	0.93	2.02	1.40	0.87	2.71	2.57	2.37	2.59	2.24	3.69	3.34	2.67	2.56	1.94
Na_2O	4.99	3.38	4.06	4.00	4.47	3.60	4.32	4.40	3.85	5.75	5.74	5.37	5.38	6.30	5.16	4.95	5.63	5.25	5.10
K_2O	1.74	4.66	4.91	3.90	3.78	5.12	4.10	4.40	5.10	2.14	1.50	1.55	1.78	2.08	0.62	1.15	1.85	3.04	3.38
TiO_2	0.32	0.20	0.08	0.28	0.28	0.11	0.28	0.09	0.13	0.22	0.27	0.24	0.25	0.16	0.30	0.31	0.27	0.45	0.25
Trace elements																			
Ba		742	448	733	807	651		572	592		383	290			146	170	197	551	502
Sr	928	189	116	257	290	156		208	207	486	523	573	589	366	627	564	406	110	104
Rb	46	159	183	242	166	210		67	154	60	52	42	54	57	16	35	55		
La											18.00	13.00	20.40		17.00	9.90	16.00		
Ce		108.00	63.20	97.90	72.10	35.30		44.20			27.00	25.00	34.60		15.00	22.00	18.00		
Sm		4.28	3.51	4.55	3.49	2.04		2.96	6.58		2.50	1.30	2.42		1.30	1.00	1.70		
Eu		0.641	0.394	0.801	0.783	0.430		0.497	0.646		0.620	0.540	0.660		0.510	0.480	0.520		
Gd		2.20	3.00	2.88	2.24	1.72		2.27				1.20	2.36		1.20	0.670			
Tb											0.240	0.160			0.160	0.080	0.220		
Yb		0.520	0.723	0.696	0.595	0.514		0.216	0.460		0.680	0.280	0.300		0.250	0.240	0.330		
Lu		0.104	0.121		0.101	0.084		0.037			0.110		0.053				0.060		
ΣREE		115.75	70.95	106.83	79.31	40.09		50.18			49.15	41.48	60.79		35.42	34.37	36.83		
Eu/Eu*		0.57	0.36	0.63	0.80	0.69		0.57			0.82	1.30	0.84		1.23	1.69	0.96		
La/Yb											27	46	68		68	41	49		
CIPW Norms																			
Q	15.27	31.36	27.53	27.64	26.19	28.99	23.81	26.11	27.89	21.26	24.17	25.37	23.38	21.71	25.38	27.08	23.34	20.89	20.07
Or	10.67	27.83	29.07	23.27	22.69	30.49	24.46	26.08	30.43	12.63	8.92	9.31	10.55	12.15	3.71	6.87	10.99	18.18	20.14
Ab	45.56	30.64	36.49	36.23	40.74	32.54	39.12	39.58	34.88	51.51	51.81	48.97	48.40	55.84	46.88	44.89	50.78	47.55	46.12
An	16.67	5.62	3.24	7.35	3.60	4.12	8.95	6.76	4.16	7.91	8.05	11.55	12.35	5.94	17.93	16.14	9.42	5.43	8.25

	7			GR 8	GROUP 9			GROUP 10				
Sample No. / Oxides	104	105	DALM	KAAP	33	STOLZ	ST-AN	H1214	H1279	SWZ15	SWZ16	SWZ18
SiO_2	69.72	70.57	69.30	68.60	69.56	71.10	68.40	71.51	71.26	65.44	69.15	72.85
Al_2O_3	15.29	14.52	14.80	15.40	15.33	15.00	16.33	14.40	14.46	16.42	15.61	14.60
Fe_2O_3	2.30	2.45	2.84	4.84	1.80	1.62	2.33	2.64	2.19	4.62	4.45	1.61
MgO	0.95	0.97	1.03	2.58	0.90	0.74	1.07	0.65	0.84	1.43	1.07	0.68
CaO	1.72	2.04	2.22	4.33	2.01	2.32	3.11	2.33	1.80	3.98	3.86	2.72
Na_2O	4.72	4.74	4.76	4.72	6.20	6.48	5.35	4.55	4.65	5.03	4.71	4.79
K_2O	3.46	2.93	3.23	1.55	2.15	1.67	1.49	2.40	2.55	1.24	0.93	1.41
TiO_2	0.32	0.35	0.37	0.51	0.16	0.23	0.32	0.27	0.37	0.70	0.41	0.27
Trace elements												
Ba	700	540	880	450		508	519					
Sr	483	523	692	552	714	667	767			727	414	529
Rb	121	103	105	59	27	39	39			18	10	29
La	52.00	52.00	63.00	19.00		16.00				59.50	24.70	15.40
Ce	98.00	58.00	126.00	31.00		20.00				103.80	41.40	23.90
Sm	6.40	6.70	8.60	3.00		1.80				6.15	3.24	1.26
Eu	1.70	1.60	2.00	1.00		0.560				1.75	1.44	0.91
Gd	4.40	4.50										
Tb	0.540	0.52	0.450	0.400		0.160				0.560		
Yb	0.920	1.10	1.40	1.00		0.360				0.660	0.520	0.210
Lu			0.190	0.180						0.141	0.106	0.049
Σ REE	164.02	124.42	201.69	55.58		38.88				172.56	71.41	41.73
Eu/Eu*	0.93	0.84	0.83	1.04		1.05				0.95		
La/Yb	53	47	45	19		44				90	48	73
CIPW Norms												
Q	22.88	24.84	21.88	17.16	18.73	20.22	22.19	28.40	28.07	19.71	25.84	30.92
Or	20.70	17.56	19.38	9.31	12.79	9.83	8.89	14.44	15.39	7.42	5.53	8.45
Ab	42.87	43.12	43.36	43.01	55.96	57.92	48.46	41.56	42.59	45.69	42.52	43.57
An	7.44	9.06	9.61	16.30	7.69	6.88	14.58	11.16	8.24	18.32	18.47	13.21

GROUP II

Sample No.	1518	1519	1525	1526	1527	1531	1533	1535	1541	1542	1543	1545	1546	1548	1549	1551	1511	1512	1513	1514	1515	1516	1517
Oxides																							
SiO_2	69.57	72.22	68.92	71.98	74.11	70.95	71.44	68.52	71.15	69.78	74.22	73.70	74.41	74.46	75.26	74.99	68.09	65.94	70.29	69.13	72.72	70.55	71.21
Al_2O_3	13.85	14.59	15.13	14.56	13.02	14.03	13.91	14.88	14.12	14.26	13.32	13.59	13.61	14.66	14.02	14.31	15.72	15.79	14.68	14.94	15.31	14.41	13.89
Fe_2O_3	3.98	1.73	3.88	0.32	1.52	2.60	2.32	3.43	2.48	3.36	1.25	1.24	1.17	0.87	1.21	1.13	3.09	4.56	2.72	3.22	0.71	2.95	2.47
MgO	1.93	1.04	1.14	0.49	0.60	1.06	1.15	1.60	0.95	1.21	0.70	0.63	0.46	0.24	0.29	0.23	1.19	1.39	0.95	1.18	0.61	1.76	1.05
CaO	3.27	1.80	2.45	0.42	0.90	1.94	1.78	3.15	1.82	2.42	1.43	0.96	0.90	0.32	0.32	0.31	2.30	2.90	2.00	2.12	1.94	1.54	1.23
Na_2O	4.16	3.73	5.63	2.76	3.56	4.48	4.13	4.87	3.90	4.10	3.79	3.97	3.82	6.64	6.12	6.67	4.47	4.92	4.18	4.25	5.61	4.77	3.53
K_2O	1.09	3.78	0.64	8.14	4.80	2.44	3.20	1.50	3.88	3.16	3.97	4.43	4.75	1.46	1.36	1.05	3.49	2.40	3.84	3.62	2.48	1.64	4.99
TiO_2	0.32	0.24	0.36	0.01	0.12	0.35	0.32	0.39	0.39	0.52	0.15	0.12	0.11	0.01	0.01	0.01	0.40	0.66	0.35	0.49	0.06	0.37	0.29
Trace elements																							
Ba																							
Sr																							
Rb																							
La																							
Ce																							
Sm																							
Eu																							
Gd																							
Tb																							
Yb																							
Lu																							
Σ Ree																							
Eu/Eu*																							
La/Yb																							
CIPW Norms																							
Q	29.26	25.96	25.38	21.78	30.59	28.60	28.30	24.10	27.01	25.73	31.09	29.02	29.56	27.36	31.41	29.22	20.99	18.64	24.30	23.14	23.65	29.14	26.11
Or	6.62	22.67	3.86	48.87	29.00	14.79	19.34	9.01	23.38	19.03	23.91	26.65	28.45	8.64	8.10	6.2.	20.87	14.40	23.00	21.69	14.61	9.90	30.09
Ab	38.36	33.95	51.58	25.15	32.65	41.23	37.88	44.42	35.67	37.47	34.65	36.25	34.73	59.61	55.33	58.97	40.58	44.80	38.01	38.65	50.15	43.71	32.32
An	16.13	8.59	11.60	1.98	4.23	9.13	8.35	14.54	8.40	11.16	6.96	4.45	4.19	0.80	0.81	0.75	10.61	13.33	9.26	9.66	9.23	7.27	5.56

Sample No. / Oxides	GROUP 12 B	GROUP 12 F	GP 13 S	GROUP 14 LAW-T	GROUP 14 L-LG	GROUP 14 L²-LT	GP 15 MER-2	GROUP 16 S76-30	GROUP 16 S76-31	GROUP 16 S77-101	GP 17 III	GP 17 V
SiO_2	73.15	73.17	65.70	64.97	74.39	74.85	66.11	71.96	69.78	71.72	66.88	66.15
Al_2O_3	14.29	14.37	17.40	15.60	13.97	13.15	15.07	15.14	15.32	15.36	15.66	15.56
Fe_2O_3	1.78	1.80	4.10	4.27	0.82	1.28	5.41	1.81	2.38	0.97	3.92	4.78
MgO	0.44	0.47	1.70	2.11	0.21	0.43	1.35	0.40	0.76	0.57	1.57	1.94
CaO	1.65	1.70	3.60	3.78	1.05	0.94	4.53	2.78	3.09	1.99	3.56	4.65
Na_2O	4.10	4.34	4.50	4.46	4.95	5.41	3.97	4.64	4.82	5.18	3.84	3.90
K_2O	4.10	3.78	2.30	2.16	3.65	2.18	1.55	2.02	1.65	2.44	3.07	1.42
TiO_2	0.24	0.25	0.50	0.63	0.08	0.08	0.52	0.26	0.34	0.20	0.57	0.62
Trace elements												
Ba			642	1208	533	458	340	848	491	891		
Sr			563	833	195	307	287	509	546	853		
Rb			69	90	121	64	73	45	47	60		
La												
Ce												
Sm												
Eu												
Gd												
Tb												
Yb												
Lu												
Σ REE												
Eu/Eu*												
La/Yb												
CIPW Norms												
Q	27.64	27.30	19.03	18.94	27.30	30.58	23.70	29.09	26.52	25.63	21.77	23.75
Or	24.42	22.45	13.61	13.03	21.69	13.09	9.42	12.10	9.95	14.57	18.42	8.55
Ab	37.07	39.13	40.41	40.83	44.65	49.31	36.64	42.17	44.11	46.95	34.97	35.66
An	7.72	7.88	16.56	16.49	5.04	4.40	19.25	13.17	14.63	9.31	16.52	21.14

[1]Sample Data Source

1) UK-1, UK-2, UK-3, UK-9, UK-4, UK-5, UK-6, UK-7, UK-10, UK-11, UK-8, UK-14, UK-18, UK-15, UK-17, UK-12, UK-13, UK-16, from Arth et al., 1978

2) DDH-4, SM-63, SH-63, DL-7, MN-28A, DLNW-30, DLSE-6, DLNW-10, KA-2A, KA-2B, V-5 from Arth and Hanson, 1975

3) VG-18, V17, VG1C, VD19, 3J, H1214, H1279 from Viljoen and Viljoen, 1969

4) THEES, NELSH, DALM, KAAP, Stolz from Condie and Hunter, 1976

5) 106, 117, 118, 104, 105 from Glikson, 1976

6) TR1, SWZ15, SWZ16, SWZ18 from Hunter et al., 1978

7) ST-AN from Anhaeusser, 1974

8) 1511, 1512, 1513, 1514, 1515, 1516, 1517, 1518, 1519, 1525, 1526, 1527, 1531, 1533, 1535, 1541, 1542, 1543, 1545, 1546, 1548, 1549, 1551 from Oversby, 1976

9) B, F from Archibald et al., 1978

10) 5 from Ermanovics et al., 1979

11) LAW-T, L-LG, L-LT from Cooper et al., 1978

12) MEB-2 from Glikson, 1979

13) S76-30, S76-31, S77-101 from Sutcliffe, 1978

14) III, V from Nockolds, 1954

PRELIMINARY MAP, GEOLOGY OF THE ROUND LAKE BATHOLITH,
KIRKLAND LAKE, ONTARIO

MAP 1

LEGEND

Scale 1:100 000

0 1 2 MI

0 1 2 KM

PHANEROZOIC

PALEOZOIC

[14] Guiques, Bucke, Thornloe and Dawson Point Formations: Limestone, dolostone, sandstone, shale

PRECAMBRIAN

PROTEROZOIC

APHEBIAN

[13] Nipissing Diabase

HURONIAN SUPERGROUP

[12] Lorrain Formation: orthoquartzite, arkose, wacke

[11] Gowganda Formation: conglomerate, argillite, wacke, arkose

ARCHEAN

SYENITIC PLUTONS: Cairo, Holmes, Otto, Lebel Stocks

[10] 10a - syenite; 10b - diorite; 10c - quartz syenite; 10d - nepheline syenite; 10e - contaminated syenitic rocks; 10f - porphyritic syenite

ROUND LAKE BATHOLITH

[9] Younger, massive intrusions: Indian Chute, Hope Lake, Crooked Creek Stocks: granodiorite-tonalite

[8] Older intrusions: 8a - tonalite (A - agmatite zone, tonalitic gneisses; 8b - poikiloblastic (microcline) granodiorite; 8c - hornblende tonalite; 8d - foliated, cataclastic tonalite; 8e - gneissic, cataclastic granodiorite

ABITIBI SUPERGROUP

[7] Timiskaming Group: trachytic lavas, conglomerate, sandstone, argillite

[6] Kinojevis Group: pillow basalt, intermediate to felsic lavas, volcaniclastic sedimentary rocks

[5] Larder Lake Group: 5a - ultramafic lava, pillow basalt, amphibolite; 5b - felsic tuff; 5c - wacke, argillite; 5d - iron formation; 5e - syenite; 5f - gabbro, peridotite

[4] Skead Group and equivalent rocks: 4a - basaltic to rhyolitic lavas and pyroclastics, iron formation; 4b - quartz-feldspar

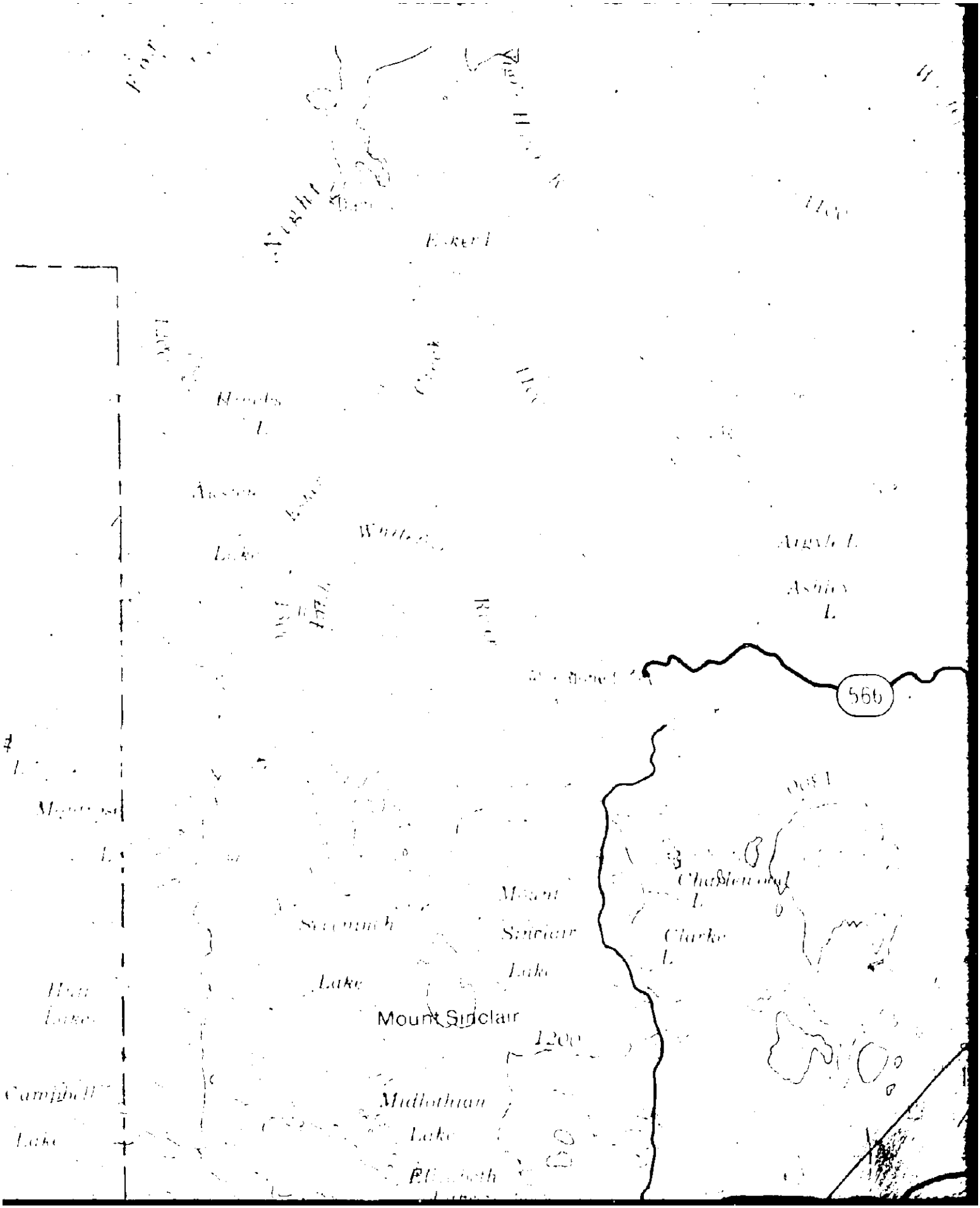
566
Mount Sinclair
1200

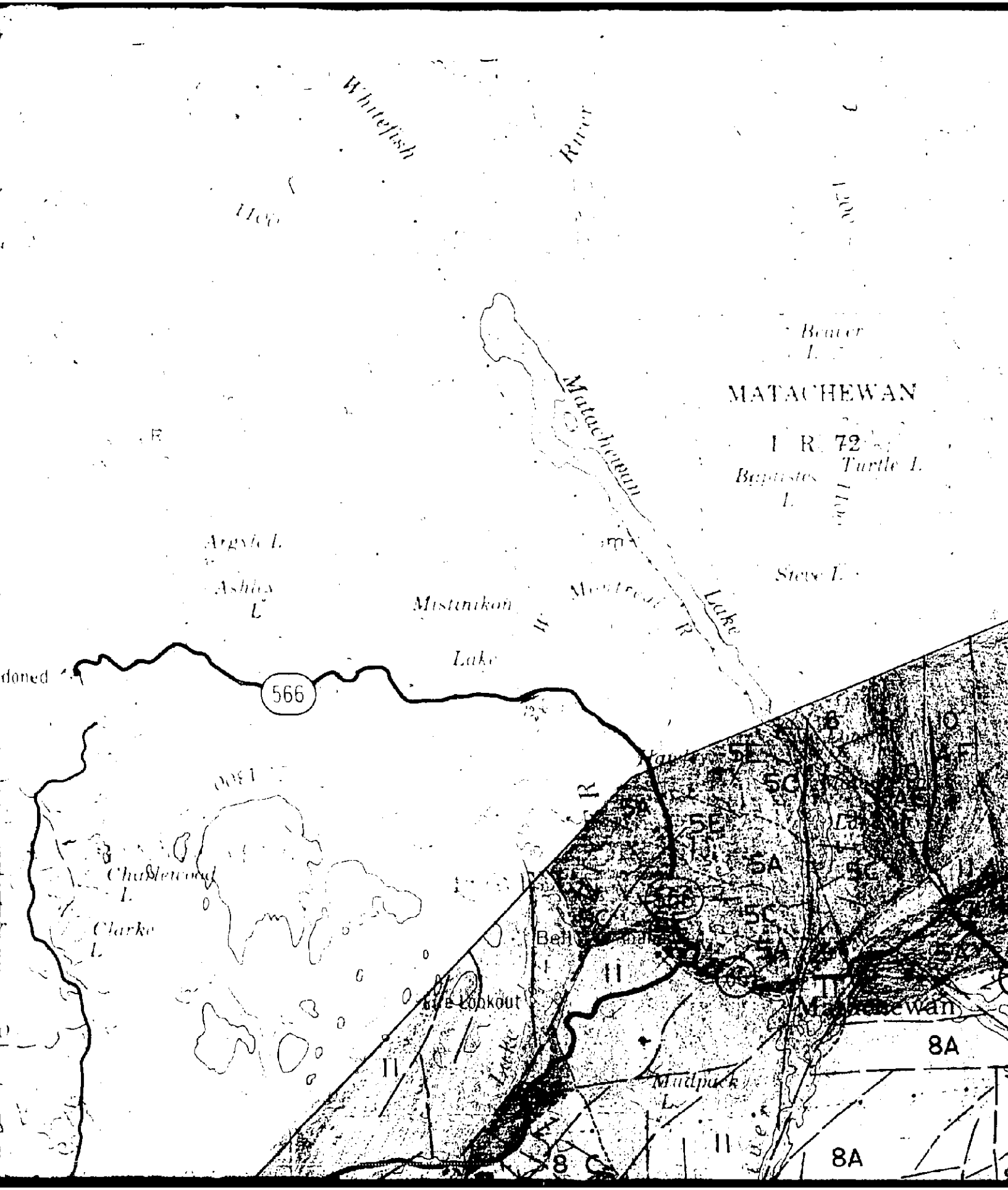
Whitefish
River
Beaver
L.
MATACHEWAN
I R 72
Turtle L.
Matachewan
Lake
Argyle L.
Ashley
L.
Mistanikon
Lake
566
Clarke
L.
Bell
Lookout
Matachewan
Mudpark
L.
5E
5C
5A
8A
8C
11

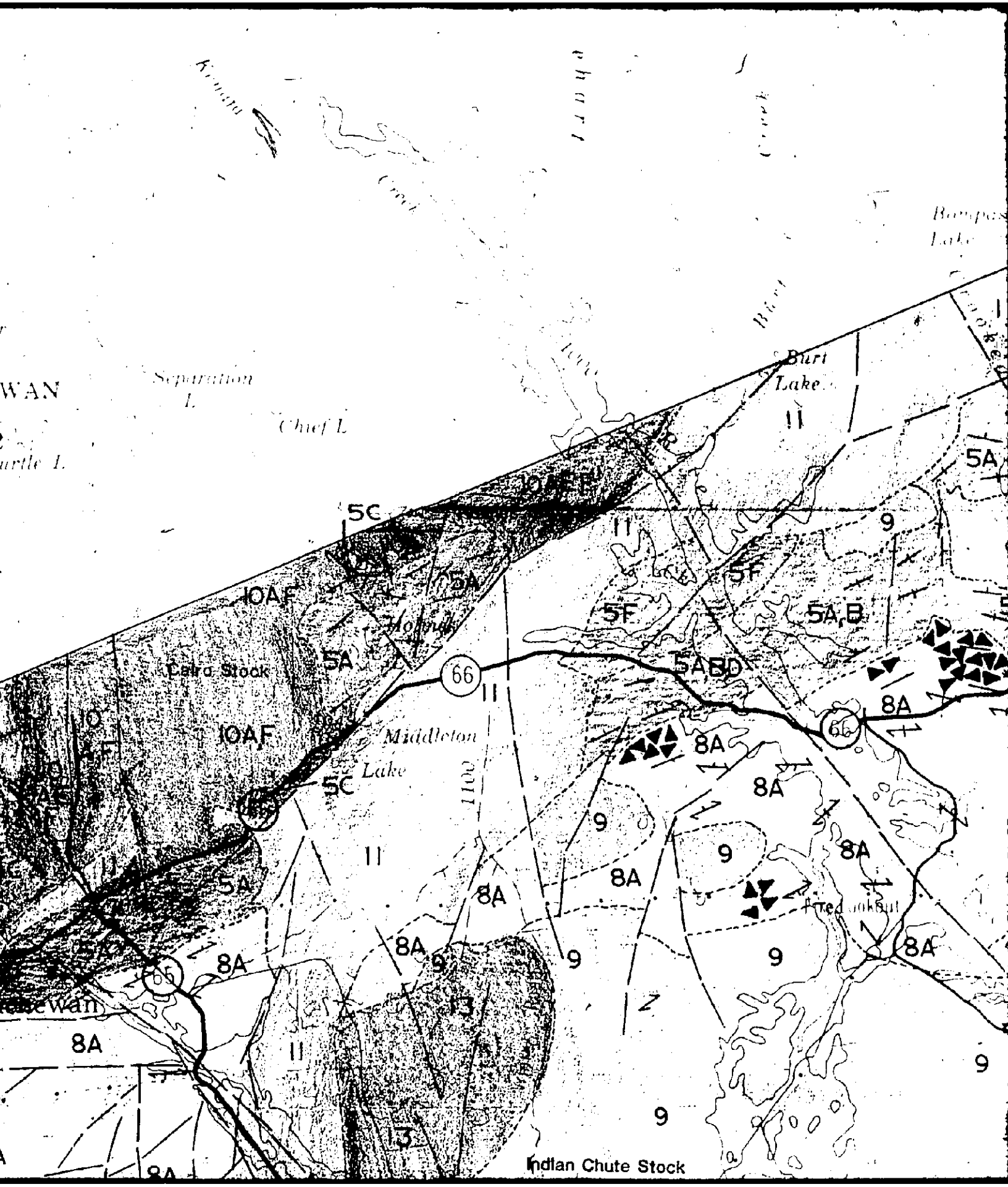
Separation L.
Chief L
Burt Lake
Middleton Lake
Laird Stock
Indian Chute Stock
10AF
5C
5A
5F
5A,B
5ABD
8A
9
11
13
66

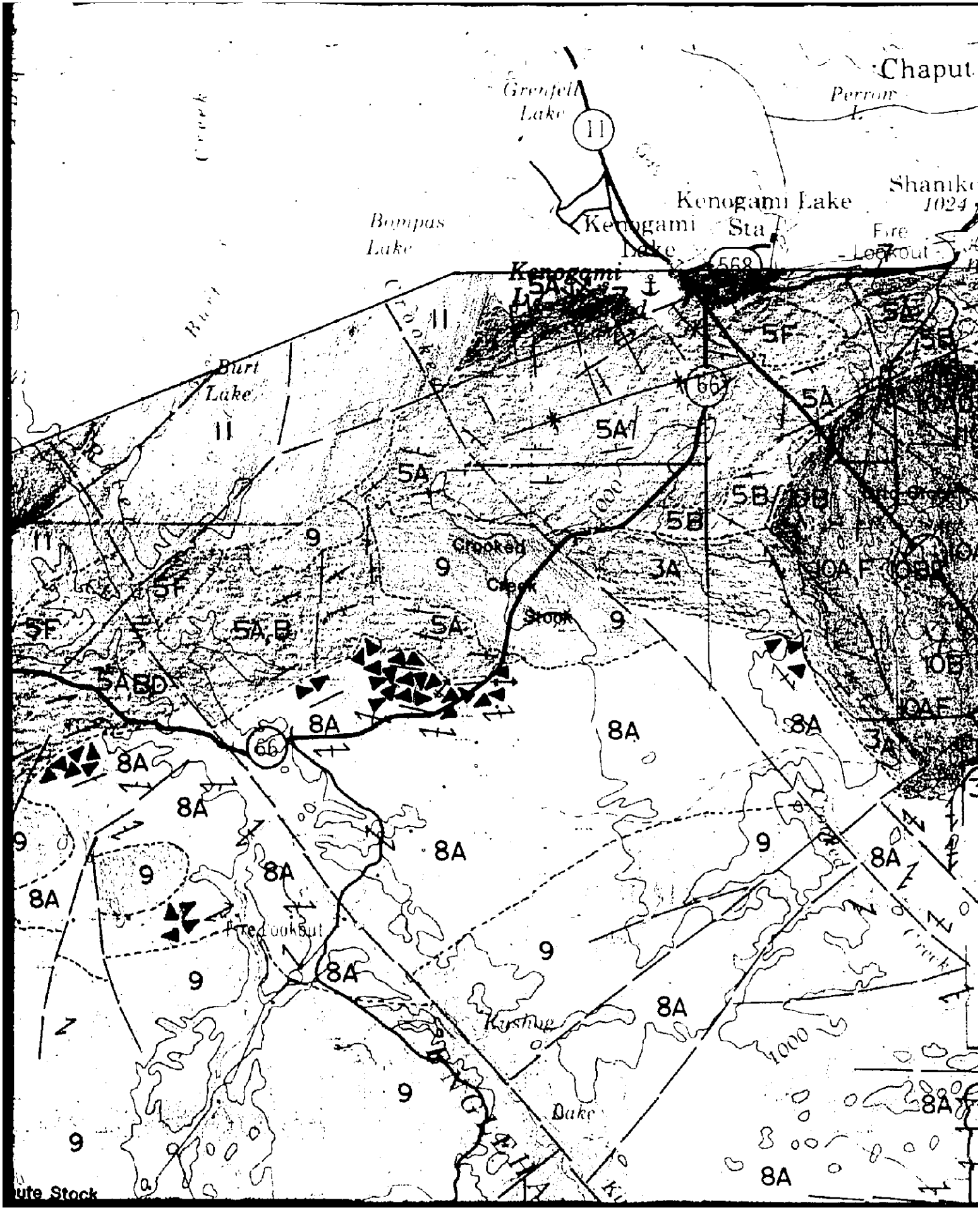
Chaput
Grenfell Lake
Perron
11
Kenogami Lake
Kenogami Sta
Bompas Lake
Fire Lookout
568
Kenogami Lake
5A
5F
5B
Burt Lake
66
11
5A
5B
9
Crooked Creek
3A
10A
10B
5F
5A,B
5A,B,D
8A
9
Fire lookout
Kashue
Lake
1000
Stock

Chaput Hughes
Mine Area
Shaniko
1024
Swastika
Fire Lookout
King Kirkland Sta.
North Park
Lobel Stock
5ABC
5A
5B
5C
5E
4A
3A
2A
1
10AF
10AC
10B
Round Lake
Tarzwell
66
112
11
FIG 25
8A
8B
8E
South Mindoka
Laskowski Breccia Zone
Hough Lake Breccia Zone
Hough Lake
Krugerdorf
48°00′

4 Skead Group and equivalent rocks: 4a - basalt; [illegible] rhyolitic lavas and pyroclastics, iron formation; 4b - quartz-feldspar porphyry

3 Catharine Group and equivalent rocks: 3a - pillowed and massive basalt, amphibolite, volcaniclastic sedimentary rocks; 3b - gabbro, peridotite

2 Wawbewawa Group; 2a - ultramafic lava, pillowed and massive basalt, amphibolite, felsic tuff; 2b - gabbro, peridotite

1 Pacaud Tuffs; mafic to intermediate volcaniclastic sedimentary rocks; pillow basalt, amphibolite; iron formation; quartz-feldspar porphyry, gabbro

Geological contact

Foliation (inclined: 0^{o}-29^{o}; 30^{o}-59^{o}; 60^{o}-89^{o}; vertical)

S_0-S_1 - bedding and stratiform foliation

Gneissosity

Axial plane of minor fold

Lineation, axis of minor fold

Lineation: M - mineral; P - deformed pillow; S - slickenside

Lineament: CLF - Cross Lake Fault; MRF - Montreal River Fault

Shear zone **(shear sense not implied)**

Sources of information: Compilation by J. Lafleur, 1981.

Geology from Moorhouse, 1944; Lawton, 1954, 1957; Grant, 1963; Lovell, 1964, 1967, 1972; Moore, 1966; Mackean, 1968; Pyke et al. 1973; McIlwaine, 1978; Jensen, 1978, 1980; Sinclair, 1979; Johns, 1980.

Additional geology from Lafleur, 1979, 1980.


Elizabeth Lake
Lloyd Lake
Mount Collins
Rankin Inlet
WEST
Otto Lake
Lehmann Lake
Melan Lake
Penpisi Lake
Obushkong Lake
Lake
11
13
3A
8A
8B
81°00'
13

8A
Sisseney
Lake
8A
11
8A
Zigzag
9
MONTREAL
WEST
Rankin
11
8A
11
13
8A
Wookey
Lake
8B
8A
11
13
Shillington
Lake
8B
8A
8A
Penrost
8A
8A
Lake
Obushkong
8A
12
11
12
8A
Wigwam
Lake
12
11
3A
3A
13
12
4A
3A
4A
3A
12

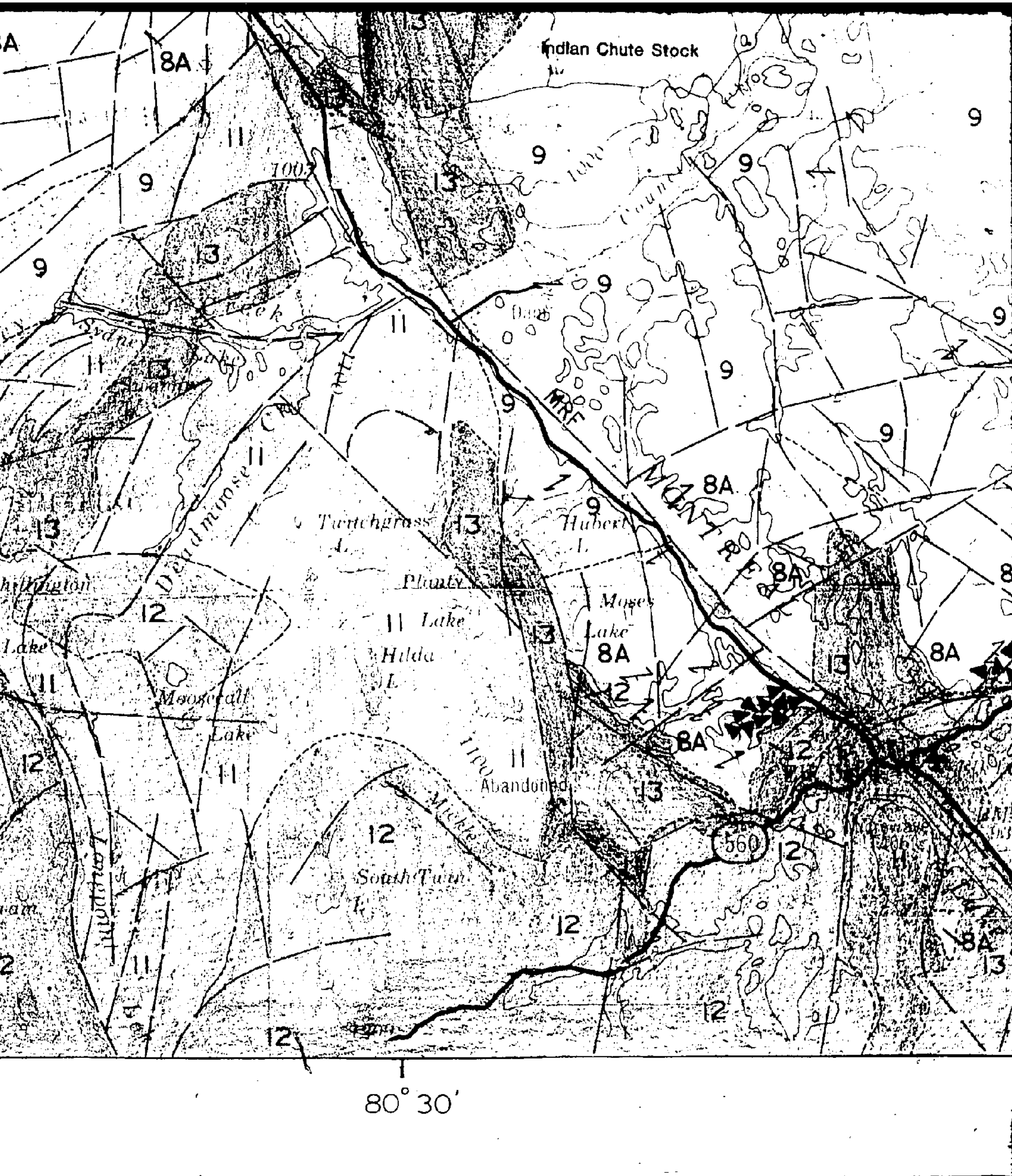

Indian Chute Stock
8A
9
11
13
12
Twitchgrass L.
Plenty
Lake
Hilda L.
Hubert L.
Moses
Lake
South Twin L.
Abandoned
560
MRF
80° 30'

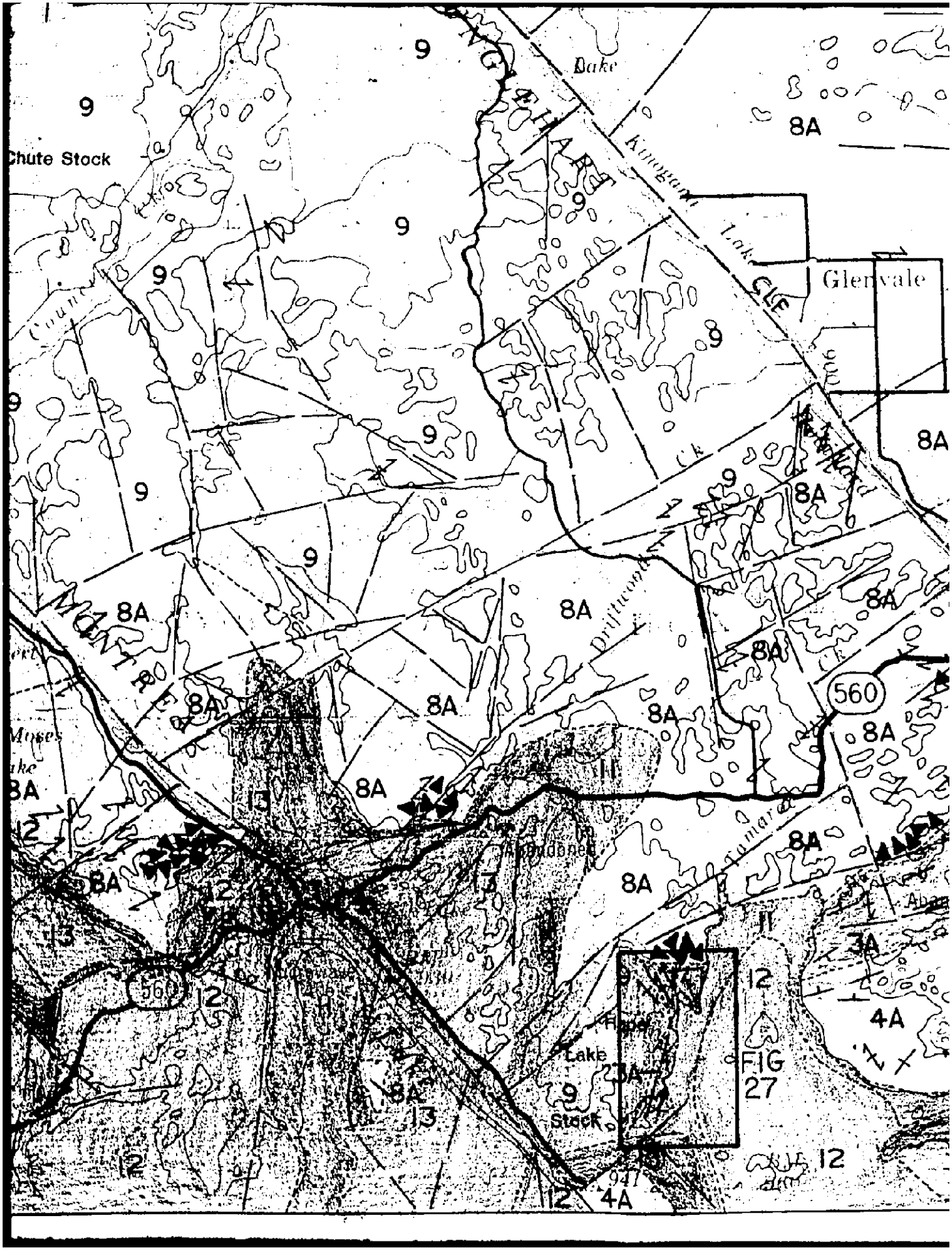
Chute Stock
Glenvale
Lake
Stock
560
FIG
27

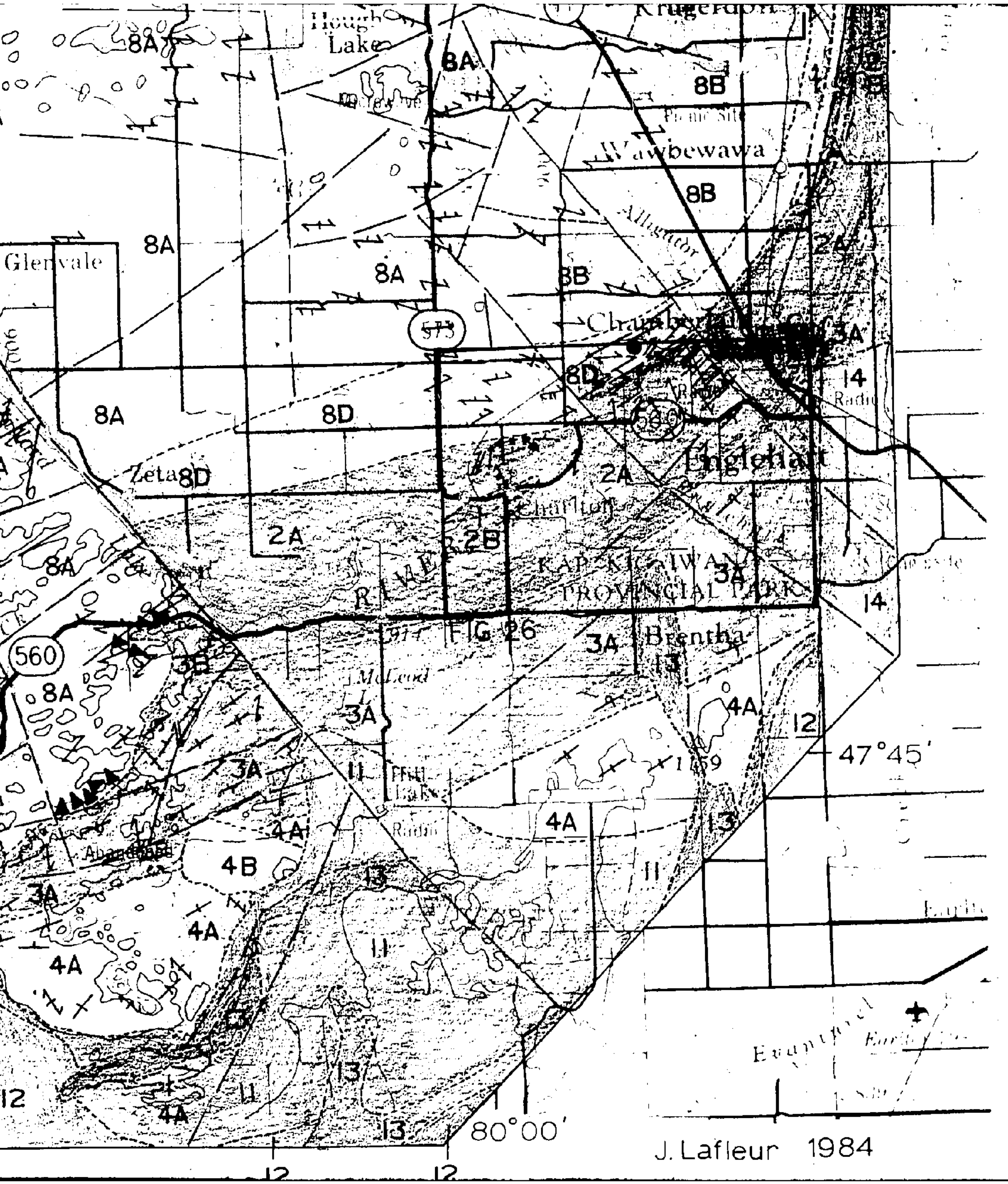

Hough Lake
Krugerdorf
8A
8B
Wawbewawa
Glenvale
Alligator
Chamberlain
575
560
Englehart
Zeta
8D
Charlton
2A
2B
3A
3B
14
KAP-KIG-IWAN
PROVINCIAL PARK
FIG 26
Brentha
McLeod L.
4A
4B
11
12
13
47°45′
Radio
80°00′
J. Lafleur 1984